INFORMATION TO USERS

This manuscript has been reproduced from the microfilm master. UMI films the text directly from the original or copy submitted. Thus, some thesis and dissertation copies are in typewriter face, while others may be from any type of computer printer.

The quality of this reproduction is dependent upon the quality of the copy submitted. Broken or indistinct print, colored or poor quality illustrations and photographs, print bleedthrough, substandard margins, and improper alignment can adversely affect reproduction.

In the unlikely event that the author did not send UMI a complete manuscript and there are missing pages, these will be noted. Also, if unauthorized copyright material had to be removed, a note will indicate the deletion.

Oversize materials (e.g., maps, drawings, charts) are reproduced by sectioning the original, beginning at the upper left-hand corner and continuing from left to right in equal sections with small overlaps. Each original is also photographed in one exposure and is included in reduced form at the back of the book.

Photographs included in the original manuscript have been reproduced xerographically in this copy. Higher quality 6" x 9" black and white photographic prints are available for any photographs or illustrations appearing in this copy for an additional charge. Contact UMI directly to order.

UMI

A Bell & Howell Information Company
300 North Zeeb Road, Ann Arbor MI 48106-1346 USA
313/761-4700 800/521-0600

SPATIALLY DISTRIBUTED HYDROLOGICAL MODELING OF STORM EVENTS USING A GEOGRAPHIC INFORMATION SYSTEM (GIS) WITH INSIGHT INTO TURBIDITY

By

Yuri Gorokhovich

A dissertation submitted to the Graduate Faculty in Earth and Environmental Sciences in partial fulfillment of the requirements for the degree of Doctor of Philosophy, The City University of New York

1999

This manuscript has been read and accepted for the Graduate Faculty in Earth and Environmental Sciences in satisfaction of the dissertation requirement for the degree of Doctor of Philosophy.

1/11/99
Date

Victor Goldsmith
Dr. Victor Goldsmith,
Chair of Examining Committee

1/25/99
Date

Dr. Frederick Shaw,
Executive Officer

Dr. Reza Khanbilvardi

Dr. Lorraine Janus

Dr. Keith Clarke

Supervisory Committee

THE CITY UNIVERSITY OF NEW YORK

Abstract

SPATIALLY DISTRIBUTED HYDROLOGICAL MODELING OF STORM EVENTS USING A GEOGRAPHIC INFORMATION SYSTEM (GIS) WITH INSIGHT INTO TURBIDITY

by

Yuri Gorokhovich

Adviser: Professor Victor Goldsmith

Distributed hydrological modeling of turbidity in streams is important because turbidity is an optical indicator of water clarity and indirectly linked with different kinds of pollutants in streams. One of the fortuitous properties of turbidity monitoring is that measurements can be recorded continuously.

As an optical measured parameter turbidity can be linked with suspended sediment concentration. This relationship is based on statistical regression. Regression allows one to predict suspended sediment concentration continuously during storms. It also allows one to apply modeling techniques available for suspended sediment concentration, for turbidity. Because these techniques are based on flow rate, such an approach requires development of a spatially distributed model of flow.

Spatially distributed modeling of flow during storm events is an important basis for any environmental modeling. During the initial phase of a rain storm surface runoff is the

main contributor of flow. To provide the spatial components for distributed hydrological modeling a Geographic Information System (GIS) was used to map and visualize contributing areas around a stream channel. Stream segments were defined using the hydrologic response unit (HRU) concept. Lateral flows used in the kinematic routing equation were derived from GIS output for each segment of the stream and at each time interval of the rain storm. This approach is new in hydrological modeling and can be used to enhance many existing simulations.

After flow values were calculated, suspended sediment concentration was estimated through the Yang's unit stream power equation (Yang, 1972) and afterwards was used to estimate turbidity values.

Model estimates of turbidity showed high correlation with measured discharge values and low correlation with turbidity. In most cases the accuracy of modeling, expressed as root mean square error, did not exceed 100%, but ranged from a minimum value of 25% to a maximum value of 534% for the verification dataset.

Based upon "in situ" measurements of discharge, a good comparisons with model computations of discharge, it is concluded that the methodology presented can be used in its current form for spatially distributed modeling of flow during storm events, and therefore provides a solid basis for turbidity or sediment transport modeling.

Acknowledgements.

I would like to express my gratitude to all members of my advisory committee for their support and advise that helped me to accomplish my work. I believe I had the best possible combination of members, with each of them uniquely contributing to my scientific research and work on the thesis.

I am indebted to Dr. Victor Goldsmith (Hunter College, NY) for his almost parental guidance of my professional career in the United States after I emmigrated from the Ukraine in 1989. Victor introduced me to the GIS field, and because of his warm personal attitude and exciting introduction to American geoscience and the scientific community, I stayed in New York, moved into the GIS field, and applied for the Ph.D. Program at CUNY. I appreciated his trust in me when he offered me a teaching assistantship at Hunter College and involved me in many GIS technical projects which gave me the necessary experience, without which, this work would be impossible.

I would like to thank Dr. Keith Clarke (University of Santa Barbara, CA) for his excellent GIS courses, programming classes and especially for the seminars on scientific research at the Graduate Center. These seminars helped me to select a topic for my dissertation, which is in my opinion the most difficult initial step. Dr. Clarke's seminars had great inspiring energy and they forced me to be fully immersed in scientific literature analysis and reading. They helped me to look at scientific areas of my interest from a different points of view, and stimulated my imagination to find the topic I am presenting in my thesis.

Dr. Reza Khanbilvardi (City College, NY) was the main dynamic force behind the

most complicated part of my dissertation - hydrological analysis. Because of his persistence and wise guidance my work changed direction from an original simple idea to a more complicated and interesting scientific development. His accurate and strong comments forced me to apply all my knowledge of GIS technology to create hydrological visualization and analysis in its current way.

I greatly appreciate Dr. Lorraine Janus's (New York City Department of Environmental Protection, Valhalla) work on guiding me through the analysis of my data and results. Besides scientific comments she helped me tremendously with my writing style and to express of my thoughts in a clear and understandable fashion. She helped me to recognize the importance of "multispectral" data analysis when all data sets, including measured and modeled, are treated from different points of view using different statistical methods.

During the field work on my thesis I used equipment which was bought through the grant from the New York State Electrical Research and Development Agency (NYSERDA), Drs. Khanbilvardi and Goldsmith, PI's.

All measured hydrological data on Malcolm Brook were supplied by the East of Hudson Hydrology Group, New York City Department of Environmental Protection (NYCDEP). I would like to thank Mr. Dale Borchert, current supervisor of the group, and Ms. Pat O'Hara, former supervisor of the group, for their support and valuable exchange of ideas about hydrological measurements and modeling. Ms. Kelly Seelbach (Data Coordinator, NYCDEP) provided prompt delivery of the data.

I appreciate the fine editing work on my dissertation by Mr. Anthony Grande (Hunter College, NY) who fearlessly undertook this enterprise and corrected my original

text.

I would like especially thank my parents, Anatoly and Molly Gorokhovich for their belief in me in fullfilling this task and encouragement. My wife, Svetlana and daughter Mila deserve special appreciation for bearing with me and my thesis all these years.

Table of Contents

List of Tables

List of Figures

1. Introduction.

1.1 Problem Statement.

In 1991, the Federal Surface Water Treatment Rule of the Safe Drinking Water Act (SDWA) came into effect. This rule states that all surface water supplies must be filtered prior to distribution to the public, unless it can be demonstrated that a certain level of purity exists and can be maintained. In December 1991, New York City Department of Environmental Protection (NYC DEP) obtained a resolution from the New York State Department of Health that said "...the City [could] be issued filtration avoidance status" (DWQC DEP Annual Report, 1993). To comply with this status, extensive work is planned to maintain certain water quality parameters within specific ranges. One of those parameters is turbidity.

The turbidity of water in streams is an important determinant of how and where point and non-point source pollutants mix and become dispersed throughout a hydrologic system. According with the Environmental Protection Agency (EPA) regulations (40 CFR Parts 141 and 142, 1989) the turbidity level cannot exceed 5 NTU in representative samples of water immediately prior to the first or only point of disinfectant application. These regulations make turbidity one of the most important factors in water quality monitoring activity. High levels of turbidity can reduce disinfection performance and therefore decrease drinking water quality or increase cost of disinfection.

There is also a direct link between turbidity and other water pollutants as described in Chapter 2. For example, pathogens and pesticides tend to be absorbed to the colloidal particles of soil and get carried with them into reservoirs. High levels of turbidity have

been noticed in many streams and reservoirs in the Catskill watershed system as well as in the Croton system. To design management practices, there is a need for a turbidity model which will allow a rapid assessment of turbidity levels for large watershed areas and for projected or unexpected changes from natural and manmade events. The model can guide application of best management practices to meet filtration avoidance requirements.

1.2 Description of New York City Drinking Water Supply.

The New York City drinking water supply consist from three separate systems, the Catskill, Delaware and Croton Systems, that collectively deliver more than 1.5 billion gallons of water every day. The distribution system consists of a 6000-mile gridwork of water mains ranging in size from 2 to 84 inches in diameter, with roughly 180,000 valves and 100,000 hydrants (Iwan, 1987). Through the system's gravity head and the use of regulating valves, a head pressure of 3560 psi is achieved. This pressure is sufficient to supply water upwards five or six stories without pumping. The water system has been considered one of the foremost public works projects of the 19th and 20th centuries.

The current water supply system has been in operation since 1842. In 1835, the Common Council approved plans to bring water to New York City from Westchester County by constructing a dam and the Croton Aqueduct. Pure Croton water entered New York City for the first time on July 4, 1842. It was delivered to the Old Central Park and Murray Hill reservoirs. Due to the population growth, in 1883 construction of a new aqueduct and reservoir supply to meet the high demand was approved. The New Croton Aqueduct was completed in 1890 and the New Croton or Cornell Dam was completed in

1907. At 234 feet it was the highest dam in the world.

The methods used to determine water quality improved between 1835 and 1910 as the link between disease and contamination by living organisms was being recognized and the agents of typhoid fever, yellow fever and cholera were discovered. In 1868, Drs. Elisha Harris and C.F. Chandler stated: "The sanitary importance of the excellent water supply which New York City enjoys cannot be overestimated, nor can we sufficiently prize the safeguards by which its continued and constant purity shall be insured...[to] prevent every source and possibility of defilement of the stream." (Harris, 1868). In 1905 Thomas Darlington, commissioner of the New York City Department of Health, expressed concern over the pollution of the watershed, the growth of New York City area, the suggestion of using Hudson River water, and the contribution of 'dead ends' i.e closed ends of pipes in the distribution system to disease. He advocated filtration, but cautioned:"The plan of filtration herein recommended does not mean that the City should guard any less the source of supply." (Darlington, 1905). In 1905 New York embarked upon filtration of the water supply, but by 1910 filtration was no longer considered a viable alternative. New York established its first calcium hypochlorite disinfection of Croton water in 1920 at Dunwoodie, New York and gas chlorination two years later at the same location. Chlorination remains the major source of protection agains bacterial disease today. Formal monitoring of the New York City water supply began in 1897 with establishment of Mt. Prospect Laboratory situated at Mt. Prospect Reservoir in Brooklyn and continues today at five laboratories throughout the watershed, including New York City.

The passage of state laws of 1905 opened the way for acquisition of new watershed property and the Catskill (1907 - 1927) and Delaware (1927 - 1965) watershed systems

were developed. Watersheds were progressively equipped with further technological advancements in chlorination, developments in copper sulfate technology for algal control, use of activated carbon filtration, improved water quality standards and increased Federal and State legislated water quality criteria and regulations.

The current system of five laboratories, responsible for the monitoring of New York City waters is under the administration of the NYC DEP. Within the NYC DEP's Bureau of Water Supply, the Drinking Water Quality Control (DWQC) laboratories provide monitoring of the water quality and associated scientific research and investigation.

1.3 Approach.

Hillel (1986) identified four principles that should guide model development:

1. Parsimony: "A model should not be any more complex than it needs to be and should include only the smallest number of parameters whose values must be obtained from data."

2. Modesty: "A model should not pretend to do too much. There is no such thing as THE model."

3. Accuracy: "We need not have our model depict a phenomenon much more accurately than our ability to measure it."

4. Testability:"A model must be testable" and we need to know "if it is valid or not, and what the limits of its validity are."

A turbidity model should consist of a set of hydrological equations describing

behavior among related hydrological parameters and turbidity origination. Solving these equations and using statistically supported regressions will make it possible to predict turbidity. Some equations will have spatial variables such as landuse areas, stream length and slope, that will be stored and handled by the geographic information system (GIS). The last stage of the modeling exercise will be the visualization of the results. This can be also done most efficiently, using a GIS. Two main parts of the modeling system can be easily identified: the hydrological component and the GIS component.

The hydrological component consists of two parts:

1. Rainfall and associated processes, such as rainfall intensity and surficial runoff;

2. Open channel flow and associated processes, such as sediment deposition, sediment entrainment and suspended sediment transportation.

These parts deal with forces that move particles of loose sediments, products of weathering and other fine grained material. Particles are moved toward the lowest gradient of the terrain and transported along stream beds or rills by water movement. Since turbidity is a water property and can be measured only within the water column, it can be modeled only if substituted by or represented through the factor that causes it. Most appropriate causal factor for turbidity is suspended matter, which directly changes the optical characteristics of water and statistically correlates with turbidity. Therefore, treating turbidity as a result of the total suspended matter appearance allows one to predict it using hydrological analytical methods. These methods usually deal with the total sediment transport and suspended sediment concentration as a part of it. One part of the total sediment transport is a bedload that moves through the stream channels by saltation.

This part generally is not suspended and consists of the coarse material, such as gravel or coarse to medium size sand, moved along the bottom of the channel. Chapter 3.6 describes temporal characteristics of the turbidity model and includes field data, showing that simulation of turbidity can be limited to the time interval of rainfall. Therefore there is no need to use hydrological model to derive hydrograph at its full length, i.e. untill final flow value will be equal to initial value.

Hydrological analytical methods, dealing with the sediment transport are well described by Julien (1995) who used both chronological description and practical examples in his study. The landmark method was developed by Einstein (1942). His method was simple and most useful for calculations under conditions where the bedload would constitute the most significant portion of the total load. His method was used by Colby (1964) and Simons (1981). A different physical basis for sediment transport problem was explicitly laid by Bagnold (1966) who considered energy balance and mechanical equilibrium to derive the mathematical expression relating the rate of sediment transport as bedload and suspended load to the expenditure of power by a statistically steady flow of water, i.e the available power of the flow supplies the energy to transport the sediments. Bagnold was one of the first scientists who mentioned stream power in relation to the sediment transport, and in 1973 Yang (1973) treated stream power not just as a velocity expression, but as a product of velocity and slope.

By increasing the importance of slope in the calculations, Yang brought more significance to the whole geomorphological aspect of the modeling. In hydrology, slope serves generally to calculate velocity or discharge, while in geomorphology it is used as one of the main parameters for description of the land patterns. In key papers by Strahler

(1952, 1957), he indicated that geomorphic processes are " the various forms of shear, or failure, of materials which may be classified as fluid, plastic, or elastic substances, responding to stresses which are most commonly gravitational." Under geomorphological principles, gravitational stresses act upon all earth materials and slope is a basic property of the landscape that causes gravity movements and the erosional-transportational fluids. These processes utilize energy which is the potential energy of elevation. All earth materials are moving from higher to lower elevations and the potential energy transforms into kinetic energy of motion or heat. This is one of the basic principles of Strahler's dynamic approach.

One of the first practical investigations, linking elevation and sediment loss was done by Schumm (1954), who statistically showed such correlation. A similar study, linking watershed area and sediment delivery ratio, was done by Roehl (1962). Both studies consider terrain as a natural structure that affects processes of sediment transport and delivery rates. Using this point of view, GIS appears to be the most appropriate method in dealing with terrain models and its spatial characteristics such as slope and aspect.

The GIS component of the study is a set of tools for collecting, storing, retreiving, transforming and displaying spatial data from the real world for a particular set of purposes (Burrough, 1986). According to Burrough, geographical data describe objects from the real world in terms of (a) their position with respect to a known coordinate system, (b) their attributes as they are interrelated to position (as color, cost, pH) and (c), their spatial interrelationship (topological relations) which describe how they are linked together.

A GIS can exist in two main formats, defined as being either vector and raster types. Vector-based GIS deals with such topological entities as point, line, polygon. These entities have a unique identifier that is linked with an attribute table. An attribute table can have many user defined fields containing information about the represented feature. Raster GIS deals with a grid that is defined by cell size, number of rows and number of columns. The only one numeric value can be attached to a grid cell. The advantage of the grid GIS is high speed of the spatial analysis and simplicity of the data structure. Vector-based GIS provides a more accurate and readable data display, but lacks the speed of the spatial analysis and has much more complicated attribute table management procedures.

GIS has proved to be an excellent tool to help manage a watershed and assist in solving water quality related problems for New York City's water supply, (Gorokhovich and Janus, 1996). A GIS is composed of software programs run by a computer operating system. This feature allows the user to program GIS applications, customize them or use commercially available software. GIS also serves as an ideal framework for automated cartography (Clarke, 1995), allowing the visualization of data or the results of spatial analysis.

GIS has been extensively used for the environmental modeling purposes (NCGIA, 1996). General datasets which are widely utilized for modeling consist of soils data (polygons or raster data), stream network (lines or connected cells), landuse (polygons or raster data) and digital elevation models (raster data). These data have various attributes which can be utilised in calculations, such as landuse areas, soil moisture coefficients, slope, stream length. The hydrological core when embedded into a GIS framework, can allow rapid data input and display of the model results.

2. Literature Review.

2.1 The role of turbidity in water quality concerns.

Clarity of water is an important factor in any drinking water distribution system. Turbidity, a measure of clarity, can be caused by suspended matter, such as clay, silt, fine particulate organic and inorganic matter, soluble colored organic compounds, plankton and other microscopic organisms. Turbidity is an expression of the optical property that causes light to be scattered and absorbed rather than transmitted in straight lines through a water sample. Therefore turbidity can serve as an indirect indicator of different water quality parameters which obscure light transmission.

Among research topics related to turbidity are studies of measurement methods, sources, linkages with organic compounds, suspended solids, fecal coliforms and hydrological parameters. The main reason that turbidity is included in such a broad range of studies is its ease of measurement and therefore its potential for use in:

- modeling different water quality parameters;
- reducing significantly the cost of laboratory measurements and field sampling, when it can be used as a surrogate mesurement; and
- monitoring and preventing high levels in water supply systems to avoid filtration plants or control quality after treatment.

Turbidity measurement is mandatory for regulatory purposes.

As mentioned in EPA Rules and Regulations, Surface Water Treatment Rule (1989), to avoid filtration, a water system should demonstrate on an ongoing basis that the

turbidity of the water prior to disinfection does not exceed 5 NTU, based on measurements taken at least every four hours.

2.1.1 Turbidity Measurements.

According to "Standard Methods for Examination of Water and Wastewater" (1994), turbidity traditionally was measured using the Jackson candle turbidimeter. The lowest turbidity value that could be read with this device was 25 Jackson turbidity units (JTU) . The method was totally visual, since the scientist evaluated light scattering using his unaided eyes. Most commercial turbidimeters measure intensity of light scattered in one particular direction, predominantly at right angles to the incident light. Because there is no direct relationship between the intensity of light scattered at a 90 degree angle and JTU's, there is no valid basis for the practice of calibrating a nephelometer in terms of candle units. In terms of precision, sensitivity, and applicability over a wide turbidity range, the nephelometric method is usually preferable to visual methods. Therefore the Jackson candle method is no longer used.

Nevertheless, some authorities viewed turbidity measurements as not reliable for use. In 1976, the United States Geological Survey (USGS) issued an open-file report describing a standard approach toward turbidity measurements (Pickering 1976). This document stated that "...the following principles are to be used in selecting methods for the measurement of light transmitting characteristics of natural waters: (1) standard instruments and methods are to be adopted to measure and report in optical units, avoiding 'turbidity' as a quantitative measure; (2) reporting of 'turbidity' in JTU's, Hellige units, severity, or NTU's will be phased out; ". Despite this negative proposal, the majority of

water quality reports, including USGS reports, have turbidity values expressed in NTU's. Moreover, for the past 10 years there is a growing trend toward usage of turbidity measurements in hydrological practice.

Nephelometric method is based on a comparison of the intensity of light scattered by the sample under defined conditions with the intensity of light scattered by a standard reference suspension under the same conditions. The higher the intensity of scattered light, the higher the turbidity. As a reference suspension formazin polymer is used. Standard commercial turbidimeters consist of nephelometer with a light source for illuminating the sample and one or more photoelectric detectors with a readout device to indicate intensity of light scattered at a 90 degree angle to the path of incident light. Figure 2.1 shows the essential components of a turbidimeter.

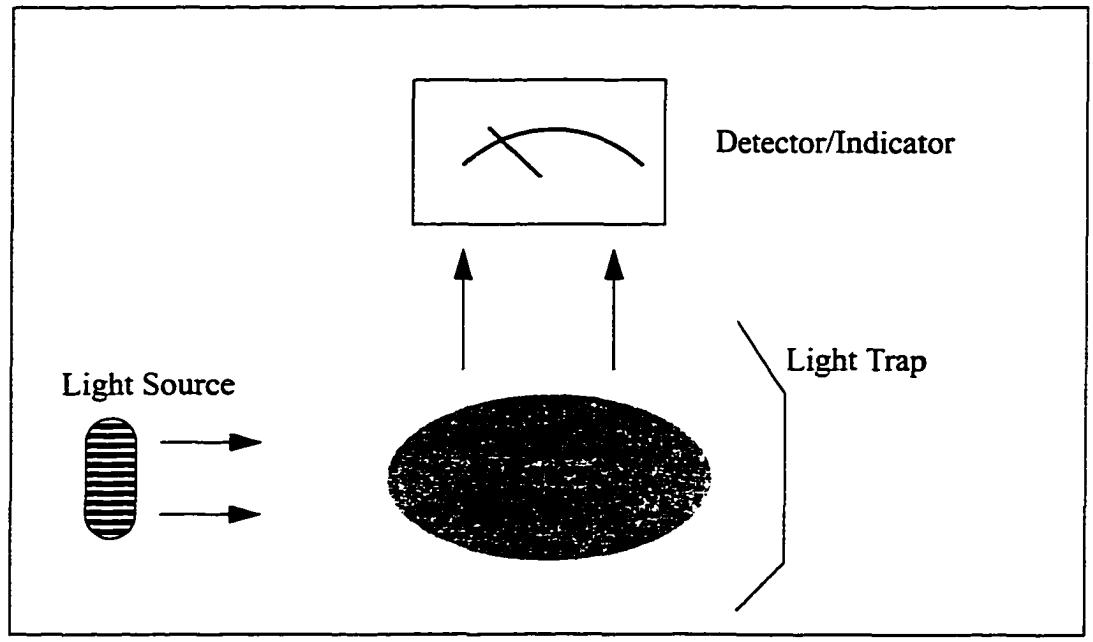

Figure 2.1 Essential Components of a Turbidimeter. (adapted from Letterman, R.D.(1994)).

2.1.2 Turbidity in Natural Environments.

Causes of turbidity vary with the environment where turbidity is measured, i.e. rivers, bays, ocean, lakes or urban areas.

N. Strunk (1992) performed a study in two small catchments in the Mosel region of Germany that showed how different sources of the suspended sediments can influence turbidity. In addition to the remobilization of sediment and channel erosion, he identified such inputs as sewage treatment plants, road discharge, topsoil and interflow.

Study of Effler and Johnson (1987) showed calcium carbonate precipitation as a significant turbidity source. In their field work on the Otisco Lake in New York they measured tubidity on the lake before and after acidification. Their conclusion was that calcium carbonate represented 32 percent of the turbidity and sometimes up to 70 percent. Therefore, calcium carbonate precipitation or 'whiting' should be taken into account for the high pH waters.

Turbidity sources can also have seasonal variations. While studying variation of the bottom turbidity layer in Etauchi Bay in Japan, Tanimoto and Hoshika (1992) found that this layer was produced by phytodetritus produced in the surface water layer, rather than by resuspension of bottom sediments in Etauchi Bay.

2.1.3 Suspended Solids and Turbidity.

Many studies relate turbidity to the amount of suspended solids in a water. The net transport of suspended solids is primarily a function of fresh water discharge. Study was done in Copper River, South Carolina (Althausen and Kjerfve 1992). However, N.Strunk

(1992) suggested that the transport of suspended solids was not only controlled by discharge magnitude but also sources of suspended solids.

The first suggestion to use turbidity for the computation of sediment loads was stated in the study done by the Pennsylvania Department of Transportation and USGS in 1975 and presented by Truhlar, J.F. (1976). The field study that was done by both agencies intended to evaluate sediment-control measures used during highway construction. The field data "revealed a good correlation between daily mean discharge-weighted turbidity and daily mean discharge-weighted suspended sediment concentration". In this study, missing data for the suspended sediment concentration were replaced by the values derived from the turbidity-sediment correlation and used with the daily mean water discharge to calculate a daily sedment load.

At the same time, the suggestion to use suspended solids as a measure of turbidity was documented in Emmett's (1975) study. Though he used Jackson Turbidity Units, a formula linking turbidity and suspended solids concentration was derived and used in some Idaho river studies.

The relationship of turbidity with inorganic compounds can be found in studies of Stewart and Martin (1982). While attempting to assess the potential relationship between asbestos in drinking water and cancer, Severson (1981) found a significant correlation between turbidity and asbestos levels in the Sultan River Basin watershed in Washington.

Clay discharge (as a result of mining) studies were done by Quinn *et al.*, (1992). They showed that mean turbidity was increased by 7 to 154 NTU above background (mean 1.3 to 8.2 NTU) by the mine discharges. Patterns of increase in suspended solids (strongly correllated with turbidity, r=0.95) were similar. Decamps *et al.*, (1979) found

that the mixture of suspended matter (45% mineral and 55% organic) corresponds to 4.4 Formazin Turbidity Units. Gippel (1989) established preliminary relationships between turbidity and suspended sediment concentration. One of the valuable conclusions of this study was a suggestion that the presence of hysteresis indicated changing sediment properties. He suggested that these variations could indicate changing source areas during storm events.

The same hysteresis was found by L.A. Kelly (1992) for suspended solids and discharge variables. He performed a 14-month study of bedload and suspended sediment generation in three gauged subcatchments of a small coniferous forested upland drainage basin in the southern Pennines of the United Kingdom.

Letterman (1991) plotted a log-log graph of particle count versus turbidity. The concentrations were reported for particles in the 2 to 60 micrometer range. The graph was used to reveal limitations of the turbidity measurements when it is used to monitor the performance of filtration systems with high particle removal efficiencies. The graph shows very good correlation below 0.5 NTU, between turbidity and particle concentrations for the raw water.

One of the latest studies on the subject belongs to Jack Lewis (1996) who concluded that for estimating suspended sediment concentration in rivers, turbidity is generally a much better predictor than water discharge. In his experiment, the five loads were estimated by predicting suspended sediment concentration from regressions on turbidity. Using simple linear regression, the five loads were estimated with root mean square errors between 1.9 and 7.7%, compared to errors of 8.8 to 23.2% for sediment estimates based on rating curves for the same samples.

2.1.4 Organic Compounds and Turbidity.

Turbidity is linked with existence of organic matter in natural waters. Organic components can increase or decrease turbidity. Following papers studied turbidity phenomenon in relation to organic matter.

Oksiiuk *et al.*, (1992) showed that decreased water turbidity allowed growth of phytoplankton.

Quinn J.M. *et al.*, (1992) provided data that taxonomic richness of invertedrate densities in their study of six streams on the west coast of the South Island, New Zealand were significantly lower at downstream sites where mean turbidity was 23 to 154 NTU's. They found that downstream densities as a proportion of those upstream were negatively correlated with the logarithm of the turbidity loading ($r = -0.82$).

Davies-Colley *et al.*, (1992) while studying the same six streams on the west coast of the South Island in terms of the optical properties, found that clay suspensions (40% between 0.55 and 0.001 mm) seeping into the streams from gold mines were colloidally stable. They attenuated light with near maximum efficiency which lead to severe degradation of stream optical quality. This reduction in light proportionally reduced benthic primary productivity downstream of mining activity. In turn, this reduced benthic algal biomass and lowered the phototrophic content of the epilithon.

Experimental studies of Liang, McCarthy *et al.*, (1993) in which oxygenated water with high levels of natural organic matter was injected into a sandy aquifer, showed that at the locations where dissolved oxygen remained constantly low, the turbidity increase was moderate.

Described papers indicate that high turbidity negatively affects biomass and

benthic productivity due to the reduction of light.

2.1.5 Pathogens and Turbidity.

In EPA-issued Rules and Regulations (USEPA,1989), turbidity level was considered a measure of particulate matter in water and an indicator of the effectiveness of treatment processes that control pathogens, including *Giardia*, in systems using surface water. Parasite densities and turbidity were studied by different authors and were found to be related. The relation between *Giardia, Cryptosporidium*, turbidity and particle counts were evaluated by LeChevallier and Norton (1992) in raw-water and filtered effluent samples from three different locations. In general, indicators of pollution (coliforms, turbidity, particle counts) correlated with parasite densities. They also stated that removal of particles greater than five microns and turbidity were useful predictors of *Giardia* and *Cryptosporidium* removal. The same authors (1991) also found significant correlations between *Giardia* and *Cryptosporidium* densities and turbidity while performing tests of source waters of 66 surface water treatment plants in 14 states and one Canadian province. For this reason, prediction of particle transport as measured by turbidity is an important aspect of water supply management.

2.1.6 Hydrological Parameters vs. Turbidity.

There are many studies that have examined the relationship between turbidity and hydrological parameters. The practical meaning of these studies is very important because such relationships can be utilized in models. One of these studies was done by A.

Spangberg and J. Niemczynowicz (1992). Their project aimed at delivering water quality data with the very fine time resolution necessary to discover deterministic elements of the complex processes of pollution wash-off from an urban surface. Measurements of rainfall, runoff, turbidity, pH, conductivity and temperature with 10-second time resolution were performed on a 270 sq. meter surface drained by one inlet. A cross-correlation between all measured parameters was calculated for all events with and without a time lag, and showed that turbidity was strongly correlated with rainfall intensity and runoff. It was noticed that the peak of turbidity came shortly after a peak of rainfall intensity and earlier than the peak of discharge.

Similar observations were reported by Y. Gorokhovich and P. O'Hara (1995). A turbidity study of a small watershed basin of New York City drinking water supply showed high correlation of turbidity and the rain intensity ($r^2 = 0.7$). An analysis of the turbidity curve overlain by the hydrograph and cumulative rainfall curve showed that the turbidity response to rainfall occurs before the discharge peak. A previously published report by New York City Department of Environmental Protection (1994) shows that turbidity levels are related to discharge rates and rainfall intensity.

Besides correlation with rainfall intensity there are reported correlations with velocity, found by Mack (1988). He analysed 76 samples collected within the Crooked Creek basin, Alaska and used as variables turbidity, suspended solids and velocity. The multiple regression model with suspended solids and log velocity as independent variables produced an r^2 of 0.85.

2.2 Modeling Accuracy.

Model's accuracy is important to know because eventually model's performance has to be evaluated. It is difficult to know how well model performs until some other criterias can be utilized. Accuracy varies with different models and applications. Several literature sources were studied to ascertain the results of existing models showing comparison between modeled and observed data.

There are two main output components of the proposed model, flow and turbidity. Since no models exist for turbidity in streams, data on suspended sediments were used instead.

2.2.1. Flow Modeling.

In order to evaluate accuracy of flow modeling, a few publications were reviewed to evaluate differences between measured flow and modeled flow. One of the most widely used flow model is HEC-1 (U.S.Army Corps of Engineers, 1994). Some examples presented at the HEC-1 workshop (Rutgers University, 1995) for the Waller Creek Basin, shows accuracy of modeling within 20 to 200%.

M.A. Collins and R.O. Dickey (1989) used the stohastic method to simulate a hydrograph. Their results showed generally good agreement between observed and computed hydrographs with accuracy of 10 to 100%.

J.C. Panuska et al. (1991) applied the AGNPS model and found that errors in flow prediction ranged from +25% to -75%.

In 1997, HydroQual, Inc., applied the SWMM model for the Kensico Tributaries

Management Plan (HydroQual, Inc., 1997). SWMM is a storm water management model which predicts flow for selected drainage basin using rainfall as an input. For two storm events within drainage basins surrounding Kensico Reservoir, its modeling accuracy was within 10 to 300%.

2.2.2. Suspended Sediments Modeling.

One of the most useful publications for comparing the effectiveness of sediment transport and sediment delivery models was "Effectiveness of Soil and Water Conservation Practices for Pollution Control" (Haith and Loehr, 1979). It was found that three most widely used models, Universal Soil Loss Equation (Wischmeier and Smith,1965), Onstad-Foster (Onstad and Foster, 1975) and Williams (Williams, J.R. 1975), overpredicted soil losses by values 50 to 100 times larger than observed. In some cases, the discrepancy between observed and modeled values reached 4000%. The authors concluded that "no model was found to be clearly more accurate than the others in all cases."

Better results, with accuracy of 28 to 270% were presented by Foster *et al.*. (1977), who used the USLE with modified factors.

Another model, AGNPS Young *et al,* (1987) was applied by Panuska , Moore, and Kramer (Panuska *et al.*, 1991) to interface with terrain analysis methods. The authors found that the sediment yield values ranged from a maximum underprediction of 60% to maximum overprediction of 1,420%.

3. Methodology.

There are three main components presented in the methodology below: the GIS component, the hydrological component and the suspended sediment concentration/ turbidity component. They are integrated through visualization of the runoff pattern, including contributing areas, and extraction of original flow and lateral flow for the modeling. This means that the hydrological component handles finite element matrix calculations; the GIS component provides initial flow data (for each time interval) as an input to the matrix, and also preserves static images of the runoff pattern at each time interval for each segment on a stream. Most of the current hydrological, non-point source pollution models use GIS as a front end for the model or tool for database handling and visualization (Gorokhovich and Janus, 1996; Krysanova *et al.* 1996; DePinto *et al.*1994; Gao, X., *et al.* 1993; Engel, B., *et al.* 1993; Harris, J., *et al.* 1993). In these models, GIS provides either initial data for models and final visualization of results, or a visual interface for handling and displaying the original spatial databases. According to Maidment (1993), " it is possible to do some hydrologic modeling directly within GIS systems, so long as time variability is not needed". He mentioned that theoretically it is possible to model one-dimensional and two-dimensional steady-state flow computations explicitly using a GIS database. The methodology presented here attempts to use GIS data generated for each time interval of a rain storm. The GIS provides lateral flow and initial channel flow for each time interval and segment on a stream. Unlike raster systems that use a constant cell size, vector GIS was used to define hydrological response units that divide the stream channel into segments.

Suspended sediment concentration model served as a basis to model turbidity

through developed regression equation. In this study turbidity assumed to be an indication of suspended sediments in stream channel and indirectly reflects its concentration.

3.1 Application of a Geographic Information System .

3.1.1 The GIS Method.

GIS, according to Burrough (1986) "is a set of tools for collecting, storing, retrieving at will, transforming and displaying spatial data from the real world for a particular set of purposes." In much wider sense, Dueker and Kjerne (1989) defined GIS as "a system of hardware, software, data, people, organizations, and institutional arrangements for collecting, storing, analyzing, and dissemenating information about areas of the Earth."

All objects within a GIS should have three main characteristics: a coordinate system, attributes, and a topological type.

A coordinate system is essential to locate objects within a space. Because of the digital nature of a computer's memory, the traditional geographic coordinate system that consist of degrees, minutes and seconds is not usable. It exists in decimal degree format. Most common systems are Universal Transverse Mercator coordinate system (in meters) and the State Plane coordinate system (in feet). Both systems represent land surface as a combination of flat grids.

Attributes are needed to characterize objects. Traditional geographic attributes are area, length and direction. Other attributes may be added and can include chemical, physical or descriptive characteristics. These characteristics can be either in numerical or

character format. A numerical format can be values for specific conductivity, pH and similar variables. Characters can be place names, rock types or soil description.

Topological type defines spatial relation between objects. There are three basic examples of topological types: point, line, area (polygon). Each type has a specific attribute, i.e. point - location X and Y., line - length, polygon - area and perimeter. These attributes allow the answer to such common questions as 'How many points?', 'How many segments?' and 'What area?'. By using the attributes of these objects, very powerfull queries and databases can be developed.

GIS methodology for hydrological and surface process modeling is comprehensibly described by David Maidment and Ian Moore (Goodchild et. al., 1993). GIS provides modelers with spatial data analysis and visualization capabilities. Time series and modeling parameters (i.e., coefficients) are entered either through the modeling interface or stand alone files. Moreover, modeling equations are generally compiled separately and from this point of view can be tested or calibrated independently from the GIS. Maidment noticed that "it is hard to see how the differential equations describing the conservation of mass, Newton's second law, the first law of thermodynamics, and the processes inherent in dispersion and transformation of constituents can be explicitly captured within a GIS system. What can be captured are snapshots of these processes at particular points in time, or time-averaged values of process variables over a long interval, such as a year, within which many of the intrinsic physical variations have been accumulated or averaged". The "happy" marriage between hydrological, or even other kinds of modeling and GIS must be based on using the advantages of both technologies: spatial data manipulation from GIS and description of specific processes in the form of

equations from hydrology.

Spatial data manipulation within GIS should be based on the particular GIS data type and structure. There are two main types of GIS - raster and vector. Both are well described by Burrough (1986) in applications for land use management, and by Clarke (1995) in relation to automatic cartographic visualization. The choice of using either a raster or vector GIS system should depend on the specific application. While working with stream networks and tracing water flow through channels, vector-based GIS is most appropriate.

Raster structure is simple. Its smallest component is the cell and total structure can be represented by combination of cells, a grid. Such data as satellite images or scanned images are readily available in raster format. Analytical computations with grids, also called map algebra, are simple and fast. Data overlays can be done quickly. But, there are three disadvantages:

1. Data redundancy - high volumes of cells representing each object.

This disadvantage is not only a problem related to the computer memory capabilities, but within a modeling framework, has direct impact on data accuracy. This means that within certain areas there can exist as many cells as a modeler can define by their size. Their values will be the same and data quality will also be the same. The reason that this is mentioned here is that in GIS-related modeling studies, questions of the cell size for the model have gained significant importance, especially for distributed modeling projects. This issue is linked directly with the size of the data and the map scale.

The scale of the map is a vector category by definition (relationship between distance units on a map and distance units on terrain). But after geocoding map units,

especially square units, these map units can represent data values (attributes) as well, and final maps will represent special areas, such as concentrations of elements or land use categories. This means that the map scale should have enough statistically supported field based or remotely sensed measurements of the mapped values to support attached attribute. Thus for each square unit of the map, there should be enough measurements to support definition of the area as 'residential' or '20 mg/l of phosphorus'. Therefore, by reducing or increasing cell size, data accuracy will never be gained. Also, data values within the area will never be changed if computations are done from cell to cell. The only time cell size is an important factor is during interpolation, when the number of cells and the size of resulting grid define final result. This issue is very important when creating digital elevation models and then, deriving stream networks or other data from them.

2. Poor visual representation of data - representation appears "squared" or boxy with an angular outline.

3. Grid orientation - cell sides are always oriented either north to south or east to west.

This disadvantage is important to consider when direction of flow should be taken into account or required correct linear distances between segments.

Vector structures can represent cartographic entities such as lines more closely and completely lack the redundancy of raster systems. Topology can be completely described by the vector structure in a simple form. Linear networks, such as rivers or transportation routes can be represented by vectors very effectively. At the same time, such operations as data overlay can be very intensive and require considerable amount of computer time. In this format, high quality printing can be expensive and time consuming. Previously, these

disadvantages created a barrier against the utilization of vector GIS for modeling and visual persentation of the results. Today, with multi-processing, high speed and large memory computers, vector GIS can be used effectively for any application.

3.1.2. Choice of Appropriate GIS Technique.

Essentially, there are only two options for linking environmental models with GIS. The first option is to run the model outside of a GIS framework and then use GIS for the data storage and display. The second option is to integrate a model in the GIS by utilizing GIS functions, command or SQL language, or map algebra.

The first option has advantages when the modeled process is complex enough to use specific computer language or software. The disadvantage of this is a need to convert data formats and constantly move between compiled code and GIS system. Examples of such modeling are WASP4 model (DePinto et. al., 1993) and TR-20 model (Cahill et. al., 1993).

The second option has the advantage that both the model and the GIS use a single database and share functions. The disadvantage is if the model is too complicated, then the GIS may not have enough tools or capacity to accomplish the goal of the modeling. It is only a true disadvantage for the commercial GIS's which are based on a proprietary codes and have a limited number of functions. In case of public domain GIS, the code is usually open, allowing the user to implement any changes or to use the full capabilities of the programming language functions. A perfect example of such a GIS is the GRASS software, developed by US Army Corps of Engineers. It is written in C language.

Excellent examples of model integrations within this GIS can be found in Proceedings of the Seventh Annual GRASS Users Conference (Waggoner, 1993).

Since turbidity modeling will be based on some empirical methods which do not require complicated computations, the second option is more practical and attractive. Another consideration which favors the integration of GIS and a modeling algorithm is that the result of the modeling will be a cartographical display of the final data. The modeler, in this case, will be able to manipulate the display options and data processing from one single place on the screen. The time gained by such integration can convert the modeling process from a tedious data/format exchange into a dialog between scientist and model.

3.1.3. Choice of the GIS Type.

The choice of using either a raster or vector GIS type should depend on the specific application that a scientist has in mind. While working with stream networks and tracing water flow through channels, vector-based GIS can be most effectively utilized. This kind of GIS will also be advantageous for hydrologists who will use the resulting model.

Most of the widely utilized hydrological models, such as HEC-1, HEC-2, TR-55, use the concept of segments or set of segments which is usually oriented toward the direction of outflow. In these models, all segments are numbered and organized in a tabular form. This organization allows the calculation of hydrological parameters for each segment and then builds a linear graph or bar diagram representing distribution of a modeled parameter (usually discharge) along the selected network. Data associated with

segments are stored in the table and may also contain information about areas surrounding stream network. Usually these include various landuse, soil, and gradient data, to name a few.

More often, these data are represented by grid-based or raster GIS because spatial analysis can be performed faster. In the case where data are integrated within GIS models, map algebra can be conveniently utilized.

The main types of GIS models, used in hydrology include hydrologic response units (HRUs), triangulated irregular networks (TIN), and grid-based and contour-based models (Moore *et al.*, 1991). These models have one thing in common - they represent certain areas which have single homogeneous properties. While TINs and grid-based and contour models deal with elevations, their only attribute, HRUs are hydrologically similar areas derived by overlaying landuse properties (landuse classes) and soil properties (hydric groups). Hydrological properties in this case are runoff and infiltration, derived from combinations of landuse classes and hydric soil groups. HRU data structure is therefore suited for hydrological modeling purposes and can be modified according to the modeling ideas.

Because the turbidity model will be linked with stream unit power values, HRUs should have more information besides landuse classes and soil types. This enhancement can be done by including such data as topography (slope) and rainfall (depth). Therefore, each unit can have several attributes that will be used in computations.

3.1.4 GIS Spatial Analysis

All spatial analysis in this study was done using commercial type GIS called ARCINFO, produced by Environmental Systems Research Institute (ESRI). One of the main advantages of this specific software is its modular structure. All software modules can be utilized separately or together, in raster format or vector. It also has powerful macro-language capability which allows one to run macros and batch files; it also communicates easily with the operating system and C programming language.

The spatial analysis here consists of the following main steps:

1. Create a catchment boundary and select stream reaches for analysis.
2. Create HRU matrix for the catchment.
3. Segment the stream using the HRU coverage.
4. Define the initial point on the stream line (using highest elevation) from which calculations start.
5. Select contributing areas for stream segments.
6. Produce output (define flow values and contributing areas for each stream segment at each time step and save visual frames for animation).

The following is a more detailed explanation of each of these steps:

1. Create a catchment boundary and select stream reaches for analysis:

The catchment area was derived from contour lines. For this study, the watershed boundary was derived from a USGS 24K contour map.

2. Create HRU matrix for the catchment:

Creation of HRUs requires an overlay procedure to combine several datasets: soils,

landuse and slope. The resulting dataset looks like a mosaic consisting of multiple HRU planes, each with a single runoff value. This dataset or coverage has unique hydrological characteristics of the catchment. For each specific storm pattern, values of runoff can be calculated using the rational method. After calculations, the HRU matrix has an attribute table with peak runoff values for each time interval of the storm event. This makes the HRU matrix multi-dimensional in time and unique for each storm pattern. Figure 3.1 depicts the general structure of HRU elements. Input data for the model contain only rainfall information which is presented as rainfall depth (inches) per time interval (T_1....Tn). After applying the rational method, each polygon in the HRU matrix is assigned a value of potential surface runoff (Q_1...Qn)

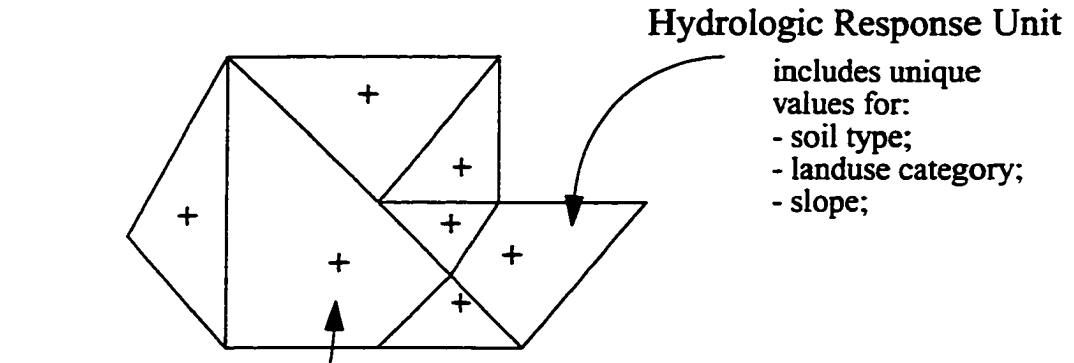

Attribute Table of the Label Point :

Item	Explanation
AREA	Area of the HRU, m
PERIMETER	Perimeter, m
RUNOFF_COV#	Unique Label Point #
RUNOFF_COV-ID	Coverage ID #
LANDUSE	Landuse Category
SOIL-TYPE-NYC	Soil Type
SLOPE	Slope, %
C	Runoff coefficient C
Q1	Runoff at time interval 1
Q2	Runoff at time interval 2
Q3	Runoff at time interval 3
Q4	Runoff at time interval 4
Q5	Runoff at time interval 5
Q6	Runoff at time interval 6
Q7	Runoff at time interval 7
Q8	Runoff at time interval 8
Q9	Runoff at time interval 9
Q10	Runoff at time interval 10

Figure 3.1 Element of the HRU matrix from the GIS coverage RUNOFF_COV.

The triangular shape of the matrix elements is due to the triangulation irregular network (TIN) structure. This structure represents elements of the terrain with label points having values for the slope. Other spatial datasets, as soils and landuse are represented by irregular polygons, but TIN elements prevail because of the better resolution: one polygon of specific soil type can contain several TIN elements. Example of the HRU matrix for Malcolm Brook watershed is depicted in Figure 3.2

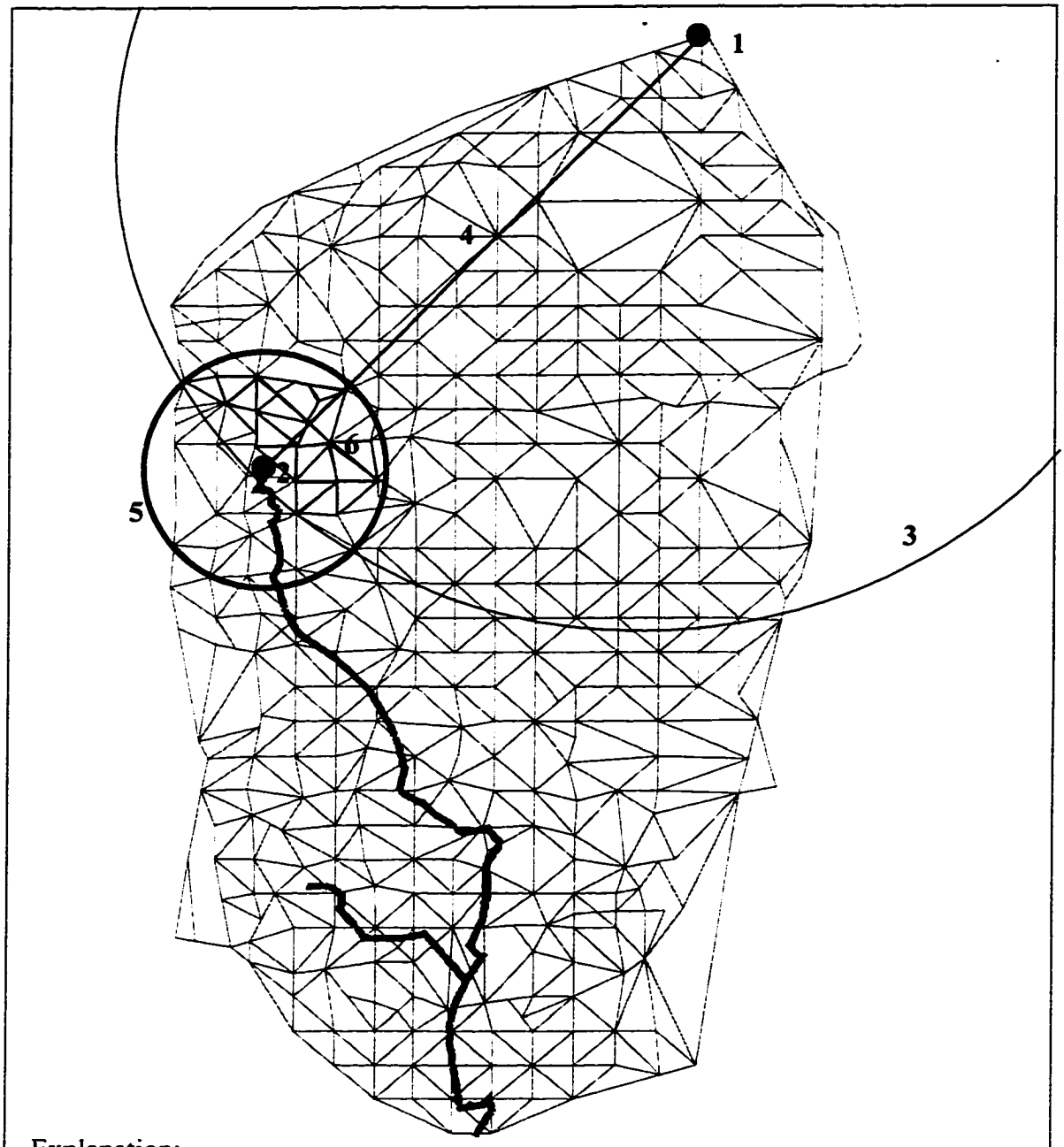

Explanation:

1. Selection of farthermost point on the watershed;
2. Selection (in this case, first) segment of the stream;
3. Creation of the radius to select allpotentially contributing HRU's;
4. Distance, used to develop radius (3);
5. Circle, drawn using the radius, interpolated from the distance (4);
6. Shaded area represent HRU's selected from the rest of HRU units, using 'high elevation' rule and 'within' or 'passthru' option (in this case 'within' option) ;

Figure 3.2 Spatial iterations within GIS to obtain contributing areas for each stream segmentusing the Malcolm Brook watershed as an example.

The next step in this procedure requires rainfall data for the matrix. Data are structured in an ASCII type file, which is automatically created through a customized interface. Figure 3.3 shows an example of this file. It is created from a larger data file with four columns: Discharge, Date, Time, Rainfall. The ARCINFO built macro requests the desired number of intervals, breaks the original data file into the requested number of intervals, and calculates the cumulative rainfall for each time interval. It then writes the results into a separate file depicted by Figure 3.3.

```
/* June 3, 1997 rain storm, 5 hours, start 1:50;
/* Time interval = 20 min; 20 min x 60 sec = 1200 sec;
/* Rain started 6/3/97, 1:50

&sv .P1 = 0.02
&sv .P2 = 0.01
&sv .P3 = 0.01
&sv .P4 = 0.02
&sv .P5 = 0.01
&sv .P6 = 0.01
&sv .P7 = 0.02
&sv .P8 = 0.01
&sv .P9 = 0.01
&sv .P10 = 0.01
&sv .P11 = 0.01
&sv .P12 = 0.01
&sv .P13 = 0.01
&sv .P14 = 0.01
&sv .P15 = 0.01

&sv .cycle = 15
&sv .time_interval = 20
```

Figure 3.3. Rainfall input file for the model. P_1 ... P_n consist of rainfall depth per time interval.

Upon setting up this data file, another ARCINFO built macro creates the

corresponding HRU matrix, calculates runoff for each spatial element of the matrix and assigns attributes Q_1 .... Qn for each element's attribute table.

3. Segment the stream using the HRU coverage:

After the HRU matrix has been created, it is superimposed on the stream line. It is a simple procedure that results in dividing the stream into many segments with different lengths.

Each segment is assigned an unique number as the label point from the HRU matrix coverage

4. Define the initial point on the stream line (using highest elevation) from which calculations start:

To define the segment that hydrological calculations will start from, a simple assumption, that water flows from highest to lowest elevations is made. Therefore, to define the head of the reach, it is necessary to compare elevations at both ends of the stream. The segment with highest elevation is the first one, the adjacent connected segment is the second, etc.

5. Select contributing areas for stream segments:

Selection of contributing areas around stream segments is necessary to define lateral and channel flow for each stream segment. These numbers are used for the channel flow routing and subsequent turbidity estimation. During the rainfall at each time interval, only part of the catchment contributes to surface water flow. Chow et al. (1988) designates boundaries of these areas "isochrones" (meaning equal time). The time at which the entire watershed contributes to channel flow is defined as the time of concentration. This is the time it takes for flow from the farthest point on the watershed to reach the outlet. Figure

3.4 shows isochrone positions relatively to the stream channel on the watershed. This simple model can be applied for each segment of the stream by considering the end of each segment the outlet of the watershed.

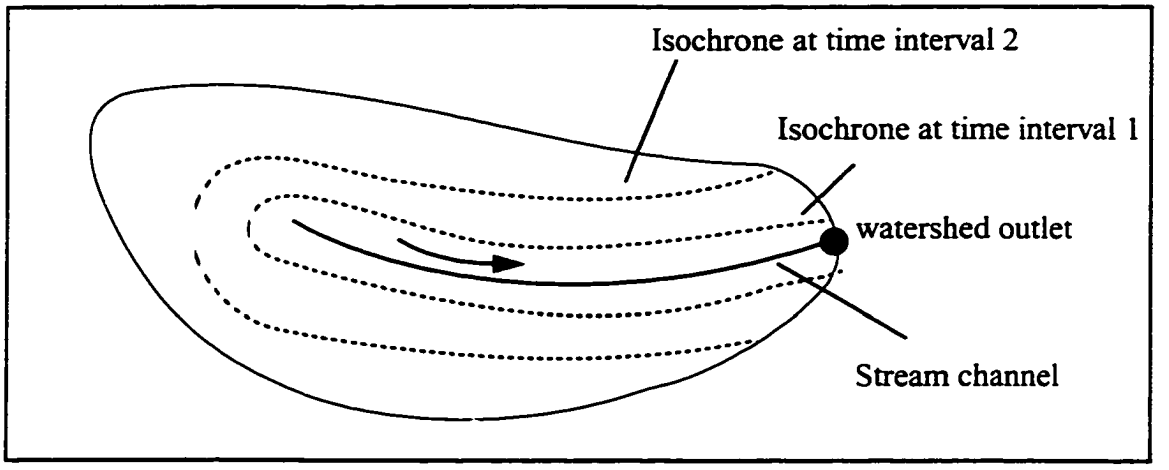

Figure 3.4 Contributing areas of the stream, bounded by isochrones.

Several soil erosion studies have indicated importance of contributed areas. In soil erosion processes described by Lal et. al. (1994), sediment transport models show that detachement by shear forces occurs mainly in areas where water is concentrated (e.g., rills) rather than over a broad areas. Therefore, they subdivided suspended sediment sources by rill erosion and overland flow. Also they indicated that despite the fact that shear stress acts uniformly around the wetted perimeter, re-entrainment of sediments will take place mainly from the base of the rill. Novotny and Chesters (1989) mention the study of Dickinson and Pall (1982) which showed that sources of stream sediments do not necessarily coincide with major soil erosion areas because of the differences in capacity of different parts of a watershed to transport sediments. The authors underline that a source

with a high soil erodibility located far from established channels may not contribute as much pollution to a stream as a less erodible source near stream. Walling (1996) mentions importance of contributing areas and sediment sources for calculating phosphorus loads. In Walling's paper he uses such terms as "minimum active contributing areas", defined as a percentage of the total catchment area, in accord with the variable source area concept of storm runoff production (Kirkby, 1978).

The selection of contributing areas for each stream segment can be accomplished through different methods used in hydrology to calculate time of concentration. There are two essential geometrical parameters within these equations: slope and distance from the outlet to the most distant point on the watershed boundary (see element 1 on Figure 3.2). Distance can be defined by using coordinates of both points. Slope can be obtained from the HRU polygon attribute table as the average of the slopes of the contributing areas for the specific time intervals (see element 4 in Fig.3.2).

After obtaining the time of concentration, it is possible to interpolate the distance for each time interval to obtain the circumference of the circle bounding contributing areas (see element 4 on Figure 3.2). For example, if the most distant point in the watershed is 800 meters from the outlet and the estimated time of concentration is 40 minutes, then for the first 10 minute interval of the storm, water will contribute to the studied segment from areas within the distance of 200 meters, for the second 10 minute interval water will contribute from areas within 400 meters and so on. This is a simple approximation that produces distances necessary for spatial selection by the GIS. Linear interpolation was tried first as a simple solution, but after several model runs it was replaced during calibration by a non-linear function of the type $Y = aX^b$, where Y = distance and X = time. This is quite simple approximation that produces distances, necessary to use by GIS

for spatial selection (see element 5 on Figure 3.2) . Using obtained distance as a radius, it is possible to select all surronding HRU's (see element 6 on Fig. 3.2) with two different options - HRU's polygons totally inside or partially inside. The choice of option depends on the modeler and can be used for model calibration. In first case, resulting areas will be much smaller than in the second case. Another option was considered when the circle can serve as a cookie-cutter. In this case, results would be much more accurate, but procedure would considerably increase time of calculation and make spatial modeling more complex and time consuming.

The next step in the GIS analysis eliminates HRU's with lower elevation values than the elevation of the HRU through which the current stream segment flows (see element 6 on Figure 3.2). This is done using the assumption that water flows only from higher elevations to lower ones (high elevation rule).

The elimination of unnecessary polygons is done with a duplicate of the original HRU runoff matrix. After this selection process, only the polygons not eliminated are kept for further analysis, and GIS iterations continue for each segment along the stream.

6. Produce output (define flow values and contributing areas for each stream segment at each time step and save visual frames for the future animation):

During each calculation of the discharge, a graphical image of the watershed and contributing areas was captured as an image file. Series of these images were combined together to produce a continuous animation.

3.1.5 Final Visualization.

The outcome of the model is a visual representation of expected turbidity levels related to specific precipitation conditions. Since modeling will be done within a GIS framework, it will be natural to utilize internal functions of the GIS and apply them to visualization. Most often, hydrological modeling visualization can be found in the forms of linear graphs, bar diagrams or scatter plots.

Hydrological visualization will consist of animation showing growth of contributing areas. Images for this animation are produced by the GIS module which calculate lateral flows. Using available animation software it is possible to combine necessary images into one animation file, usually in GIF format. Changing sequence of images allows modeler to view area which contributes lateral discharge to the stream channel at each time interval. This visualization attempted to reproduce isochrones depicted on Figure 3.4.

Since routed discharge values and turbidity values will be in a form of comma delimited ASCII tables, it is possible to link them with the stream coverage attribute table. Both tables have one common field - unique segment number for stream segments. This field serves as a primary key to join tables. After tables are "joined", it is possible to build a chart or line graph for each segment on a stream coverage, showing either hydrograph or turbidity distribution during storm event. Both steps are shown on Figure 3.5.

This procedure can be easily done within ESRI product ARCVIEW. ARCVIEW can allow to program such procedure using its own language - AVENUE. Even without programming it is relatively easy to join tables and display graph or chart using individual

fields as primary keys. Then graph can be redisplayed for each stream segment just by clicking on a segment within "View" graphical display.

Besides graphs or charts it si possible to use table values to display streams with different symbols, using turbidity or discharge values as a symbol attribute, i.e. thickness, size, etc. A series of such maps, where measured turbidity was displayed by different width, were presented during 1995 annual meeting of AGU in Baltimore (Gorokhovich and O'Hara, 1995). Maps were evaluated by most of the participants as clear and understandable.

In most cases, to visualize the distribution of certain parameters along a linear network, modelers use colors, like those used on the transit maps to show the different routes. Sometimes a line can have a label attached to it, which will be repeated over certain distances.

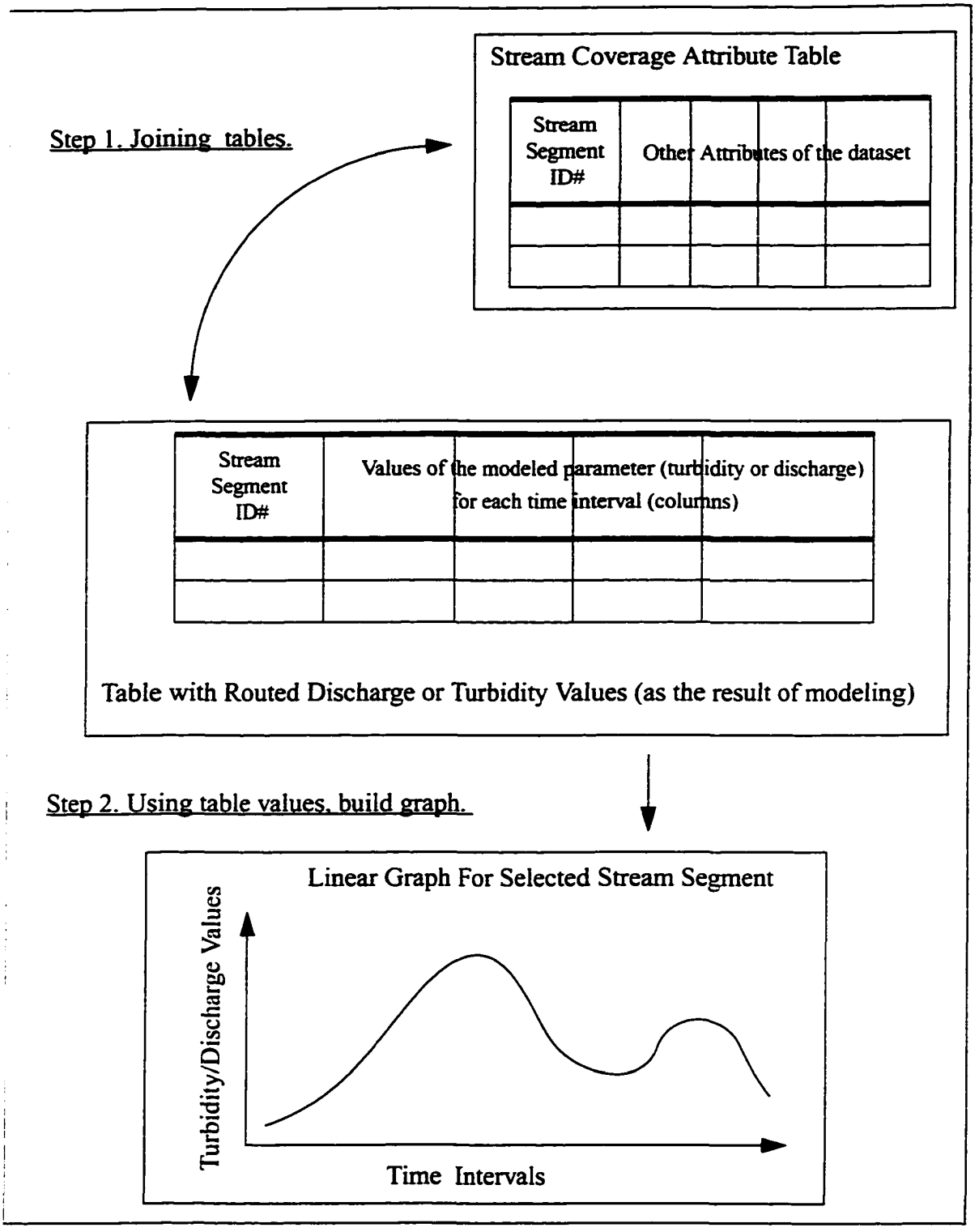

Figure 3.5 Building Final Visualization.

Other methods utilize indicators (lines or arrows) linked with pie-charts, bar diagrams or just single values. One of the techniques being used is line thickness, which can be associated with different properties, for example, road classification on modern transportation maps. Despite the fact that this technique shows only qualitative attributes of a particular feature, it can be also used to show quantity. This particular technique was used first probably by Charles Joseph Minard (1781-1870) in 1864. According to Tufte (1983), Minard gave quantity as well as direction to the data measures located on the world map in his portrayal of the 1864 exports of French wine. Line thickness showed the amount of exported wine and the direction showed to where the wine was exported. His other fascinating work utilizing the same technique was a map showing the terrible fate of Napoleon's army in Russia. This map, drawn in 1861, was a combination of data map and time series. One of the variables, the size of Napoleon's army at different times, was expressed by different band widths. The resulting graph gives an obvious understanding of this variable distribution along the mapped path.

One of the peculiar points of such visualization is that lines assume continuous distribution of the measured or modeled parameter along segments. Using McCutcheon's (1989) description of steady-state hydrological modeling, this peculiarity can be explained from the modeling point of view. He showed an example where loads at the head of the stream and at the point source were specified as constant values, and the results were reported as a constant value at the end of the stream or at any point within the stream. This provides a good justification for the use of above mentioned visualization technique from the modeling point of view. Figure 3.6 shows an example of such visualization where modeled turbidity values for each segment on a stream are shown by line symbols with

different thicknesses.

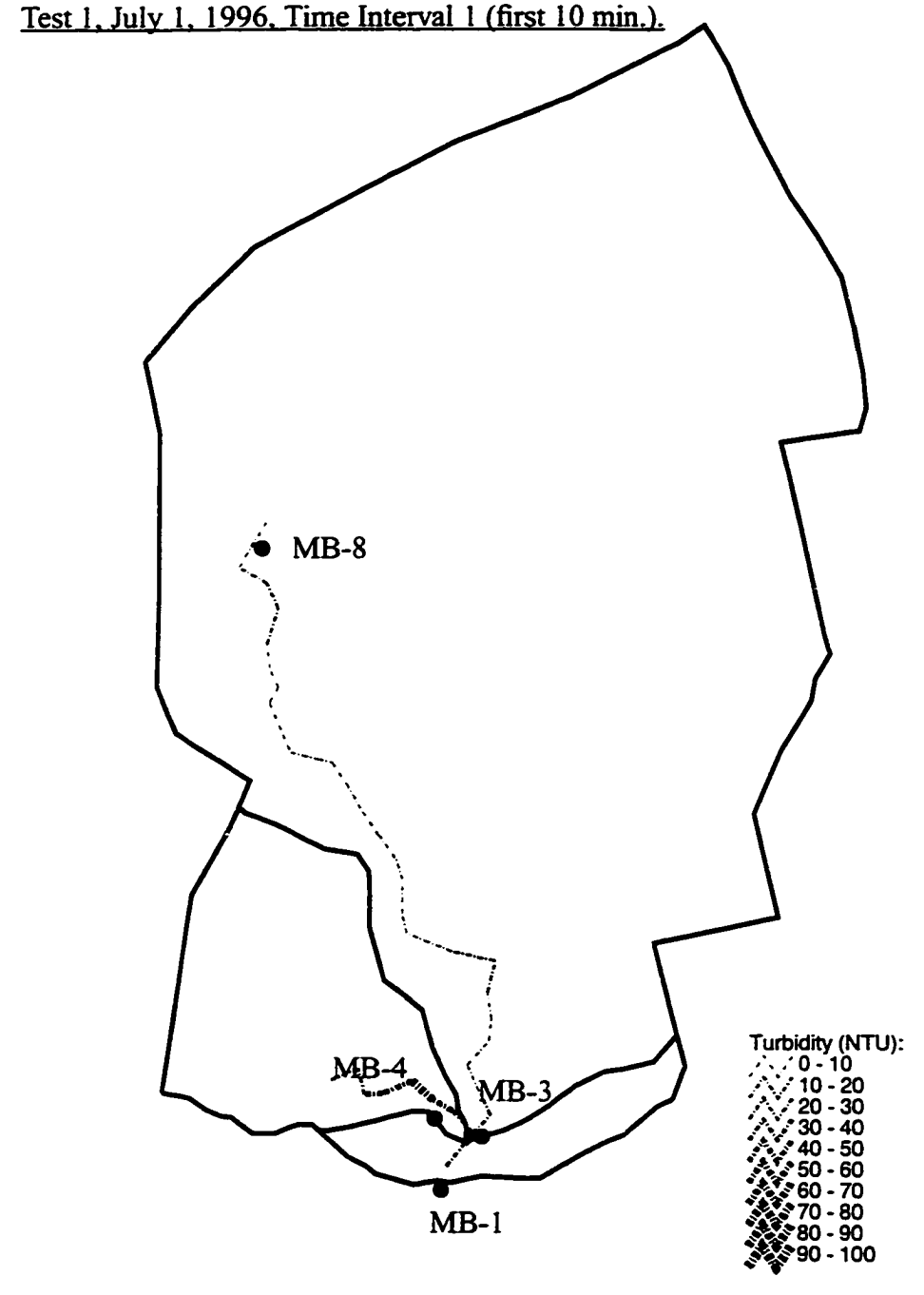

Figure 3.6 Example of the visualization of turbidity modeling results on Malcolm Brook.

3.2 Hydrological Module.

The hydrological module includes mainly calculations of the excess of rainfall. Excess of the rainfall is a volume of runoff during a rainstorm. It shows the depth of the runoff across landscape areas. Using it along with the average slope of the area, it may be possible to calculate the velocity and critical shear stress applied to the sediment particles.

The most common method utilized to calculate excess runoff is one, developed by the Soil Conservation Services (SCS) and called SCS Curve Number Procedure (SCS, 1972). In this approach infiltration losses are combined with average storage by the relationship:

$$Q = \frac{(R - Ia)^2}{(R - Ia + S)}$$

where,

Q - accumulated rainfall excess (in.)

R - rainfall (in.)

S - parameter

Ia - initial abstraction (in.) that includes storage, interception and infiltration prior to runoff, equal 0.2S.

Parameter *S* is represented by the following formula:

$$S = \frac{1000}{CN} - 10$$

where:

CN - curve number, which is a function of the ability of soils to infiltrate water, landuse and soil water conditions prior to the rainfall.

To define CN, it is necessary to know the soil group (A,B,C,D) and landuse description. Then, using SCS tables, it is possible to define CN value.

It appears that this method was developed based on 24-hr. rainfall-runoff data. It limits itself to the calculation of runoff depth and does not explicitly take into account temporal variations of rainfall intensity (Ponce, 1989). Since storms produce most of turbidity and pollution, it is important to look at the rainfall process through small time intervals and take into account variations of rainfall intensity. The most widely used method of dealing with runoff from small areas is called the rational method. This method is restricted to small catchments with areas up to 12.5 sq.km (Ponce, 1989). Its main assumptions are constant rainfall in space and time and a storm duration exceeding the time of concentration. The rational method is based on the following formula:

$$Q = 1.008\ C\ I\ A$$

where: Q = peak discharge, corresponding to a given rainfall intensity, $ft.^3/sec$;

C = runoff coefficient (a dimensionless empirical coefficient);

I = rain intensity, in/hr;

A = catchment area (acres);

Peak discharge is equal to the sum of rainfall for specific time and area.

The specific runoff coefficient is a ratio of the observed peak runoff to the

potential runoff rate. It can range from 0 to 1, but in practice ranges from 0.05 to 0.95. At C = 0.95 runoff is 95% of rainfall, as in the case of asphalt streets or parking lots. Lawns with a mild gradient might yield only 5% of the runoff, C = 0.05. Runoff coefficients depend also on the slope range (e.g., 0-2%, 2-7%, > 7%) and the character and condition of soil and vegetation. There are some tables available in the hydrology and engineering literature which can be used as a reference (Ponce, 1989; Chow, et al., 1988; Maidment, 1993). These values can be modified within reasonable ranges and used for the calibration of hydrological models.

According to the original rational method, rainfall intensity is estimated from storm duration and total rainfall. Storm duration has to equal the time of concentration to define a concentrated catchment. In this study, rainfall intensities were calculated from rainfall data as amount of rainfall per time interval. This was done because the size of areas for which calculations have to be done is relatively small, ranging from 350 to 1950 m^2. This is the size of single components of the HRU matrix as a result of the spatial overlay of landuse, soil, and slope polygons. Combined together, these polygons form an irregular grid of small HRU planes. At this point it is assumed that such small areas will be covered uniformely by the rainfall. This is a requirement of the concentrated catchment which is a essential assumption of the rational method. The catchement area is determined from GIS data.

After runoff coefficients are selected it is possible to create HRU matrix for specific storms. If coefficients has to be changed, then matrix should be changed also according with new values of coefficients.

3.2. I. Time of concentration and runoff volume calculations.

The time at which maximum discharge for the hydrograph occurs, i.e., the entire watershed area contributes to flow, is referred to as the time of concentration. There are several formulae available to calculate the time of concentration as a function of some watershed characteristics. Most of them are empirical and have several basic parameters: slope, distance from the studied point to the fartherst point on the watershed, rainfall and roughness. There are several basic formulae available, including Kirpich's (Kirpich, 1940), Hathaway's (Hathaway, 1945) and FAA (Federal Aviation Agency, 1970) formulae.

Kirpich Formula:

$$t_c = \frac{0.06628\ L^{0.77}}{S^{0.385}}$$

Hathaway Formula:

$$t_c = \frac{0.606(Ln)^{0.467}}{S^{0.234}}$$

FAA Formula:

$$t_c = \frac{1.8\ (1.1 - C)\ L^{0.5}}{S^{0.66}}$$

where:

t_c = time of concentration (hr.)
L = length of the principal watercourse (m)
S = slope between maximum and minimum elevations (m/m)
n = roughness factor (dimensionless)
C = rational method coefficient (dimensionless)

The FAA formula was selected because its development and testing included

evaluation of the C coefficient which is an essential part of the rational method. In the case of drainage areas with several different C values, the C coefficient is calculated as a weighted average in accordance with the respective areas.

Calculations of runoff have to take into account the fact that contributing areas increase until the whole watershed area reaches saturation. This means that during each time step for each segment on the stream there is both channel flow from upstream and from contributing areas that yields a certain amount of runoff in the form of lateral flow. During the first time step, the amount of runoff, delivered to the stream channel is equal to lateral flow, the total runoff value for the given contributing area. In the next time steps, the contributing area becomes larger and delivers runoff developed during the previous time step. Therefore, this runoff is taken into account as well. Figure 3.7 shows the calculation for this process.

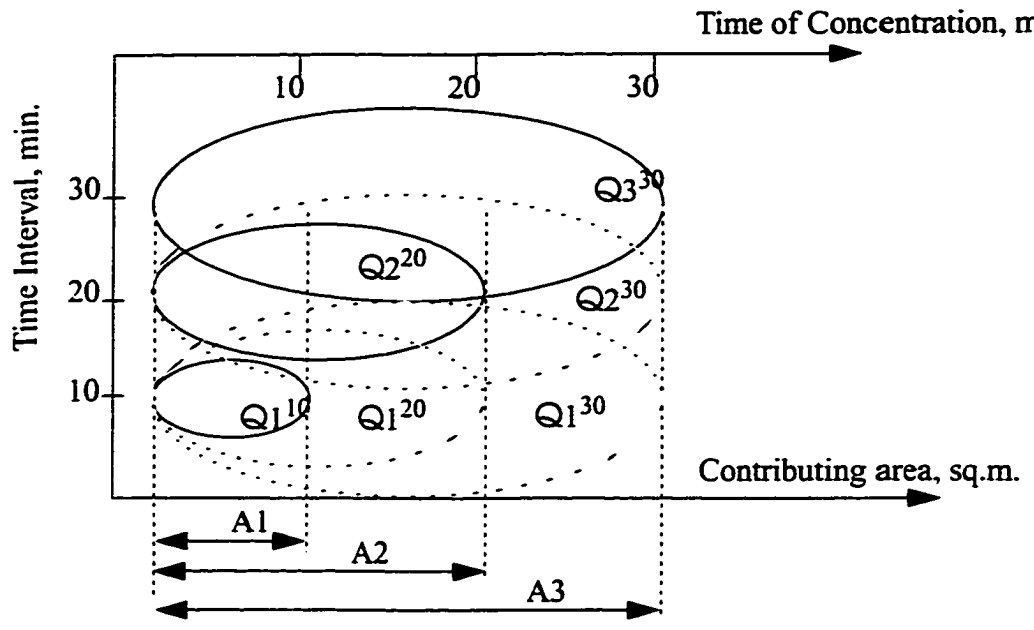

$$Q1^{10} = Q1^{10}$$

$$Q2^{20} = \frac{(Q2^{20} * A2) + [(Q1^{20} - Q1^{10}) * (A2 - A1)]}{A2 + (A2 - A1)}$$

$$Q3^{30} = \frac{(Q3^{30} * A3) + [(Q2^{30} - Q2^{20}) * (A3 - A2)] + [(Q1^{30} - Q1^{20}) * (A3 - A2)]}{A3 + [(A3 - A2)] * 2}$$

where:

$Q1^{10}$ - discharge for the first time interval (10 min), first contributing area;

$Q2^{20}$ - discharge for the second time interval (20 min), second contributing area;

$Q3^{30}$ - discharge for the third time interval (30 min), third contributing area;

A1, A2, A3 - contributing areas at time 1,2,3;

Figure 3.7 Calculations of runoff (Q, L/sec) during modeling.

The general form for the previously described routine of calculating lateral flow is:

$$Q_n^t = \frac{(Q_n^t * A_n) + \sum_{i=1}^{n-1} [(Q_i^t - Q_i^{(t-1)}) * (A_n - A_{(n-1)})]}{A_n + \sum_{i=1}^{n-1} [(A_n - A_{(n-1)})]}$$

where:

Qn^t = discharge for the time interval t (min), for the given contributing area n

A_n = contributing area for the current time interval (m^2)

After the GIS module captures an image of contributing areas, it also stores all discharge values in a table. Following is an example of such a table (Table 3.1):

Table 3.1: Output file with discharge values after GIS simulation.

Segment # (assigned by GIS)	Length (m)	Slope	Discharge at time step 1 (L/sec)	Discharge at time step 2 (L/sec)	Discharge at time step 3 (L/sec)
238	10	0.02	0.05	0.08	0.17
345	12	0.03	0.06	0.07	0.11
355	8	0.03	0.04	0.07	0.10
360	20	0.05	0.02	0.10	0.20
410	18	0.04	0.02	0.06	0.12
415	11	0.02	0.05	0.08	0.10
427	10	0.01	0.03	0.06	0.11
500	22	0.02	0.08	0.11	0.21

Discharge data are used as input for the Kinematic Wave Routing method to route flow from upstream to downstream and estimate the hydrograph for each segment on the

stream. Code was written in C language to speed up calculations since the programming language of GIS (ARC/INFO macro language) is slow. An algorithm for the code was taken from "Applied Hydrology" (Chow, Maidment and Mays, 1988).

The following equation is a numerical solution of a kinematic wave through a linear scheme:

$$Q_{i+1}^{j+1} = \frac{\left[\frac{dt}{dx} Q_i^{j+1} + \alpha\beta Q_{i+1}^{j} \left(\frac{Q_{i+1}^{j} + Q_i^{j+1}}{2} \right)^{\beta-1} + dt \left(\frac{q_{i+1}^{j+1} + q_{i+1}^{j}}{2} \right) \right]}{\left[\frac{dt}{dx} + \alpha\beta \left(\frac{Q_{i+1}^{j} + Q_i^{j+1}}{2} \right)^{\beta-1} \right]}$$

where: Q_{i+1}^{j+1} = routed flow, L/sec;

q_{i+1}^{j+1} = lateral flow,Ll/sec;

α, β = hydrological coefficients;

i = time interval;

j = distance interval;

The notation j refers to time and i refers to distance. Two parameters, α and β, are exponents in hydrological momentum equations, relating flow to area, velocity, depth and width. Leopold and Maddock (1953) showed how are these power equations are related to flow:

$$U = aQ^b$$
$$H = \alpha Q^\beta$$
$$B = cQ^f$$

where: U = velocity (m/sec)

H = mean depth (m)

B = mean width (m)

The coefficient β in the Kinematic Wave equation is derived from an area-flow correlation. A detailed explanation can be found in (Chow et al., 1988). Manning's equation was used with a hydraulic radius expressed through area and wetted perimeter. In this case, $\beta = 0.6$ and $\alpha = [nP^{2/3} / S^{0.5}]^{0.6}$, where n = Manning's coefficient and S = slope. To calculate α from this equation it is necessary to obtain a value for P (wetted perimeter). For shallow streams wetted perimeter can be approximated by width, therefore we used the width-flow correlation with coefficients f = 0.05 and c = 0.80. With these values, the simulated width was in agreement with the measured width.

The Kinematic Wave equation also has a necessary (but insufficient) condition for stability. It is called the Courant condition (Courant and Friedrichs, 1948). This condition is:

$$dt \leq \frac{dx}{C_k}$$

where C_k = kinematic wave celerity

Another parameter used in the Kinematic Wave equation was Manning's roughness coefficient. This parameter can range from 0.030 to 0.070 for mountain streams or wooded streams. In this study a value of 0.060 was selected.

The routing process starts with the first row of Table 3.1. The first segment on a stream ususally receives more flow than other segments because its contributing area is larger. Flow within segments is considered channel flow. The next segment (second row, Table 3.1), receives lateral flow from its contributing areas combined with channel flow from the first segment. The lateral flow value is obtained from the table, while channel flow is calculated during each iteration using the flow value from the upstream segment. The same scheme applies to all segments in the stream. After the routing procedure, all flow values are written into a file. The first column in the file is a unique number for each segment and other columns have discharge values for each time interval. Therefore, this file can be linked with the HRU matrix and GIS data. In practice, it is possible to display the hydrograph for each stream segment by selecting it on the GIS graphic interface.

3.3 Sediment Concentration Per Unit Volume of Suspension

3.3.1 Importance of Turbidity/Suspended Solids Relationship.

The basic assumption for the proposed methodology is that turbidity has a strong correlation with suspended solids. Since there are no exisiting models for turbidity modeling, the most reasonable approach would be to use available sediment transport models that can be substituted or used for turbidity modeling. In this case, it is necessary to find an appropriate parameter within existing sediment transport models that could be linked with turbidity. After revisiting the literature and available data on turbidity and associated parameters, suspended solids (usually represented by the fine sediment particles or so-called washload) were chosen as the most suitable for the purpose of turbidity modeling. There are several factors which should be considered before describing methodology for the modeling of turbidity:

1. Since turbidity is an expression of the optical property that causes light to be scattered and absorbed, the optical property can be affected by anything that is immersed within the water column. Generally, the matter immersed in the water column is represented by the fine sediment particles or the floating organic matter. In streams, where the water body constantly moving, organic matter does not accumulate, but can be observed in quiet reaches of the stream. Fine sediment particles constitute the majority of the immersed matter that is reflected in a residue from the total suspended solids analysis. Therefore, suspended particulates can be considered to be an important factor that influences the optical property of water, and this can be recorded by turbidity measurements.

2. The best indicator of physical linkage between total suspended solids and turbidity should be a statistical correlation between these two parameters. A literature review and analysis of the New York City watershed data strongly supports this correlation.

3. Numerous existing models, which describe sediment transport in streams, can be used as prototypes for the modeling of turbidity.

The most important statistical factor in the study is a correlation between turbidity and suspended particulates. With this purpose, 562 samples from the Catskill/Delaware region of the New York City watershed for the period of 1989-1995 were analysed. Statistical analysis revealed a high correlation ($r = 0.94$, $r^2 = 0.88$) between suspended solids (SS) and nephelometer turbidity units (NTU). Table 3.2 contains the information about regression analysis and Figures 3.8 and 3.9 show graphical representation of the correlation between the two parameters.

Since the work on model development was planned to be done on a small watershed, 444 samples from the Malcolm Brook watershed for the period 1993 - 1995 were statistically analyzed and the same high correlation was found between SS and NTU's. Malcolm Brook watershed is located within the Croton District of the New York City watershed area and it has a completely different geological composition than the Catskill/Delaware region. Nevertheless, statistical analysis supported the idea of a strong correlation between SS and NTU's ($r=0.75$, $r^2 = 0.56$). Table 3.3 contains the results of this analysis.

Table 3.2 Statistical Analysis of the Catskill/Delaware District Data.

Coefficient of correlation (r)	0.75
r^2	0.563
Significance F	1.36e-14
P-value	1.36e-14
Intercept coefficient	0.58
x1 coefficient	0.63
Resulting linear formulas	NTU = 0.63SS + 5.8

Table 3.3 Statistical Analysis of the Malcolm Brook Watershed Data.

Coefficient of correlation (r)	0.93
r^2	0.86
Significance F	4.3e-194
P-value	4.1e-09
Intercept coefficient	9.93
x1 coefficient	0.56
Resulting linear formulas	NTU = 0.6SS + 9.9

Some results were available from other geographical regions, such as Alaska (Mack 1988), Texas (Collins and Dickey, 1989), Australia (Gippel, 1989), and England (Walling and Webb, 1988). The report published by Stephen Mack (Mack, 1988),

contains detailed description of statistical analysis between suspended solids and turbidity in Alaska. His database contained 1,100 observations from approximately 140 sites in seven different basins. By the end of the analysis, he came to conclusion that "a strong, if not perfect, relationship exists between total suspended solids and turbidity. Excess amount of sediment which cause ecological and aesthetic damage can be accurately monitored or estimated by either parameter, and this report has demonstrated a way to estimate sediment loads with a minimum amount of total suspended solids analysis". However, he warned "... analyses indicated that regression equations should be used with care if developed for more than site, if used on sites that did not contribute data to the model development."

Statistical analysis represented in Tables 3.2 and 3.3 is supported by the study of Collins and Dickey (1989), which included a linear regression analysis between SS and NTU for the Lake Ray Hubbard reservoir basin in Texas, near Dallas. This analysis produced the following relationship:

$$Y = 0.86X - 2.2, \text{ where } Y = SS \text{ (mg/l) and } X = \text{turbidity, NTU}$$

The linear correlation coefficient in the study was 0.97 which indicated an excellent linear relationship between SS and turbidity. Using this relationship, the authors were able to convert the continuous field turbidity measurements into a continuous graph of SS concentration versus time for each storm event monitored.

In Australia, while studying Latrobe River Basin, Grayson (1994) found linear correlations between turbidity and total suspended soilids. In his study turbidity was

measured in Formazin Attenuation Units (FAU) which differs from nephelometric turbidity units (NTU) by the direction of the light sensor in relation to the measured substance. Despite this fact, he obtained perfect (r^2 = 0.86 - 0.91) correlations expressed by the following examples of described relationship:

$Y = 0.92X - 0.76$, $Y = 0.976X + 32.6$,

where Y = SS (mg/l) and X = turbidity, FAU

In another publication, probably using the same data from Latrobe River (Australia), (Gippel, 1995), the author gave the following example of the linear model relationship derived from 108 cases with $r^2 = 0.88$:

$Y = 0.85X - 1.97$, where X = SS (mg/l) and Y = turbidity, FAU

He also mentioned that Walling (1977) found such a close relationship between turbidity and suspended solids concentration that he used continuous turbidity records to define the 'true' sediment load.

Described statistics and their results allow the construction of the proposed methodology composed of two main components - hydrological/soil part and GIS part. The hydrological part will consist of equations, predicting possible sediment concentrations within the water flow during storm events. Through established correlation between sediment concentration and NTU which also serve as a calibration device for the future model, it will be possible to predict turbidity during storm events. The GIS part will

serve as a framework for the modeling and the base from which to study spatial distribution of the turbidity along stream network.

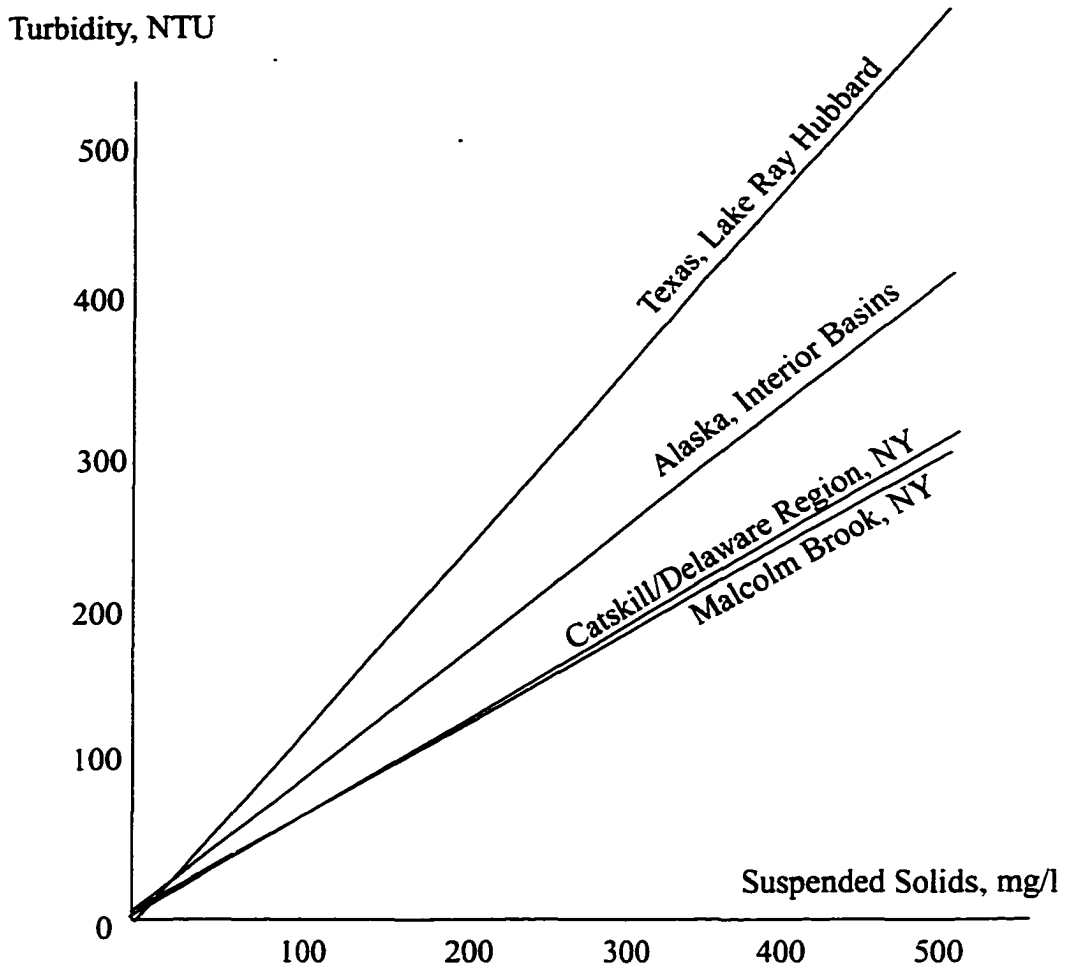

Figure 3.8 Relationship between turbidity and suspended solids, using data from different geographical areas.

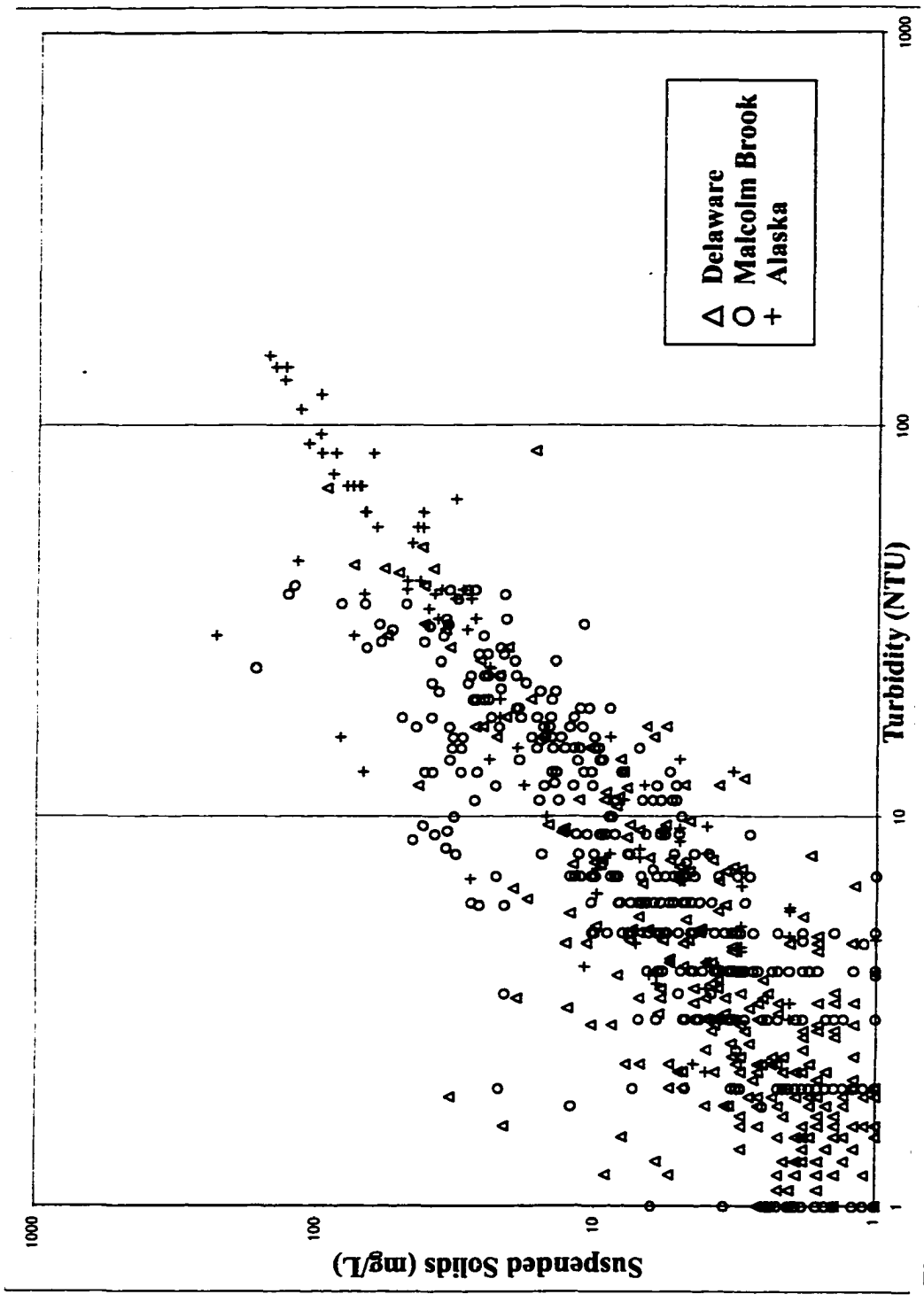

Figure 3.9 Relationship between turbidity and suspended solids, based on data from Malcolm Brook, Delaware and Alaska.

3.3.2 Calculations of the suspended sediment concentration.

Turbidity in streams is a result of either organic or inorganic material suspension. To be suspended, material has to be moved from its resting place. The original movement of particles is a result of the dynamic impact of water, wind or any other mass movement. Each type of impact has its own mathematical description, based on the physical nature of the driving forces. The driving force in case of stream channel is a water flow. The flow can be described in terms of velocity. High water velocity allows particles to move along the stream channel. Low velocity results in particle deposition. Sediment yield or discharge of suspended material is a product of the water velocity, density of particles and the cross sectional area through which the flow passes. Turbidity can then be derived from the amount of suspended particles per water volume. Lal (1994) indicated that a description of soil processes involves description of the hydrology of surface flow and a description of the various erosion processes that add to sediment concentration, C.

The basic hydrological model used to describe velocity employs the Chezy or Manning equation (Dunne and Leopold, 1978). The result is a water velocity, which is a function of slope (S), hydraulic radius (r) and the condition of the surface along which water flows (n).

$$V = \frac{r^{2/3} S^{1/2}}{n}$$

where,
V = velocity of flow (m/s); r = hydraulic radius (m); S = energy gradient ($\sin\alpha$); n = Manning coefficient of resistance.

Discharge can be defined as a product of velocity and cross-sectional area through which water flows:

$$Q = V * A,$$

where A = cross-sectional area (sq.m)

Using velocity, it is possible to make a link toward suspended solids concentration through the unit stream power.

Unit stream power was defined through the Yang's equation, utilizing velocities and slope gradients (Yang 1972):

$$P = \frac{dY}{dt} = \frac{dx}{dt}\frac{dY}{dx} = V * S$$

where,

P = stream unit power (m/s); Y = elevation above datum (m); x = longitudinal distance (m); t = time (s); V = velocity of flow in the x direction (m/s); S = energy gradient ($\sin\alpha$);

Suggesting the use of the stream unit power for the study of the total sediment concentration, Yang understood the whole complexity of the processes that are involved with sediment transportation and concluded that it is extremely difficult to associate a fraction of unit stream power with a particular mode of transport. Therefore, he considered the problem of sediment transport as a whole regardless of the difference between bed load and suspended load. This postulate was built on the consideration that at equilibrium condition, the total sediment concentration is always at its maximum, and that a definite

amount of effective unit stream power is used in transporting this maximum or equilibrium total sediment concentration for a given sediment and fluid character.

In his first study of stream morphology, Yang (1972) concluded that the unit stream power, defined as the time rate of potential energy expenditure per unit weight of water in an alluvial channel, is the dominant factor in determining total sediment concentration or vice versa. He expressed the relationship between unit stream power and total sediment concentration as:

$$\log Cstr = a + b \log(P - VcrS)$$

where,

Cstr = total sediment concentration; P = stream unit power
VcrS = critical unit stream power required at the incipient motion;
P - VcrS = effective unit stream power; a, b = parameters.

Yang addressed some problems with this equation (Yang 1973) by stating :

1. VcrS parameter is not related to sediment and flow characteristics.
2. Equation is not dimensionally homogeneous.

The main improvement of the unit stream power application toward the calculation of the total sediment concentration was the inclusion into equation of shear velocity, U and hydraulic properties of sediments, w, which is a terminal fall velocity for the specific particles with a median sieve diameter = d. The following final equation was used to define the total sediment concentration:

$$\log Cstr = 5.435 - 0.286 \log \frac{wd}{v} - 0.457 \log \frac{U}{w} +$$

$$\left(1.799 - 0.409 \log \frac{wd}{v} - 0.314 \log \frac{U}{w} \right) \log \left(\frac{VS}{w} - \frac{VcrS}{w} \right)$$

where:
Cstr = total sediment concentration (mg/l);
w = terminal fall velocity;
d = median sieve diameter (cm);
v = kinematic viscosity;;
U = shear velocity;
Vcr = critical average water velocity at incipient motion;
S = slope;
V = average water velocity;

Yang (1973) also mentioned that the high correlations between the total sediment concentration and effective unit stream power can exist only if the condition that sediment particles are always transported at the maximum or equilibrium condition for the given effective unit stream power and constraints is satisfied. Considering the total sediment concentration and water discharge as independent variables of a natural stream, then the natural stream will adjust its unit stream power through the process of scour and deposition so that the (VS - VcrS)/C ratio can reach a minimum value which is determined by the constraints applied to the stream.

In the formula, the incipient motion is introduced by the factor Vcr/w, which can be defined from the following equations:

$$\frac{Vcr}{w} = \frac{2.5}{\log\left(\frac{U\,d}{\nu}\right) - 0.06} + 0.66, \quad \text{if} \quad 0 < \frac{U\,d}{\nu} < 70$$

$$\frac{Vcr}{w} = 2.05, \quad \text{if} \quad 70 < \frac{U\,d}{\nu}$$

These equations were derived by Yang from concepts generally accepted in fluid mechanics and boundary layer theory. The coefficients in these equations were determined from reliable data independently collected by eight different investigators and, according to Yang (1973), they should provide engineers with a useful criterion for incipient motion.

One of the main components in this study is a size of the material analyzed. Yang's minimum size was 0.062 mm, which correspond to the sedimentary term 'very fine sand' or 'coarse silt'. This size is usually attributed to a part of the sediment that cannot be seen individually on the streambed surface and called washload by Maidment (1992). As Maidment indicated, washload cannot be directly related either to the flow condition at the stream reach or to the sediment composition of the streambed. This definition exactly describes the physical state of the matter that causes turbidity and gets measured as the 'total suspended solids' in the field of environmental hydrology.

To describe the size of suspended sediments quantitatively, it is necessary to find a physical criterium. Einstein (1950) suggested to use the d_{10} size, which is a size of 10% of the sample from the material size distribution. Chien and Wan (1983) propose d_5 for the same criteria. Assuming that turbidity for the most part is caused by the washload with an

average size of particles = 0.062 mm, this number can be taken as maximum value for the modeling purposes.

After estimating the total amount of suspended sediments, it is possible to use the statistical correlation between turbidity and suspended solids that was described previously. The estimation should be used with a certain caution under the following assumptions:

1. The source of suspended solids is predominantly re-deposited sedimentary material .

2. The turbidity pattern on a hydrograph or pollutograph coincides with a 'first flash', i.e. first peak of rainfall intensity.

3.3.3 Elements of the Suspended Sediment Model.

Constants:

1. Kinematic viscosity, v, depends on temperature and was defined as 0.0000013 m^2/s for the water temperature T = 10°C and water density p = 1,000;

2. Particle size was expressed by d (median diameter) and was defined as 0.000031 m, which corresponds to the medium-coarse silt boundary.

3. Fall velocity, w, was defined as 0.00067 m/s for the water temperature T = 10°C and water density p = 1,000 for medium-coarse silt particle size;

4. Sediment density, p_s, was defined as 2650 kg/m^3;

5. Manning coefficient, n, was defined as 0.045 which corresponds to the conditions of the mountainous forested water courses.

Variables:

1. Reynolds Number (Re).

This number in relation to the sediment transportation describes the ratio of kinetic to viscous forces applied on a moving particle. In general it describes the relationship between shear velocity, particle diameter and kinematic viscosity of the surrounding substance.

$$Re = U^* d / \nu;$$

The Reynolds Number combined with Shields parameter can serve as an indicator of the threshold of motion for granular material (Julien, 1995). Fig. 3.10 shows this relationship. Shields parameter is a dimensionless shear stress defined from the ratio of hydrodynamic forces to the submerged weight.

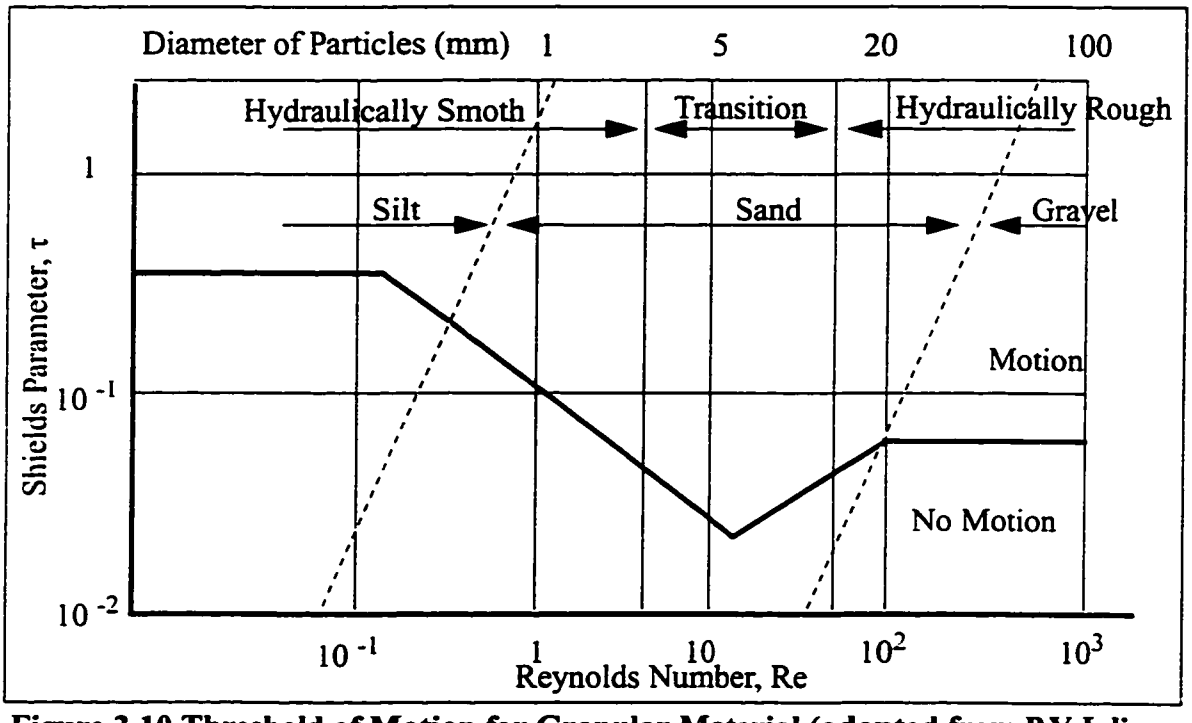

Figure 3.10 Threshold of Motion for Granular Material (adapted from P.Y.Julien, 1995).

2. Shear Velocity (U)

Shear velocity is a function of the boundary shear stress and fluid density. It is widely used in most hydrological applications and often refers to friction. Physically, this parameter represents a measure of the intensity of turbulent fluctuations. It is expressed in the formula:

$$U = \sqrt{\tau/\rho}$$

where :
τ - is the boundary stress
ρ - is the fluid density

In this formula boundary stress τ is a measure of a 'tractive' force per unit surface and also reffered to as shear stress and drag force (Graf, 1984). It is expressed in the general equation:

$$\tau = \gamma\, r\, S$$

where:
y - is a specific weight of fluid;
r - hydraulic radius;
S - slope;

Specific weight is a gravitational force per unit volume of fluid and equals the product of mass density p times the gravitational acceleration g (constant equals 9.81 m/ s^2). It is expressed by the formula:

$$y = pg$$

At 10°C water has a specific weight 9,810 N/m^3. It varies slightly with temperature and therefore can be used as a constant.

After substituting t and y equations into basic shear velocity equation, we will obtain the following equation:

$$U = \sqrt{g\,r\,S}$$

3. Hydraulic Radius (r).

Hydraulic radius is defined by the ratio of the net area (A) of the cross section in which flow takes place to the wetted perimeter (P). Wetted perimeter is a function of the channel geometry and depends on the channel shape.

For a trapezoidal shaped channel (Figure 3.3.4.2), the following equations are applied:

$$A = (b + ky)y; \qquad P = b + 2y\sqrt{1 + k^2}\ ; \qquad r = A / P;$$

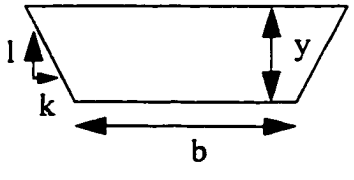

Figure 3.11 Trapezoidal Channel and its Geometrical Parameters for Hydraulic Radius Calculations.

For a triangular shaped channel (Figure 3.12), the equations are:

$$A = ky^2 \; ; \qquad P = 2y\sqrt{1 + k^2} \; ; \qquad r = A / P;$$

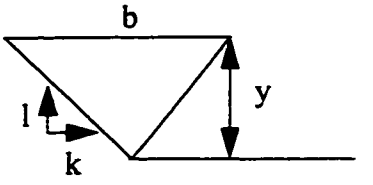

Figure 3.12 Triangular Channel and its Geometrical Parameters For Hydraulic Radius Calculations.

Because channel geometry in wooded streams is difficult to define it is useful to use one of the equations proposed by Leopold and Maddock (1953), linking mean depth with the flow. In hydrology for many practical calculations hydraulic radius is being replaced by so-called active depth which is practically average depth. Following equation has two parameters - α and β.

$$H = \alpha Q^{\beta}$$

where: H = mean depth;

These parameters can be adjusted during modeling for calibration purposes. The β value has to be within the range of 0.1 to 0.6 according to Chapra (1996). He derived this range from different literature sources on modeling. The α value can be adjusted to practically any number.

3.3.4 Sediment Routing.

The standard routing procedure (Foster and Meyer, 1972) is used to balance the amount of available eroded soil which is calculated through Yang's equation against channel flow transport capacity. Channel flow transport capacity is the maximum amount of suspended sediments which can transported in the channel. Sediments, while moving along the channel can be either deposited or transported. Yang's technique provide only potential suspended sediment concentration value depending on flow and slope steepness. If this value exceeds channel flow transport capacity then sediments will be deposited. If it will be less, than sediments will be transported. Transport capacity can be calculated from Yalin's (1963) equation:

$$T_r = 0.635\ (p_s - p_w)\ m\ (ghB)^{1/2}\ g\ (\sigma - 1 / \alpha\ \log(1 + \alpha\ \sigma))$$

where: T_r = channel flow transport capacity (weight of sediment/unit of flow width).

p_s = mass density of the soil (weight/volume),

p_w = mass density of the fluid (weight/volume),

m = soil particle diameter (length),

g = gravity acceleration (length/time^2),

h = hydraulic radius of the rill (length),

B = rill slope steepness,

$$\alpha = 2.45\ (p_w / p_s)^{0.40}\ (T)^{0.50} \quad \text{(dimensionless)}$$

$$T = \frac{p_w\ hB}{(p_s - p_w)\ m} = \frac{hB}{(p_s / p_w - 1)\ m} \quad \text{(dimensionless actual lift force)}$$

T_{cr} = critical lift force from Shields's diagram (Shields, 1936).

$$\sigma = \frac{T - T_{cr}}{T_{cr}} \quad (\sigma = 0, \text{ when } T < T_{cr}).$$

Inside the model's code, this equation compares channel flow transport capacity with the value obtained from Yang's equation. If it is greater than Yang's value, then we assume transport condition and accept Yang's value as suspended sediment concentration. If it is less than Yang's value, then we assume deposition and accept channel flow transport capacity value.

After suspended sediment concentration is defined it is possible to convert it to turbidity units, using developed empirical relationship described previously.

3.3.5 Model Flow-Chart Diagram.

Figure 3.13 shows the main components of the final model.

Input for the model consist of GIS layers, which are stored in ARCINFO format. Two files - rainfall data and runoff coefficient are stored as an ASCII text files and supplied to the model at the beginning.

The GIS module uses only ARCINFO data format. Using values from all supplied data sources, HRU matrix for the model is being formed. This matrix exists as a GIS layer, which is also in ARCINFO format. For each model run with different rainfall and runoff coefficient data, the matrix should be re-calculated without GIS spatial transformations. If any of GIS data layers were changed, then the martrix has to be re-recreated using GIS first. Upon working through the matrix and creating isochrone boundaries for each segment on a stream, the GIS module also stores images during each iteration. This images can be stored as SUN rasterfile format or postscript and then converted into any of more suitable formats for visualization, such as GIS or JPEG for animation purposes. Another output of GIS module is an ASCII file containing all necessary information for the further flow routing for each time step.

The hydrological module consists of the C code, which reads an ASCII file produced by GIS module. After collecting all necessary information from that file, such as length of the stream segment, slope, flow, routing technique is applied for all values, starting from the first segment and first time step. The hydrological module creates an output ASCII file with all discharges produced by routing routine. These values can be used for verification or even as an end result if only flow has to be modeled. The same

table exist virtually in a buffer and get accessed by the suspended sediment module.

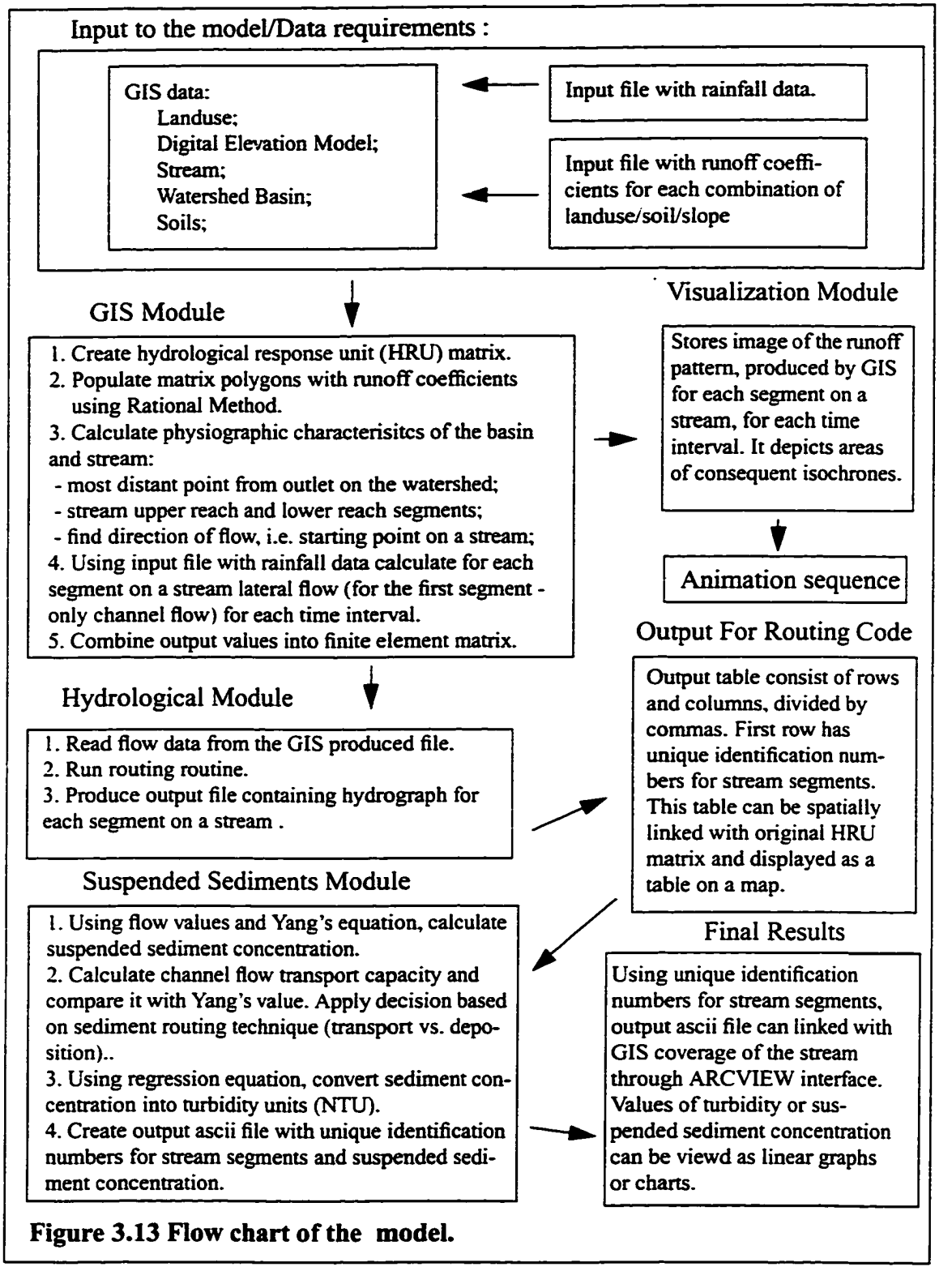

Figure 3.13 Flow chart of the model.

Suspended sediment module applies Yang's equation and sediment routing routine to all flow values. It is written in C and embedded into the hydrological module code. For each discharge value the module identifies potential suspended sediment concentration and through regression equation converts it to nephelometer turbidity units (NTU).

Final result of the model are two tables, which can be used together or separately - flow table from the hydrological module, containing routed discharge values for each segment on the stream during the modeled rainfall, and turbidity table which has turbidity values for each segment on the stream during the modeled rainfall. These tables can be easily joined with original GIS stream coverage or HRU matrix using unique identification number for stream segments as a common field. Upon joining tables, data from them can be visualized through many options, offered by ARCVIEW interface, which include line graphs, bar diagrams, etc.

While GIS can serve as an excellent tool for spatial analysis, its programming capabilities are limited. For example, in many GIS packages there are no decimal logarithms and exponential functions which are essential to many models. Because GIS was never considered to be a programming language, there are also problems associated with the speed of calculations. Therefore, the optimal solution is to use GIS capabilities for spatial manipulations and a programming language, such as C, for time consuming and data abundant calculations.

3.6 Model's Temporal Characteristic.

The proposed model does not explicitly cover typical hydrological model temporal scale which is usually cover the beginning and end of the hydrograph. During this period of time, water flow increases to its maximum value and then returns to original flow level. The scope of conducted modeling is turbidity, which behaves quite differently then water flow. While peak discharge can be distributed over long time periods, depending on land cover and infiltration coefficients, turbidity, like suspended sediments has sharp peaks during short periods of time. D.E.Walling (1996) provided examples of concentration-duration and load-duration curves, developed for the River Creedy, Devon, UK. These curves were based on a detailed 7.75 year record assembled using continuous turbidity recording equipment. They emphasize that most of the total sediment load is transported during a short period of time. In that case the majority of the load was transported during only 5% of the time when sediment concentration exceeded concentration 100 mg/l. Therefore it is possible to make an assumption that most rivers will behave similarly. During analysis of data collecetd during 1996-1997, it was found that Malcolm Brook reveals similar pattern. This affect was noticed by NYCDEP hydrologists in many other watersheds, including those of Delaware region and Catskill Mountains. Associated pollution peaks acquired term "first flush", which refers to the first outbreak of pollutant triggered by the rain storm.

Another phenomenon associated with turbidity behaviour is the fact that after rain stopped turbidity level would decrease considerably while flow could be rising at the same time. Figures 3.14 and 3.15 show two examples of turbidity-flow interrelation for the

Malcolm Brook watershed.

Since model goal is to predict possible turbidity rates during storm events, model's duration will cover only the period of beginning and the end of rain storm. This would provide modeler with an idea about flow and turbidity behavior during particular rain storm, but not afterwards.

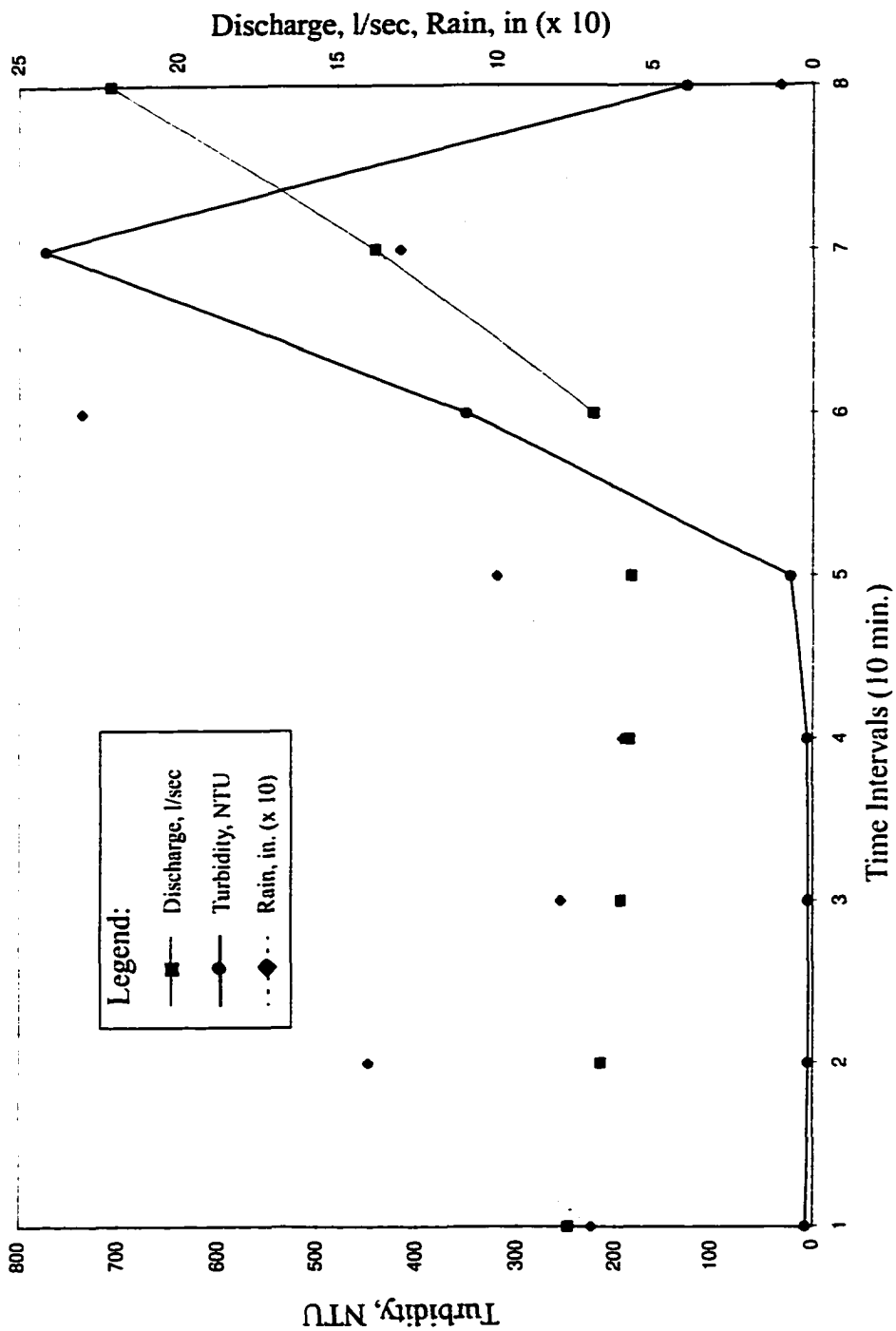

Figure 3.14 Turbidity-Flow Interrelation For The Malcolm Brook Watershed, July 1, 1996.

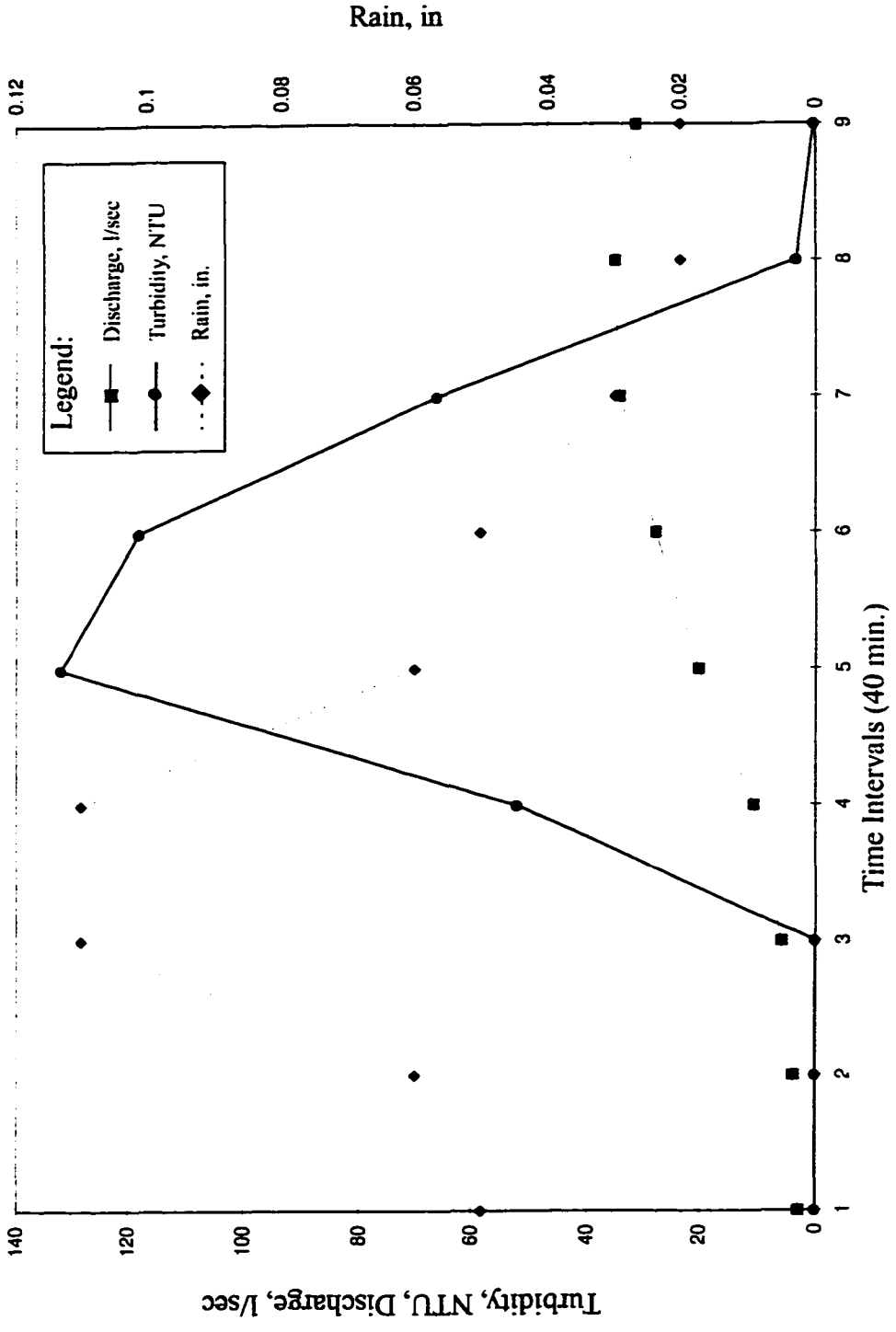

Figure 3.15 Turbidity-Flow Interrelation For The Malcolm Brook Watershed, June 30, 1996.

4. Turbidity Model Application.

4.1 Site Description.

The study site, Malcolm Brook, is a sub-basin located on the western side of the Kensico Reservoir which is part of the Catskill/Delaware watershed system (Figure 4.1.1). Kensico Reservoir delivers drinking water to New York City and is the terminal reservoir for water coming through aqueducts from the Catskill and Delaware systems. Because of this, water quality is extremely important and it is measured daily at numerous hydrological and limnological sampling locations.

The total area of the Malcolm Brook sub-basin equal 0.36 sq.km. Figure 4.2 shows Malcolm Brook's stream network and monitoring sites used in this study. Dashed lines show stream channels that pass through the wetland area. These channels are not seen well in aerial photography, but they were traced during the winter season when the wetlands were frozen and the bush was not dense. Open channels are visible on USGS 24K quadrangles and also they were mapped using the Global Positioning System (GPS) to verify their current location. During this survey which was conducted in 1994, the morphological parameters, such as depth and width were measured. Table 4.1 shows the average depth and width for different segments of the stream, designated A, B, C, D (Figure 4.2).

Table 4.1 Stream Channel Morphometry

Channel Segment	Average Depth (m)	AverageWidth (m)
A	0.14	1.30
B	0.02	0.42
C	0.05	0.72
D	0.04	0.70

These numbers refer to the summer base flow in July, 1994.

The total number of observation points was four. These sites served as the main source of continuous data collection during storm events.

Site MB-1 was established by NYCDEP hydrological group in 1993 and represents a cemented weir that collects water from upstream. Inside the weir there is a plastic tube attached to the Sigma Streamline 800SL auto-sampler. The water pump, located inside Sigma, through the tube takes water samples during storm events. The sampler was programmed to initiate sampling at a one centimeter rise in the stream. The first sample is usually taken 15 minutes after the program has been initiated and then at half-hour intervals. This site provided data for several storms during 1994 - 1995 interval. Data included fecal coliform bacteria, turbidity, specific conductivity and discharge. During 1996, only discharge data were available.

Site MB-3 was established in 1996 and equipped with a SOLOMAT hydrological unit which has flow, turbidity and temperature sensors. The SOLOMAT unit provides continuous monitoring of the mentioned parameters during the storm and stores all information in a memory. Data logging is done at 15 minute intervals. During the base flow, water depth is 0.08 m and width is 0.5 m. Three metal rods serve as a mounting

platform for the unit and its sensors.

Site MB-4 was equipped similar to Site MB-3. It is located by bare rocks at the more confined channel section, therefore providing better flow measurement conditions than site MB-3. During the base flow, water depth is 0.05 m and width is 0.4 m.

Site MB-8 was equipped similar to Site MB-3 and MB-4. During the base flow, water depth is 0.04 m and width is 0.1 m.

The field survey was conducted in the following way:

1. Every day the weather report was checked through the Internet by connection to the 'NYC Weather Report' ("http://www.intellicast.com/weather/lga/").

2. Before an anticipated storm event, two sites were equiped with SOLOMAT data logging devices, calibrated and initialized for the coming storm.

3. After storm event data from data loggers were downloaded and processed.

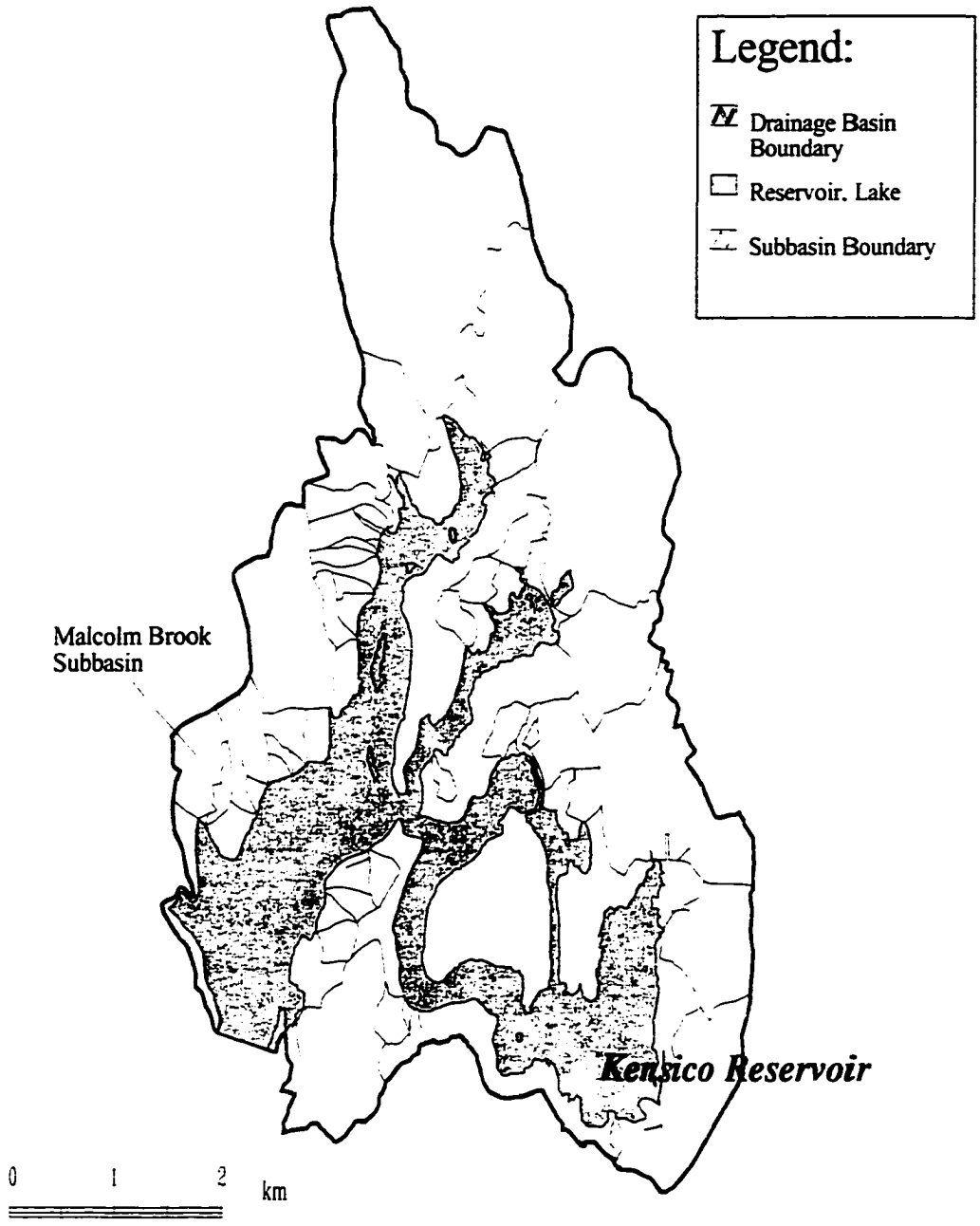

Figure 4.1 Kensico Reservoir Drainage Network.

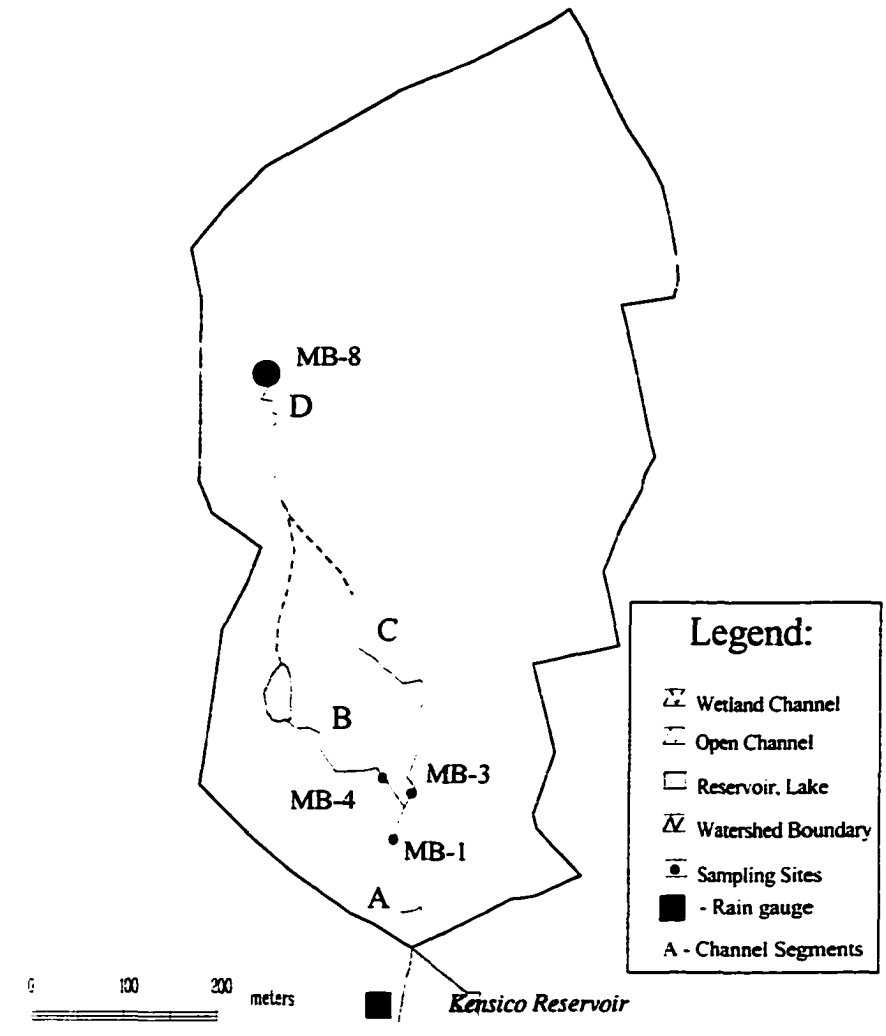

Figure 4.2 Malcolm Brook Watershed.

3. After the storm event, SOLOMAT units were collected from the field and data were downloaded into a PC and saved on a hard drive.

4.2 Hydrological Data Collection Methods

Data collection included one Sigma Streamline 800SL auto-sampler and two SOLOMAT data logging devices.

Sigma Streamline 800SL auto-sampler initiates sampling when the water level rises or rainfall increases. Rotating carousel held up to 30 bottles which get filled with the water from the stream at half-hour or preselected other time intervals. After the storm event ended, all bottles were delivered to the laboratory for the water quality analysis. Such hydrological characteristics as discharge and velocity were defined from the hydrograph. The hydrograph from Sigma Streamline 800SL is based on the stage height which was recorded every 10 minutes. Stage height is a water depth inside the channel and it is measured by the pressure transducer, connected with Sigma.

SOLOMAT data logging devices are hand-held, water resistant portable units. They consist of the data processing unit which can be programmed and also store collected digital information. It can store up to 52,000 data records. Three C-size batteries provide power for more than 70 hours. Data from different sensors, such as turbidity sensor, flowmeter and temperature sensor are recorded by the unit. Stored data can be retrieved and analysed through the laptop or desktop PC using SOLOMAT analytical software.

Rain data were obtained from the rain gauge installed at the nearby shaft next to the site. The rain gauge (Figure 4.2) provided continuous data every 10 minutes on the rainfall depth.

Figure 4.3 shows locations where digital photos were taken to view particular stream segments.

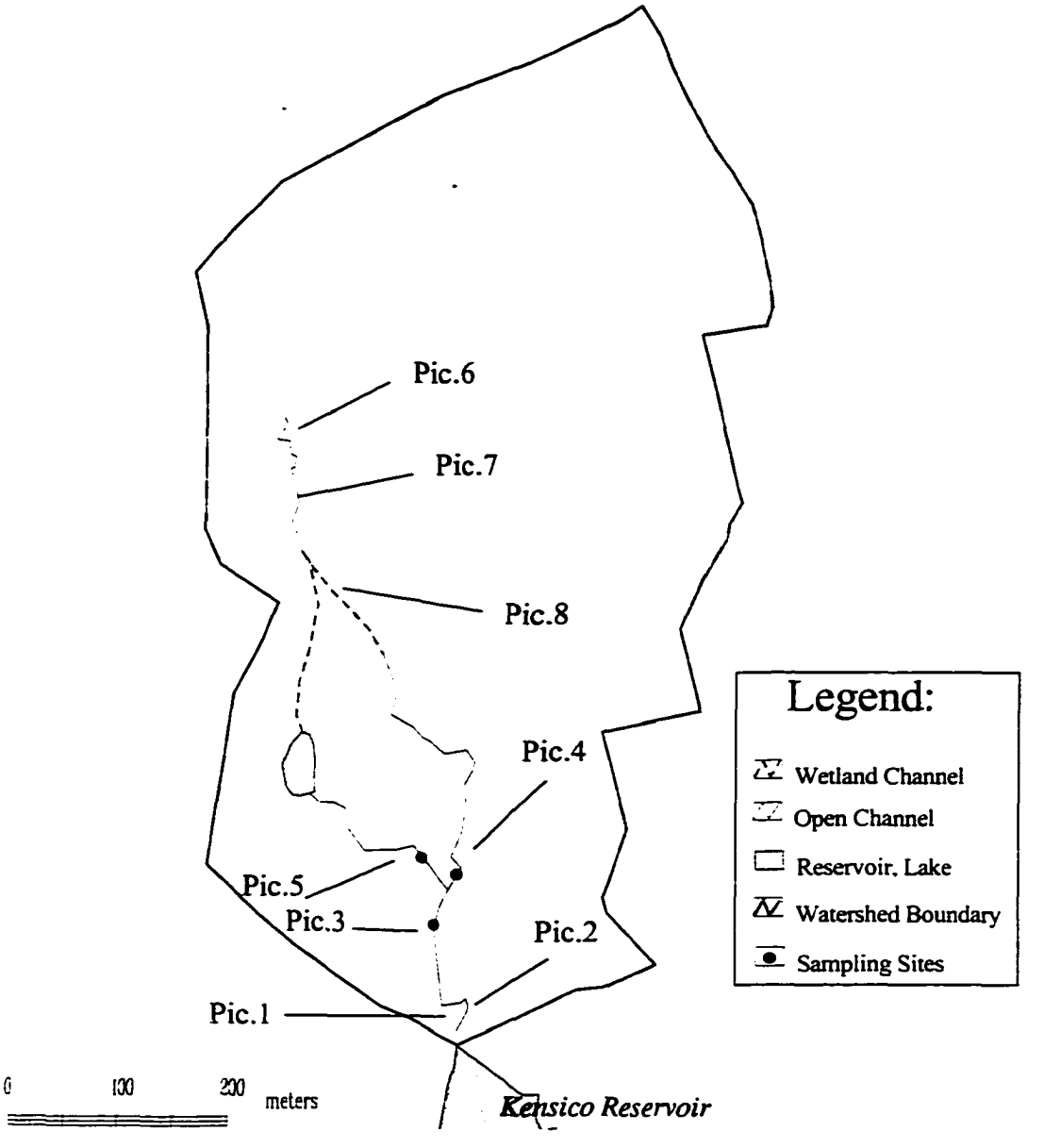

Figure 4.3 Locations of Digital Images.

Pic. 1

Pic. 2

Pic. 3

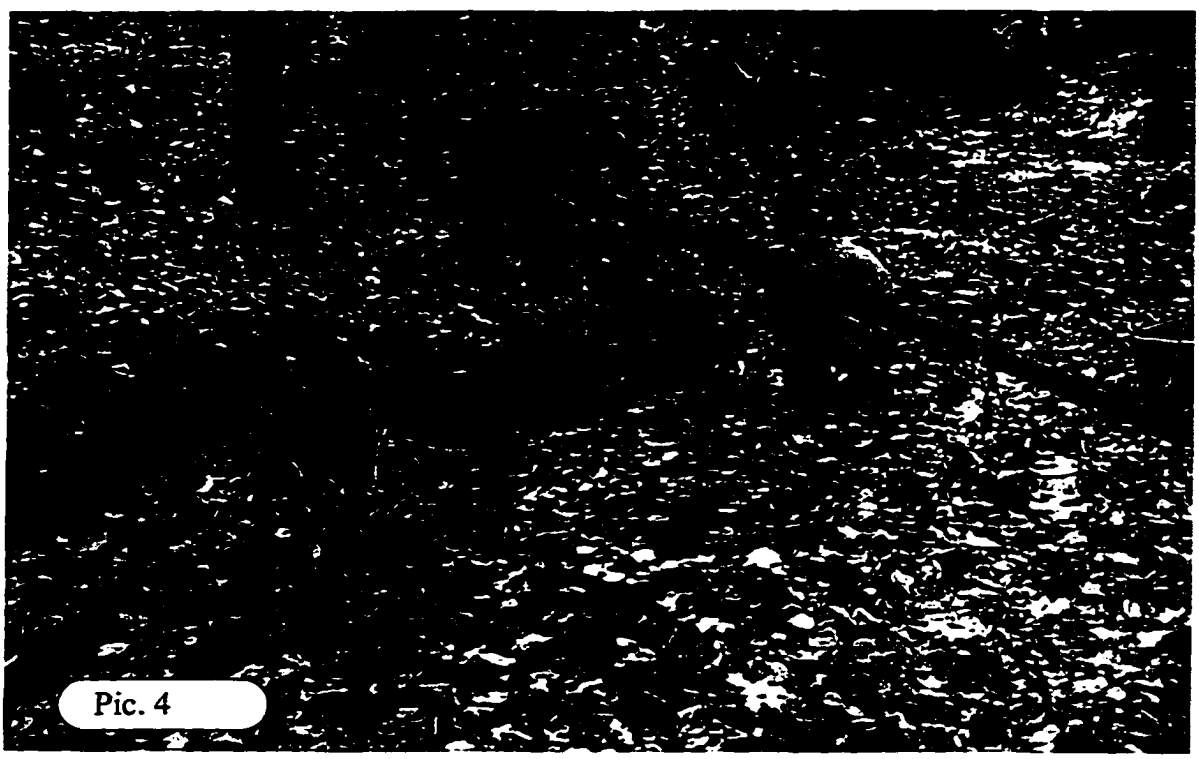

Pic. 4

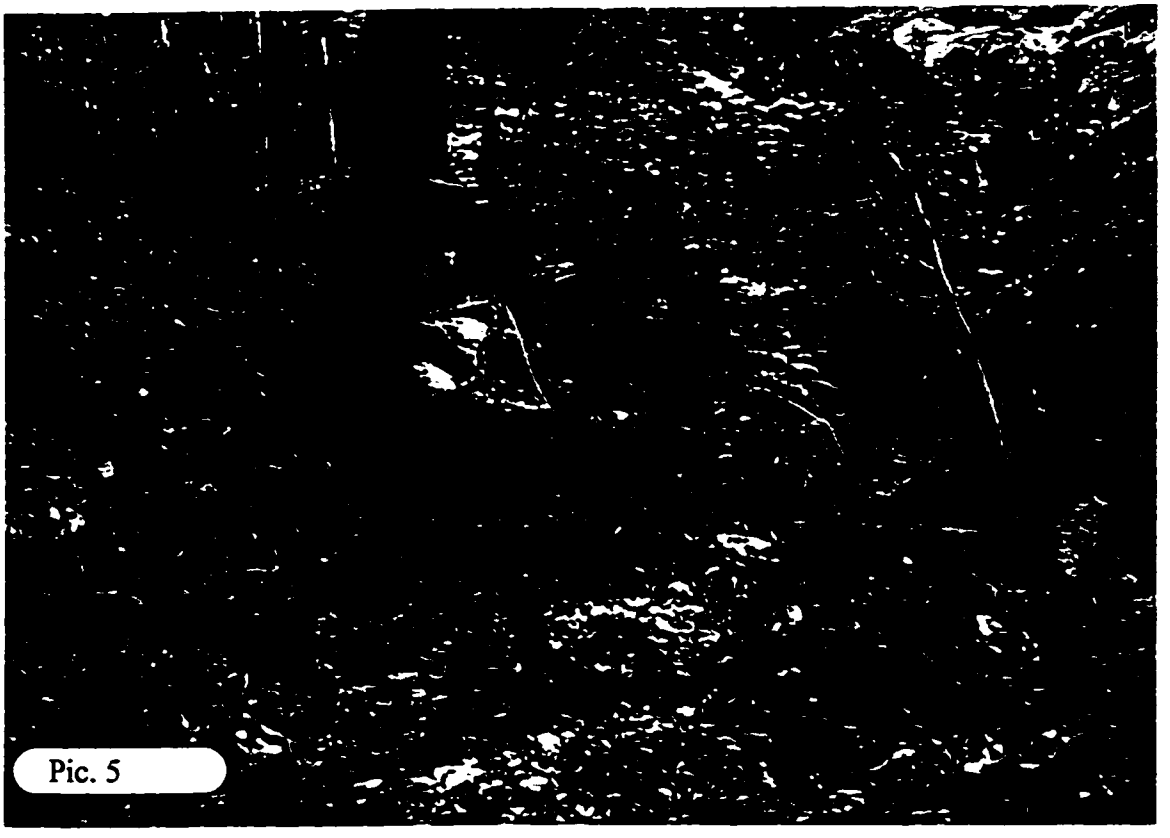

Pic. 5

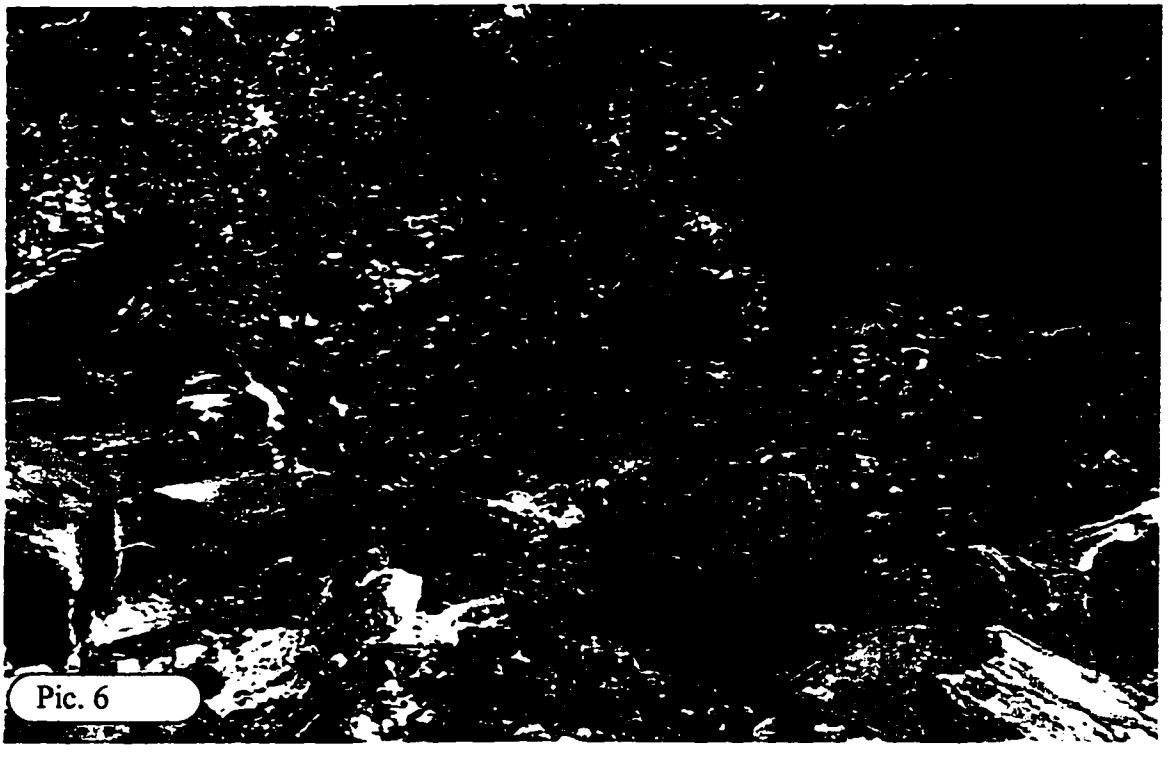

Pic. 6

Pic. 7

Pic. 8

4.3 GIS Data.

GIS data for this project consist of the set of spatial data in ARC/INFO format (coverage). These data sets serve to derive spatial measurements and provide visualization framework. GIS data collection was based mostly on the scale of 1:24,000, because the majority of the available GIS data on state and regional level linked with the United States Geological Survey (USGS) quadrangles or derived from them.

4.3.1 Stream Network.

The stream network was derived from a Global Positioning System (GPS) survey, conducted by NYCDEP on Malcolm Brook in 1994. This delineation was necessary to build a field map that would serve to place field observation sites more accurately than would has been done using USGS data. The GPS survey was conducted using standard Trimble Navigation ProXL units. During the survey, characteristic stream channel points, i.e. turn points, were defined and surveyed. On each characteristic point, 180 - 200 coordinate measurements from satellites were taken. Then all measurements were downloaded into computer and corrected using data from the Environmental Protection Agency base station, located in Edison, New Jersey. After correction, all points were converted into the linear data set, representing accurate stream delineation. The Trimble GPS unit allowed the collection of points in Universal Transverse Mercator (UTM) format.

After the GPS survey, all data were transformed into ARC/INFO line format. This line coverage is a basic data layer used for modeling and visualization.

4.3.2 Landuse Data

Landuse areas for the Malcolm Brook watershed were delineated from the low altitude infrared color photography. There are only three land uses for the watershed: open space, mixed forest; medium density residential and commercial.

Data were derived by outlining polygons with the same landuse characteristics from the image. After delineation, data were built as polygon coverage and then georeferenced through the use of control points available within the watershed. Figure 4.4 shows different landuse classes distribution within Malcolm Brook watershed. The residential area consists mostly of suburban housing with a lot of lawn area and shrubs; this is 35% of the sub-basin. The open space, mixed forest category is 55% of the area and is mostly shrubs and trees. The commercial area is 10% of the area and includes parking lots and business complexes.

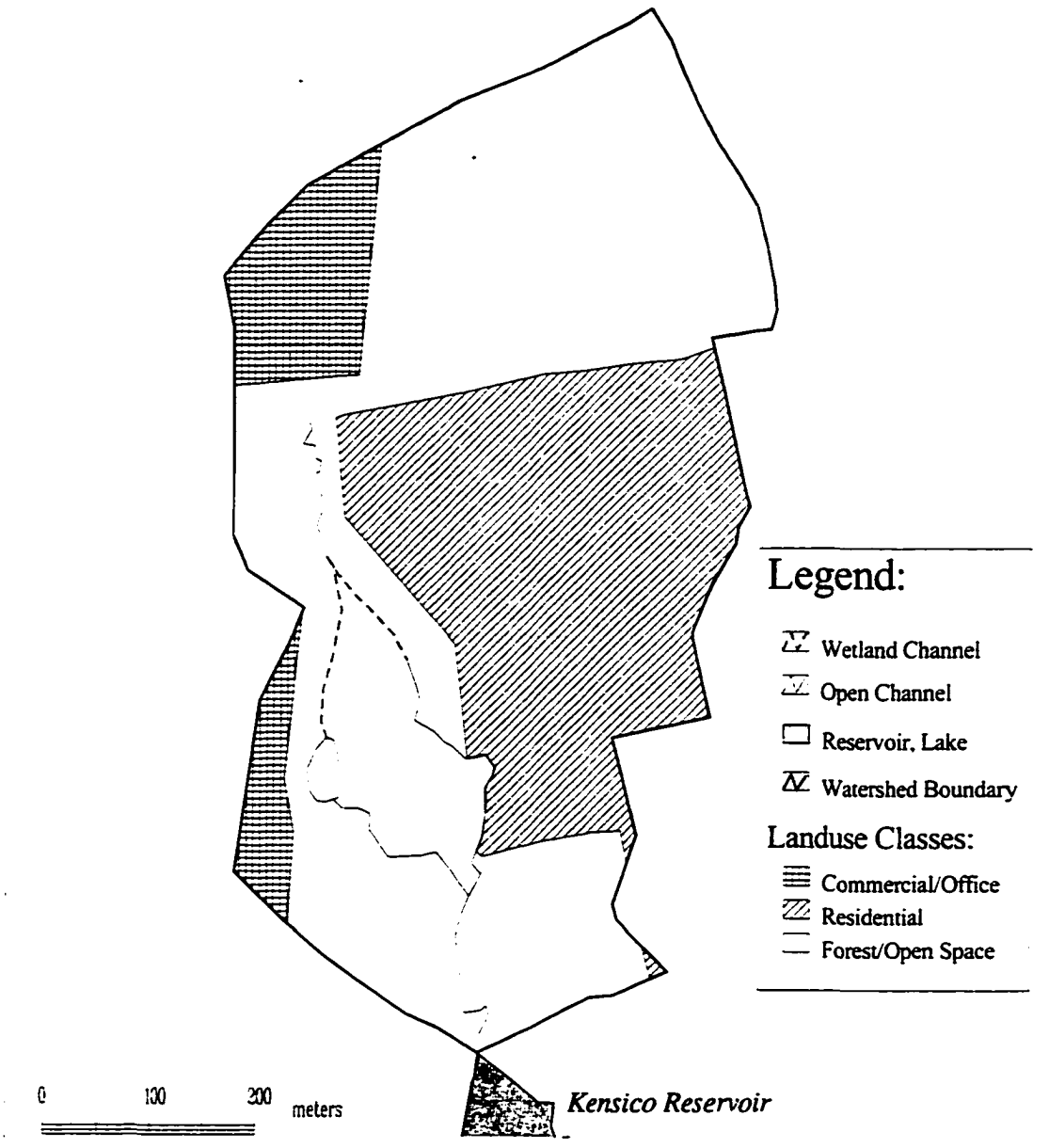

Figure 4.4 Malcolm Brook Watershed Landuse Classes.

4.3.3 Elevation data.

Elevation data used for the project were derived from the USGS digital elevation model (DEM). The only attribute associated with this dataset is elevation, expressed in meters. This model was developed from a 1:24000 USGS quadrangle contour lines. The accuracy of the dataset lies within 10-20 meters. This dataset was created by scanning contour lines and then converting them into the grid through the scanning software. Final grid was processed through the interpolation mechanism and stored as a raster data set. This dataset is a basis for the estimation of the potential energy levels of terrain. Figure 4.5 represents Malcolm Brook Watershed Digital Elevation Model, developed from USGS 24000 scale data and brought into three dimensional view. The lowest elevation of the model is 33.2 meters (109 ft) and highest elevation is 168 feet (51.2 m).

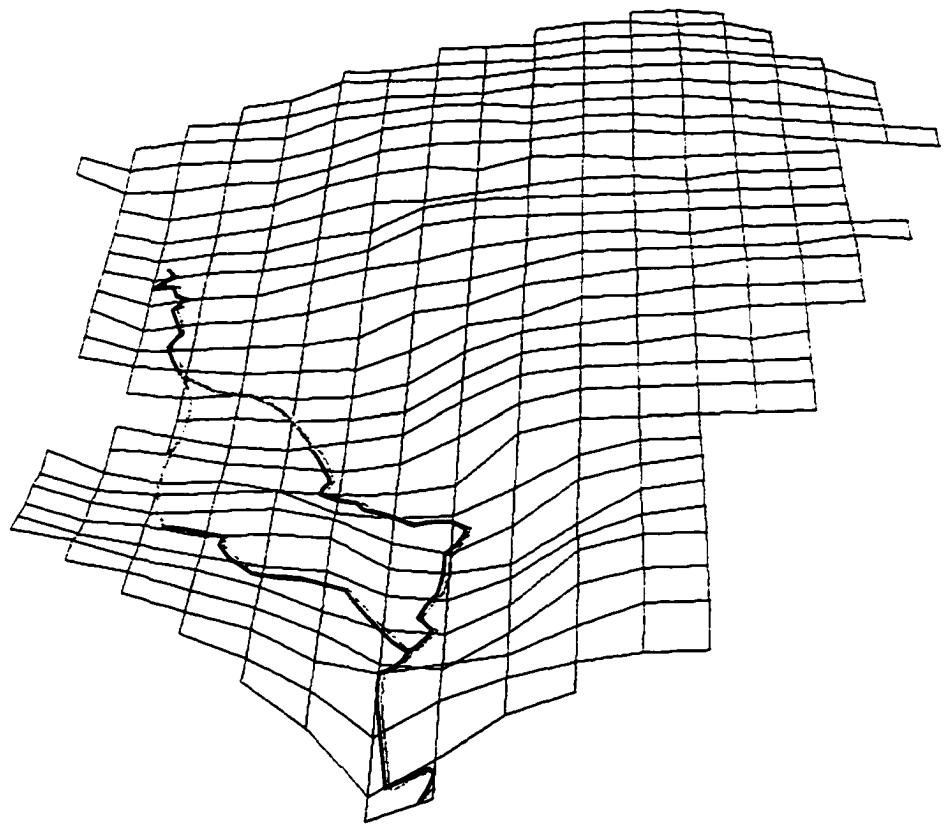

Figure 4.5 Malcolm Brook Watershed Digital Elevation Model (3D view).

4.3.4 Soil Data

Soil dataset was obtained from the Natural Resources Conservation Survey (NRCS), formerly the Soil Conservation Survey (SCS). These data were obtained from Cornell University in ARC/INFO format. Original data source were USGS 1:24,000 and 1:12,000 air photos. After interpretation all polygons, representing different soil types

were related to the soil database (Table 4.2).

Table 4.2 Malcolm Brook Soil Types and Properties

Map Unit	Area (sq.m)	Name	Hydric Group
PaxB	90817	PAXTON	C
PaxC	46524	PAXTON	C
RfA	34899	RIDGEBURY	C
Ud	2094	UDORTHENTS	A/D
Ur	3674	URBAN LAND	D
CghC	52754	CHARLTON	B
CgkD	30850	CHARLTON	B
UutB	85196	URBAN LAND	D

This database is comprehensively described in NRCS publications (1992a, 1992b).

For this research several attributes were used: map unit (soil type) and hydric group. Figure 4.6 shows soils types within Malcolm Brook watershed area.

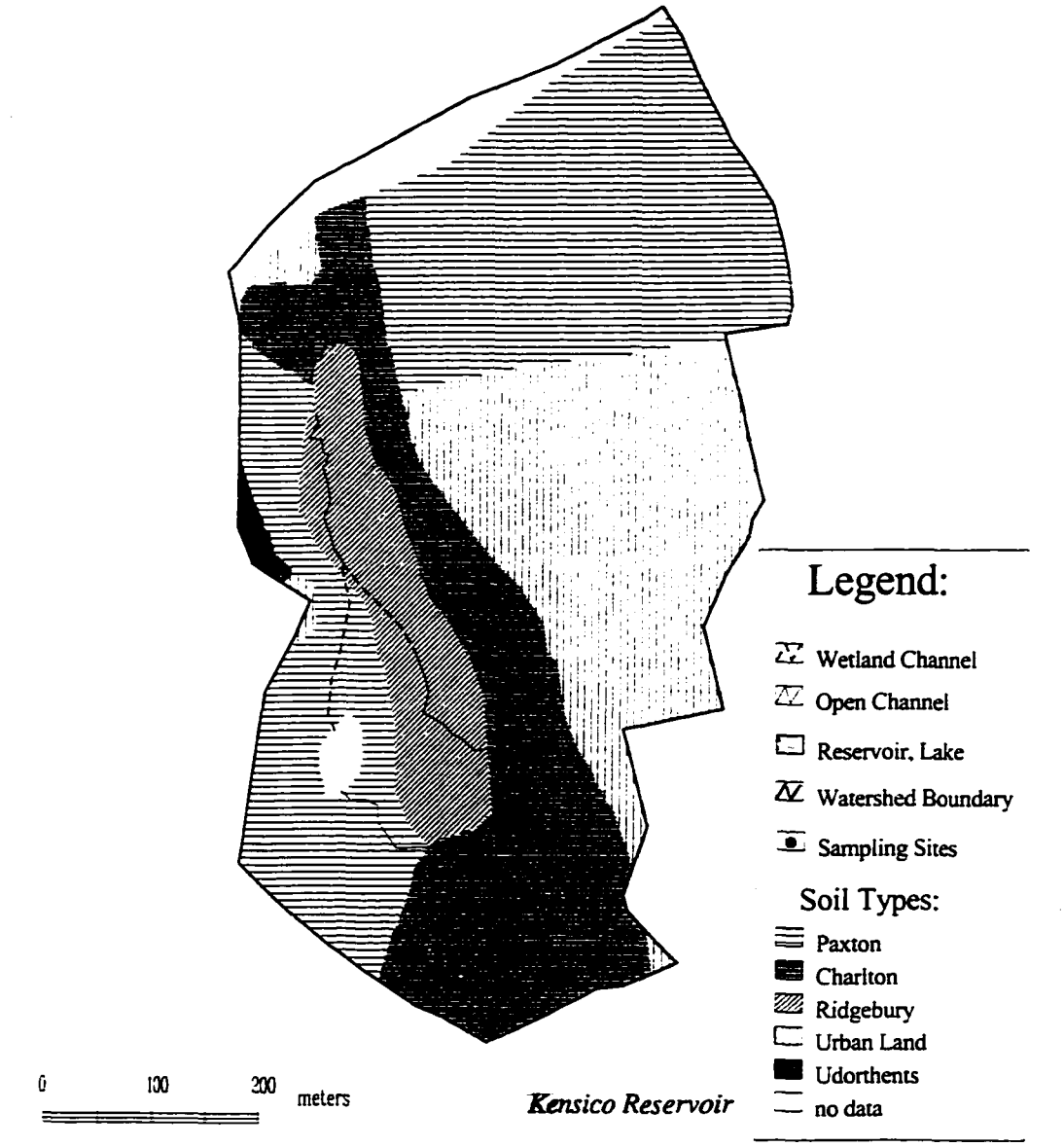

Figure 4.6 Malcolm Brook Watershed Soil Types.

4.4 Field Measurements.

Field measurements of turbidity were taken during 1996-1997 field season. Turbidity was measured by SOLOMAT turbidimeters, which were attached to the SOLOMAT produced WP4007 data logger. SOLOMAT is a company, specializing in water quality monitoring systems. WP4007 is a water quality monitoring system, designed to measure and datalog a wide range of water-quality parameters. It can be left for a long period of time under severe rain or storm conditions. Turbidity was measured by the probe which was attached to the metal rod, inserted into the stream channel (see Figure 4.7)

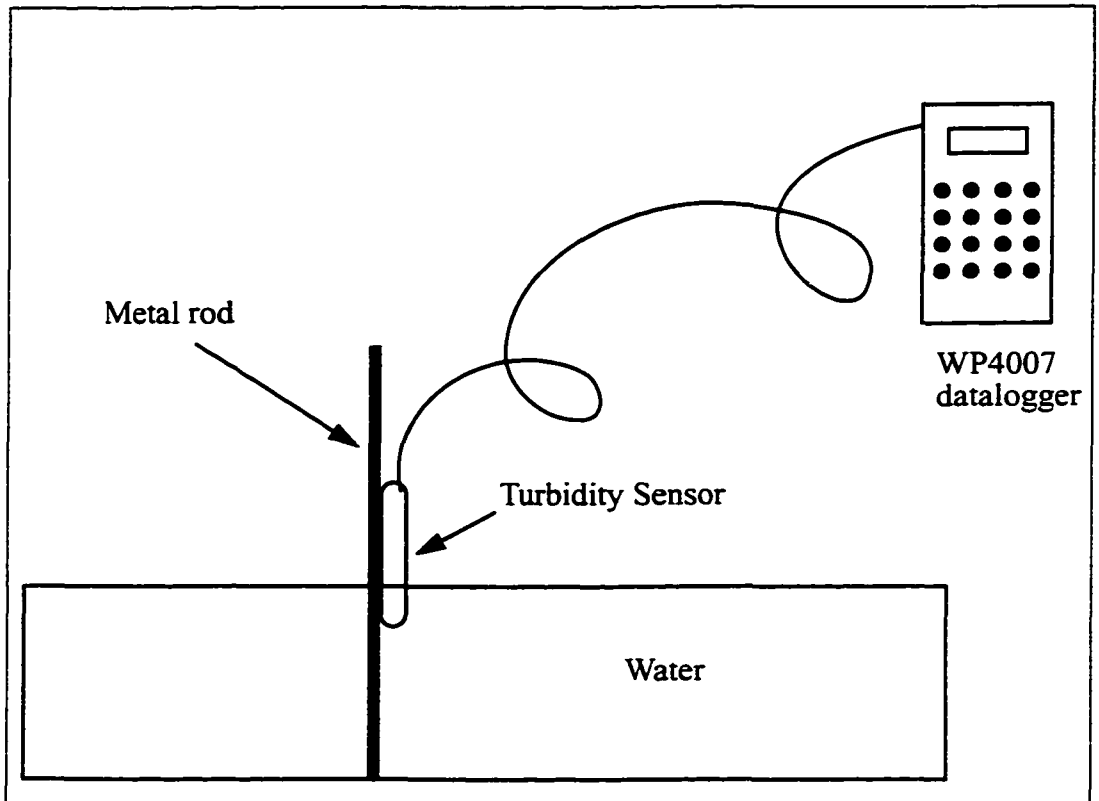

Figure 4.7 Elements of the field monitoring setup.

Power supply for WP4007 allowed unit to stay up to 3-4 days near the stream, secured in a wooden box to prevent possible damage or theft. Normally, the weather report

would be analyzed first and then WP4007 would be installed prior to anticipated event and removed after the event terminated. Turbidity sensor was cleaned after each storm event and re-calibrated with formazin solutions, corresponding to 0, 100 and 1000 NTU. Turbidity sensor measures light scattered by 90° and focussed into the water. Under normal conditions, variables such as temperature, background light and water color have negligible effect on measurements made by sensor. For all measurements, a 1110TUB sensor with a turbidity range of 0.2NTU to 4000NTU, was used.

Turbidity data from the WP4007 were transferred to the laptop computer and analyzed using SOLOMAT-designed software, CS6. This software allowed turbidity data to be downloaded and then exported to an ASCII file. These data were then merged with rainfall and flow data from site MB-1 according to the time of the record. In cases where time did not coincide, turbidity values were interpolated. Tables with measured data are represented in Appendix D.

4.5 Model Application to Malcolm Brook.

4.5.1 Flow Modeling.

During field seasons of 1994, 1996 and 1997 data on discharge and rainfall were collected for different storm events, generally for the period of May - November. Modeling was done for 1996 and 1997 years. Data from 1996 were used to calibrate the model and data from 1997 were used to verify it. Each storm event was broken into different time intervals ranging from 10 to 40 minutes. Rainfall was calculated for each time interval and used as an input for the modeling. Appendix C shows input data files

for each storm modeled in 1996 (see test #1 - test #9). Because the hydrological part of modeling was done using ARCINFO GIS software, input files were set up as ARCINFO macro language (AML) files. These files are plain ASCII files and should be located in the same directory as modeling code.

The purpose of the modeling was to obtain turbidity values using as an input only rainfall data. Therefore for each storm event an HRU matrix was developed. This matrix contained runoff values for each time interval within the "test" file from Appendix C. Matrices were created using GIS. The small interface, developed for GIS data manipulation allowed overlay of soil/landuse/slope data. After the GIS data were combined, a reference table was used to assign runoff coefficient values for each HRU using rational method formula. The reference table is presented in Table 4.3. This table is also an ASCII file which is used by ARCINFO software.

Table 4.3 Reference table with runoff coefficient values C.

Landuse	Hydro-group	Slope 1 - < 2% 2 - 2 - 8% 3 - > 8%	C
Commercial/Office	A	1	0.51
Commercial/Office	A	2	0.51
Commercial/Office	A	3	0.51
Commercial/Office	B	1	0.51
Commercial/Office	B	2	0.52
Commercial/Office	B	3	0.52
Commercial/Office	C	1	0.52
Commercial/Office	C	2	0.52

Table 4.3 Reference table with runoff coefficient values C.

Landuse	Hydro-group	Slope 1 - < 2% 2 - 2 - 8% 3 - > 8%	C
Commercial/Office	C	3	0.52
Commercial/Office	D	1	0.52
Commercial/Office	D	2	0.52
Commercial/Office	D	3	0.52
Forest/Space	A	1	0.05
Forest/Space	A	2	0.10
Forest/Space	A	3	0.14
Forest/Space	B	1	0.08
Forest/Space	B	2	0.13
Forest/Space	B	3	0.19
Forest/Space	C	1	0.12
Forest/Space	C	2	0.17
Forest/Space	C	3	0.24
Forest/Space	D	1	0.16
Forest/Space	D	2	0.21
Forest/Space	D	3	0.28
Residential	A	1	0.09
Residential	A	2	0.14
Residential	A	3	0.17
Residential	B	1	0.12
Residential	B	2	0.16
Residential	B	3	0.21
Residential	C	1	0.15
Residential	C	2	0.20

Table 4.3 Reference table with runoff coefficient values C.

Landuse	Hydro-group	Slope 1 - < 2% 2 - 2 - 8% 3 - > 8%	C
Residential	C	3	0.26
Residential	D	1	0.19
Residential	D	2	0.23
Residential	D	3	0.30

The landuse column has values taken from the GIS landuse data. The hydro-group column has values taken from the GIS soil data and refers to hydrological group of soil. Slope values are in percentage and were obtained from digital elevation model. Values of the C coefficient were obtained from the references (Ward and Elliot, 1995) according to other three parameters.

After creating HRU matrix for the selected strom event using selected C coefficients, main ARCINFO macro code "discharge.aml" has to be utilized. This code uses "test" file as an input and also has to utilize such GIS files as watershed boundary, stream channel, digital elevation model and HRU matrix. Because Malcolm Brook has two stream channels, merging into the main one, basin boundaries for each stream channel were delineated within GIS and then "discharge.aml" code worked on each stream route separately. Fig 4.8 shows Malcolm Brook sub-basins and routes. Following description of the modeling procedures refers only to one main route 1, while the results of modeling will be shown for both.

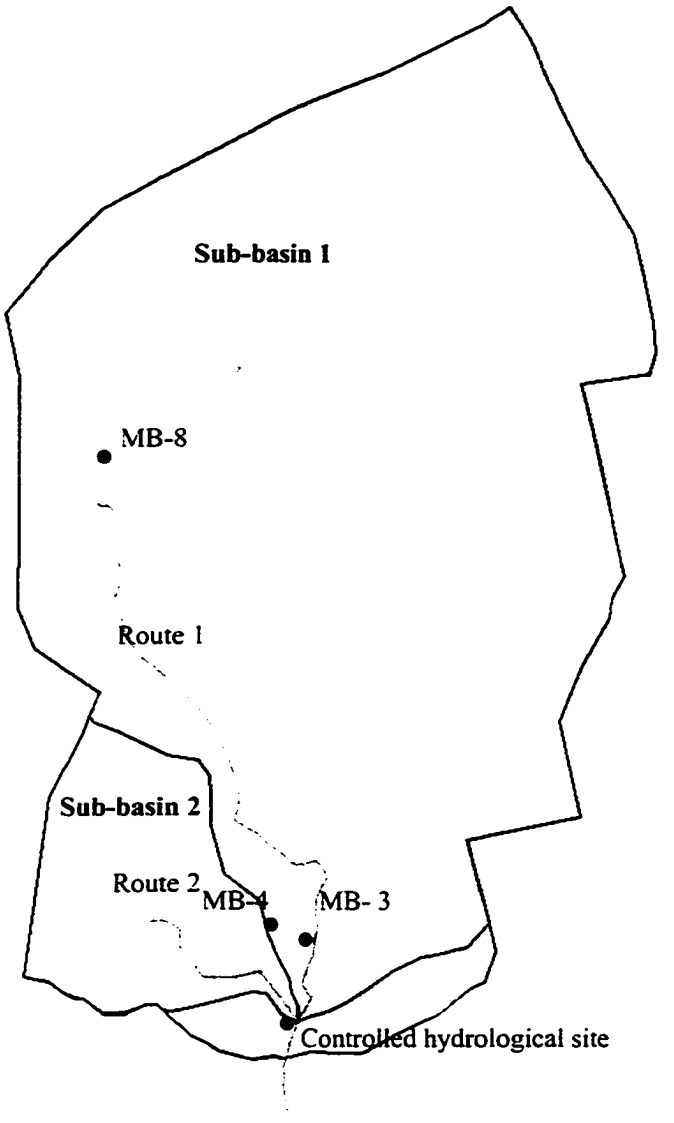

Figure 4.8. Malcolm Brook Basins and sampling sites.

There are two main functions which are performed by the code: 1 - calculate discharge values for each stream segment; 2 - visualize contributing areas and runoff:

First function result in a file containing discharge data for each stream segment and

segment unique numbers from GIS database. Example of such file is in a Table 4.4

Table 4.4 Output file from GIS macro "discharge.aml"

ID#	Length (m)	Slope %	Q1 l/sec	Q2 l/sec	Q3 l/sec	Q4 l/sec	Q5 l/sec	Q6 l/sec	Q7 l/sec	Q8 l/sec
238	12	0.07	1	5	10	14	23	50	53	33
254	31	0.09	1	2	3	3	5	12	9	5
255	15	0.09	1	1	1	1	3	4	3	2
273	13	0.09	1	2	2	3	4	8	9	5
274	28	0.09	1	2	3	3	4	10	11	6
298	14	0.04	1	3	3	3	5	10	9	5
325	33	0.04	1	2	3	3	4	8	8	5
330	10	0.00001	1	2	2	2	4	7	6	1
358	5	0.06	0	0	0	1	1	2	1	1
360	7	0.06	0	1	1	2	2	8	5	0
353	10	0.06	0	1	1	1	1	3	3	2
354	17	0.04	1	1	1	1	2	7	4	0
385	14	0.04	1	1	2	2	2	5	7	4
380	14	0.03	0	1	1	2	2	10	5	3
381	18	0.03	1	2	2	2	3	6	6	3
407	6	0.06	1	2	2	2	3	7	7	4
408	10	0.06	0	1	1	1	1	3	3	0
409	12	0.07	1	1	1	1	2	4	5	3
410	7	0.07	1	1	2	1	2	10	7	4
432	17	0.09	1	1	1	1	2	8	6	3
431	14	0.000001	2	4	5	4	6	12	12	2
445	12	0.03	1	1	2	1	3	9	7	0
452	24	0.03	1	2	2	3	4	16	13	1
473	11	0.000001	0	0	0	0	0	1	1	0

Table 4.4 Output file from GIS macro "discharge.aml"

ID#	Length (m)	Slope %	Q1 l/sec	Q2 l/sec	Q3 l/sec	Q4 l/sec	Q5 l/sec	Q6 l/sec	Q7 l/sec	Q8 l/sec
464	14	0.03	1	2	2	2	5	8	7	0
465	14	0.03	1	1	2	2	3	6	5	0
489	5	0.06	0	0	0	0	0	0	0	0
490	4	0.1	0	1	1	1	2	4	2	0
503	15	0.1	1	2	2	2	3	11	3	0
492	10	0.1	0	0	0	0	0	0	0	0
491	13	0.04	0	1	1	1	1	2	2	1
504	13	0.19	1	1	2	1	3	5	2	1
505	11	0.19	0	1	1	1	2	4	4	0
513	5	0.06	1	2	2	2	3	7	5	3
512	36	0.000001	2	5	6	6	8	23	18	1
548	2	0.03	0	0	1	1	1	1	1	0
555	21	0.03	2	4	4	3	4	11	9	1
576	34	0.06	3	5	5	4	5	12	10	1
575	21	0.06	2	3	2	2	2	4	4	2

ID# column shows the unique number of the stream segment which is also the unique number of the HRU plane from the matrix. These numbers allow one to link the HRU matrix and the output file to create a hydrograph.

Length (m) is a length of the stream segment which will be used later within kinematic routing module.

Slope (%) is a slope of HRU plane and also stream channel slope. In some cases, because of the coarseness of DEM, slope was assigned value '0' because of the flat terrain. Since '0' will annihilate all consecutive calculations and in the real world, it is difficult to

find a perfectly flat spot, slope values of '0' were substituted by 0.000001 value which reflects very low energy level or gradient. It would also reduce potential hydrological parameters, such as water velocity and discharge.

Q1 ... Q9 are discharges from a surface into the stream. The first row contains discharge values for the first segment on the stream. These values are usually larger than the numbers in other rows because the contributing area for the first segment is larger than any of the other segments. For the first segment, runoff value is a combination of lateral and channel flow, while for the other segments, runoff from modeling is represented only by the lateral flow. Therefore, for the second segment on the stream, total flow will be equal to channel and lateral discharge from the first segment plus lateral discharge from the second segment and so on. Visual representation of the process can be seen in Figures 4.9 and 4.10 which were created for the first and second segment on the stream for the first time interval.

Second function results in a visual representation of runoff and the contributing area for each stream segment at a given time interval. Figure 4.9 shows the first stream segment (marked with a dot) and the surrounding contributing area for the first time interval of the rainstorm. Figure 4.10 shows the same for the next segment. Because part of the watershed already delivered runoff to the previous (first) segment, only small part of contributing area delivers water as a lateral flow into this segment. Therefore, flow into the second segment is visualized as a small strip. However, the size of the strip (visual width) does not exceed the estimated size of the contributing area. After the model finished its run for the first time interval and stopped at the last segment, then the total size of contributing area for this time interval can be seen (Figure 4.11). The boundary of the blank space on

the image is an isochrone of the first time interval. Figure 4.12 shows the same isochrone for the second time interval. During the "test1.aml" run rainfall was not intensive enough to saturate the whole watershed. Therefore, last time interval on Figure 4.13 does not show a fully saturated watershed.

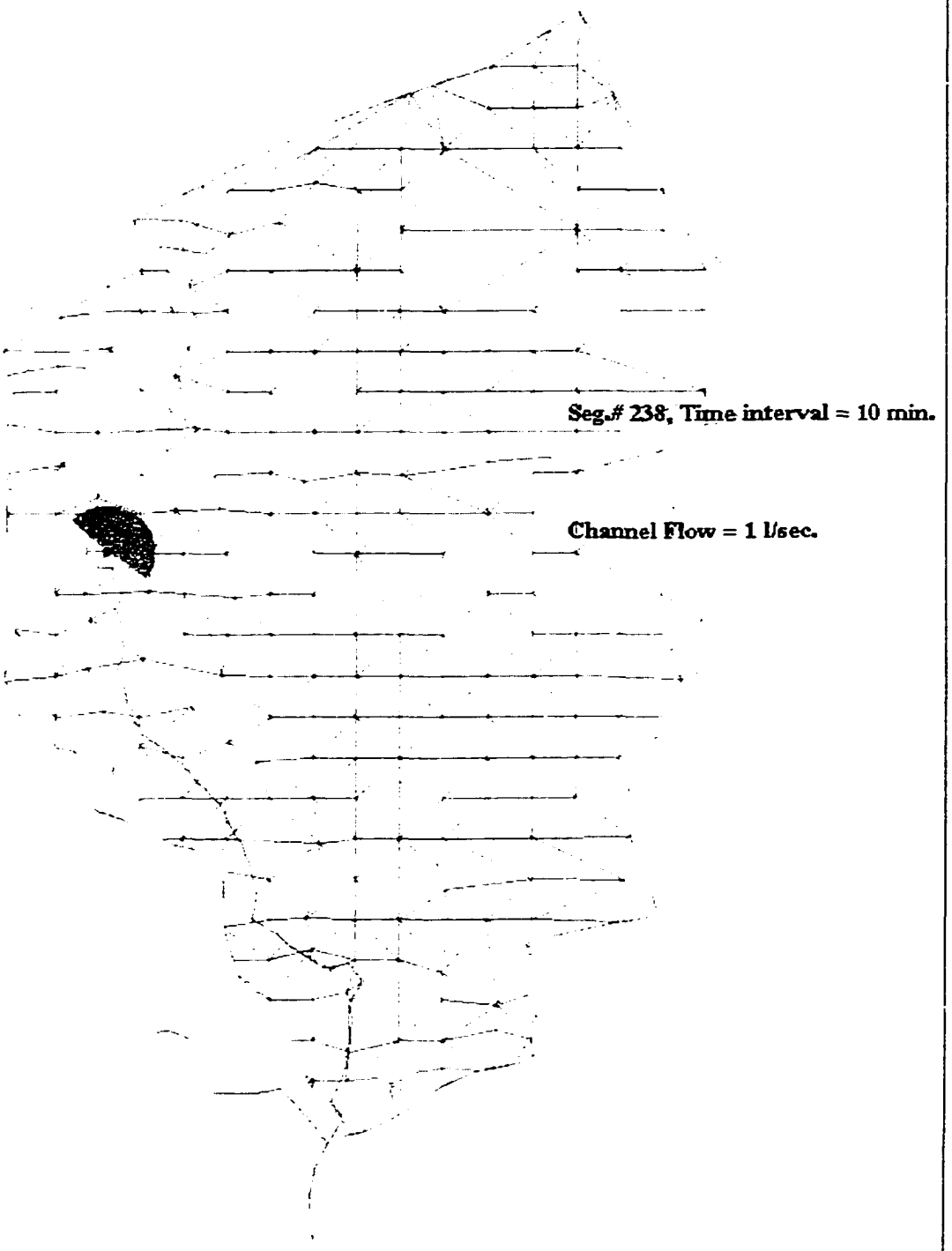

Figure 4.9. Visualization of runoff and contributing area for the first segment on the stream for the first time interval.

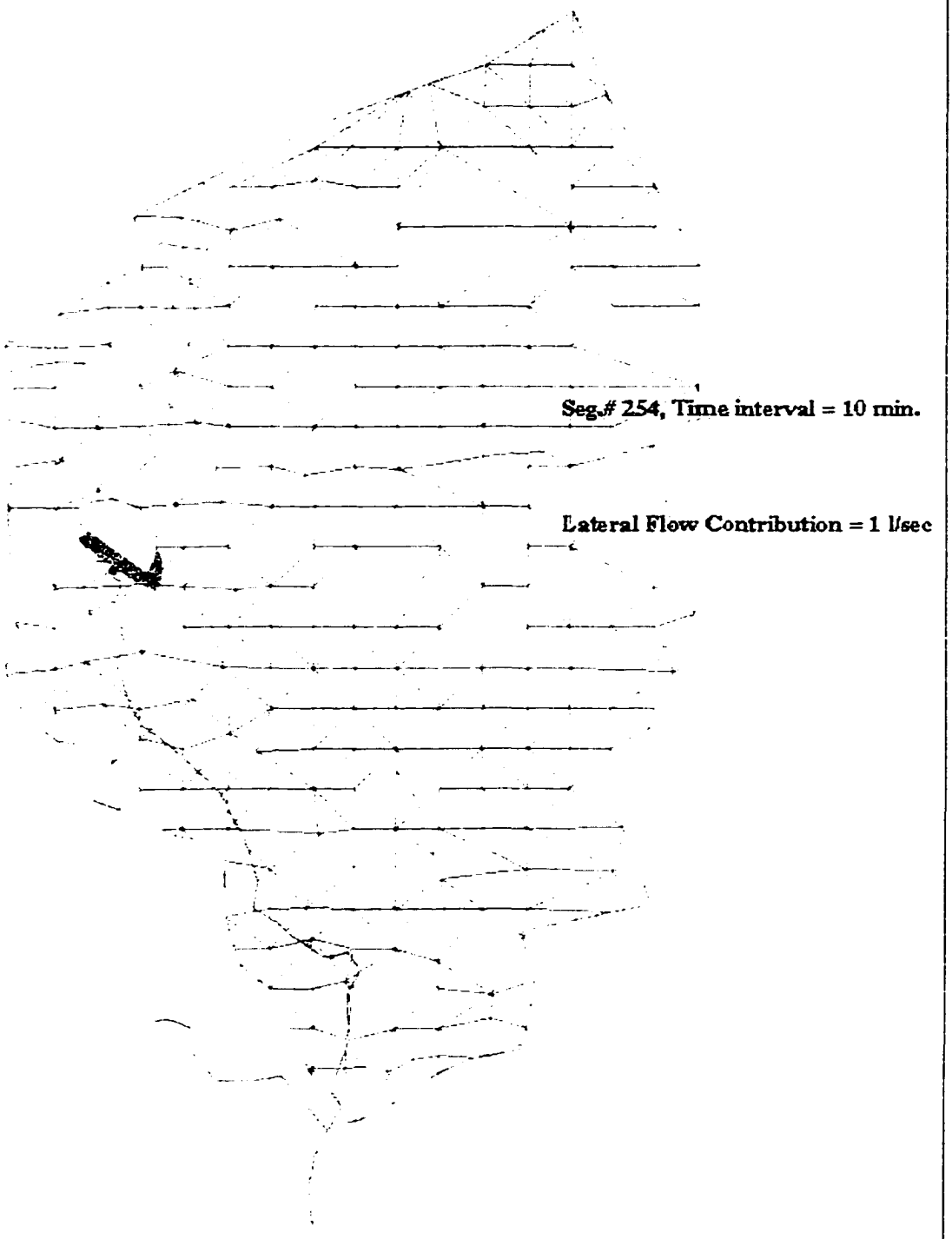

Figure 4.10. Visualization of runoff and contributing area for the second segment on the stream for the first time interval.

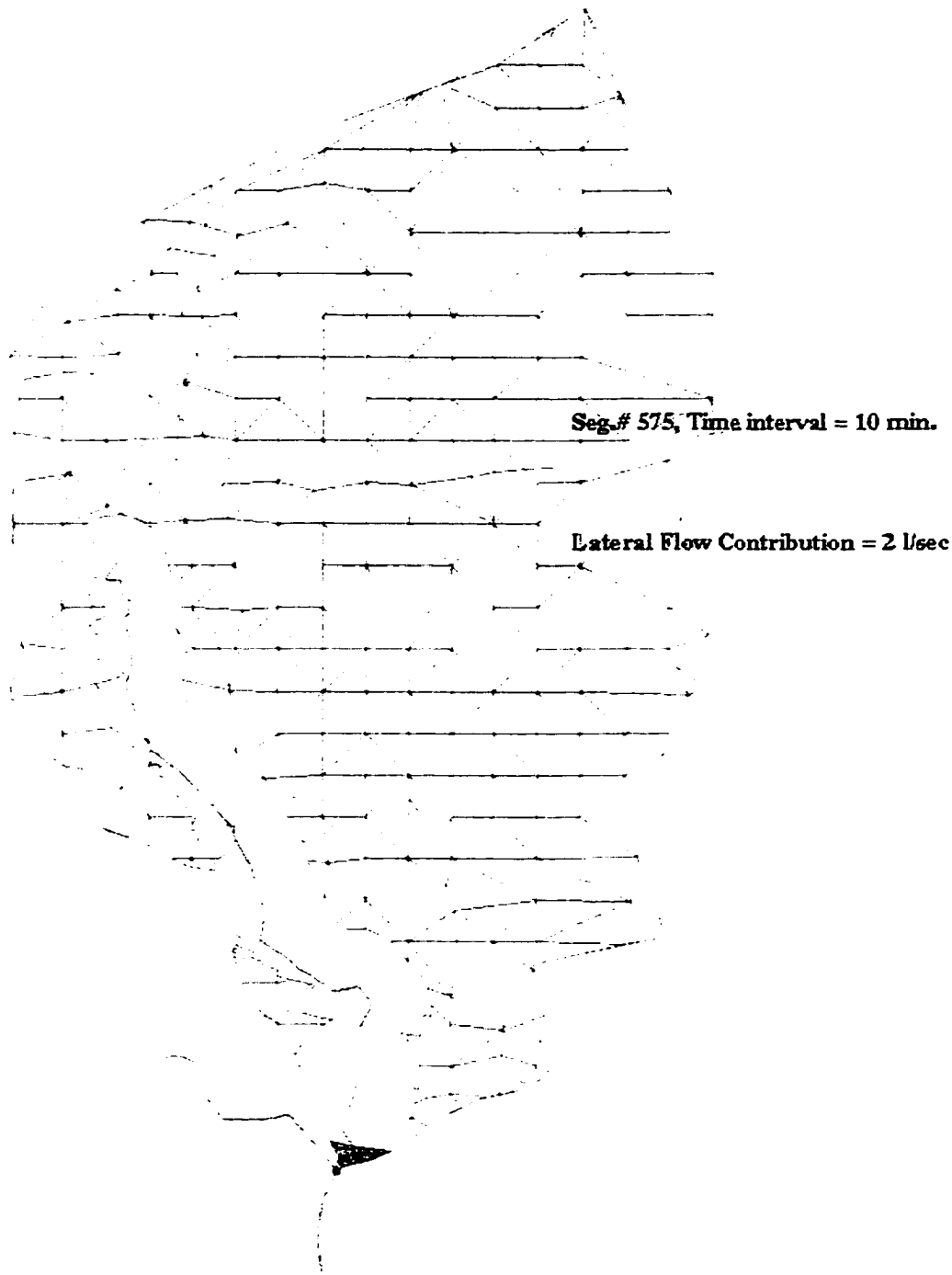

Figure 4.11. Visualization of runoff and contributing area for the last segment on the stream for the first time interval.

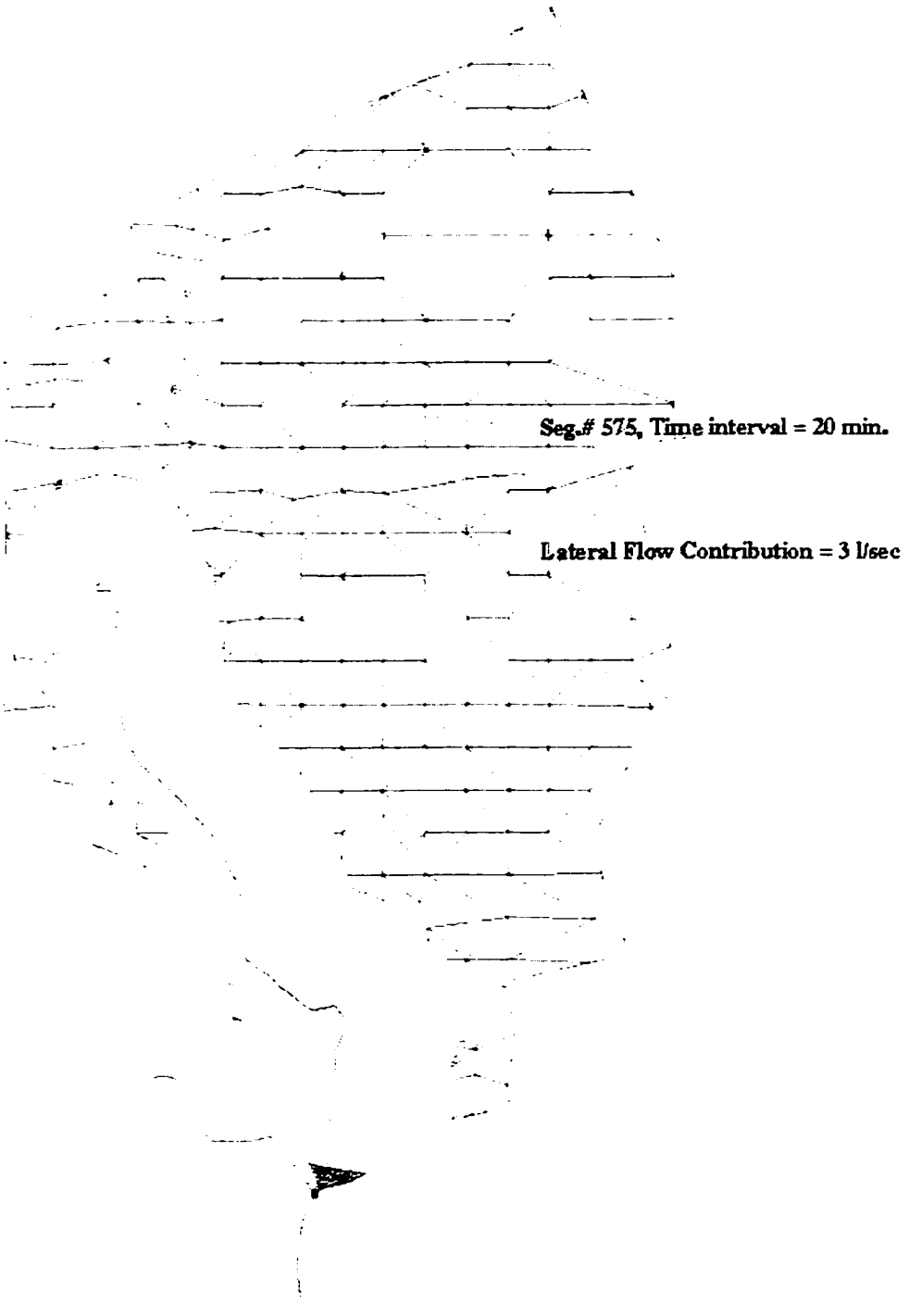

Figure 4.12. Visualization of runoff and contributing area for the last segment on the stream for the second time interval.

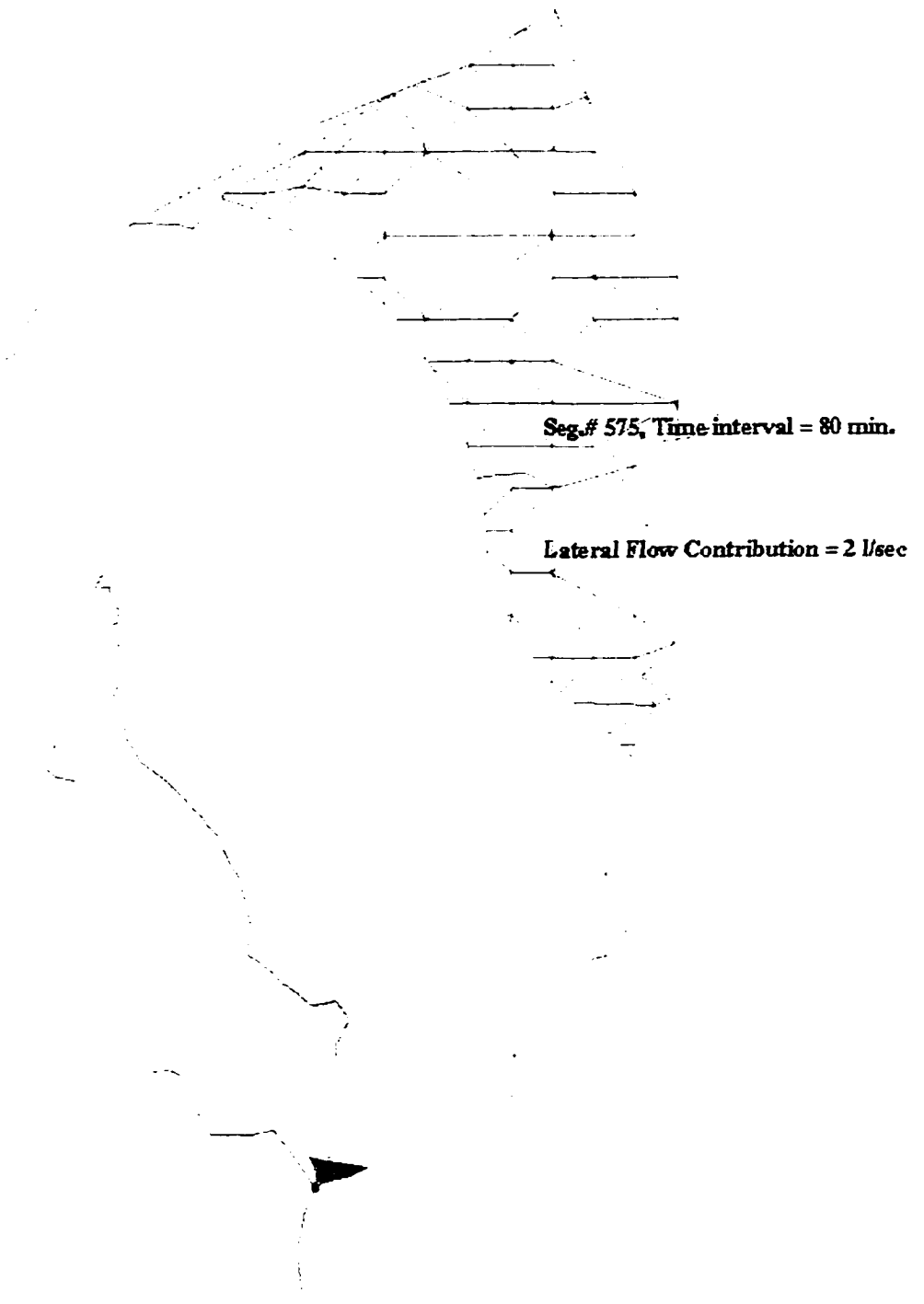

Figure 4.13. Visualization of runoff and contributing area for the last segment on the stream for the eighth time interval.

Graphical outputs for each segment can be combined later into an animated video display of changing contributing areas and discharges.

The next step in modeling was the discharge routing, using resulting values to calculate turbidity. Discharge was routed using kinematic wave equation described earlier. It was programmed in C language to speed up and simplify calculations and named "kinematic". Input for the code "kinematic" was presented in Table 4.4. This file contains the main characteristics of the stream - length, slope and discharge. Table 4.5 shows the output table of "kinematic" code. Values for the base flow were assumed to be equal 1 L/ sec which is an average flow for the Malcolm Brook during normal spring-summer conditions. Base flow can be chosen and used in this model according to the modeled or anticipated conditions.

Table 4.5. Output of the "kinematic" code with routed flow values.

ID#	Q1	Q2	Q3	Q4	Q5	Q6	Q7	Q8
238	1.000	5.000	10.000	14.000	23.000	50.000	53.000	33.000
254	1.000	5.111	10.207	14.316	23.535	51.150	54.253	33.919
255	1.000	5.103	10.184	14.295	23.510	51.086	54.201	33.955
273	1.000	5.097	10.164	14.278	23.490	51.033	54.161	33.988
274	1.000	5.085	10.122	14.243	23.444	50.921	54.077	34.061
298	1.000	5.077	10.096	14.220	23.415	50.848	54.020	34.105
325	1.000	5.058	10.033	14.164	23.344	50.673	53.882	34.206
330	1.000	4.880	9.54	13.722	22.764	49.269	52.747	4.813
358	1.000	4.877	9.537	13.715	22.755	49.247	52.729	34.824
360	1.000	4.874	9.524	13.706	22.742	49.219	52.704	34.840
353	1.000	4.869	9.505	13.693	22.723	49.178	52.669	34.861

Table 4.5. Output of the "kinematic" code with routed flow values.

ID#	Q1	Q2	Q3	Q4	Q5	Q6	Q7	Q8
354	1.000	4.858	9.468	13.663	22.683	49.086	52.595	34.903
385	1.000	4.850	9.442	13.639	22.650	49.012	52.535	34.938
380	1.000	4.840	9.413	13.613	22.615	48.934	52.471	34.978
381	1.000	4.828	9.371	13.580	22.570	48.833	52.387	35.027
407	1.000	4.826	9.362	13.572	22.560	48.809	52.368	35.043
408	1.000	4.823	9.348	13.559	22.542	48.768	52.338	35.067
409	1.000	4.818	9.326	13.542	22.519	48.715	52.296	35.092
410	1.000	4.815	9.317	13.532	22.506	48.690	52.275	35.110
432	1.000	4.808	9.295	13.510	22.478	48.638	52.230	35.149
431	1.000	4.583	8.675	12.926	21.680	46.764	50.699	35.837
445	1.000	4.578	8.659	12.906	21.654	46.705	50.652	35.862
452	1.000	4.564	8.615	12.863	21.596	46.583	50.550	35.908
473	1.000	4.397	8.153	12.412	20.961	45.137	49.354	36.340
464	1.000	4.389	8.123	12.387	20.927	45.060	49.289	36.361
465	1.000	4.382	8.099	12.364	20.896	44.986	49.228	36.383
489	1.000	4.379	8.092	12.356	20.885	44.963	49.209	36.389
490	1.000	4.378	8.087	12.352	20.879	44.949	49.196	36.393
503	1.000	4.376	8.068	12.337	20.859	44.907	49.152	36.408
492	1.000	4.372	8.056	12.325	20.842	44.871	49.118	36.419
491	1.000	4.364	8.030	12.303	20.810	44.800	49.060	36.437
504	1.000	4.361	8.016	12.290	20.793	44.761	49.025	36.450
505	1.000	4.358	8.006	12.280	20.780	44.729	48.998	36.459
513	1.000	4.357	7.999	12.274	20.772	44.712	48.983	36.468
512	1.000	3.929	6.775	11.024	18.934	40.568	45.499	37.487
548	1.000	3.928	6.774	11.022	18.929	40.559	45.491	37.488
555	1.000	3.920	6.745	10.996	18.886	40.459	45.405	37.500
576	1.000	3.914	6.719	10.956	18.822	40.329	45.293	37.517

Table 4.5. Output of the "kinematic" code with routed flow values.

ID#	Q1	Q2	Q3	Q4	Q5	Q6	Q7	Q8
575	1.000	3.909	6.707	10.931	18.781	40.243	45.219	37.527

4.5.2 Flow Calibration.

Two parameters, α and β, are exponents in hydrological momentum equations, relating flow to area, velocity, depth and width. Leopold and Maddock (1953) showed how are these power equations are related to flow:

$$U = aQ^b$$
$$H = \alpha Q^\beta$$
$$B = cQ^f$$

where: U = velocity;

H = mean depth;

B = mean width;

The product of these coefficients should not exceed 1, because Q = UHB, and therefore $b + \beta + f = 1$. Chapra (1996) presented a table with average values and ranges of these exponents in hydrogeometric correlations (Table 4.6):

Table 4.6 : Average Coefficients for Basic Hydrological Equations

Correlation	Exponent	Value	Range
Velocity-flow	b	0.45	0.30 - 0.70
Depth-flow	β	0.40	0.10 - 0.60
Width-flow	f	0.15	0.05 - 0.25

The Kinematic Wave equation also has a necessary (but insufficient) condition for stability. It is called the Courant condition (Courant and Friedrichs, 1948). This condition is:

$$dt \leq \frac{dx}{C_k}$$

where C_k = kinematic wave celerity;

As (Chow, et al., 1988) mention, the Courant condition requires that the time step be less than the time for a wave to travel the distance dx (i.e. segment length). If dx is so large that the Courant condition is not satisfied, then there is, in effect, an accumulation or piling up of water. To avoid this, it is necessary to check the Courant condition for each iteration and, if necessary, adjust segment length and time interval. Upon checking it was found that time intervals and stream lengths has to be changed. For example, at an average size of 350 m^2 for HRU the stream segment defined by this area can vary from 5 to 30 m. Assuming the smallest time interval equal to 10 minutes (600 sec.), dx/dt = 0.01 to 0.05 m/sec. This value is far smaller than potential wave celerity and actual precision of the flow meter. This means that existing conditions do not satisfy Courant condition. But, with this methodology, a final grid or finite element matrix is created after a time interval is chosen and GIS simulation finished. Moreover, stream segment length cannot be changed because it was obtained as a result of the HRU matrix overlay on the stream channel. Stream segments preserve their uniform hydrological properties as well as HRU elements when produced in this way. Also, GIS iterations take a lot of time to run through the watershed modeling procedures and with additional requirements would run even

slower. Therefore, to avoid water accumulation as a result of not meeting the Courant condition, other means were found. After evaluating available geometrical measurements of stream channel, it was assumed that wetted perimeter can be approximated by width, since the stream is shallow and wide.

Therefore, wetted perimeter P in the equation for α can be substituted by the so-called "active width" parameter. This parameter can have a calibrating coefficient which substitutes for the Courant condition and fulfills a similar task, i.e. avoids high accumulations of water and excessive, unrealistic flows. For every reach on a stream it can differ, therefore model would require to evaluate several different numbers for each stream reach.

After many runs of the model, it was found that the best values of "active width" parameter are 4000P and 30000P for longest and shortest reaches of the Malcolm Brook, respectively.

Figure 4.14 - 4.16 show results of the flow modeling for selected storms. Appendix D contains results of all conducted tests. Tests 1-8 served as calibration datasets, while tests 9-16 were used for the model testing. These tests were taken at different year (1997) and therefore can be considered as independent.

Appendix C shows input files.

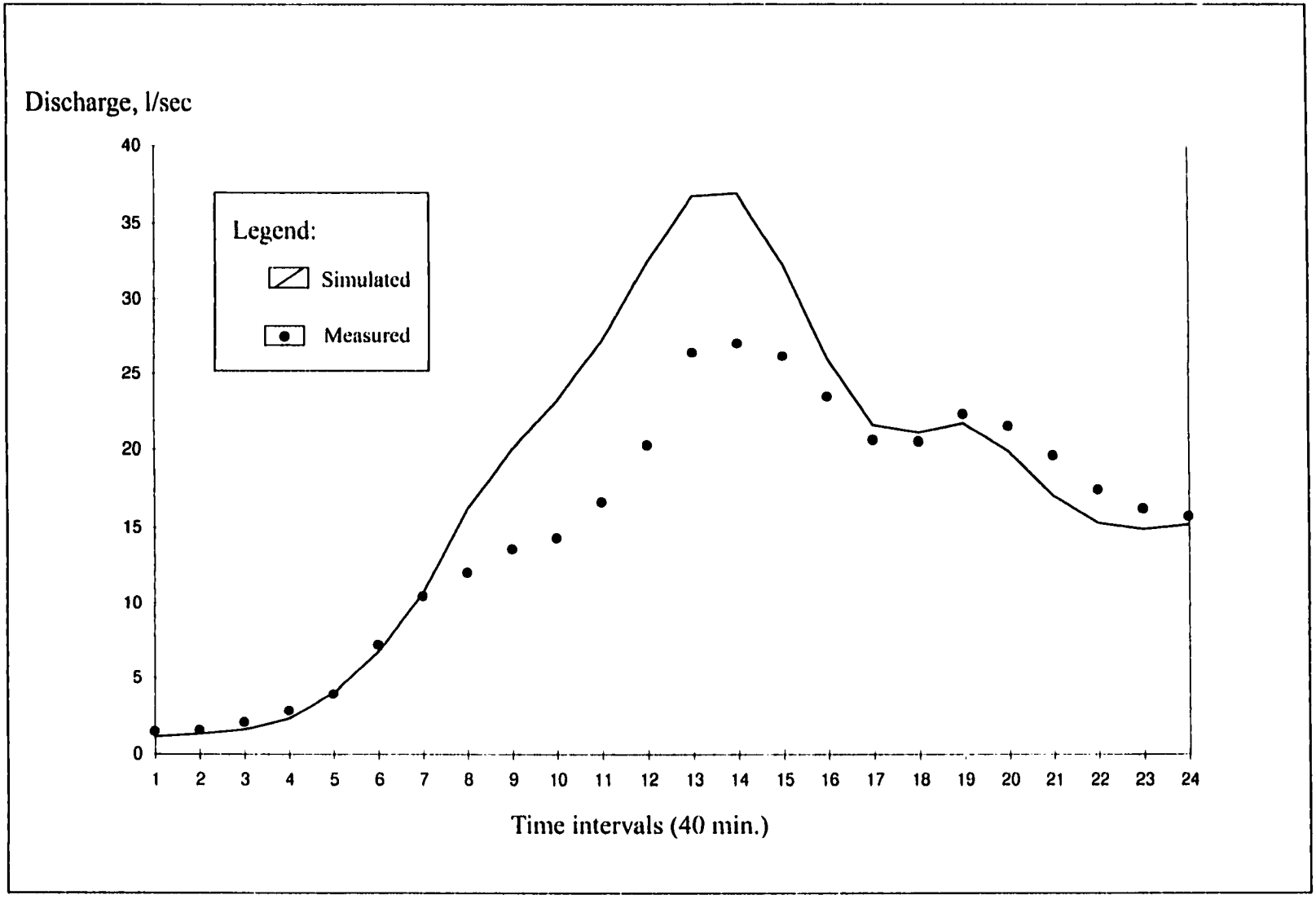

Figure 4.14. Flow modeling results for test9, comparison between measured and simulated values.

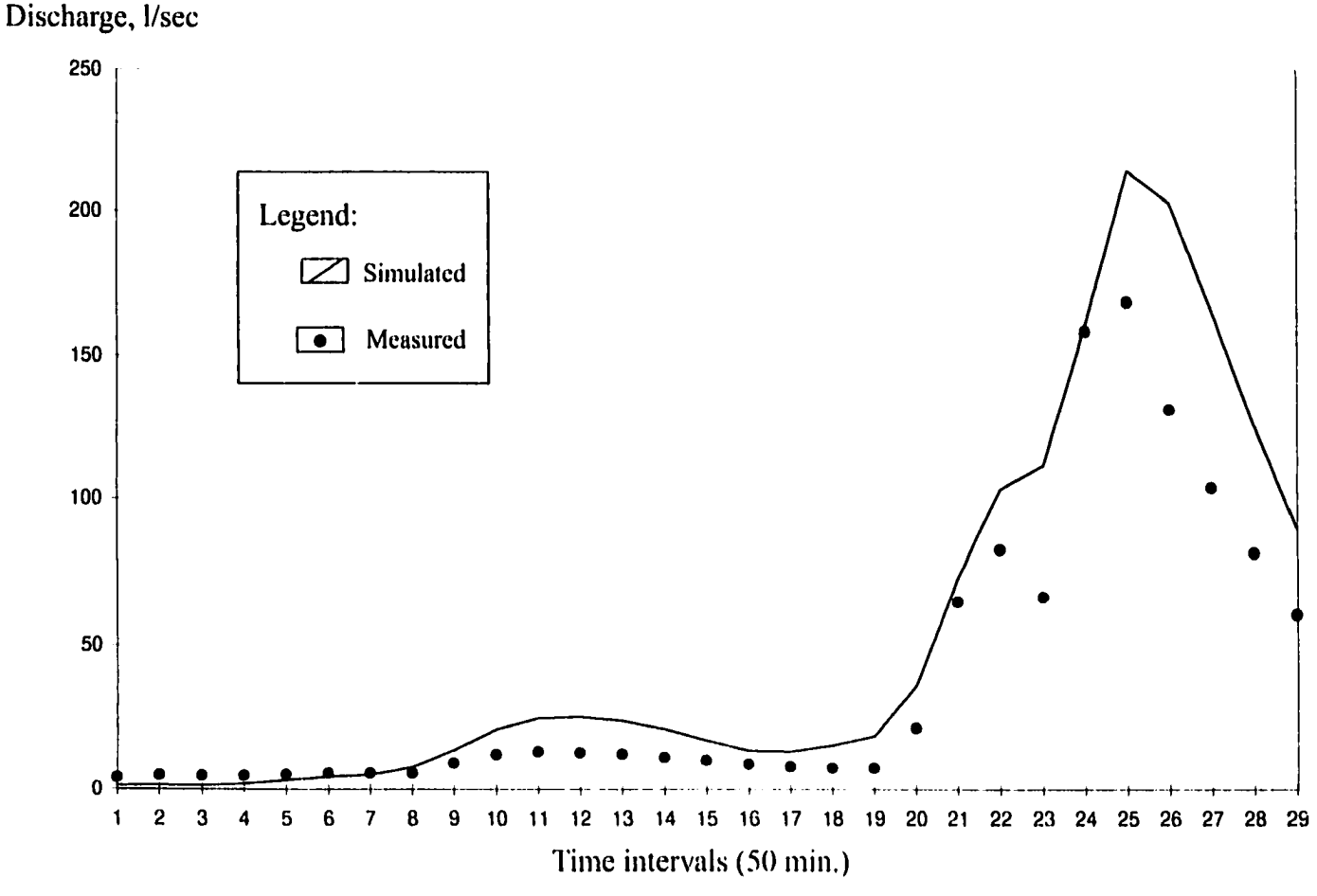

Figure 4.15. Flow modeling results for test 13, comparison between measured and simulated values.

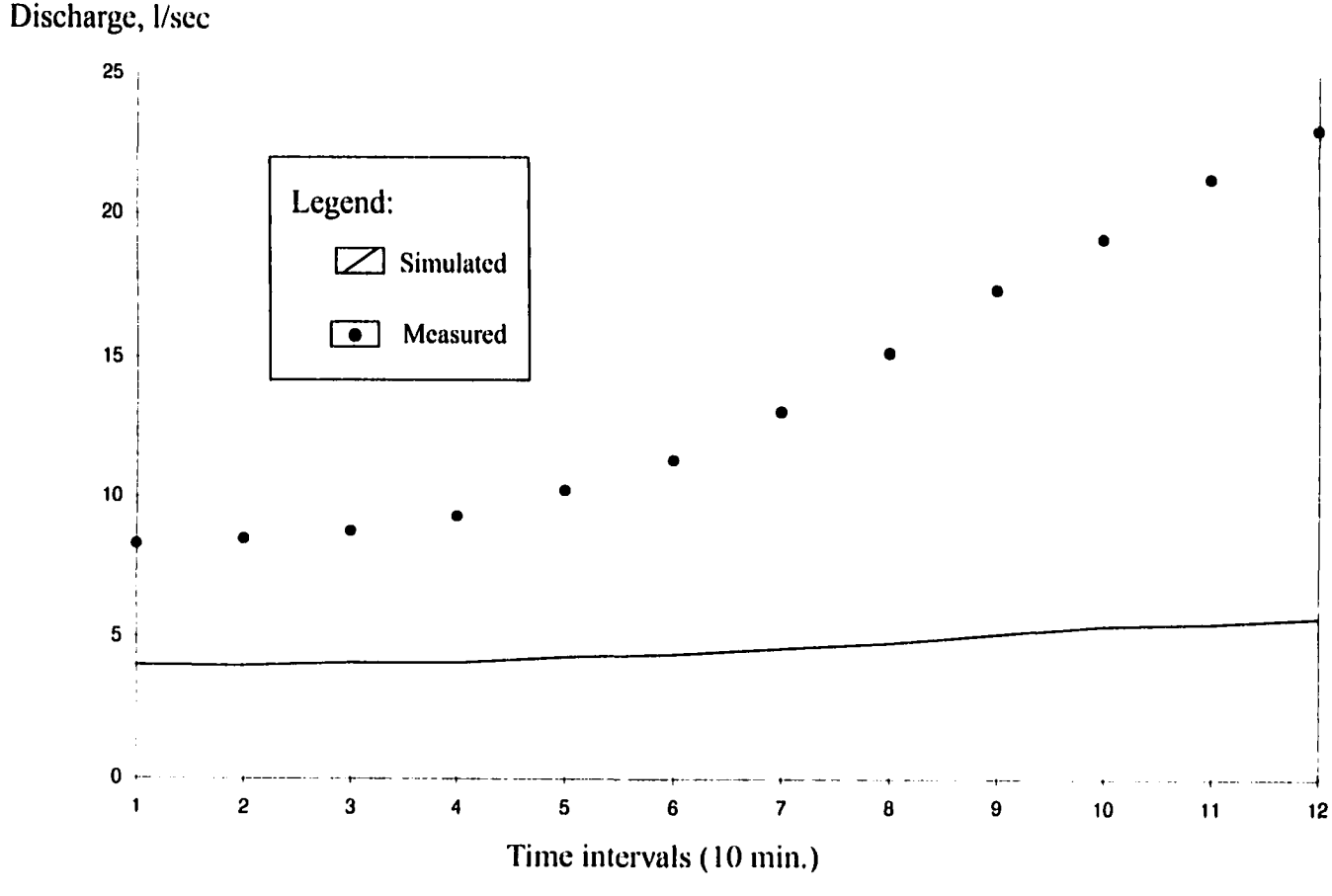

Figure 4.16. Flow modeling results for test 11, comparison between measured and simulated values.

4.5.3. Turbidity Modeling.

After a flow matrix with the routed flow data is formed, it is used as an input for Young's equation. The software component for this procedure is documented in Appendix A as "Kinematic Wave Routing and Turbidity Modeling Code".

Following three steps are being performed consequently:

1. Calculation of the sediment concentration;
2. Calculation of the channel flow transport capacity;
3. Sediment routing through the stream channel and conversion of units from mg/l to NTU, using statistical regression.

Resulting turbidity values are stored in an ASCII, comma delimited file (Table 4.7).

Table 4.7 Output of the "kinematic" code with turbidity values.

ID #	Slope	T1	T2	T3	T4	T5	T6	T7	T8
238	0.07	9.9	9.9	9.9	9.9	10.6	15.0	16.3	13.6
254	0.09	9.9	11.9	15.7	17.7	27.6	72.7	86.5	55.0
255	0.09	9.9	13.1	18.3	20.5	31.7	80.5	97.6	64.7
273	0.09	10.0	14.5	22.1	26.3	41.2	99.5	124.7	88.5
274	0.09	10.2	17.2	29.2	35.8	53.7	122.1	155.3	114.1
298	0.04	9.9	9.9	10.1	10.4	11.7	18.4	22.6	18.0
325	0.04	9.9	9.9	10.3	10.8	12.1	19.3	24.0	19.2
330	0.00	9.9	9.9	9.9	9.9	9.9	9.9	9.9	9.9
358	0.06	10.3	11.4	15.9	19.5	26.5	53.5	73.4	60.1
360	0.06	10.4	11.6	16.3	19.9	27.3	55.3	76.2	62.9
353	0.06	10.6	11.9	16.8	20.7	28.6	58.5	81.2	65.7
354	0.04	9.9	9.9	10.6	11.6	13.7	23.0	30.9	25.2
385	0.04	9.9	9.9	10.8	11.8	14.2	24.5	33.6	26.9

Table 4.7 Output of the "kinematic" code with turbidity values.

ID #	Slope	T1	T2	T3	T4	T5	T6	T7	T8
380	0.03	9.9	9.9	9.9	10.0	10.7	14.9	19.0	15.8
381	0.03	9.9	9.9	9.9	10.1	10.8	15.4	19.8	16.4
407	0.06	12.5	14.6	21.3	27.0	38.3	81.5	115.7	90.2
408	0.06	12.8	14.9	21.9	27.8	39.4	83.7	118.9	92.2
409	0.07	16.9	20.6	32.4	42.1	61.3	131.2	187.2	148.3
410	0.07	17.3	21.4	34.0	44.0	63.7	135.6	193.4	153.8
432	0.09	33.3	43.1	69.8	90.4	131.0	271.9	382.7	304.4
431	0.00	9.9	9.9	9.9	9.9	9.9	9.9	9.9	9.9
445	0.03	9.9	9.9	10.1	10.6	11.8	17.8	24.9	22.3
452	0.03	9.9	9.9	10.2	10.7	12.1	18.7	26.4	23.6
473	0.00	9.9	9.9	9.9	9.9	9.9	9.9	9.9	9.9
464	0.03	9.9	9.9	10.2	10.7	12.1	18.5	26.8	25.4
465	0.03	9.9	9.9	10.2	10.8	12.4	19.0	27.6	26.1
489	0.06	0.0	0.0	0.0	0.0	0.0	103.5	159.5	0.0
490	0.10	68.0	72.9	106.0	142.2	203.4	391.2	581.2	548.0
503	0.10	70.4	76.7	111.3	148.7	212.6	407.3	601.2	564.3
492	0.10	71.2	77.4	112.0	149.4	213.2	408.1	602.2	0.0
491	0.04	11.2	11.5	13.6	16.1	21.2	39.6	60.4	56.2
504	0.19	410.7	449.7	627.3	808.1	1115.2	1978.3	2789.0	2633.4
505	0.19	418.8	459.4	639.8	822.3	1133.9	2007.0	2823.6	2664.6
513	0.06	21.5	23.6	33.1	43.5	62.7	123.4	186.7	173.7
512	0.00	9.9	9.9	9.9	9.9	9.9	9.9	9.9	9.9
548	0.03	10.0	10.1	10.5	11.4	13.2	19.9	29.8	31.4
555	0.03	10.0	10.1	10.7	11.6	13.7	21.3	31.9	33.2
576	0.06	26.5	30.2	39.6	50.1	70.2	136.0	212.0	209.5

ID# refers to unique numbers of the stream segments. T1 ... T8 are turbidity values for each modeled time interval.

4.5.4. Turbidity Model Calibartion.

Turbidity phenomenon unlike flow doesn't have directly related variables, like for example channel width or depth. At the same time turbidity is a parameter related to suspended sediment concentration. This gives an opportunity to use variables, related to suspended sediment concentration, such as channel depth or width. Since width was already used for flow calibration, depth was chosen as calibration parameter. It considerably affects channel flow sediment capacity (Tr) and dimensionless actual lift force (T). The depth-flow ratio, $H = \alpha Q^{\beta}$, where H is depth and Q is discharge, described earlier, was used for calibration of turbidity. Parameter α was found to produce satisfactory results with values 0.002 for MB-3 and MB-8 sampling sites and 0.04 for site MB-4. These values will differ for other watersheds, depending on channel morphometry.

5. Results.

5.1 Measured Field Data.

Figures and tables in Appendix B represent measured data: rainfall, discharge and turbidity. Discharge was measured at site MB-1, turbidity at sites MB-2, MB-3 and MB-8, and rain was measured by the rain gauge located near the outlet of the Malcolm Brook basin. Most of the data in the figures of Appendix B display the following pattern of behavior: the peak of rain is followed by the peak of turbidity, and the peak of turbidity is followed by the peak of discharge. In some cases, the peak of turbidity coincides with the peak of discharge (storms 6, 7, 15). This also occured twice during storm 8.

Table 5.1 contains a summary of general hydrologic characteristics of storm data. The most lengthy storm (storm 13, 23.3 hr.) was observed on July 24, 1997. The shortest storm (storm 1 , 1.2 hr.) was observed on July 1, 1996. Storm intensity ranged from 0.01 in/hr (storms 12, 14, 16) to 0.68 in/hr (storm 1). Cumulative rainfall was calculated as the sum of rainfall depth per time interval, multiplied by the watershed area (0.33 km^2) and converted into liters to comply with the discharge units of measurements. Cumulative discharge was calculated as the sum of discharge rates (L/sec) multiplied by the time interval in seconds. Calculated runoff coefficients represent the ratio of cumulative discharge and cumulative rainfall. Coefficients range from 0.01 to 1.10. The maximum value of this ratio can be only 1.0. The value of 1.10 can be explained by an additional water source discharging into the stream during the storm. Time lags between peak rainfall and peak discharge were calculated from the graphs in Appendix B (measured data). These values range from 20 to 120 minutes.

Table 5.1 Observed hydrological characteristics of storm events measured at Malcolm Brook.

Storms	Duration (hr.)	Intensity in/hr	Cumulative Rain, Lx 10^5	Cumulative Discharge, L x 10^5	Calculated Runoff Coefficients	Time Lag between peak rainfall and peak discharge (min)
1	1.2	0.68	67.3	0.5	0.01	20
2	5.3	0.10	41.9	4.1	0.10	100
3	2.5	0.21	42.7	1.5	0.04	60
4	8.5	0.15	105.1	9.7	0.09	120
5	11.5	0.19	178.0	35.9	0.20	120,60,60
6	8	0.08	52.6	4.4	0.08	120
7	6.7	0.17	92.3	15.1	0.16	40, 40
8	20	0.22	356.0	116.9	0.33	120, 120, 60
9	6	0.05	23.0	10.7	0.46	60
10	1.8	0.10	14.8	0.6	0.04	20
11	1.8	0.12	18.1	0.9	0.05	70
12	4.7	0.01	5.8	1.6	0.28	60
13	23.3	0.02	32.0	35.0	1.10	90
14	8.7	0.01	8.2	5.6	0.68	40, 80
15	10.8	0.02	14.8	4.5	0.31	50
16	15.3	0.01	7.4	7.0	0.95	120, 90

A few storms (5, 7, 8,14, 16) have 2 or 3 peaks of rainfall and discharge, therefore resulting in more than one time lag. Normally, all consequent time lags are less than previous ones, except storm 14, when the second time lag is longer than the first one. Simulated travel time during model runs did not exceed 140 minutes, which corresponds well with the maximum lag time recorded, which is 120 minutes.

5.2 Hydrological Modeling

Calibration of the hydrological model was described in section 4.5. Hydrological modeling may be broken down into two main parts: GIS and kinematic wave routing. In presented model both parts were programmed with different software. GIS software works very slowly (approximately 7-12 hours per simulation). Therefore, the calibration process was very slow and had to be done manually, using the method of comparison between measured and predicted datasets. Figure 5.1 shows the scatter plot of all data used for calibration.

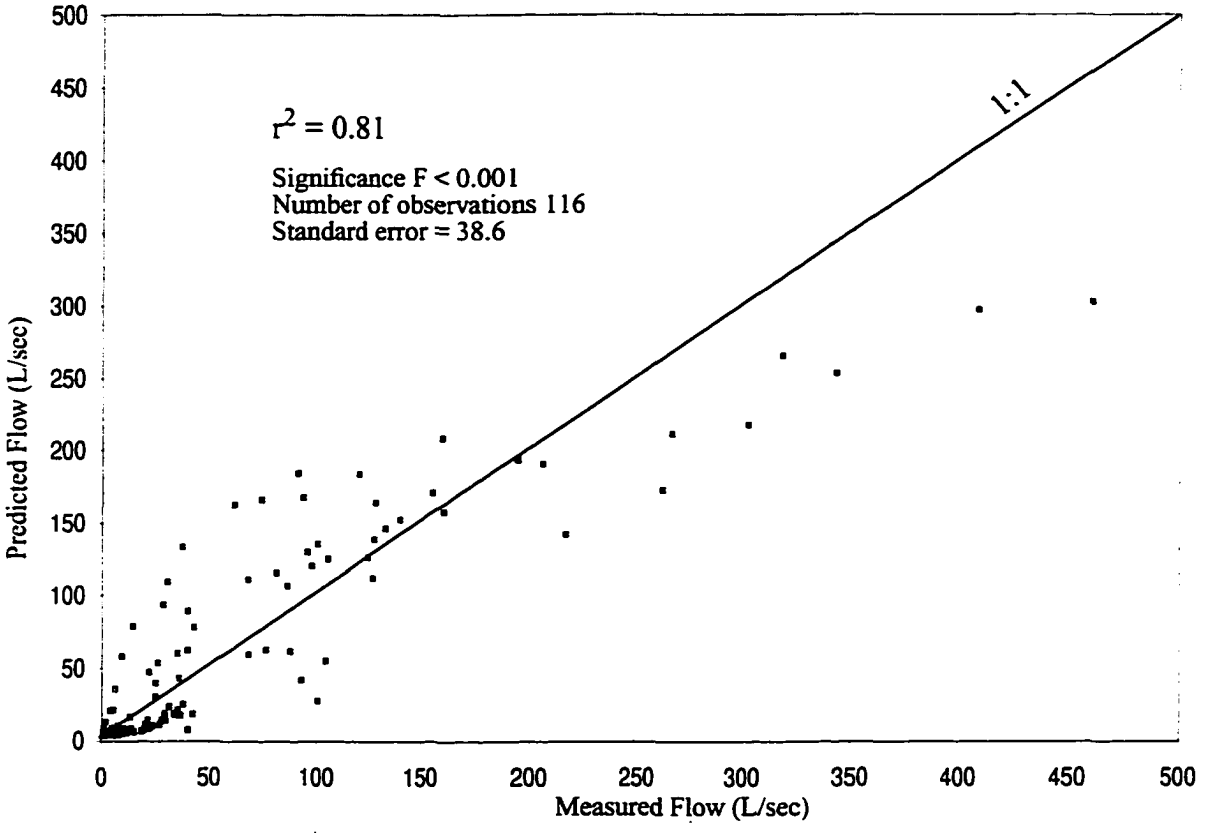

Figure 5.1 Predicted *vs.* measured flow for the 8 storm events, used for model calibration

Figure 5.2 shows a scatter plot of all data used for verification i.e., eight storms. It displays the relationship of measured and simulated data to the 1:1 line. The majority of model runs are above the 1:1 line indicating that the model tends toward overprediction of flow. The correlation coefficient (r^2) is a measure of the degree of closeness of the linear relationship between measured and simulated values. For all the verification data included here (Figure 5.2), r^2 equals 0.85. Appendix D contains the results of all individual storms.

Table 5.2 shows statistical parameters for each storm. These parameters include the number of points, i.e., the number of modeled intervals for the storm, the coefficient of correlation, the root mean square error (RMSE), the measured peak discharge, the modeled peak discharge, and the difference of these in discharge rate (L/sec) and percentage (%) of measured peak discharge. RMSE is an estimate of the average error between simulated and measured values. RMSE is given in both percentage and flow units and ranges from 22% to 386%. Peak discharge is important as a design parameter for the storm drainage systems. Differences indicate how well the model can predict discharge peaks.

For the eight individual storm tests used for verification (tests 9 through 16), r^2 ranges from 0.80 to 0.99. Four individual model runs of simulated flow for 1997 data are illustrated in Figures 5.3 through 5.6. These were chosen for more detailed display and discussion because they represent both overpredicted (Figures 5.3, 5.4) and underpredicted (Figures 5.5, 5.6) results. Each plot displays the simulated and measured flows vs. time (i.e., hydrographs).

Storm 16 displayed in Figure 5.3 was modeled using rainfall data divided into 24 time intervals of 40 minutes each. The total length of this storm was 15.3 hours. The

maximum measured rainfall was 0.06 inches at time interval 12. This run shows the lowest RMSE (21%) and a correlation coefficient (r^2) of 0.85. The first peak in discharge at time interval 14 was predicted with an accuracy of 37%. The second peak in discharge at time interval 19 was predicted with an accuracy of 3%.

Storm 13 displayed in Figure 5.4 was modeled using rainfall data divided into 29 intervals of 50 minutes each. The total length of this storm was 23.3 hours. The maximum measured rainfall was 0.56 inches at time interval 24. This run showed an RMSE of 59% and high correlation ($r^2 = 0.95$). The first peak discharge at time interval 12 was predicted with an accuracy 88%, the second peak discharge at time interval 22 was predicted with accuracy 25% and the third peak discharge at time interval 25 was predicted with an accuracy 27%.

Storm 11 displayed on Figure 5.5 was modeled using rainfall data divided into 12 intervals of 10 minutes each. The total length of the storm was 1.8 hour. The maximum measured rainfall was 0.03 inches at time interval 5. This run shows an RMSE of 63% and highest correlation ($r^2 = 0.99$). There are no distinct peaks in discharge. Storm was weak and represents light rainfall rather than a storm event.

Storm 10, displayed in Figure 5.6 was modeled using rainfall data divided into 12 intervals of 10 minutes each. The total length of the storm was 1.8 hour. The maximum measured rainfall was 0.04 inches at time interval 8. At time intervals 3,4 and 9 the rain stopped and rainfall input values were equal to zero. This run has a good RMSE of 41% and a correlation coefficient of 0.81. Similar to the case of storm 11, there are no distinctive peaks and the data represents a rain event rather than a more intense storm event.

Appendix C shows input files (test 9 - test 16) which were used for calibration. Appendix D contains results of all hydrological predictions for individual storms.

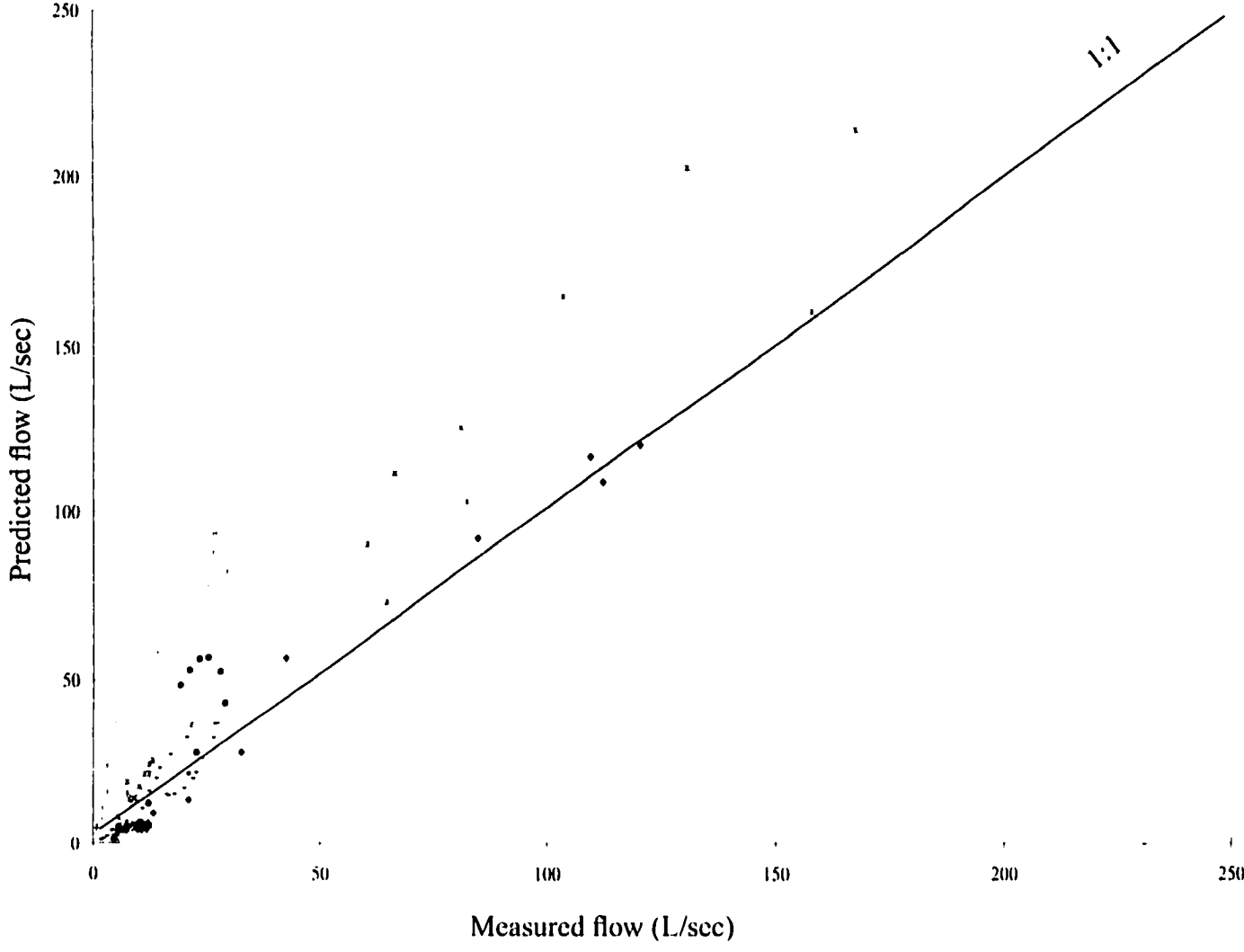

Figure 5.2 Predicted *vs.* measured flow for the 8 storm events, used for model verification.

Table 5.2 : Statistical parameters of hydrological predictions

Model Runs:	Number of points	r^2	RMSE, L/sec	RMSE, %	Measured peak, L/sec	Predicted peak, L/sec	Peak Difference L/sec (%)
Calibration Data Sets:							
Storm 1, July 3, 1996	8	0.75	5	27	22	9	-13 (59)
Storm 2, June 30, 1996	9	0.91	9	32	35	21	-14 (39)
Storm 3, July 31, 1996	16	0.97	9	44	42	19	-23 (55)
Storm 4, Sept. 16, 1996	18	0.85	54	354	128	164	+36 (28)
Storm 5, Oct. 8, 1996	24	0.86	30	50	38 105 266	25 125 211	-12 (67) +20 (19) -55 (21)
Storm 6, Aug. 13, 1996	9	0.96	15	110	40	63	+23 (58)
Storm 7, Sep. 28, 1996	11	0.63	34	66	100	28	-72 (72)
Storm 8, Oct. 19, 1996	21	0.91	62	49	160 461	158 303	-2 (1) -159 (34)
Verification Data Sets:							
Storm 9, Nov. 9, 1996	13	0.99	7	32	121	120	-1 (1)
Storm 10, May 1, 1997	12	0.81	4	41	12	6	-7 (55)
Storm 11, May 6, 1997	12	0.99	10	63	23	6	-17 (75)
Storm 12, June 3, 1997	14	0.85	4	36	14	12	-2 (14)
Storm 13, July 24, 1997	29	0.99	25	59	13 83 168	25 103 214	+12 (88) +21 (25) +46 (27)
Storm 14, Aug. 20, 1997	14	0.80	19	68	29	43	+13 (45))
Storm 15, Oct. 24, 1997	14	0.96	40	386	29	82	+53 (181)
Storm 16, Oct. 26, 1997	24	0.85	5	21	27 22	37 22	+10 (37) -1 (3)

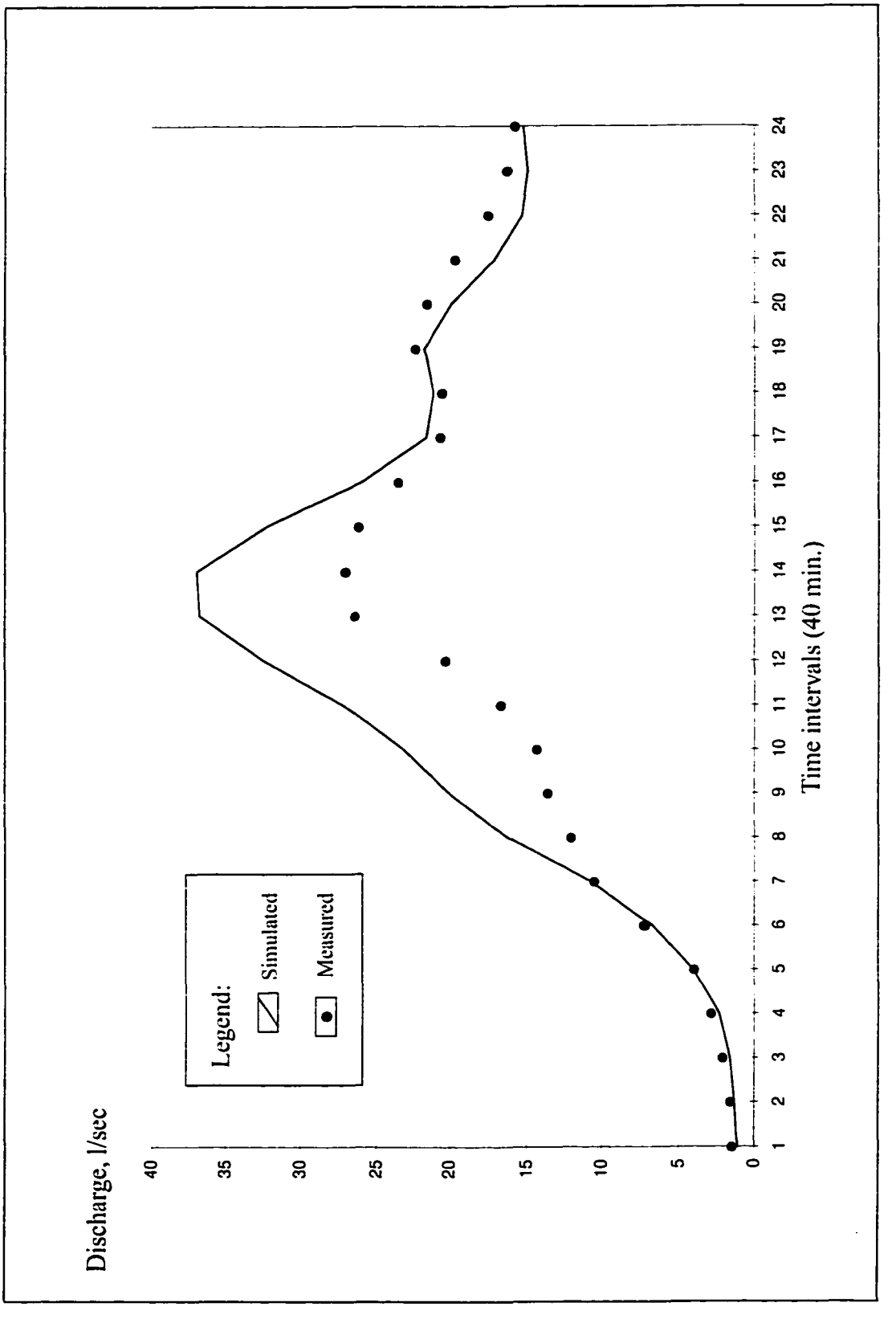

Figure 5.3 Storm 16, October 26, 1997. Comparison between measured and simulated hydrographs.

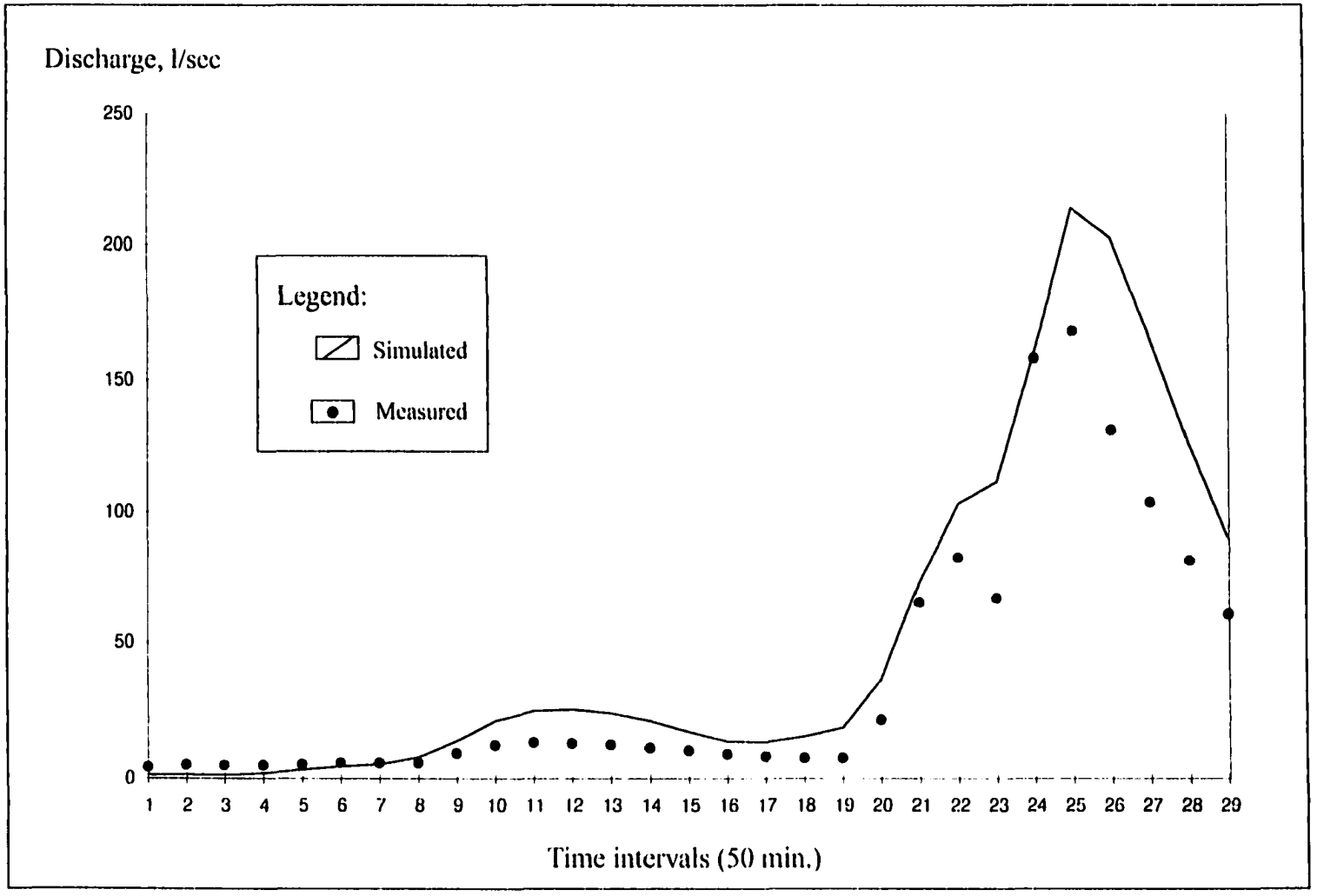

Figure 5.4 Storm 13, July 24 1997. Comparison between measured and simulated hydrographs.

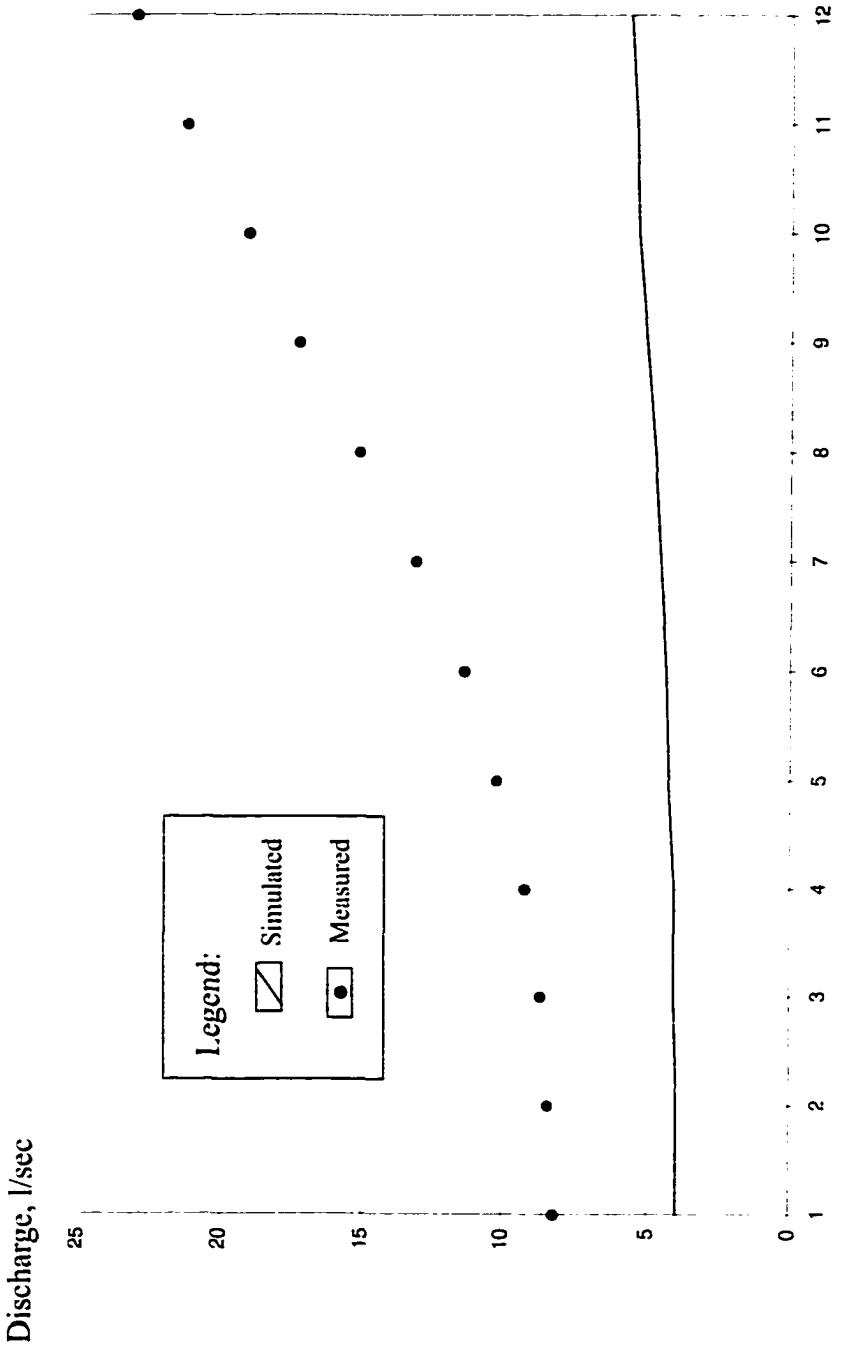

Figure 5.5 Storm 11, May 6, 1997. Comparison between measured and simulated hydrographs.

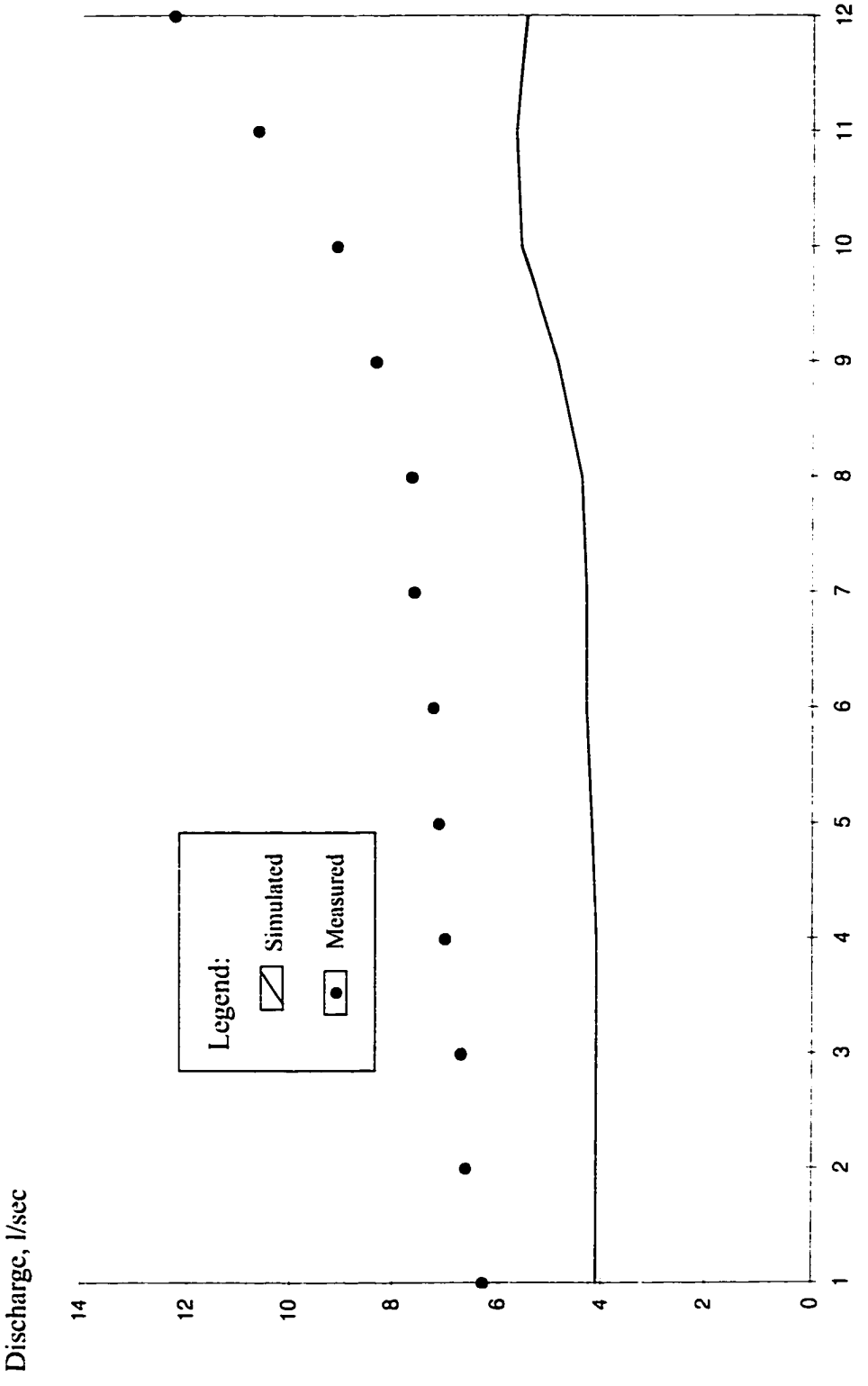

Figure 5.6 Storm 10, May 1, 1997. Comparison between measured and simulated hydrographs.

5.3 Turbidity Modeling

The input flow values for turbidity modeling was the discharge output obtained from hydrological modeling. In the hydrological modeling step, simulated discharge was calibrated using data from site MB-1. Upon obtaining satisfactory results, discharges for sites MB-3, MB-4 and MB-8 were taken from simulated hydrographs. Therefore, turbidity predictions were based on simulated hydrographs for three specific sites. The advantage of the hydrological modeling proposed here is that it is spatially distributed, therefore allowing predictions for any place on the stream channel.

Results of simulation for three sites were combined together. Figures 5.7 through 5.9 show scatter plots of simulated *vs.* measured turbidity data for three sites: MB-3, MB-4, MB-8. If storms are combined for each site, results show low correlation. The best correlation ($r^2 = 0.40$) was achieved for the site MB-8. For sites MB-3 and MB-4, r^2 equalled 0.04 and 0.13, respectively. Higher correlations were achieved for single storm events such as test 4, sites MB-3 and MB-4, test 6, sites MB-3 and MB-4, test 9, site MB-3, test 10, MB-8, test 11, site MB-8, test 14, site MB-4. Appendix E contains results of turbidity modeling for each individual storm.

Table 5.3 shows statistical parameters for each storm. Similar parameters are described in the previous section on hydrological modeling. RMSE ranges from 60% to 16636%. For the verification dataset (storms 9 through 16), RMSE ranges from 25.3% to 534%. The difference between measured and predicted peaks for the verification dataset ranges from 1% to 108%.

Table 5.3 Statistical parameters of conducted turbidity tests

Test	Number of points	r^2	RMSE, NTU (%)	Measured Peak, NTU	Predicted Peak, NTU	Peak Difference,* NTU (%)
Calibration Data Sets:						
Test 1, July 3, 1996						
MB-3	8	0.44	297 (91)	773	12	+761 (98)
MB-4		0.91	35 (16636)	15	52	-37 (264)
Test 2, June 30, 1996	9					
MB-3		0.003	4 (60)	61	12	+49 (81)
MB-4		0.56	8 (11487)	132	85	+47 (35)
Test 4, Sep. 16, 1996	18					
MB-3		0.90	62 (38)	110	139	-30 (27)
				188.	295	-107 (57)
MB-4		0.79	49 (43)	143	136	+7 (5)
				160	176	+16 (10)
Test 5, Oct. 8, 1996	24					
MB-3		0.22	124 (81)	190	14	+177 (93)
				215	193	+22 (10)
				688	305	+383 (56)
MB-4		0.19	782 (149)	127	129	-2 (1)
				893	102	+791 (89)
				2202	151	+2051 (93)
Test 6, Aug. 13, 1996	9					
MB-3		0.78	36 (372)	165	89	+76 (46)
MB-4		0.69	205 (122)	570	99	+471 (83)
Test 7, Sep. 28, 1996	11					
MB-3		0.11	108 (61)	247	24	+223 (90)
MB-4		0.29	37 (34)	133	136	-3 (2)
Test 8, Oct. 19, 1996	21					
MB-3		0.39	299 (604)	38	38.	0 (0)
				127	210	-83 (66)
				114	433	-319 (281)
MB-4		0.47	81 (181)	90	85	+5 (5)
				96	156	-60 (63)
				156	226	-70 (45)
Verification Data Sets:						
Test 9, Nov. 9, 1996	13					
MB-3		0.92	41 (31)	280	183	+98 (35)
Test 10, May 1, 1997	12					
MB-4		0.002	21 (437)	28	29	-1.4 (5)
MB-8		0.78	8 (365)	5	11	-55 (108)

(table continued on the following page)

Table 5.3 Statistical parameters of conducted turbidity tests (continued)

Test	Number of points	r^2	RMSE, NTU (%)	Measured Peak, NTU	Predicted Peak, NTU	Peak Difference,* NTU (%)
Test 11, May 6, 1997	12					
MB-4		0.25	22 (40)	56	31	+25 (44)
MB-8		0.44	50 (81)	84	11	+73 (88)
Test 12, June 3, 1997	15					
MB-4		0.10	19 (58)	30	31	+1 (3)
				30	53	+23 (77)
MB-8		0.02	35 (67)	65	11	-54 (84)
				66	11	-55 (84)
				54	21	-33 (62)
Test 13, July 24, 1997	29					
MB-4		0.40	45 (60)	109	70	+39.4 (36)
				65	52	+12.7 (20)
				147	146	+1.4 (1)
				174	212	-38.3 (22)
MB-8		0.42	110 (60)	60	31	+29 (48)
				270	110	+160.3 (59)
				697	270	+427.4 (61)
				290	79	+211.2 (73)
Test 14, Aug. 20, 1997	14					
MB-4		0.59	26 (25)	125	70	+54.8 (44)
MB-8		0.10	312 (57)	64	44	+20.0 (31)
Test 15, Oct. 25, 1997	14					
MB-4		0.17	49 (535)	90	79	+11 (12)
MB-8		0.02	41 (111)	60	86	-27 (44)

* difference = measured - predicted; % = difference / measured;

Most of the peak differences show overprediction of turbidity values for the verification dataset. Underprediction values range from 5% to 84%.

As was mentioned before, individual storms show a better correlation than the total number of storms for a specific site. Figures 5.10 through 5.12 show results of three tests. Two tests show examples of good and average correlations and one test shows examples of poor correlation which reflects total average result. Each plot displays simulated and measured turbidity vs. time intervals.

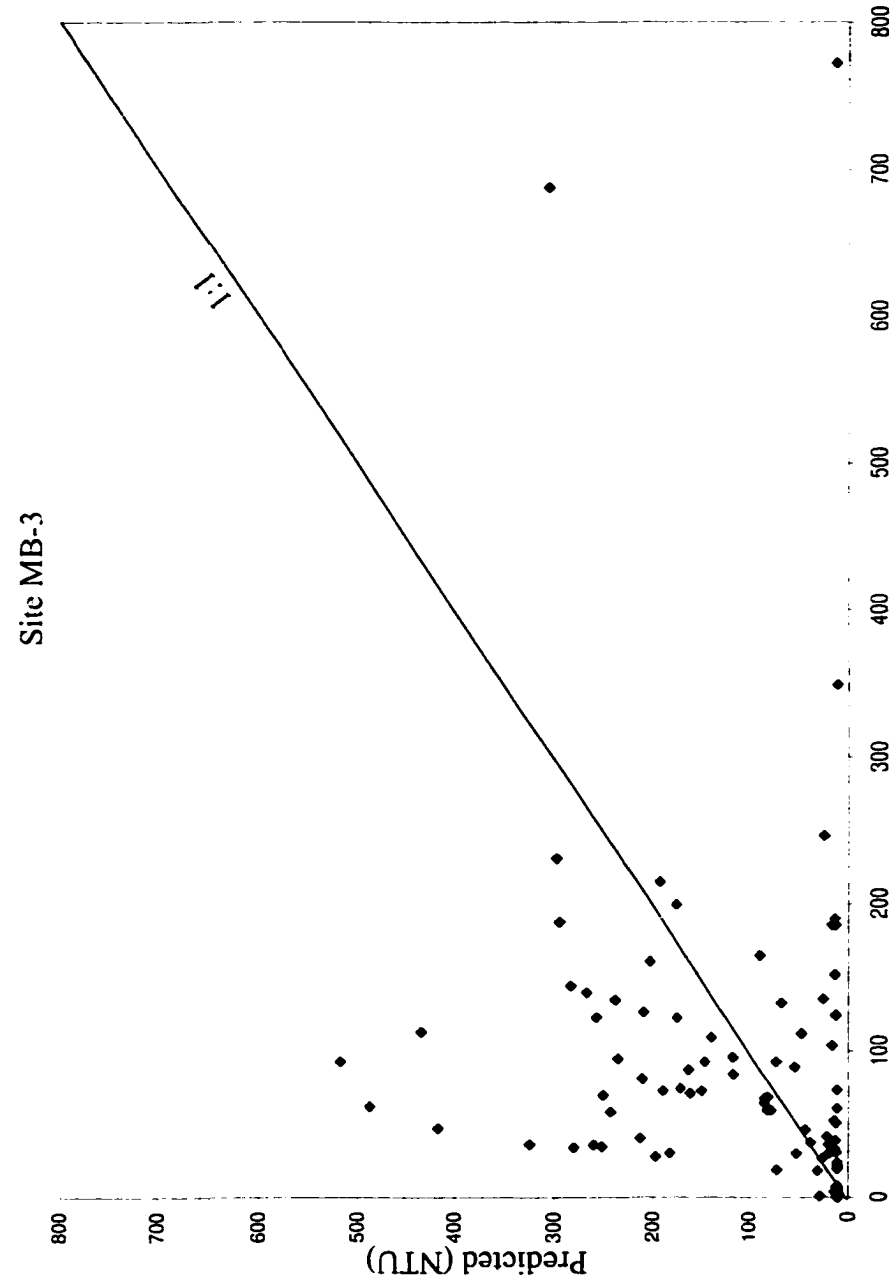

Figure 5.7 Storms at site MB-3. Comparison between measured and simulated turbidity.

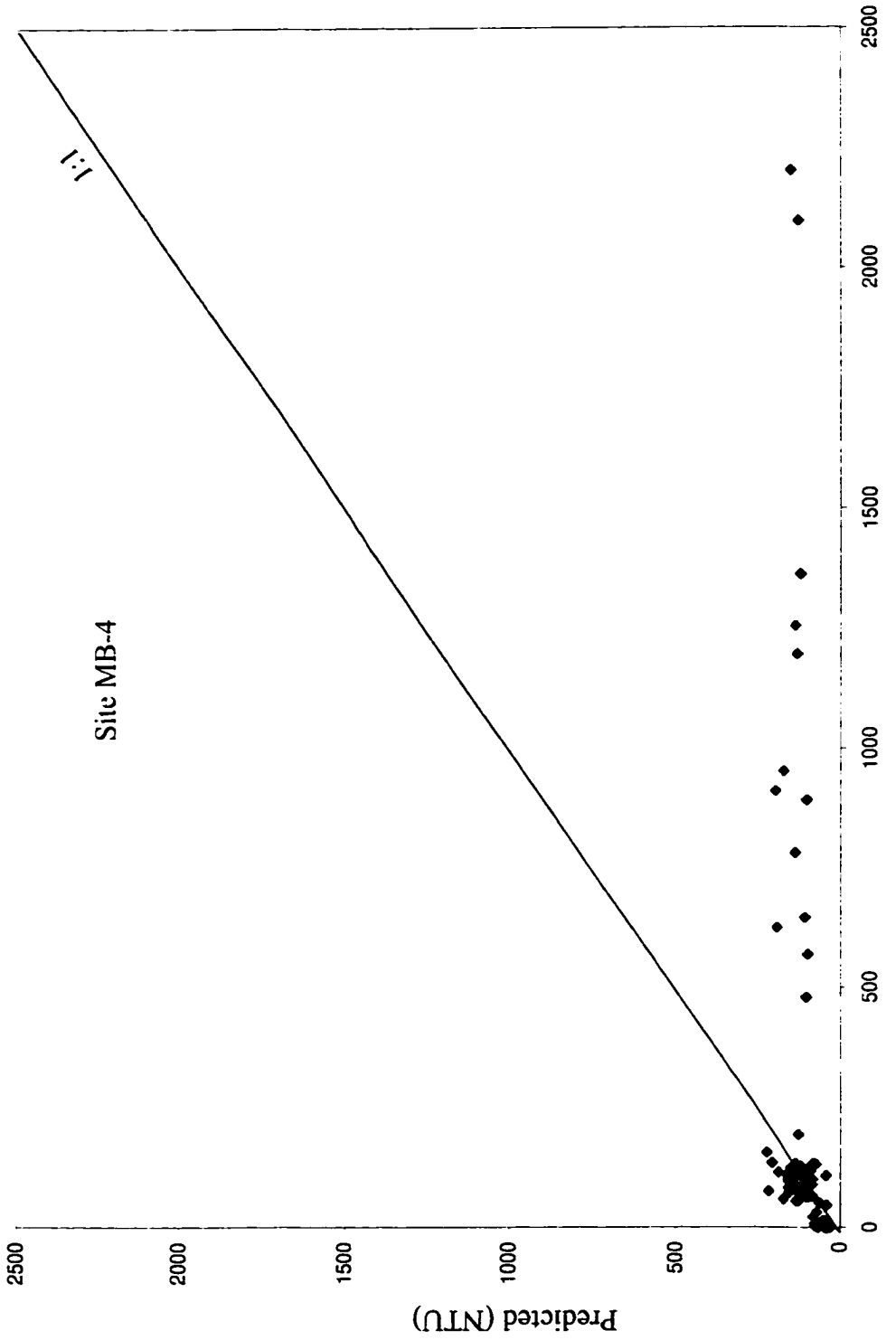

Figure 5.8 Storms at site MB-4. Comparison between measured and simulated turbidity.

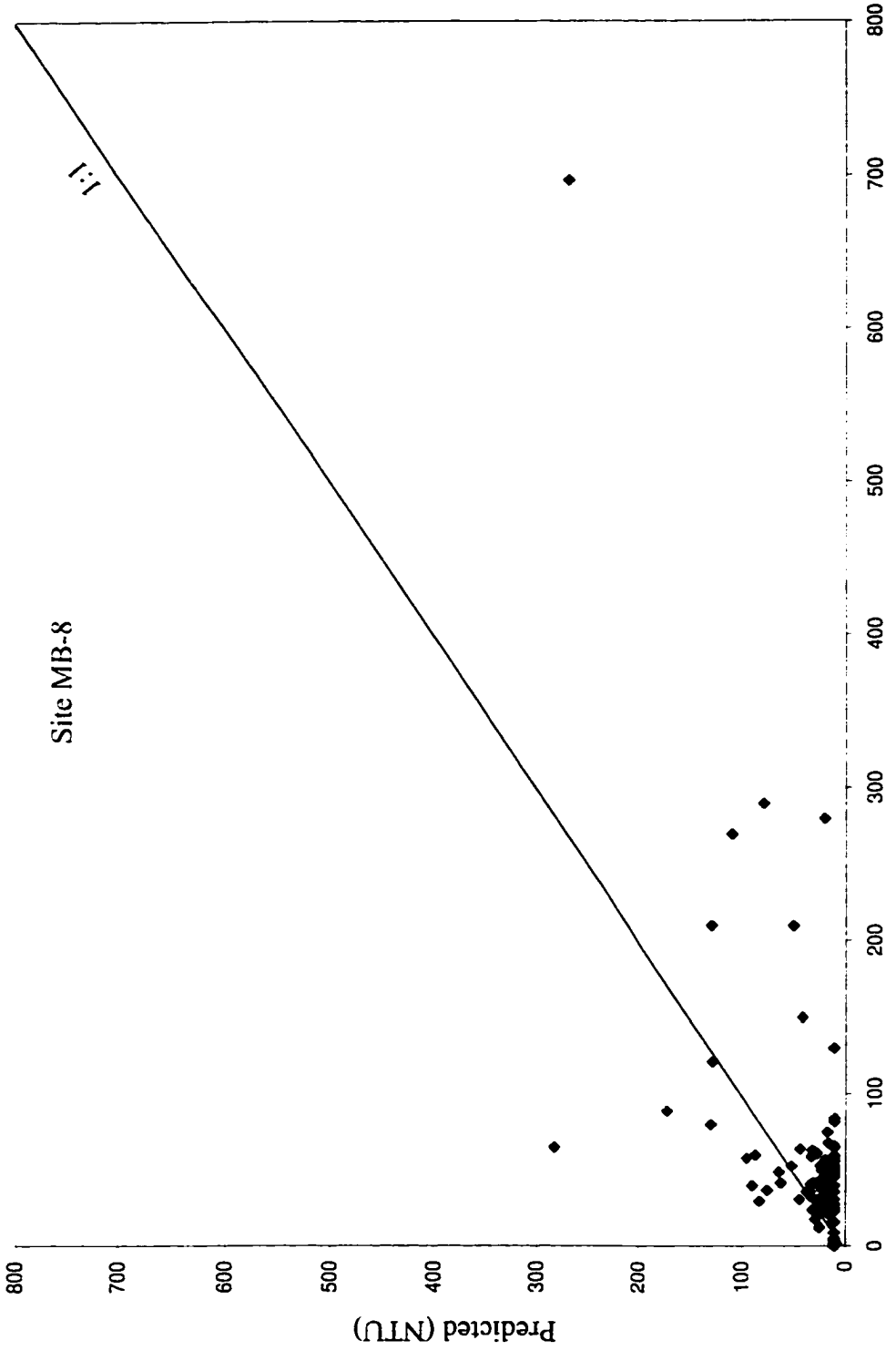

Figure 5.9 Storms at site MB-8. Comparison between measured and simulated turbidity.

Storm 9 (November 9, 1996), site MB-3, displayed on Figure 5.10 is a "classic" storm. The turbidity peak occurs right after the rain peak and before the discharge peak. This storm produced highest coefficient of correlation of 0.92% with a RMSE of 31%. It also showed excellent correlation for hydrological modeling ($r^2 = 0.99$) with a RMSE = 32%. Modeled time intervals equal 30 minutes.

Storm 13, site MB-4, displayed on Figure 5.11 is an example of an average storm, having a relatively low correlation ($r^2 = 0.40$). The RMSE equals 60%. Nevertheless, the simulation curve followed all main peaks at time intervals 6, 10, 22 and 25. Peak differences range from 1% to 36%. During this storm, turbidity peaks followed peaks of rain and preceded discharge peaks for most of the storm's duration. This test, despite low statistical coefficients, shows good simulation pattern for the longest modeled storm (23.3 hr.) divided into 29 intervals, 50 minutes each. At time intervals 2, 14, and 24, measured turbidity values were relatively high and therefore changed statistical parameters. During hydrological modeling, this simulation produced high ($r^2 = 0.95$) coefficient of correlation with RMSE of 59%. Three peak discharge values were modeled with the an error ranging from 25% to 88%.

Storm 15, site MB-8, displayed on Figure 5.12 is an example of the low correlation ($r^2 = 0.02$) with RMSE of 111%. At the same time, simulation shows a good matching pattern within time interval 9 - 14 when both turbidity and discharge increased. Error at the peak equals 44%. During this storm, three peaks of rain were observed. In all cases, the turbidity peak followed the rain peak immediately. The discharge peak occurred only once, at the end of the storm, and coincided with high turbidity. Hydrological modeling for this storm produced a coefficient of correlation $r^2 = 0.96$ and a RMSE of 386%.

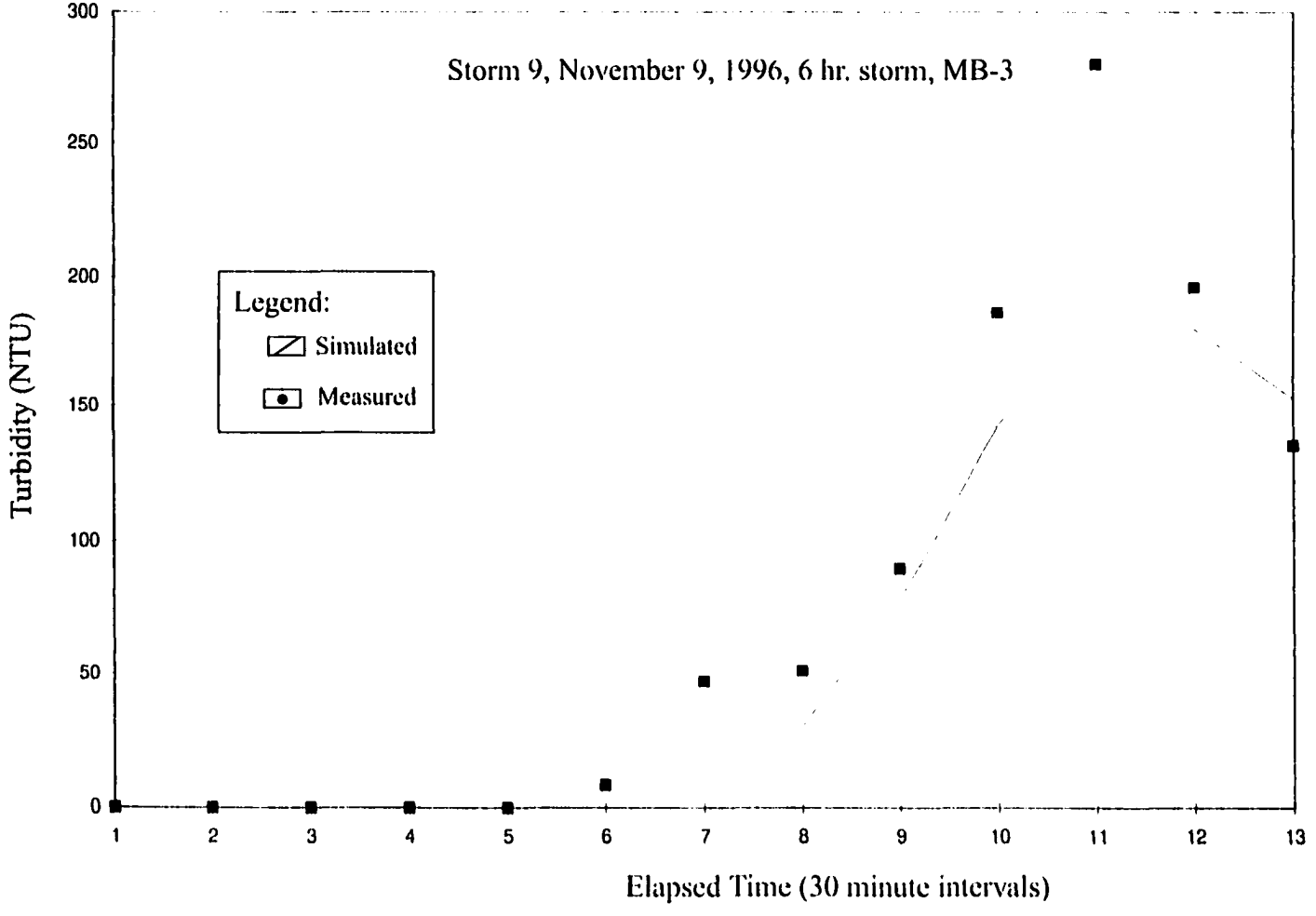

Figure 5.10 Storm 9, Site MB-3. November 9, 1996. Comparison between measured and simulated turbidity.

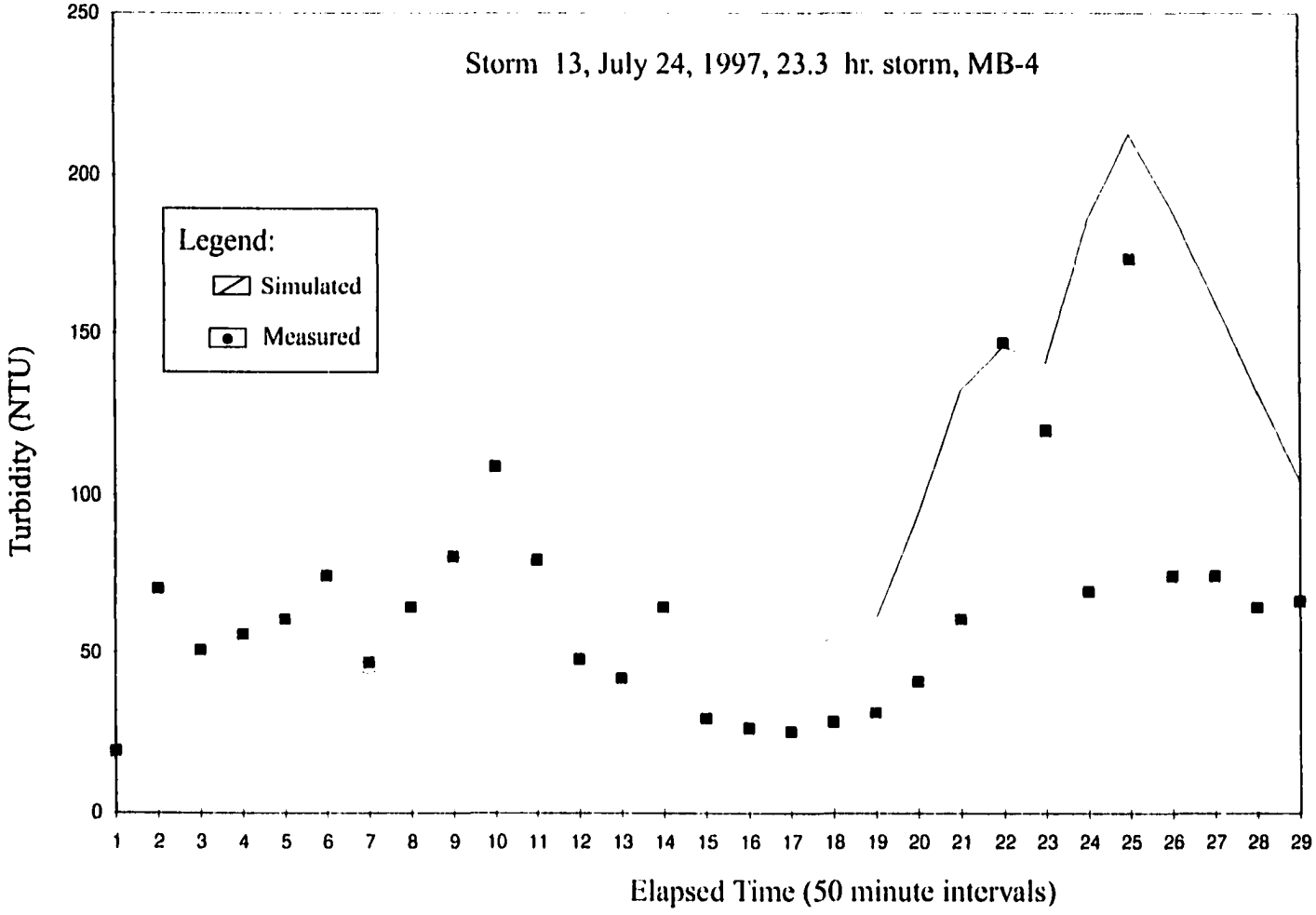

Figure 5.11 Storm 13, Site MB-4. July 24, 1997. Comparison between measured and simulated turbidity.

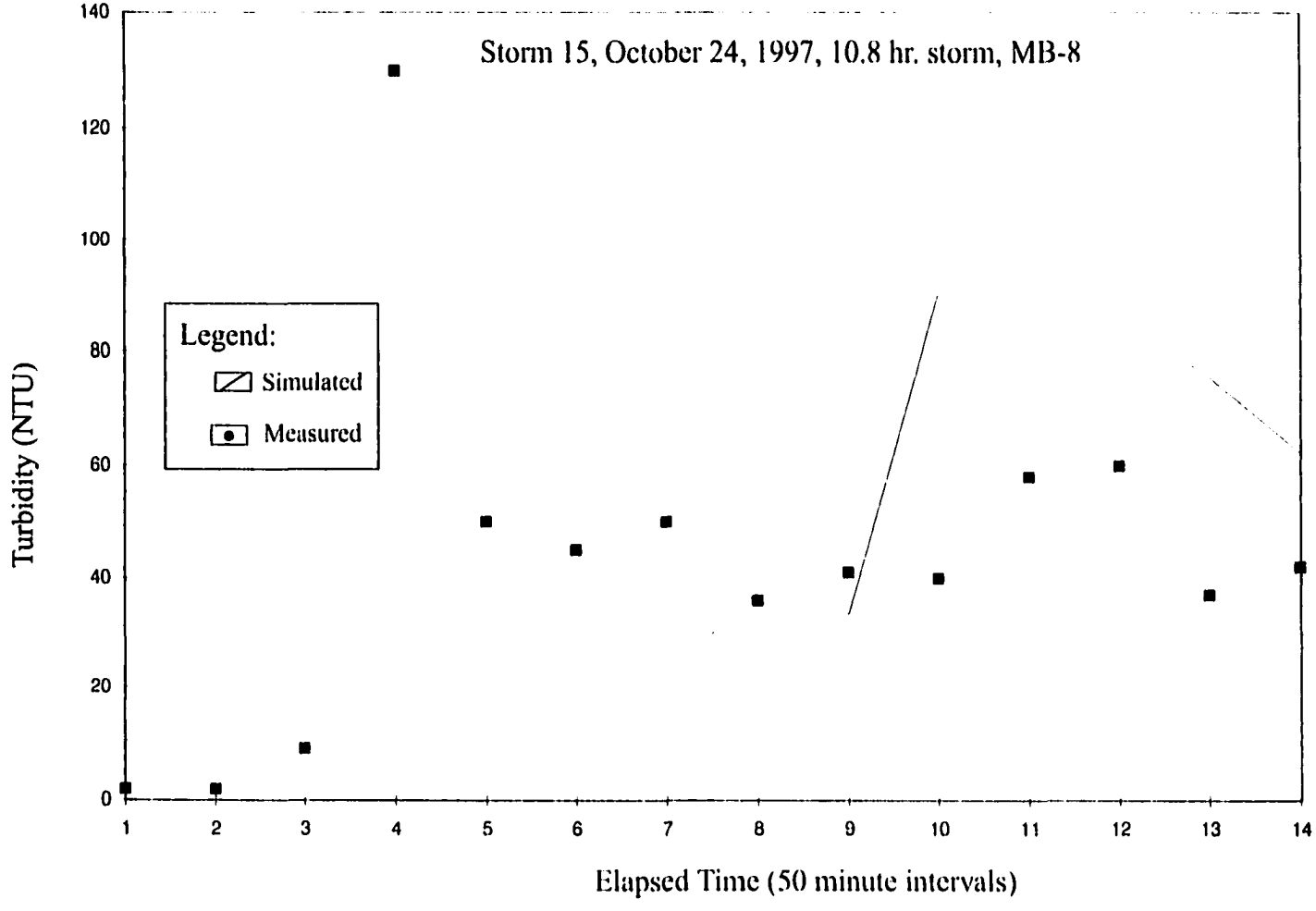

Figure 5.12 Storm 15, Site MB-8. October 25, 1997. Comparison between measured and simulated turbidity.

6. Discussion.

6.1 Measured Field Data.

The duration of rainstorms ranged from 1.2 (storm 1) to 23.3 hours (storm 13). This is based upon actual storm data, in which autumnal storms appeared to be longer (8.5 to 20 hrs.) and summer storms were shorter (1.2 - 8.7 hrs.). Summer storm 13 with 23.3 hrs. duration is an exception among 1996 and 1997 rainstorm data. Intensity of summer storms ranged from 0.01 in/hr to 0.68 in/hr. Autumnal storms intensity ranges from 0.01 in/hr to 0.22 in/hr. Summer storms tended to be shorter, but more intense.

Because the Malcolm Brook watershed is small, and a rain gauge was located within 50 meters from the basin outlet, it was assumed that precipitation was evenly distributed over the area. This is important for spatially distributed modeling because under uneven rainfall distribution over the watershed, the model would have to take this factor into account. This means that the model would have to accept as an input file, a two-dimensional matrix with a variable rainfall distribution, rather than a one-dimensional scalar variable.

Discharge measurements were done at the weir, with a known geometry. Flow stage at the weir was calibrated with discharge according to USGS methodology.

Turbidity measurements were done on three sites using turbidimeters connected with data loggers. Sites MB-3, MB-4 and MB-8 respond differently to turbidity measurements because they have different hydrological and geomorphological settings. Site MB-3 has a wider (when flooded, up to 4 m) bed than the other sites. During normal conditions (base flow) water is running and channel is always wet; it represents a

perennial channel. Site MB-4 is located in a confined V-shaped trench with steep slopes. It can be dry during the summer and autumn depending on rainfall. As soon as rain starts, changes in flow can be dramatic. Surrounding trees are very close to the channel and during high winds can bend. Bending causes roots to move and additional sediment from this activity can influence turbidity. This example was observed during 1997 and 1998 field seasons. A wetland with a small pond is located at the head of this stream segment. Site MB-8 is located at the head of Malcolm Brook. This site can also be dry during rainless days. Its channel when flooded can be 2.5 meters wide. The surronding trees under high winds produce a similar effect to site MB-4, root systems move and supply some additional amount of fine sediments to the channel. Thist does not happen at site MB-8, but happens at some downstream locations.

Turbidity data during storm 3 were measured only at site MB-4. After data were analyzed, it was found that turbidity values were "0". Apparently the data logger did not download data due to a technical problem. Therefore the results of the turbidity simulation for this storm were not included in the table and appendices.

The main factors affecting turbidity measurements were dry channel conditions before storm events and debris clogging the turbidity sensor. Because of the dry conditions, the channel sometimes did not have enough water to cover the sensor. Therefore, the turbidity sensor was hanging in the air until water would reach it, and then the sensor would start storing turbidity data. Floating debris would ocassionally clog the sensor. In this case, turbidity measurements would show extremely high turbidity values until the debris got washed out. Clogging would also create a favorable environment for microorganisms to build up on the surface of the optical elements. This was noticeable as

high values of turbidity (up to 50 NTU) at the end of the storm event, even after the stream became clear. After cleaning the optical elements at the site, the sensor would show normal (0.1 to 2 NTU) characteristic values.

At the beginning of field work in 1996, sensors were tightly attached to the holding rod in the stream channel. During the first two storms it was noticed that this attachement caused accumulation of leaves and debris around the sensor. This problem was eliminated by fastening the sensor's wire to the rod and leaving the sensor itself hanging freely. Thus, under the pressure of accumulated leaves or branches, the sensor would move and release debris to provide access of the flowing water to the sensor.

Measured data with problems described above, were discarded for two of 16 storms when the source of error was identified during storm events by field inspection. In cases, when error was suspected but not verified, data were used in their original form. Better and probably more costly turbidity measurement techniques should be used in further studies.

6.2 Hydrological Modeling.

6.2.1 Model Performance.

The hydrological model presented here conceptualizes how different variables on the watershed influence flow rate and surficial runoff (i.e., channel and lateral flow to the stream). The variables analyzed are coefficients of the surface runoff, contributing areas and slope. This model works on the time scale of a single storm event that may last for a few days using time intervals during the storm ranging from 10 to 50 minutes. Therefore,

some large variability in RMSE can be expected as the result of a dynamically changing environment (e.g. the sharp transition from antecedent conditions, high winds, rain gusts, and channel blockage by falling trees, etc.). Tests 4 and 15 show the highest RMSE, 354% and 386%, respectively. These tests also show high correlation of measured and modeled flows (0.85 and 0.96). The main reason for these high RMSE values are differences between modeled and measured baseflow values. While modeled base flow was 4 L/sec, the measured baseflow was only 0.9 L/sec. This already gives an error of 344%. In the case of the test 14, measured base flow was equal to 0.72 and simulated flow was 4 L/sec, which produced RMSE value equal to 364%. Such errors are inevitable at such fine time scales and flow units of measurement until base flow value can be better predicted. Upon analysing the results, it was found that the value of most flow peaks were predicted with 25-30% of accuracy, while the rest of the curve was highly variable, and it is that variability which increased the average RMSE up to 386%. This variability is the result of large discrepancies on a percentage basis in the modeled vs. simulated results for the baseflow part of the hydrograph. These values highly influenced the RMSE which was calculated as an average for all values of the hydrograph. Figure 5.4 shows that measured discharge values are 2 - 3 times higher than simulated values because of the base flow influence. This happens within time intervals 1 to 4 until time interval 19, after which simulated and measured discharge values vary by 20 to 30%.

Most of the modeled storm simulations overpredict flow. Two simulations of short, 2 hour storms show underprediction. The reason for the model overprediction lies in application of the rational method. According to its description, rational method estimates maximum flow value for the given area. Therefore, simulated flow represent maximum

values. Despite calibration process, verification dataset could cause overprediction due to the antecedent moisture conditions (AMC). Underprediction can be possibly explained by the short time interval of storms, low discharge values and antecedent moisture conditions. Time periods in both simulation equalled 10 minutes which is a time interval of actual measurements. In this case, accuracy of the flow gauge becomes important factor. Both storms have also low flow, i.e. the same magnitude as the baseflow. If under these conditions flow gauge would provide higher flow values, then model would show underprediction. AMC are important factor as well. During model calibration runoff coefficients were calibrated according to the wide range of storm conditions, as for the average AMC. If actual AMC would be wet or saturated, then the model would underpredict. Most of the simulated storms differ considerably from underpredicted ones in terms of duration, seasonality and rain intensity. To account for all different conditions, runoff coefficients were adjusted to satisfy all of them. This could explain the fact that some storms became underpredicted.

GIS allows one to model contributing areas and lateral flow as an input to the hydrological flow routing model. Spatial modeling took into account different watershed characteristics, as well as their location and potential influence on runoff, depending on travel time. A linear relationship was replaced by an exponential one to obtain the radius of contributing areas after extremly high volumes of runoff were predicted during several of the first time steps. From the hydrograph for site MB-1, it was observed that the beginning of the hydrograph rise was accompanied by small discharge values and after a while, the curve would increase rapidly. This lag in response is explained by the process of runoff infiltration into soils. During the initial time intervals, soils act as a sponge,

absorbing water and storing it. After soils become saturated, they release water into the stream. Therefore, surface runoff and ground water combine to contribute water flow into the channel. This process depends on many variables, such as soil conductivity, antecedent moisture conditions, vegetation and geological structures. The best calibration was obtained with coefficient values of 0.1 for *a* and 1.05 for *b*, where *a* and *b* are power coefficients from Leopold and Maddock (1953) equations linking discharge and mean depth. Coefficients were derived empirically during calibration. Leopold and Maddock's equations are widely used in hydrology for variety of streams, but during their original research were derived from rivers in Great Plains and Southwest.

6.2.2 Model Applicability.

This model can be applied successfully on streams with similar characteristics of the Malcolm Brook, a rolling hill stream (average slope equal 3 degrees) within small, less than one square kilometer watershed area, a shallow (< 0.20 m during base flow conditions) and narrow (< 2 m during base flow conditions) stream channel and dense vegetation. Before applying the turbidity model, it is necessary to establish the regression equation between turbidity and suspended solids during storm events. This regression should be verified and statistically tested. If results do not show high correlation between suspended sediments and turbidity, the model should not be applied. The model was tested with widely available GIS data at scales of 1:12000 - 1:24000. Therefore, smaller or larger scale of spatial data could produce erroneous results. The model should be applied to storms with a duration 2 to 24 hours. Time intervals for simulation can be selected by

modeler according to the purpose of the modeling with a lower limit equal to 10 minutes and an upper limit equal to 1 hour. These are the ranges of conditions where it would be expected that the model would best predict. Table 6.1 shows model shortcomings and strength. Model speed is among major shortcomings. This affects time which modeler spends to calibrate model and actually run it. Spatial and temporal distribution of the model parameters make it powerfull to deal with complex modeling schemes at a fine time scale..

Model should be applied cautiously considering all listed weeknesses. Future work to overcome these shortcomings discussed in section 8.

Table 6.1 Model shortcomings and strength.

Model Shortcomings	Model Strength
Flow error could be $\pm$100%	Predicts qualitatively where high and low flow occur along the stream channel during each time interval.
Turbidity error could be $\pm$ 534%	Predicts qualitatively were turbidity peaks occur along the stream channel during each time interval of the simulation.
Does not predict turbidity values lower than 20-30 NTU	Predicts time and location of maximum turbidity values.
Antecedent moistute conditions are not explicitly accounted for over and underprediction.	Simulates behavior of the long, high flow storms. Can identify time intervals and stream segments where peak of the hydrograph can be expected .
Model only predicts hydrograph for duration of rainfall.	Predicts qualitatively rising limb of hydrograph and distinguishes individual peaks.
Difficult to calibrate	Easy to use GIS data and input files. GIS spatial analysis allows derivation of contributing areas.
Slow performance	Easy to use output files for animation.

6.3 Turbidity Modeling.

The turbidity model presented is one of the first attempts to model this hydrologically dependent optical phenomenon at the storm event time scale. Turbidity modeling was attempted as a continuous variable through the storm events using different time intervals ranging from 10 minutes to 1 hour.

The basis of the turbidity modeling presented is a regression between suspended sediment concentration (SSC) and turbidity. This regression was shown to exist in different geological regions, and it is location specific in terms of regression coefficients. The first task in turbidity modeling is therefore to evaluate such coefficients. Turbidity is a difficult parameter to measure due to the variety of measuring devices, calibration techniques and changing environmental conditions during monitoring. Field work during 1996-1997 revealed that the most influencial factor during turbidity measurements was the rapidly changing environmental conditions in the stream during storm events. This included fallen leaves, soil washed into the stream from moving tree roots during wind gusts, pieces of grass and floating garbage. All these sources of debris influenced turbidity measurements by clogging sensors or completely blocking them. Other conditions affected measurements, such as accumulation of algae or microorganisms on the surface of the optical part of the turbidity sensor. It was found that while "real" turbidity in the stream can be 0.8 NTU, a sensor with dirty optics can produce values of 30 NTU or more. In this case, measurement error equal 3750%. Recently, turbidimeters equipped with small fans or jets, that constantly wash the surface of the optical unit have been produced to avoid the problem. Another way to measure turbidity more effectively would be to

pump water from the stream and pass it through a turbidity sensor. This equipment would be more expensive, but apparently more effective in terms of accuracy. The resulting measurements would create a substantial basis to develop the relationship of turbidity with suspended sediments. Alternatively, one could frequently visit the measuring site during storm events, in order to remove debris.

Results of turbidity modeling do not show high coefficient of correlation for the different sites when all tests are combined together. The main factor of this is a temporal scale of modeling and modeling method. At the temporal scale modeled all variables are changing rapidly. Peaks of the rainfall and discharge, on which turbidity depends, occur at different times. The model has to be improved to account for this much better. In terms of RMSE, simulated values are within the same order of magnitude as measured values. RMSE for verification dataset, comparing measured and simulated values, doesn't exceed 534%. In most cases, RMSE is within 100% and RMSE for the peak values are within 108%. This means that turbidity can be at least assessed more accurately than now in terms of maximum and average NTU values. By modeling turbidity in a spatially distributed way before and after implementation of engineering projects, it would be possible to evaluate their effectiveness at any location on the stream channel.

The modeling method presented in this study does not include such function as the rainfall influence on turbidity. It is known that rain drops affect sediment particles and move them. This dynamic force is apparently responsible for the turbidity response in the stream channel immediately after the rainfall peak because a lot of sediment has accumulated at the stream bank. This process requires special study and can be added to the model later. The methods presented in this study is mainly based on water discharge

and therefore can not account for the mentioned process.

7. Conclusions.

This study attempts to design and test a methodology for the spatially distributed hydrological modeling at a fine temporal scale of tens of minutes. A fine temporal scale allows one to study the behavior of dynamic natural events such as storms or heavy rainfalls with time intervals between 10 and 50 minutes and durations of several hours. At the same time, the small size of these intervals increases complexity of the modeling algorithm due to the differences in the behavior of modeled parameters revealed at such fine scale. For example, the discharge peak has to follow the rainfall peak, peak of turbidity generally follows peak of rainfall, but preceeds the peak of the discharge. These patterns would be barely noticeable if time intervals represent average daily or monthly values, but for the time intervals expressed in tens of minutes they have to be simulated. At this point, travel time becomes one of the main characteristics of the model. It had to be calculated for each segment on the stream with a purpose to estimate runoff. This iteration also made necessary contouring of contributing areas and their visualization. Thus, more tasks associated with spatial analysis for contributing area delineation have to be accounted for, and model complexity increases drastically.

Spatial distribution results in increasing numbers of computer commands iterations within the modeling code and complex GIS structure of the input data. This complexity slowed down the simulation process. ARC/INFO GIS software, used for the main part of the programming, like most other commercial GIS packages, utilizes macro language. Macro language differs from the regular programming language because it is not compiled. Therefore, performance of the programming code is slow and an average model run takes 7 to 12 hours of computer time.

Nevertheless, a spatially distributed model allows the analysis and study of particular portions of the watershed which might be affected by the point source pollution, or implementation of specific engineering projects. By using this distributed modeling approach, it became possible for the first time to visualize boundaries of areas, contributing surface runoff to stream segments.

This flow modeling produced satisfactory results, compared with other hydrological models, mentioned in the literature review. It predicts results within a range of 25% to 100% of observed values. Predictions are generally better when storm durations exceed 2 to 4 hours and time intervals are greater than 15 minutes.

However, the model does not predict flow after rainfall ceases. The main reason relates to the original purpose of the modeling, which is to simulate turbidity behaviour. Field measurements showed that turbidity is associated with both rainfall and discharge. After the rain stops, sediment material does not reach the stream, and turbidity in the channel decreases. Therefore, future behavior of the flow after the rain stopped was not necessary to simulate. This can be of interest for the more complicated hydrological model, dealing primarily with discharge and attempts to simulate the hydrograph from the beginning to the end.

Turbidity predictions and suspended sediment predictions are less precise than flow predictions. It was difficult to compare modeling results with accuracy ranges obtained from the literature sources because there are no similar suspended sediment or turbidity models with such temporal resolution. In summary, the model presented produces results which are highly variable and generally, within 500% of observed values.

Results were animated, showing expansions of contributing areas with each time

interval. This is one of the first attempts to visualize boundaries of contributing areas - isochrones and convert them into spatial objects. File formats used for the visual frames are GIF's (Graphics Interchange Format) and can be used by most of the commercial and shareware animation software packages.

8. Recommendations For Future Studies.

8.1 Hydrological Modeling

The model presented is a new tool which has to be tested on a large variety of conditions. As was mentioned in "Discussion", most of storms were overpredicted, while two were underpredicted. Model testing should involve use of several statistically representative datasets which would account for a wide range of the following conditions: seasonality, rainfall intensity, rainstorm duration. After all tests should be conducted, analysis of variances (ANOVA) could have been applied to reveal which conditions cause overprediction and which underprediction.

Rainfall is one of the main input parameters in any hydrological model. Generally it is assumed to be equally distributed over the area of the watershed. In fact, for the large watershed basins, greater than several square kilometers, spatial distribution of the rainfall might not be even. Some parts can get more rainfall than others. This issue directly affects simulation of the surface runoff and it was addressed recently by the new remote sensing technology - NEXRAD (Next Generation Weather Radar). This technology allows the assessment of precipitation across areas greater than 4 square kilometers and creates a raster data set with pixels, representing rainfall depth. This grid, combined with other GIS data, can serve as an input for the model and enhance accuracy of estimated surface runoff across HRU matrix.

Hydrograph can be simulated by the model presented after the development of a module which should include groundwater infiltration and discharge. This represents very complex modeling associated with geological and soil properties of the watershed. To

model groundwater infiltration and discharge it is important to know how fast water infiltrates specific soil types and when it will be discharged back to the stream channel. This might require some field work and experiments.

Contributing areas in this study were estimated through empirical equation, which was experimentally derived. However, there is a need for the field experiments, which would allow the better understanding of contributing areas as a spatial phenomenon. Such a study would also support coefficients, used in non-linear interpolation of contributing areas, described in the methodology presented here. These experiments should allow the observation of relations between the rainfall depth, duration and growth of contributing areas.

The distance between point of observation and most distant point on the watershed is an important parameter used by the time travel formula. The most distant point on the watershed is usually selected arbitrarily from a map, showing watershed basin, or through computer by simply calculating length. Nevertheless, this length can vary, depending on topographical complexity, as height of hills, number of depressions and valley shapes. Future enhancement of the travel time computation should include a better estimation of the distance between point of observation and most distant point on the watershed, using GIS capabilities.

8.2 Turbidity Modeling.

Future work should be done on improving turbidity measurements and verifying model results with better data. This is a critical part of the study, since collected data are used to calibrate the model. Tubidity measurement methods are improving and becoming more reliable, especially methods where the optical part of the sensor is constantly washed by the water flow, preventing organic and inoragnic components from accumulating on its surface. Using these data, models can be tested and calibrated again to provide better results.

In methodology presented here, the main source of turbidity was suspended sediments from the stream channel and not the nearby slopes because of the vegetation cover. Models can be enhanced considerably by accounting for the sediment particles impacted by the rain drops and eventually carried by the surface runoff into the channel. This is a separate modeling effort which can be developed through experimental study. The study would consist of measuring amount of soil moved by the rain drop and its subsequent movement.

Storm pattern when the turbidity peak occurs after the rainfall peak and before the flow peak has to be studied further to distinguish between suspended sediment dilution, when discharge volume increases, and suspended sediment concentration when rain peak passes but discharge volume is still relatively small. The process of suspended sediment dilution can be qualitatively and quantitatively modeled and added to existing model.

8.3 GIS Modeling.

Potential interest for the future application of GIS for hydrological modeling is development of an expert modeling system, which would guide modeler through different possible scenarios of the model. This system would allow the modeler to connect or disconnect different modeling functions with the purpose of managing model complexity and run time. GIS will serve in this framework as a programming tool, data management tool and database storage. Definitely, fastest modeling is done with simplest data; GIS would then allow the user to chose a data generalization method and thereby provide the necessary accuracy information.

Appendix A. Software Documentation.

Model consist of several ARCINFO macro- language codes (AML) , UNIX scripts and C codes.

MAIN MENU. (bold style indicates ARCINFO AML's which are used for modeling).

```
l
'I. Curve Number Data Entry Module'
 '1.Get C Value From Default' &r c_auto.aml
'II. GIS Data Manipulation'
 '1.Dem2TIN' &r dem2tin.aml
 '2.Stream Network Cleaning' &r stream_clean.aml
 '3.Select data for stream routing ' &r route.aml
'III. Modeling Functions'
 '1.Runoff Analysis (Rational)' &r runoff_rat.aml
'List Globals' &lv
'Terminal' &tty
'Quit' &r quit.aml
```

C_AUTO.AML

```
/* This macro allows selection of an ascii file which is set as default or use of modified
table.
/* Both tables can be prepared through ARCVIEW or using system text editor.
/* "c_table_default.txt" is a default table; "c_table_mod.txt" is modified

&type       SELECT OPTIONS:
&type
&type       1 - default table 'c_table_default.txt';
&type       2 - modified table 'c_table_mod.txt';
&type
      &if [exist c_table.dat -info] &then &sv kill [delete c_table.dat -info]
      &sv option = [response 'Select option']
      &if %option% = 1 &then
          &sv .c_table_name = c_table_default.txt
      &else
          &sv .c_table_name = c_table_exp.txt

      tables
       DEFINE C_TABLE.DAT   /* Creates new table in INFO format */
       LANDUSE,30,30,C      /* Following four lines specify data format */
       HYDRO-GROUP,1,C
       SLOPE,3,3,I
       C,5,5,N,2
```

```
        [unquote ' ']
/* Following line specifies command which reads data from ascii file into INFO format */

        ADD LANDUSE HYDRO-GROUP SLOPE C FROM %.c_table_name%
        q
&type                       FINISHED!
&return
```

DEM2TIN.AML

```
/* Purpose of this AML is data conversion from regular grid into TIN format.

/* Set up initial variable values
&sv .set_cover =
&sv cover = DEM

/* Uses ESRI prepared AML "browse.menu" and "browse.aml" to select DEM grid
/* from directory. "browse.aml" was modified and saved as "browse_dem.aml".

&r browse_dem init %cover%

&if [NULL %.set_cover%] &then
 &do
   &type No Value Entered
   &return
 &end

/* Checks existence of old temporary GIS datasets and deletes them from directory
&if [exist tmp -TIN] &then kill tmp all
&if [exist terrain -POLY] &then kill terrain all

/* Converts DEM into TIN structure using very small vertical tolerance value and
/* moderate maximum number of points. For more detailed TIN, more points required.
latticetin %.set_cover% tmp 0.001 600

/* Converts dataset from TIN structure into ARC structure with polygon topology
/* Resultant coverage assigned name "terrain".
tinarc tmp terrain poly percent

/* Checks for the existence of the field "slope" within ARCINFO database.
&if [iteminfo terrain -POLY slope -EXISTS] = .TRUE. &then
dropitem terrain.pat terrain.pat slope

/* In CIA runoff model slopes are needed.
/* with intervals 0-2, 2-6, >6. Following line adds field "slope" to ARCINFO database
additem terrain.pat terrain.pat slope 3 3 i
```

```
/* In 'TABLES' module of ARCINFO classifies slope field by intervals and populates it
/* using values 1 ( 0-2), 2 (2-6)  and 3 (> 6)
tables
sel terrain.pat
resel percent_slope ge 0 and percent_slope lt 2
calc slope = 1
aselect
resel percent_slope ge 2 and percent_slope lt 6
calc slope = 2
aselect
resel percent_slope gt 6
calc slope = 3
aselect
q

/* Following iteration is for adding X and Y coordinates and "elevation" field to
/*coverage "terrain" for the future use.

addxy terrain point
additem terrain.pat terrain.pat elevation 9 9 N 2

/* Using GRID module assigns elevation values to the field "elevation"
/* in "terrain" coverage.
grid
display 9999 size 5 5
cursor tmp declare terrain.pat info rw
   cursor tmp open
   &do i = 1 &repeat %i% + 1 &untill %:tmp.AML$NEXT% = .FALSE.
     &sv .height = [show cellvalue dem [value :tmp.X-COORD] [value :tmp.Y-COORD]]
     &if [type [value .height]] = 1 &then &type NODATA
       &else
       &sv :tmp.ELEVATION = [value .height]

    cursor tmp next
    &end
cursor tmp remove

q
display 9999 size 700 800   /* Restores graphic device and its size*/

&return
```

STREAM_CLEAN.AML

```
/* This AML takes ARCINFO dataset representing stream and eliminates nodes
```

```
/* to reduce number of segments, because this coverage are used later in conjunction
/* with HRU matrix. When HRU polygons overlay stream coverage, it is used to define
/* hydrologically 'meaningful' segments.

/* Removes old variable
&dv .stream_cover

/* Sets up new variables
&sv cover = stream
&sv .set_cover = .stream_cover
&sv .type = COVER

/* Uses ESRI prepared AML  "browse.aml" to select stream coverage
&r browse init %cover% %.type%

&if [NULL %.stream_cover%] &then &return

/* Deletes old dataset if it exists
&if [exist stream_cov -COVER] &then kill stream_cov all

/* Checks if the field 'null' exist in coverage.
&if [iteminfo %.stream_cover% -LINE null -EXISTS] = .TRUE. &then
dropitem %.stream_cover%.aat %.stream_cover%.aat null

/* Adds field 'null' to the coverage
additem %.stream_cover%.aat %.stream_cover%.aat null 1 1 I
&type
&type       Removing unnecessary nodes ...
&type
/* Eliminates unnecessary nodes
dissolve %.stream_cover% stream_cov null line

/* Adds few fields to the stream coverage database to store values of velocity, depth,
width,
/* manning equation coefficient, discharge, and turbidity
&type
&type       Adding fields ...
&type
additem stream_cov.aat stream_cov.aat depth 7 7 N 3
additem stream_cov.aat stream_cov.aat width 7 7 N 3
additem stream_cov.aat stream_cov.aat mann 7 7 N 3
additem stream_cov.aat stream_cov.aat velo 7 7 N 3
additem stream_cov.aat stream_cov.aat discharge 7 7 N 3
additem stream_cov.aat stream_cov.aat turbidity 7 7 N 3
&type
&type                    FINISHED!
```

```
&return
```

ROUTE.AML

```
/* This AML helps to define appropriate routes along the stream coverage. Basically this
/* AML brings user to ARCEDIT module of ARCINFO and allows selection of routes
/* interactively, then adds values to appropriate fields.

/* Selects stream network coverage
&sv .stream_file = [entryname [getfile * -DIRECTORY 'Choose stream coverage' -NONE
-OTHER]]
&type
&if [null %.stream_file%] &then &type Nothing entered...Stop...
&if [null %.stream_file%] &then &return
&if [exists [value .stream_file] -ARC] = .FALSE. &then &type Coverage %stream_file%
Doesn't Exist! Check covername...
&if [exists [value .stream_file] -ARC] = .FALSE. &then &return
&type
&severity &error &ignore

/* Checks if necessary field 'route' exists in coverage and adds it if not present
&if [iteminfo %.stream_file% -LINE null -EXISTS] = .TRUE. &then
dropitem %.stream_file%.aat %.stream_file%.aat route
additem %.stream_file%.aat %.stream_file%.aat route 3 3 i

/* Brings user to ARCEDIT environment, draws stream network; then user
/* can select desirable stream attributes and enter route values into field 'route'
/* associated with stream coverage database.
ae
display 9999
edit %.stream_file%
editf arcs
drawenv arcs
draw
&return
```

RUNOFF_RAT.AML

This AML spatially overlays three datasets: soil, landuse and terrain. After physical overlay, the resultant coverage will receive all necessary attributes in preparation for modeling. Practically this AML creates HRU matrix and populates it with coefficients for application of of rational method. It also asks for the rainfall input datafile at the beginning. Because rainfall datafile is set as AML it creates variable for each rainfall interval. RUNOFF_RAT.AML uses these values to calculate rainfall excess for each HRU plane and time interval. Then these values are stored in fields Q_1 ... Qn.

```
/* Asks user for the rainfall input datafile
&sv test = [getfile *.aml -FILE 'Select DataFile']

&if [null %test%] = .TRUE. &then
   &do
    &type
    &type BYE!
    &type
    &return
   &end

/* Runs input file with rainfall values to set up variables for the rainfall
&r %test%

/* Prompts user to use either old HRU matrix, which is named 'runoff_cov' or create
/* a new one. If answer is 'yes' then RUNOFF_RAT.AML will use existing 'runoff_cov'.
/* This makes sense if basic coverages such as soil, landuse and terain were not modified.
/* If basic coverages were modified, then topology probably changed or other attributes
/*were modified. In this case,  the programs answers 'no' and the AML prompts to enter
 /* names of soil, landuse and terrain datasets and does spatial overlay to create a new
/* HRU matrix for use with rational method.
&if [exist runoff_cov -cover] &then
   &do
    &type
    &sv query = [query 'Do you want to use existing runoff coverage "RUNOFF_COV"'
.TRUE.]
    &type
    &if %query% = .TRUE. &then &goto continue
   &end

/* Removes old datasets
&if [exist tmp -cover] &then kill tmp all
&if [exist tmp -directory] &then kill tmp all

/* Set up name variables and uses ESRI prepared AML  "browse.aml" to select necessary
/* coverage for HRU matrix development

&sv .land_cover =
&sv .soil_cover =
&sv .terrain_cover =

&sv cover = landuse
&sv .set_cover = .land_cover
&sv .type = COVER

/* Prompts for the landuse coverage
```

```
&r browse init %cover% %.type%

&if [NULL %.land_cover%] &then &return
/* Prompts for the soil coverage
&sv cover = soil
&sv .set_cover = .soil_cover
&sv .type = COVER

&r browse init %cover% %.type%

&if [NULL %.soil_cover%] &then &return

/* Prompts for the terrain coverage
&sv cover = terrain
&sv .set_cover = .terrain_cover
&sv .type = COVER

&r browse init %cover% %.type%

&if [NULL %.terrain_cover%] &then &return

/* Removes old HRU matrix if it is exists
&if [exist runoff_cov -DIRECTORY] &then kill runoff_cov all
&sv .runoff_cover = runoff_cov

/* Creates HRU matrix by combining all basic coverages: landuse, soil, terrain
union %.land_cover% %.soil_cover% tmp 10 join
union tmp %.terrain_cover% %.runoff_cover% 10 join
kill tmp all

/* Eliminates unnecessary fields from the database
dropitem runoff_cov.pat runoff_cov.pat
[entryname %.land_cover%-ID]
[entryname %.land_cover%#]
[entryname %.soil_cover%#]
[entryname %.soil_cover%-ID]
[entryname %.terrain_cover%-ID]
[entryname %.terrain_cover%#]
[entryname tmp#]
[entryname tmp-ID]
end

/* Using pre-fabricated INFO table 'c_table.dat' populates HRU matrix with C
/* values used in rational method
/*-----------------------------------
/* C Number coding
```

```
/*-----------------------------------
/* Checks for the necessary fields and adds them if necessary
&if [iteminfo runoff_cov -POLY c-code -EXISTS] = .TRUE. &then
dropitem runoff_cov.pat runoff_cov.pat c-code
additem runoff_cov.pat runoff_cov.pat c-code 30 30 c
&if [iteminfo c_table.dat -INFO c-code -EXISTS] = .TRUE. &then
dropitem  c_table.dat c_table.dat c-code
additem c_table.dat c_table.dat c-code 30 30 c

/* In INFO module of ARCINFO combines (concatenates) landuse, soil and slope values
&data arc info
arc
SEL RUNOFF_COV.PAT
CONCATENATE C-CODE FROM LANDUSE, HYDRO-GROUP, SLOPE
SEL C_TABLE.DAT
CONCATENATE C-CODE FROM LANDUSE, HYDRO-GROUP, SLOPE
Q STOP
&end

/* Merges HRU's database with 'c_table.dat' to populate field containing C coefficient
joinitem runoff_cov.pat c_table.dat runoff_cov.pat c-code c-code

/* For the impervious surface coverage assigns C values = 1.0 which means 100%
/* of runoff
&if [exist imperv -cover] &then
  &do
    &if [exist tmp_cov -cover] &then kill tmp_cov all
    erase runoff_cov imperv tmp_cov poly
    tables
     sel tmp_cov.pat
     resel tmp_cov-id = 0
     resel area gt 0
     calc c = 1.0
     calc slope = 0
     calc elevation = 10000
    q stop
    kill runoff_cov all
    rename tmp_cov runoff_cov
  &end

&label continue

/* Removes old fields containing results from the rational method and adds new ones

&do k = 1 &to %.cycle%
  &sv .P = [value .P%k%]
```

```
  &if [value .P%k%] = 0 &then
   &do
     &if [iteminfo runoff_cov -POLY q%k% -EXISTS] = .TRUE. &then
     dropitem runoff_cov.pat runoff_cov.pat q%k%
     additem runoff_cov.pat runoff_cov.pat q%k% 15 15 N 2
     tables
      sel runoff_cov.pat
      resel c gt 0
      calc q%k% = 0
     q
   &end
  &else
   &do
    &sv I = [calc [calc %.P% / [calc %.time_interval%]] * 60]

    &if [iteminfo runoff_cov -POLY q%k% -EXISTS] = .TRUE. &then
     dropitem runoff_cov.pat runoff_cov.pat q%k%
     additem runoff_cov.pat runoff_cov.pat q%k% 15 15 N 2

/* Application of the rational method to all HRU planes

   /*************************************************************
   /*
   /* RATIONAL METHOD   Q = C I A
   /*     0.000247 - converts sq.meter2acres; 28 - converts cf2liter;
   /*
   /*      I - intensity, inches/hour;
   /*************************************************************
    tables
     sel runoff_cov.pat
     resel c gt 0
     calc q%k% = area * 0.000247 * C * %I% * 28
    q
   &end
   /*************************************************************
   &type
   &type              Q%k% created ... Q[calc %k% + 1] is going ...
   &type
  /*************************************************************

&end

&messages &on

&type                        FINISHED [entryname %test%]!
```

```
&return
-------------------------------------------------------------------------------
-------------------------------------------------------------------------------
```

Main AML, which uses HRU matrix for the test. In study it was called model_run.aml

MODEL_RUN.AML

```
/* Accepts file with rainfall data as an argument. It needs onlu time interval values and
/* number of time intervals to define how many runs to make.

  &args .test

/* Checks for the argument entry

  &if [null %.test%] &then
   &do
    &type Enter data file name ...
    &return
   &end
  &if [show program] eq GRID &then q
  &echo &off

/* Runs rainfall data file as AML to set up rain depths as variables for each time interval.

  &r [value .test]

/* Set up digital format for the output numbers, path for image storage

  &format 2
  &sv path_out = /local_home/images/%.test%

/* Set up of power coefficients for estimating contributing areas

  &sv trav_coeff1 = 1.05
  &sv trav_coeff2 = 0.1

/* Set up of GIS layers, representinh basin boundary, stream outline, DEM and names
/* of runoff coverage (HRU) and temporarily runoff coverage 'runoff_clip'

  &sv .basin = mb1_basin /* Basin coverage */
  &sv .stream = stream_mod /* Stream channel coverage */
  &sv .dem = dem /* DEM */
  &sv .runoff_cov = runoff_cov /* Name for the temporarily HRU matrix */
  &sv runoff = runoff_clip /* Name for the temporarily HRU matrix */
/*************************************************************************/
/* Extracting information about number of stream routes from the basin coverage and set-
```

```
timg
/* variable 'num_route' which will define number of iterations of the model i.e. loops

   &if [exist route.frq -info] &then &sv kill =  [delete route.frq -info]
   statistics %.basin%.pat route.frq
   max route-num
   end

    cursor tmp declare route.frq info rw
    cursor tmp open

     &sv .num_route = [value :tmp.MAX-ROUTE-NUM]

    cursor tmp close
    cursor tmp remove

/*************************************************************************/

/* Using 'num_route' set up loop.  'video_count' variable will be needed later to assign
*/
/* consequent numbers to image frames during conversion process from SUN raster file to
/* 'GIF' format. At the beginning it will be initialized as '0'

&sv video_count = 0

&do k = 1 &to %.num_route%

/*************************************************************************/

 /* Cleaning files, i.e. removing possible existing files from previous runs */

      &if [exist tmp_seg -cover] &then kill tmp_seg all
      &if [exist runoff_tmp -cover] &then kill runoff_tmp all
      &if [exist rt%k%_list.txt] &then &sv kill = [delete rt%k%_list.txt]
      &if [exist flag] &then &sv kill = [delete flag]
      &if [exist runoff_rt%k%.txt] &then &sv kill [delete runoff_rt%k%.txt]
      &if [exist %.test%_rt%k%.res] &then &sv kill [delete %.test%_rt%k%.res]
      &if [exist tmp_pnt -cover] &then kill tmp_pnt all
      &if [exist tmp_pnt1 -cover] &then kill tmp_pnt1 all
      &if [exist circle_runoff -cover] &then kill circle_runoff all

         &if [exist poly%k%.txt] &then &sv kill [delete poly%k%.txt]
         &if [quote [show cursors]] cn [quote seg] &then cursor seg remove
```

```
/*************************************************************************/
/* Starting  ARCINFO routine on extracitng the route basin and route outline from */
/* GIS layers defining basin and stream coverage

/* Remove any temporarily file left from previous run

    &if [exist rt%k%_poly -cover] &then kill rt%k%_poly all

/* Reselect from basin coverage first sub-basin to model

    reselect %.basin% rt%k%_poly poly
    reselect route-num = %k%
    [unquote ' ']
    N
    N

/* Remove any temporarily file left from previous run

    &if [exist rt%k%_line1 -cover] &then kill rt%k%_line1 all
    &if [exist rt%k%_line -cover] &then kill rt%k%_line all

/* Extracts part of the stream, belonging to the first modeled sub-basin

    clip %.stream% rt%k%_poly rt%k%_line1 line 0.0001

/*************************************************************************/
/* For the future need, checks if HRU matrix has any coordinates of HRU polygons
/* stored in the attribute table. If 'not', adds them

    &if [iteminfo %.runoff_cov% -poly X-COORD -exists] = .FALSE. &then
    addxy %.runoff_cov%

/*************************************************************************/
/* Remove any temporarily file left from previous run

    &if [exist runoff_clip -cover] &then kill runoff_clip all

/* Overlay extracted basin coverage with HRU matrix, therefore selecting only
/* HRU polygons within the modeled sub-basin

    identity rt%k%_poly %.runoff_cov% %runoff% poly 0.0001 join

/* Cleans stream coverage by removing all pseudo nodes from the line
/* Uses ARCEDIT module

    ae
```

```
    edit rt%k%_line1
    editf arcs
    sel all
    unsplit
    save
  q

/* Overlay stream coverage with HRU matrix to assign all HRU attributes to the stream
/* attribute table

    identity rt%k%_line1 %.runoff_cov% rt%k%_line line 0.0001
    kill rt%k%_line1 all

/*************************************************************************/
/* Getting coordinates for the supposed end and beginning of the stream */

/* Remove any temporarily files from the previous runs

      &if [exist point.sta -info] &then &sv kill = [delete point.sta -info]

      &if [exist tmp_pnt -cover] &then kill tmp_pnt all
      &if [exist tmp_pnt1 -cover] &then kill tmp_pnt1 all

/* Convert stream line coverage into point coverage

      arcpoint rt%k%_line tmp_pnt1 line runoff_cov#
      arcpoint rt%k%_line tmp_pnt line rt%k%_line#

/* Adds X, Y coordinates to points

      addxy tmp_pnt point
      addxy tmp_pnt1 point

/* Defining "min" and "max" internal numbers of  points on the stream using ARCINFO
/* 'cursors' and 'statistics' functions */

    statistics tmp_pnt.pat point.sta
    min tmp_pnt#
    max tmp_pnt#
    end

    cursor tmp declare point.sta info ro
    cursor tmp open

      &sv min_pnt_num = [value :tmp.MIN-TMP_PNT#]
      &sv max_pnt_num = [value :tmp.MAX-TMP_PNT#]
```

```
      cursor tmp close
      cursor tmp remove
/*************************************************************************/
/* Defines coordinates of the "min" and "max" internal numbers of points on the stream
/* and select first and last points on the stream

      cursor point1 declare tmp_pnt.pat info ro
      cursor point1 open

         &do i = 1 &repeat %i% + 1 &untill %:point1.AML$NEXT% = .FALSE.
          &if [value :point1.tmp_pnt#] = %min_pnt_num% &then
           &do
           &sv min_pnt_numX = [value :point1.X-COORD]
           &sv min_pnt_numY = [value :point1.Y-COORD]
           &sv init_seg_min = [value :point1.rt%k%_line#]
           &end
          &if [value :point1.tmp_pnt#] = %max_pnt_num% &then
           &do
           &sv max_pnt_numX = [value :point1.X-COORD]
           &sv max_pnt_numY = [value :point1.Y-COORD]
           &sv init_seg_max = [value :point1.rt%k%_line#]
           &end
           cursor point1 next
         &end
           cursor point1 close
           cursor point1 remove
/*************************************************************************/
  /* Getting the Total Number of Segments Along the Route */

         &describe rt%k%_line

         &sv .TOTAL_LINE_NUM = [value DSC$ARCS]
/*************************************************************************/
/* Getting elevations for the "min" and "max" segments to determine which one */
/* is the beginning of the stream reach. It is done by assuming that water runs from
/* highest elevation to lowest. This routine uses GRID module and DEM dataset

/* GRID */

grid
display 9999 size 5 5
&sv min_pnt_height = [show cellvalue %.dem% [value min_pnt_numX][value
min_pnt_numY]]
       &type [show cellvalue %.dem% [value min_pnt_numX] [value min_pnt_numY]]
&sv max_pnt_height =[show cellvalue %.dem% [value max_pnt_numX][value
```

```
max_pnt_numY]]
        &type [show cellvalue %.dem% [value max_pnt_numX] [value max_pnt_numY]]
        &if [type [value min_pnt_height]] = 1 &then

         &do
           &type NODATA ENCOUNTERED, CHECK YOUR DEM !
           &return
         &end
         &if [type [value max_pnt_height]] = 1 &then
         &do
           &type NODATA ENCOUNTERED, CHECK YOUR DEM !
           &return
         &end
      q
      display 9999 size 700 800
/*************************************************************************/
/* Assigning The Geometric Center Of the Highest Elevation On The Watershed */
/* In this case coordinates are assigned to the first sub-basin and the second sub-basin
/* manually, knowing that Malcolm Brook basin has two sub-basins. Traditionally, selec-
tion
/* of the highest point on the watershed is done subjectively upon modeler's point of view.
/* To create automatic routine, many variables should be taken into account and some fur-
ther
/* study might be required.

        &if %k% = 1 &then
         &do
           &sv .X-HIGH = 603305.489
           &sv .Y-HIGH = 4550466.932
         &end

        &if %k% = 2 &then
         &do
           &sv .X-HIGH = 602968.095
           &sv .Y-HIGH = 4549880.123
         &end
/*************************************************************************/
/* Starting the "Minor Loop" which will extract lateral flow values for each segment on
/* the stream, starting from upper reaches and working down through each segment.
/* This module uses ARC functions

/* 1. Defining the first initial segment */

      &if [value min_pnt_height] lt [value max_pnt_height] &then
        &sv .init_seg = [value init_seg_max]
      &else
```

```
        &sv .init_seg = [value init_seg_min]

/*  2. Removes old temporarily files */

      &if [exist tmp_seg -cover] &then kill tmp_seg all
      &if [exist runoff_tmp -cover] &then kill runoff_tmp all
      &if [exist rt%k%_list.txt] &then &sv kill = [delete rt%k%_list.txt]
      &if [exist flag] &then &sv kill = [delete flag]

/*************************************************************/
/* Depending on elevation, defines from which segment to start */
/* Creates ascii file with all internal numbers of segments for checking and future refer-
ences
/* This module uses 'cursor' function and set up variable' .TOTAL_LINE_NUM' which
/* defines total number of segments to be analysed

  &sv num_rec = 0
     &if [value min_pnt_height] lt [value max_pnt_height] &then
    &do
      &if [quote [show cursors]] cn [quote seg] &then cursor seg remove
      &if [exist rt%k%_list.txt] &then &sv kill [delete rt%k%_list.txt]
      &sv run_poly_num_curr = 0
      cursor seg declare rt%k%_line line ro
      cursor seg open
      &sv .init_seg = %.TOTAL_LINE_NUM%
     &do counter = 0 &repeat %counter% + 1 &untill %counter% =
%.TOTAL_LINE_NUM%
      cursor seg %.init_seg%
      &sv .next_seg = [calc %.TOTAL_LINE_NUM% - %counter%]
      &sv run_poly_num_next = [value :seg.RPOLY#]
      &if %run_poly_num_next% = %run_poly_num_curr% &then ~
      &sv run_poly_num_curr = %run_poly_num_next%
        &else
          &do
            &sv run_poly_num_curr = [value :seg.RPOLY#]
            &sys echo %run_poly_num_curr% >> rt%k%_list.txt
            &type CURR = %run_poly_num_curr%
            &sv num_rec = [calc %num_rec% + 1]
            &sv rec%num_rec% = %run_poly_num_curr%
          &end
            &sv .init_seg = %.next_seg%
    &end
    &if [quote [show cursors]] cn [quote seg] &then cursor seg remove
  &end
     &else
  &do
```

```
        &if [quote [show cursors]] cn [quote seg] &then cursor seg remove
        &if [exist rt%k%_list.txt] &then &sv kill [delete rt%k%_list.txt]
        &sv run_poly_num_curr = 0
        cursor seg declare rt%k%_line line ro
        cursor seg open
       &do counter = 0 &repeat %counter% + 1 &untill %counter% = ~
      [calc %.TOTAL_LINE_NUM% - 1]
         &sv .init_seg = [calc %counter% + 1]
         cursor seg %.init_seg%
         &sv run_poly_num_next = [value :seg.RPOLY#]
         &if %run_poly_num_next% = %run_poly_num_curr% &then ~
         &sv run_poly_num_curr = %run_poly_num_next%
           &else
             &do
              &sv run_poly_num_curr = [value :seg.RPOLY#]
              &sys echo disch%run_poly_num_curr% >> rt%k%_list.txt
              &type CURR = %run_poly_num_curr%
              &sv num_rec = [calc %num_rec% + 1]
              &sv rec%num_rec% = %run_poly_num_curr%
             &end
       &end
        &if [quote [show cursors]] cn [quote seg] &then cursor seg remove
      &end
/*************************************************************************/
/* 3. "Minor loop ", which uses number of rainfall  time intervals as number of cycles
/* Variable '.cycle' was set up at the begiining when rainfall data file was run as AML.
/* At the beginning variables 'satur_time' is set up as unrealistic '99' and 'stop' as '0'.
/* These variables serve as flags to indicate when image saving has to be stoped. It will be
/* stoped when basin will be fully saturated and visualization of contributing areas will
/* not have any sense.

    &sv satur_time = 99
    &sv stop = 0

    &do t = 1 &to %.cycle%

/* Removes temporarily files

     &if [exist %runoff% -cover] &then kill %runoff% all

/* Creates HRU matrix for the modeling, leaving original HRU matrix intact

     intersect %.runoff_cov% rt%k%_poly %runoff% poly 0.1

/* Set up variable which stores value of the modeled time interval, starting from the begin-
ning
```

```
    &sv time_interval_cum = [calc %.time_interval% * %t%]

/* Uses variable 'num_rec' to define a loop which will end at the last segment on the
stream

    &do m = 1 &to %num_rec%

    &sv run_poly_num_curr = [value rec%m%]

    &type [variable Q%run_poly_num_curr%-%t%-%t%]
    &if [variable Q%run_poly_num_curr%-%t%-%t%] = .TRUE. &then
      &do
       &type SKIPPED
       &goto skip_lateral
      &end

/* Calls main routine which calculates lateral flow and save an image of contributing area

        &call lateral_define

/* Removes old temporarily file

        &if [exist circle_covSP -cover] &then kill circle_covSP all

/* Label point, which marks the end of the flow modeling

        &label skip_lateral

/* End of the stream segments

    &end

/* This is the end of minor loop which ends when all time intervals of the input file are
/* worked out

  &end
/*************************************************************************/
/* Following module creates one file containing lateral flow values for all modeled seg-
ments

/* Removes all old files

    &if [exist runoff_rt%k%.txt] &then &sv kill [delete runoff_rt%k%.txt]
    &if [exist %.test%_rt%k%.res] &then &sv kill [delete %.test%_rt%k%.res]
    &if [exist tmp_pnt -cover] &then kill tmp_pnt all
```

```
        &if [exist tmp_pnt1 -cover] &then kill tmp_pnt1 all

/* Creates new ascii file for the data storage

        &sv count = [filelist disch* route%k%.list -FILE]
        &if %count% <= 0 &then &return ERROR Generating file!
        &sv unit = [open rt%k%_list.txt ok -read]
        &do i = 1 &to %count%
          &sv file = [read %unit% ok]


/* Uses UNIX function 'cat' to insert data into output file

          &sys cat %file% >> %.test%_rt%k%.res
          &sv kill = [delete %file%]
        &end

        &sv ok = [close %unit%]
        &sv ok = [delete route%k%.list]
      &type
      &type Discharges are saved in a file ...%.test%_rt%k%.res
      &type

/* Removes  'cursor' variable and all temporaryli files

     &if [quote [show cursors]] cn [quote seg] &then cursor seg remove

     &if [exist tmp_seg -cover] &then kill tmp_seg all
     &if [exist runoff_clip -cover] &then kill runoff_clip all
     &if [exist rt%k%_poly -cover] &then kill rt%k%_poly
     &if [exist rt%k%_line -cover] &then kill rt%k%_line
     &if [exist flag] &then &sv kill = [delete flag]
     &if [exist %.test%_rt%k%.var] &then &sv kill = [delete %.test%_rt%k%.var]
     &if [exist circle_runoff -cover] &then kill circle_runoff all

/* Remove all variables used to store values of HRU areas and flow

    &dv A*
    &dv Q*

/* End of the modeling

&end

/* Prints out on a screen the time when modeling was finished
```

```
&sys date

&return

/*************************************************************************
/* Main routine which calculate lateraf flow into stream segments

&routine lateral_define

/* Uses ARCPLOT module */
      ap
        DISPLAY 9999 SIZE 5 5
        mape %.runoff_cov%

/* Using segment's internal number, reselects related HRU matrix polygon  */

        reselect %runoff% poly %.runoff_cov%# = %run_poly_num_curr%
        reselect %.runoff_cov% poly %.runoff_cov%# = %run_poly_num_curr%
        reselect tmp_pnt1 point %.runoff_cov%# = %run_poly_num_curr%

/*************************************************************************/
/* Getting all necessary information about stream segment
/* Uses 'statistics' and 'cursors' to set up appropriate variables
/* Necessary information includes: slope, stream segment length
/* If slope found to be equal '0', then it will be set up as 0.000001 which
/* will refer to the very low gradient. Otherwise all calculations will result as '0'
/* '0' value of slope usually is a result of the DEM scale and preceeding interpolation

        statistics %.runoff_cov% poly
        mean PERCENT_SLOPE
        q

        &if [show statistic 1 1] = 0 &then
         &sv slope_stream = 0.000001
          &else
         &sv slope_stream = [calc [truncate [show statistic 1 1]] / 100]

       &do
        reselect rt%k%_line line RPOLY# = %run_poly_num_curr%
        statistics rt%k%_line line
        sum LENGTH
        q
        &sv total_length = [round [show statistic 1 1]]
        &if %total_length% = 0 &then &sv total_length = 1
       &end
```

```
        &sv depth_stream = 0.1
        &sv width_stream = 0.2

/*************************************************************************
/* Getting all necessary information about selected HRU polygon */
/* It includes coordinates of the polygon label, elevation, aspect

        cursor tmp1 declare tmp_pnt1 point ro
        cursor tmp1 open
          &sv .cntrX = [value :tmp1.X-COORD]
          &sv .cntrY = [value :tmp1.Y-COORD]
        cursor tmp1 close
        cursor tmp1 remove

        cursor tmp declare %.runoff_cov% poly ro
        cursor tmp open

          &sv H1 = [value :tmp.ELEVATION]
          &sv A1 = [value :tmp.ASPECT]
          &sv Num = [value :tmp.%.runoff_cov%#]

/* Calculates distance from the center of the polygon to the farthermost point on the
watershed
/* which was defined previously. This distance is stored in a variable 'RADIUS'

&sv RADIUS = [invdistance [value .cntrX] [value .cntrY] [value .X-HIGH] [value .Y-
HIGH]]

/* If calculated distance turnes to be equal '0' then radius will be considered extremely
small
/* Normally it doesn't happen, but if it will, then distance will be very small, because if
/* rain will occur, then it should drain through the area anyway and produce some kind of
runoff

        &if [value RADIUS] = 0 &then &sv RADIUS = 1

        cursor tmp close
        cursor tmp remove

/*************************************************************************
/* Calculating travel time ( 3.28 convert meters to feet)

      &sv travel_distance = [calc [invdistance %.cntrX% %.cntrY% ~
      %.X-HIGH% %.Y-HIGH%] * 3.28]

      clearselect
```

```
/* Following iterations select HRU polygons within the circle, defined by the 'RADIUS'
variable

        reselect %runoff% poly CIRCLE %.X-HIGH% %.Y-HIGH% %RADIUS%
WITHIN
        reselect %runoff% poly PERCENT_SLOPE gt 0
        reselect %runoff% poly AREA gt 0
        aselect %runoff% poly RUNOFF_COV# = %run_poly_num_curr%

/* After all relevant HRU polygons are selected, information is gathered about
/* mean values of slope, runoff, area and runoff coefficient

        statistics %runoff% poly
        mean PERCENT_SLOPE
        mean Q%t%
        mean AREA
        mean C
        end

        &sv slp = [calc [show statistic 1 1] / 100]
        &if %slp% le 0 &then &sv slp = 0.000001
        &sv run = [show statistic 2 1]
        &sv area = [show statistic 3 1]
        &sv C = [show statistic 4 1]

    &sv close = [close -ALL]

/* In a formula which calculates travel time slope value has power 0.333
/* Because ARCINFOI doesn't have appropriate power function, small C code
/* was written. Following block uses it.

    &if [exist tmp_calc1] &then &sv kill = [delete tmp_calc1]
    &sys expo %slp% 0.333 > tmp_calc1
    &sv open = [open tmp_calc1 openstatus -read]
    &sv slp_calc = [read %open% readstatus]
    &sv close = [close -ALL]

/* Travel time is calculated and variable 'time_travel is set

  &sv time_travel = [calc 1.8 * [calc 1.1 - %C%] * [sqrt %travel_distance%] /
%slp_calc%]

/* Removes temporarily file

    &if [exist tmp_calc1] &then &sv kill = [delete tmp_calc1]
```

```
/* Displays on a screen obtained values for the travel time, value of the 'RADIUS' vari-
able
/* and current cumulative time

&type
 &type TRAVEL TIME =  %time_travel%  New C = %C%  ~
 RADIUS = %RADIUS% Time Int Cum = %time_interval_cum%
&type

        clearselect

/*********************************************************************
/* Defines the radius of the contributing area and reselects HRU polygons within the
radius.

/* Checks the condition of the 'fully saturated' watershed
/* It considered saturated when travel time equal or greater than cumulative time of
/* the current model run. It sets up values for the variable 'satur_time' ('99' if not
/* saturated and value of the cumulative time if saturated) and 'stop' ('0' save images
/*  of contributing areas, '1' -  stop saving images.

&if %satur_time% = 99 &then
   &do
      &if %time_interval_cum% gt %time_travel% &then
         &sv satur_time = %t%
   &end
      &if %satur_time% = [calc %t% - 1] &then
          &sv stop = 1

/* Prints on a screen time when watershed became saturated

&type SATURATION TIME  = %satur_time%

/*/
*********************************************************************/
/* Following loop continues if watershed hasn't reached yet full saturation or is saturated
/* It calculates the radius of contributing area, using two coefficients 'trav_coeff1' and
/* 'trav_coeff2' which are set at the beginning of the code. UNIX script 'expo'
/* is used to bring variable 'dist' to the power of 'trav_coeff1'.
/*
/* The result of this loop is a variable 'distance_involved' which defines the size
/* of contributing area.
/*
/* The difference between 'saturated' vs. 'unsaturated' conditions is the way of extraction
/* necessary portion of HRU matris. If watershed 'saturated' we will need only one spatial
```

```
/* object - circle, defined by the variable 'RADIUS'. In case of 'undersaturated
/* watershed we will need also circle, defined by the variable 'distance_involved'.

      &if %stop% = 0 &then  /* Following condition applies to  'unsaturated watershed'
*/
        &do

          &sv dist = [calc %time_interval_cum% * %RADIUS% / %time_travel%]

          &sys expo %dist% %trav_coeff1% > tmp_calc1

          &sv open = [open tmp_calc1 openstatus -read]
          &sv distance_involved = [read %open% readstatus]
          &sv close = [close -ALL]
          &sv distance_involved = [calc %trav_coeff2% * %distance_involved%]

/* Print on a screen the radius of contributing area for the modeled time interval and
/* stream segment

&type
&type CONTRIB RADIUS = %distance_involved%
&type

          &if [exist tmp_calc1] &then &sv kill = [delete tmp_calc1]

/* Sets a mapping area on a graphical device

          mape %runoff%

/* Removes temporarily files

        &if [exist circle_runoff -cover] &then &sys arc kill circle_runoff
        &if [exist circle_covS -cover] &then &sys arc kill circle_covS
        &if [exist circle_covB -cover] &then &sys arc kill circle_covB

/*************************************************************************/
/* Creates temporarily coverages which will serve as a cookie cutters to
/* extract the portion of the HRU matrix which will be used to calculate
/* lateral flow for the current model run

          create circle_covS circle %.cntrX% %.cntrY% %distance_involved%
          create circle_covB circle %.X-HIGH% %.Y-HIGH% %RADIUS%
          &sys arc clean circle_covS cov_tmp1 # 0.01 poly
          &sys arc kill circle_covS all
          &sys arc rename cov_tmp1 circle_covS
```

```
        &sys arc build circle_covB

/* Extracts HRU matrix portion for the analysis

        &sys arc intersect circle_covB circle_covS cov_tmp poly 1
        &sys arc intersect cov_tmp %runoff% circle_runoff

/* Removes unnecessary temporarily files

        &sys arc kill circle_covS all
        &sys arc kill circle_covB all
        &sys arc kill cov_tmp all

/*************************************************************************/
/* Uses several conditions to extract only valuable polygons of the HRU matrix
/* These conditions are: 1) Selected polygons should have proper attribute table values;
/* 2) Selected polygons should be located at elevation higher than the current stream
/* segment elevation i.e. they should 'flow' into it.

        reselect circle_runoff poly circle_runoff-ID gt 0
        reselect circle_runoff poly ELEVATION ge %H1%
        aselect circle_runoff poly RUNOFF_COV# = %run_poly_num_curr%

      &end
    &else     /* Following condition applies to the 'saturated watershed' */
      &do

/* Removes temporarily files

        &if [exist circle_runoff -cover] &then &sys arc kill circle_runoff
        &if [exist circle_covS -cover] &then &sys arc kill circle_covS
        &if [exist circle_covB -cover] &then &sys arc kill circle_covB

/* Creates a circle, based on the value of the variable 'RADIUS'.

        create circle_covB circle %.X-HIGH% %.Y-HIGH% %RADIUS%
        &sys arc build circle_covB poly

/* Using the circel, extracts usable portion of the HRU matrix and saves it as
/* a coverage 'circle_runoff'. This coverage is the main spatial analytical object.

        &sys arc intersect circle_covB %runoff% circle_runoff poly 0.1
        &sys arc kill circle_covB all

/*************************************************************************/
/* Uses several conditions to extract only valuable polygons of the HRU matrix
```

```
/* These conditions are: 1) Selected polygons should have proper attribute table values;
/* 2) Selected polygons should be located at elevation higher than the current stream
/* segment elevation i.e. they should 'flow' into it.

        reselect circle_runoff poly circle_runoff-ID gt 0
        reselect circle_runoff poly ELEVATION ge %H1%
        aselect circle_runoff poly RUNOFF_COV# = %run_poly_num_curr%

    &end

/* Prints on a screen number of selected polygons from the HRU matrix

&type
&type [show select circle_runoff poly]
&type

/*************************************************************************/
/* Using function 'show' defines how many polygons were selected. If 'none' then it
/* assign '0' values for the discharge and area. This can happen because of complex
/* spatial interrelations between HRU matrix, stream segments and 'cookie cutting' tech-
nique.
/* For example, stream segment can be very short or previous iteration accounted for the
/* polygons because in DEM they had elevations higher than elevation of the previous
/* segment.

&if [before [show select circle_runoff poly] ,] = 0 &then
 &do
  &do i = 1 &to %t%
      &sv Q%run_poly_num_curr%-%t%-%i% = 0
      &sv Q%run_poly_num_curr% = 0
      &sv A%run_poly_num_curr%-%t% = 0
      &sv Q = 0
  &end

 /*Directs to the block of the code which enters data into output file*/

    &goto enter_disch

 &end

/*************************************************************************
/* Sets format for numbers which will be written to the output file

     &format 2

/* Removes temporarily files
```

```
&if [exist disch1] &then &sv kill [delete disch1]
&if [exist tmpA] &then &sv kill [delete tmpA]

/*************************************************************************/
/* Checks saturation conditions, extracts values of area and discharge from HRU
/* polygons and does calculations developed for these conditions and
/* described in theoretical part of the thesis

&if %stop% = 0 &then    /* Undersaturation conditions */
 &do

/* Extracts from original HRU matrix polygons for analysis

        reselect %runoff% poly OVERLAP circle_runoff poly # PASSTHRU
        reselect %runoff% poly AREA gt 0

/* Using 'statistics' module, defines total area of polygons, located inside 'circle_runoff'
/* coverage and touching it

         statistics %runoff% poly
         sum AREA
         end
         &sv AREA-TOTAL = [show statistic 1 1]

/*************************************************************************/
/* Following loop applies to current and previous time intervals, because we have to take
/* into account current runoff and runoff which occured previously, but was not accounted
/* because of the small size of the contributing area (see theoretical part of the thesis)

        &do i = 1 &to %t%

/* Calculates area and runoff within 'circle_runoff' coverage. Notice, that runoff values
/* are adjusted to the area within the 'circle_runoff' coverage. This has to happen because
/* part of HRU polygons is inside of the 'circle_runoff' coverage and part is outside.
/* However, current total runoff (Q%run_poly_num_curr%-%t%-%i%) has to be esti-
mated
/* only for the area of the 'circle_runoff' coverage.

         statistics circle_runoff poly
         sum Q%i%
         sum AREA
         end
         &sv Q%run_poly_num_curr%-%t%-%i% = [calc [show statistic 1 1] * ~
         [show statistic 2 1] / %AREA-TOTAL%]
         &sv A%run_poly_num_curr%-%t% = [show statistic 2 1]
```

```
        &end

/* Prints value of the 'circle_runoff' coverage area on the screen

        &type AREA %run_poly_num_curr%-%t% = ~
        [value A%run_poly_num_curr%-%t%] sq.m.

/*************************************************************************/
/* Following block refers to time intervals after the first one. It calculates lateral flow
/* from runoff values. obtained from HRU attribute table

&if %t% gt 1 &then
    &do
            &sv add = 0
            &sv add1 = 0

       &do i = 1 &to [calc %t% - 1]

/* Following statement compares lateral flow from the previous time interval and current
/* It then set up two variables EL1 and EL2 and redirect code to another label

        &if [value Q%run_poly_num_curr%-%t%-%i%] lt ~
        [value Q%run_poly_num_curr%-[calc %t% - 1]-%i%] &then

       &do
          &sv EL1 = 0
          &sv EL2 = 0
          &goto continue_calc
        &end

/*************************************************************************/
/* Following statement compares area value  from the previous time interval and current
/* It then set up two variables EL1 and EL2 and redirect code to another label

       &if [value A%run_poly_num_curr%-%t%] lt ~
       [value A%run_poly_num_curr%-[calc %t% - 1]] &then

         &do
           &sv EL1 = 0
           &sv EL2 = 0
           &goto continue_calc
       &end

/*************************************************************************/
/* If area and discharge from the previous time intervals are not equal '0', then code
```

```
/* calculates discharge and area using values from the current dataset and values from
/* previously set variables. For the convenience of checking the code, eqaution which cal-
culates
/* lateral flow (see theoretical part of the thesis) was broken into several pieces.
/* Variables El1 and El2 are just elements of the equation, calculated separately

      &sv EL1 = [calc [calc [value Q%run_poly_num_curr%-%t%-%i%] - ~
          [value Q%run_poly_num_curr%-[calc %t% - 1]-%i%]] ~
          * [calc [value A%run_poly_num_curr%-%t%] - [value
A%run_poly_num_curr%- ~
           [calc %t% - 1]]] + %add%]
      &sv add = [value EL1]
      &sv EL2 = [calc [calc [value A%run_poly_num_curr%-%t%] - ~
          [value A%run_poly_num_curr%-[calc %t% - 1]]] + %add1%]
      &sv add1 = [value EL2]

      &label continue_calc

   &end

/* Final calculation of the lateral flow, using previously calculated El1 and El2 elements
/* of the equation

      &sv Q%run_poly_num_curr% = [calc [calc [value Q%run_poly_num_curr%] + ~
          [calc [calc [value EL1] + ~
          [calc [value Q%run_poly_num_curr%-%t%-%t%] * ~
          [value A%run_poly_num_curr%-%t%]]] / [calc [value EL2] + ~
          [value A%run_poly_num_curr%-%t%]]]] / 2] -

      &sv Q = [format '%1%' [value Q%run_poly_num_curr%]]

 &end

/*************************************************************************/
/*  Calculates lateral flow only for the first time interval of the modeling

    &if %t% = 1 &then
    &do

     &sv Q%run_poly_num_curr%-%t%-%i% = [value Q%run_poly_num_curr%-%t%-
%t%]
      &sv Q%run_poly_num_curr% = [value Q%run_poly_num_curr%-%t%-%t%]
      &sv A%run_poly_num_curr%-%t% = [value A%run_poly_num_curr%-%t%]
      &sv Q = [format '%1%' [value Q%run_poly_num_curr%]]
       &type First step!
```

```
    &end

/* End of unsaturated conditions */

  &end

/*************************************************************************/
/*  Full saturation conditions, when the whole watershed contributes water to the stream

&else

&do

        statistics circle_runoff poly
        sum Q%t%
        end

        &sv Q%run_poly_num_curr%-%t%-%t% = [show statistic 1 1]
        &sv Q%run_poly_num_curr% = [calc [calc ~
            [value Q%run_poly_num_curr%-%t%-%t%] + ~
            [value Q%run_poly_num_curr%]] / 2]
        &sv Q = [format '%1%' [value Q%run_poly_num_curr%]]

&end

/*************************************************************************/
/* Following statement refers to the condition when stream segment is greater than
/* the radius of contributing area. This happens usually during the first or second time
/* steps. In this case lateral flow value should be extrapolated for the whole length
/* of the stream segment.

&if %distance_involved% lt %total_length% &then &sv Q = [format '%1%' [calc
%total_length% * %Q% / %distance_involved%]]

/* Prints on the screen final lateral flow value

&type DISCHARGE = [value Q]

/* Label where code starts storing flow values as variable

&label enter_disch

/*************************************************************************/
/* Stores flow value for the first time step  in an ascii file. The line stored in that file has
/* value for modeled route#, internal nimber of HRU matrix, total length of the modeled
/* stream segment, slope and value of the lateral flow for the first time step. The name of
```

```
/* the file consist of word 'disch' and unique number of the stream segment

&if %t% = 1 &then
   &do
      &if [exist disch%run_poly_num_curr%] &then &sv kill = ~
         [delete   disch%run_poly_num_curr%]
      &if %m% = 1 &then
      &sys echo "Route#","Runoff_cov#","Length","Slope",~
            "di" > disch%run_poly_num_curr%
     &sys echo %k%,%run_poly_num_curr%,%total_length%,%slope_stream%,%Q%
>> disch%run_poly_num_curr%
   &end

/*************************************************************************/
/* Stores flow value for other than first time step  in an ascii files. These files have
/* only one number - lateral flow value for the modeled time interval and stream segment
/* Following statement uses UNIX commands to append lateral flow values with comma
/* delimeter to the previously created file, storing previously derived flow, starting with
/* the first time interval.

          &else
               &do
                &if %m% = 1 &then
                &sys echo d%t% > disch%t%
                &sys echo %Q% >> disch%t%
                &sys paste -d"," disch%run_poly_num_curr% disch%t% >> tmpA
                &sv kill = [delete disch%t%]
                &sv kill = [delete disch%run_poly_num_curr%]
                &sys mv tmpA disch%run_poly_num_curr%
               &end

/* Following statement informs user about currently analysed stream segment number

     &type
     &type  POLYGON# = %run_poly_num_curr% time step  %t%
     &type

/*************************************************************************
/* DRAWING FEATURES ON THE SCREEN  AND MAKE A GRAPHIC FILE
/*************************************************************************
/* Removes old files

   &if [exist rt%k%_%run_poly_num_curr%.gra] &then ~
      &sv kill [delete rt%k%_%run_poly_num_curr%.gra]

/*************************************************************************/
```

```
/* Sets drawing parameters, such as map extent, map units, page units, page size, page
units
/* limits of the drawing, shading palette, shading symbol, colors

    &if [after %.test% est] = 2 or [after %.test% est] = 9 &then DISPLAY 9999 2
    &else DISPLAY 9999 SIZE 5 5
    mape %.runoff_cov%
    mapunits meters
    pageunits inches
    pagesize 8 11
    units page
    maplimits 0.5 0.5 10.5 10.5
    shadeset colornames.shd
    shadesymbol 26
    patch 0.03 0.0 11 11
    polygonshades circle_runoff 56

    linecolor yellow
    circle %.cntrX% %.cntrY% %distance_involved%

/* Removes old raster files

   &if [exist %path_out%/rt%k%_cyc%t%_seg%run_poly_num_curr%.rs] ~
        &then &sv kill [delete %path_out%/
rt%k%_cyc%t%_seg%run_poly_num_curr%.rs]

/* Checks that only meaningful polygons will be drawn

        aselect %runoff% poly
        reselect %runoff% poly %runoff%-ID gt 0

/*************************************************************************/
/* Sets graphical primitives for the drawing and draws image of the watershed with
/* contributing area for the modeled stream segment, stream channel and radius which
/* served to select HRU polygons form the original matrix

        linecolor green
        polys %runoff%
        linecolor cyan
        linesize 0.03
        arcs %.stream%
        linesymbol 1
        linecolor cyan
        polys rt%k%_poly

        linecolor cyan
```

```
        circle %.X-HIGH% %.Y-HIGH% %RADIUS%

/*************************************************************************/
/* Selects graphical primitives and draws symbol indicating location of the stream
/* segment used for modeling

        markerset water.mrk
        markersymbol 111
        markersize 0.1
        markercolor red
        units map
        marker %.cntrX% %.cntrY%

/*************************************************************************/
/* Seelects text properties and draws the text indicating lateral discharge value
/* and cumulative time

        units page
        move 4.5 7
        textset font.txt
        textsymbol 16
        textsize 0.2
        textcolor black
        text [quote Seg.# %run_poly_num_curr%, Time interval = %time_interval_cum%
min.]

        move 4.5 6
        &if %m% = 1 &then text [quote Channel Flow = %Q% l/sec.]
        &else text [quote Lateral Flow Contribution = %Q% l/sec.]

/* Prints on the screen directory where image will be stored

&type PATH = %path_out%

/*************************************************************************/
/* Following statement uses variable 'video_count' to assign consequent numbers 1 ... n
/* to saved images for future use in animation software which requires taht files should
/* be in order.

        &sv video_count = [calc %video_count% + 1]

/* Creates sun raster file at specified by the variable 'path_out' directory

            &if %stop% = 0 &then screensave ~
               %path_out%/ rt%k%_cyc%t%_seg%run_poly_num_curr%.sun 0 0 8 11
```

```
/* Using binaries 'convert' from the ImageMagic software, converts sun raster file
/*  into GIF format for the future animation

          &sys convert %path_out%/rt%k%_cyc%t%_seg%run_poly_num_curr%.sun
file%video_count%.gif

/*************************************************************************/
/* Following part of the code creates a coverage 'circ' containing area of the
'circle_runoff'
/* coverage. It will be used to erase already used HRU polygons from the HRU matrix
/* to avoid redundant use of them in further calculations.

     &if %stop% = 0 &then
       &do
          &if [exist circ -cover] &then &sys arc kill circ all
          create circ SELECT circle_runoff poly
          &sys arc build circ poly
       &end

/*************************************************************************/
/* Quits ARCPLOT module and returns to the regular ARC promt

        quit

/* Following procedures are done within ARC module.

/* Removes old file

          &if [exist poly_elim -cover] &then kill poly_elim all

/* Erases HRU matrix with 'circ' coverage containing already used HRU polygons

     &if %stop% = 0 &then
          erase %runoff% circ poly_elim
      &else erase %runoff% circle_runoff poly_elim

/* Removes old files

          kill %runoff% all
          &if [exist circ -cover] &then &sys arc kill circ all

/*************************************************************************/
/* Renames newly created coverage, so that it will be used again in next iterations, but
/* without already used HRU polygons

          rename poly_elim %runoff%
```

```
/*************************************************************************/
/* Followiong label is used in case if for some reason stream segment was already analy-
sed
/* and lateral discharges were already derived. This can happen sometimes as a result of
/* spatial interrelations between vertices on the stream and polygons from HRU matrix.

        &label skip_poly

/* Checks if for some reason code is still within ARCPLOT module and quits it

       &if [show program] = ARCPLOT &then q

/* End of routine
&return
/*************************************************************************/
```

Kinematic Wave routing and Turbidity modeling C code.

Both, turbidity and flow were combined together in one code because flow data are input into turbidity calculations.

```
#include <stdio.h>
#include <math.h>
main( int argc, char *argv[3])
{
    int     fcol = 4, k, i, j, C, R, dt;
    int     l, m;
    float   B, cum, SUM, baseflow, dx, alfa, beta, n, PART1, PART2, PART3, PART4,
DIS;
    double  P, S;
    char    ch;
    float   SED[100][100], Tr[100][100], DE[100][100];
    float   DATA[100][100], QBASE[100][100];
    float   CI, CJ, CO4, A, ReyNum, w, gi;
    float   nu, d, SP, U, Vcr, V, Rh, Q;
    float   SPcr, G, H, sigma, T, Tcr, al;
    double  C1, C2, C3;
    FILE    *fp;

    if(argc !=4) {
            printf("USAGE: rut #COLUMNS #ROWS dt beta alfa\n");
            exit(1);
     }

    C = atoi(argv[1]);
    R = atoi(argv[2]);
    dt = atoi(argv[3]);

/* Reading Data File */
/* Its name was fixed one, i.e. 'disch.dat' */

/* Checks if data file exist */

    if ((fp = fopen("disch.dat", "r")) == NULL) {
        printf("\n Sorry, cannot open your input file \n");
        exit();
    }

/* Following loop reads data file 'disch.dat' and create flow matrix DATA[i][j] */

    for (i = 0; i < R; i++) {
```

```
            for (j = 0; j < C; j++) {

            fscanf(fp, "%f", &DATA[i][j]);
            fscanf(fp, ",");

            }

            fscanf(fp, "%*1c");
        }
        fclose(fp);

/* Kinematic Routing Equation */
/* Baseflow is a baseflow (l/sec), n - Manning coefficient, beta - power constant */
/* Algorithm was adapted from Chow et al. (1988) */
/* Variable B is a calibrating parameter. */

    baseflow = 0.5;  n = 0.065; beta = 0.6;

 for (j = fcol; j < C; j++) {
   for (i = 0; i < R; i++) {

    DIS = 0;
    m = j - 1;
    l = i + 1;

    dx = DATA[l][2];

    if (dx == 0) { dx = 1; }

    S = DATA[l][3];

    B = 4000 * pow(DATA[i][j],0.05);          /* Width-flow relationship */

    alfa = pow((n * pow(B,0.667) / pow(S,0.5)),beta);

    if (m == fcol - 1) {
    if (DATA[i][j] < baseflow) { DATA[i][j] = baseflow; }
    PART1 = (dt / dx  * DATA[i][j]);
    PART2 = alfa * beta * baseflow * pow(((baseflow + DATA[i][j]) / 2),(beta - 1));
    PART3 = dt * (((QBASE[l][j]) / dx));
    PART4 = (dt / dx) + (alfa * beta * pow(((baseflow + DATA[i][j]) / 2),(beta - 1)));
    }
    else {
    if (DATA[i][j] < baseflow) { DATA[i][j] = baseflow; }
    PART1 = (dt / dx  * DATA[i][j]);
    PART2 = alfa * beta * DATA[l][m] * pow(((DATA[l][m] + DATA[i][j]) / 2),(beta -
```

```
1));
      PART3 = dt * ((((QBASE[l][m] + QBASE[l][j]) / dx) / 2);
      PART4 = (dt / dx) + (alfa * beta * pow(((DATA[l][m] + DATA[i][j]) / 2),(beta - 1)));
      }
            DIS = (PART1 + PART2 + PART3) / PART4;
            DATA[l][j] = DIS;
   }
}

/* Sediment module, which uses Young's stream power theory, sediment routing tech-
nique */
/* and empirical regression, converting suspended sediment concentration into turbidity
units */

/* Following constants are main hydrological parameters utilized in most models */
/* They are described in 'Methodology' chapter */

      w = 0.0006; nu = 0.0000013; d = 0.000062; SPcr = 0.002; gi = 9.81;

/* Calculations on suspended solids */
/* Inputs are: Slope, Discharge */

     for (i = 0; i < R; i++) {
      for (j = fcol; j < C; j++) {

        dx = DATA[i][2];

        Rh = 0.002 * pow(DATA[i][j],0.8);  /* 0.001 - alfa coeff for depth-flow */

        S = DATA[i][3];

        if (S < 0.01) { S = 0.001; }

        V = (pow(Rh,0.667) * pow(S,0.5)) / n;        /* Manning equation */

        U = pow((gi * Rh * S),0.5);

        ReyNum = U * d / nu;

        SP = V * S;

        C1 = w * d / nu;
        C2 = U / w;
        C3 = SP - SPcr;

/* Elements of the nit stream power equation which produces suspended
```

```
/* sediment concentration in mg/l */

        CI = 5.435 - 0.286 * log10(C1) - 0.457 * log10(C2);
        CJ = 1.799 - 0.409 * log10(C1) - 0.314 * log10(C2);
        CO4 = log10(C3);
/* Following statements refer to the calculation of the maximum sediment capacity */
/* for the given stream segment */

/* Dimensionless actual lift force */

        T = (Rh * S) / (1.7 * d);

/* Dimensionless parameter */

        al = 2.45 * pow(0.37,0.4) * pow(T,0.5);

/* Critical lift force from Schields's diagram */

        Tcr = 0.02;

/* Dimensionless parameter */

        if (T < Tcr) {sigma = 0;} else {sigma = (T - Tcr) / Tcr;}

/* Stream channel flow transport capacity */

        Tr[i][j] = (0.635 * 1700 * d * pow((gi * Rh * S),0.5) * gi * (sigma - (1 / al ) *
log10(1 + (al * sigma))));

/* Checks condition if flow = '0' and then uses regression equation to convert */
/* suspended sediments units into turbidity units */

        if (QBASE[i][j] == 0) {SED[i][j] = 0;} else {
                SED[i][j] = pow(10,(CI + (CJ * CO4))); }

/* Checks condition if estimated suspended sediment concentration greater or equal */
/* stream channel flow transport capacity. */

        if (SED[i][j] >= Tr[i][j]) {SED[i][j] = Tr[i][j];}
        if (SED[i][j] == 0) {SED[i][j] = Tr[i][j];}

    }
}

/* Following loop does sediment routing along stream channel. For each segment sus-
pended */
```

```
/* sediment concentration is treated as a sum of incoming sediment and estimated for the
*/
/* If the total sum greater than channel flow transport capacity, then suspended sediment
*/
/* concentration will be assigned value of the channel flow transport capacity */
/* Otherwise, suspended sediment concentration will be equal the sum of incoming */
/* suspended sediments from the upstream segment and suspended sediment from chan-
nel */
/* itself */
/* Variable DE was set up to indicate condition of either deposition or erosion */
/* If suspended sediment concentration is greater than the channel flow transport capacity
*/
/* DE will be assigned '1' i.e. accumulation. Otherwis eit will be assign value '0' i.e. ero-
sion */
/* This variable can be used in the future visualization to color differently stream seg-
ments */
/* Final value of the SED[i + 1][j] variable is converted into turbidity units by using */
/* empirical regression equation */

    for (j = fcol; j < C; j++) {
      for (i = 0; i < R; i++) {

        SED[i + 1][j] = SED[i][j] + SED[i + 1][j];

        if (SED[i + 1][j] >= Tr[i + 1][j]) {

            SED[i + 1][j] = (Tr[i + 1][j] * 0.6) + 9.9;
            DE[i + 1][j] = 1;
        }
        else {
          SED[i + 1][j] = (SED[i + 1][j] * 0.6) + 9.9;
          DE[i + 1][j] = 0;
        }

      }
    }


/* Exporting flow results to the output file "dis.txt" which is an ascii file  */
/* This file has fixed first 2 columns - unique identification number of the stream channel
*/
/* defined in GIS module and slope */

    if ((fp = fopen("dis.txt","w"))==NULL){
          puts("Cannot write the file\n");
          exit();
```

```
        }
    for (i = 0; i < R; i++){

      for (j = fcol; j < C; j++) {

       if (j == fcol)
         {
          fprintf(fp,"%2.0f", DATA[i][0]);
          fprintf(fp,",");
          fprintf(fp,"%3.0f", DATA[i][1]);
         }
          fprintf(fp,",");
          fprintf(fp,"%.1f", DATA[i][j]);
       }
      fprintf(fp, "\n");
    }
      fclose(fp);

    k = C - 1;

/* Exporting turbidity results to the output file "sed.txt" which is an ascii file  */
/* This file has fixed first 2 columns - unique identification number of the stream channel
*/
/* defined in GIS module and slope. Other columns refer to the time intervals of the
model */
/* and contain turbidity values and a column with the values of DE variable, showing */
/* '1' for accumulation and '0' for erosion conditions */

    if ((fp = fopen("sed.txt","w"))==NULL){
          puts("Cannot write the file\n");
          exit();
          }
    for (i = 0; i < R; i++){

      for (j = fcol; j < C; j++) {

       if (j == fcol)
         {
          fprintf(fp,"%2.0f", DATA[i][0]);
          fprintf(fp,",");
          fprintf(fp,"%3.0f", DATA[i][1]);
          fprintf(fp,",");
          fprintf(fp,"%.2f", DATA[i][3]);
         }
          fprintf(fp,",");
          fprintf(fp,"%.1f", SED[i][j]);
```

```
        }
      fprintf(fp, "\n");
    }
    if ((fp = fopen("de.txt","w"))==NULL){
        puts("Cannot write the file\n");
        exit();
        }
    for (i = 0; i < R; i++){

      for (j = fcol; j < C; j++) {

       if (j == fcol)
        {
          fprintf(fp,"%2.0f", DATA[i][0]);
          fprintf(fp,",");
          fprintf(fp,"%3.0f", DATA[i][1]);
          fprintf(fp,",");
          fprintf(fp,"%8.2f", DATA[i][3]);
        }
          fprintf(fp,",");
          fprintf(fp,"%.1f", DE[i][j]);
        }
      fprintf(fp, "\n");
    }
      fclose(fp);

}
```

EXPONENT.C

This code was compiled to use in MODEL_RUN.AML to calculate variable power of some
values because AML doesn't have this function. Output of this code was sent to a file and then
read into MODEL_RUN.AML

```
#include "math.h"
#include "stdio.h"
#include "stdlib.h"
void
main(int argc, char *argv[2])
{
    float X, Y;

    X = atof(argv[1]);
    Y = atof(argv[2]);
```

```
        printf("%f\n", pow(X,Y));
return;
}
```

Appendix B. Measured Field Data.

Test 1

Date	Time	Rain (in)	Discharge(l/sec) MB-1	Turbidity (NTU) MB-3	Turbidity (NTU) MB-4
1 July 1996	09:30	0.070	7.768	6.9	0.1
1 July 1996	09:40	0.140	6.717	4.7	0.1
1 July 1996	09:50	0.080	6.063	4.7	0.1
1 July 1996	10:00	0.060	5.759	5.3	0.1
1 July 1996	10:10	0.100	5.708	22.0	1.9
1 July 1996	10:20	0.230	6.949	350.0	10.0
1 July 1996	10:30	0.130	13.781	773.0	14.6
1 July 1996	10:40	0.010	22.117	125.0	12.5

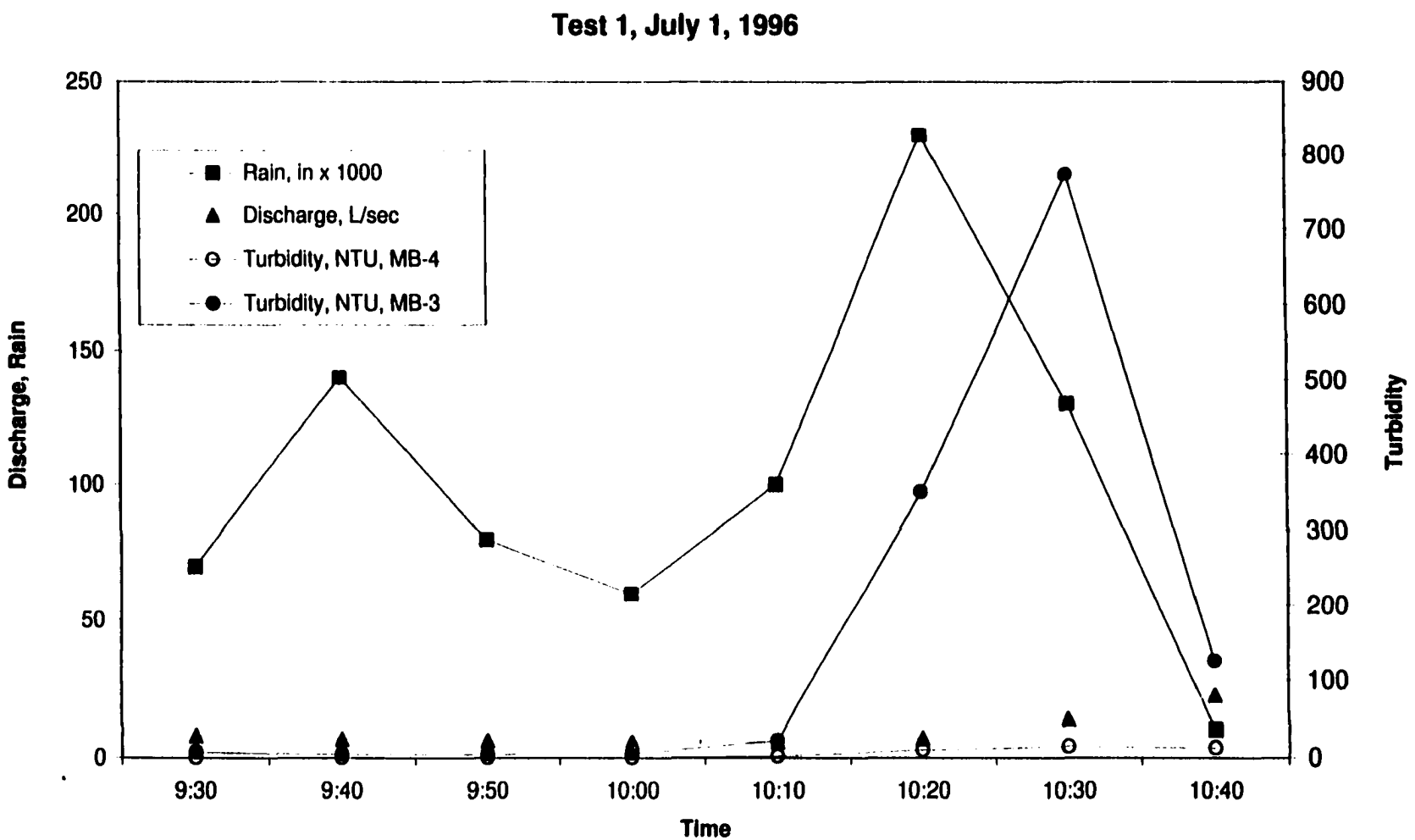

Test 2

Date	Time	Rain (in)	Discharge (l/sec) MB-1	Turbidity (NTU) MB-3	Turbidity (NTU) MB-4
30 June 1996	06:20	0.05	2.962	0.1	0.1
30 June 1996	07:00	0.06	3.755	5.5	0.1
30 June 1996	07:40	0.11	5.638	20.2	0.1
30 June 1996	08:20	0.11	10.406	61.4	52.0
30 June 1996	09:00	0.06	20.045	51.2	132.0
30 June 1996	09:40	0.05	27.561	52.8	118.0
30 June 1996	10:20	0.03	34.134	36.4	66.0
30 June 1996	11:00	0.02	35.063	26.7	3.4
30 June 1996	11:40	0.02	31.250	18.6	0.3

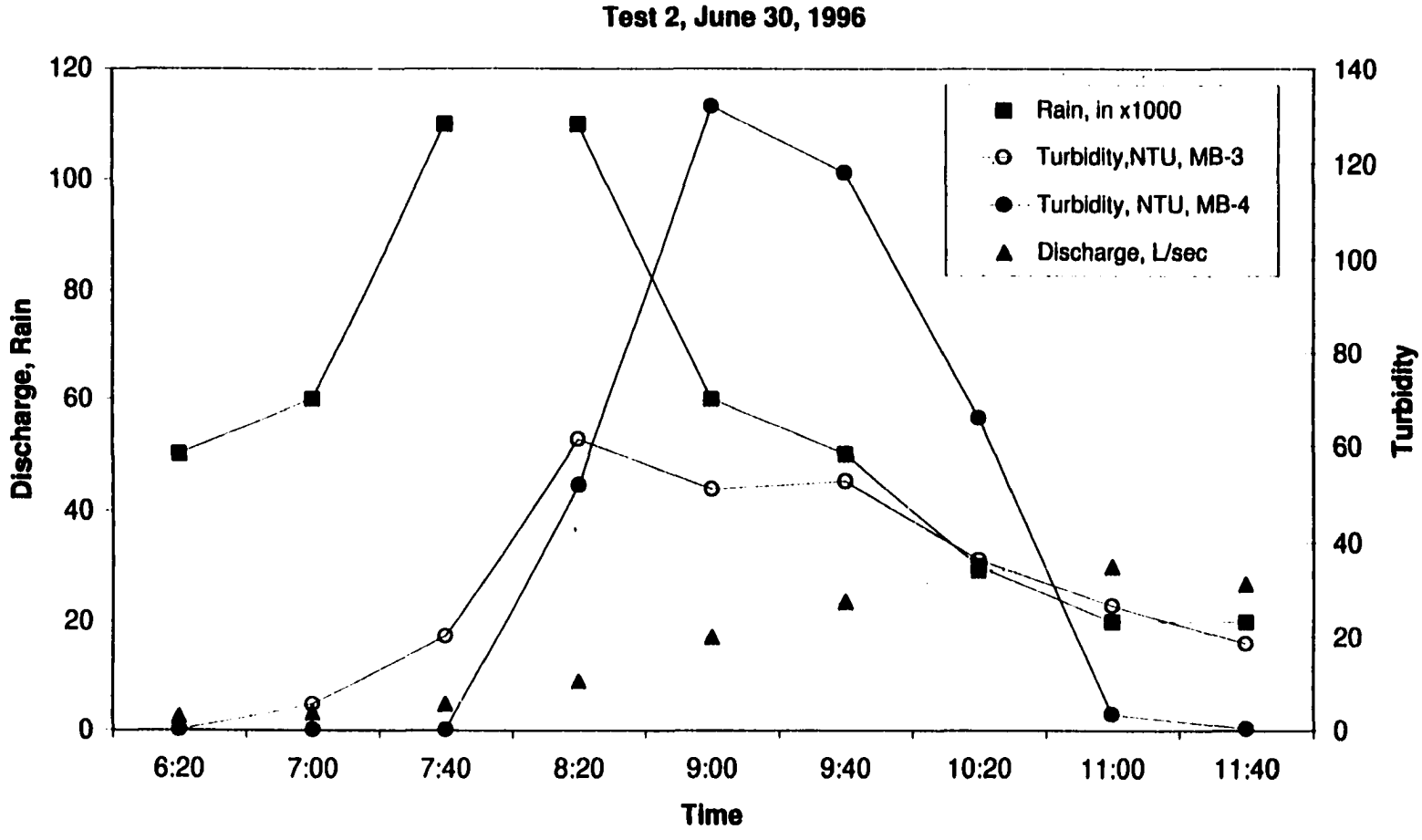

Test 3

Date	Time	Rain (in)	Discharge (l/sec), MB-1	Turbidity (NTU) MB-3
31 July 1996	09:19	0.030	5.944	0
31 July 1996	09:29	0.030	5.910	0
31 July 1996	09:39	0.020	5.893	0
31 July 1996	09:49	0.040	5.970	0
31 July 1996	09:59	0.020	6.285	0
31 July 1996	10:09	0.030	6.944	0
31 July 1996	10:19	0.030	8.394	0
31 July 1996	10:29	0.020	9.564	0
31 July 1996	10:39	0.030	11.660	0
31 July 1996	10:49	0.060	15.099	0
31 July 1996	10:59	0.050	18.602	0
31 July 1996	11:09	0.040	20.031	0
31 July 1996	11:19	0.040	23.564	0
31 July 1996	11:29	0.050	29.391	0
31 July 1996	11:39	0.020	36.371	0
31 July 1996	11:49	0.010	42.281	0

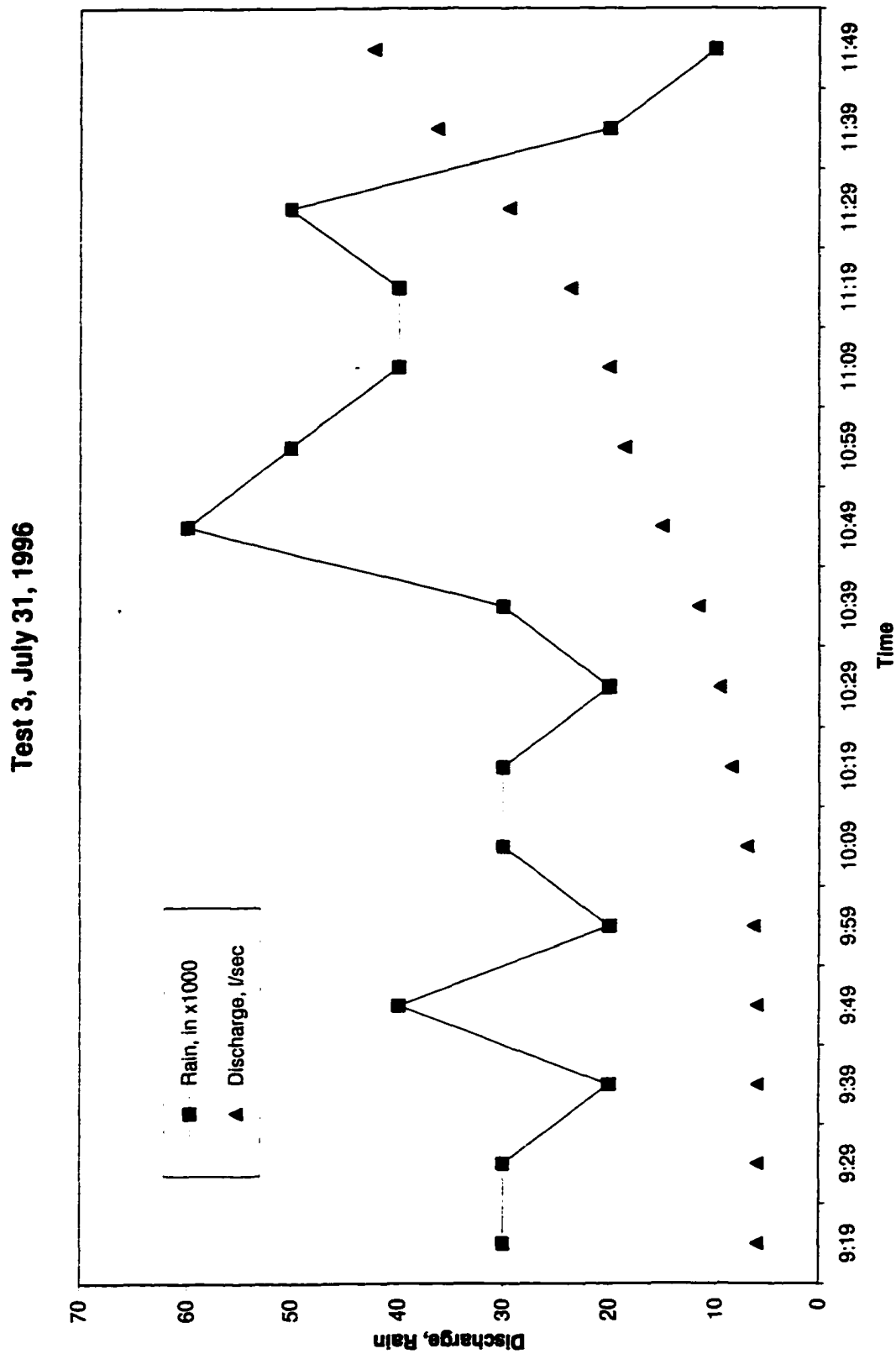

Test 4

Date	Time	Rain(in)	Discharge(l/sec) MB-1	Turbidity (NTU) MB-3	Turbidity (NTU) MB-4
16 Sep1996	22:30	0.010	0.885	0.0	0.0
16 Sep1996	23:00	0.010	0.887	0.0	0.0
16 Sep1996	23:30	0.010	0.930	0.0	0.0
17 Sep1996	00:00	0.010	0.960	0.0	0.0
17 Sep1996	00:30	0.070	1.032	0.0	0.0
17 Sep1996	01:00	0.060	1.110	24.0	0.0
17 Sep1996	01:30	0.060	1.593	39.0	0.0
17 Sep1996	02:00	0.070	3.874	42.0	23.0
17 Sep1996	02:30	0.080	5.842	46.5	66.0
17 Sep1996	03:00	0.110	9.086	69.0	48.0
17 Sep1996	03:30	0.050	14.379	96.0	73.0
17 Sep1996	04:00	0.090	28.614	109.5	110.0
17 Sep1996	04:30	0.120	30.694	87.5	143.0
17 Sep1996	05:00	0.170	37.181	161.0	134.0
17 Sep1996	05:30	0.160	61.130	123.5	125.0
17 Sep1996	06:00	0.120	91.304	188.0	160.0
17 Sep1996	06:30	0.040	120.316	145.0	150.0
17 Sep1996	07:00	0.040	128.520	135.0	134.0

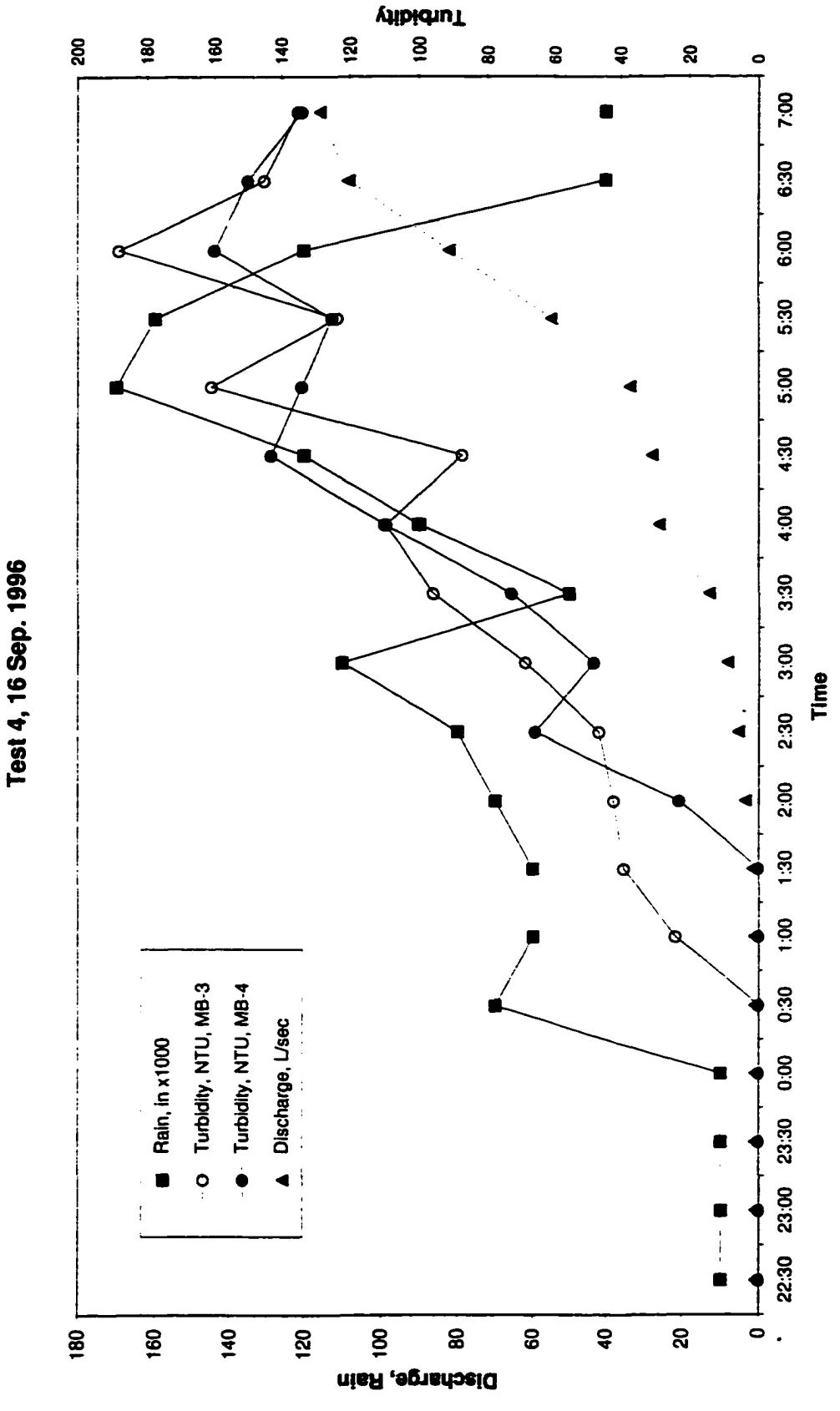

Test 5

Date	Time	Rain (in)	Discharge (l/sec) MB-1	Turbidity (NTU) MB-3	Turbidity (NTU) MB-4
08 Oct 1996	13:00	0.030	1.869	0.0	3.5
08 Oct 1996	13:30	0.070	1.772	0.0	3.5
08 Oct 1996	14:00	0.090	1.955	5.8	6.1
08 Oct 1996	14:30	0.140	3.209	19.8	14.8
08 Oct 1996	15:00	0.120	7.415	124.4	31.9
08 Oct 1996	15:30	0.070	21.054	190.3	64.8
08 Oct 1996	16:00	0.060	33.345	185.9	90.5
08 Oct 1996	16:30	0.060	37.581	135.6	108.0
08 Oct 1996	17:00	0.140	35.548	89.3	127.0
08 Oct1996	17:30	0.160	42.447	84.2	80.7
08 Oct1996	18:00	0.070	67.591	199.9	73.3
08 Oct1996	18:30	0.050	105.009	215.6	91.1
08 Oct1996	19:00	0.020	97.427	122.8	76.5
08 Oct1996	19:30	0.040	86.221	93.1	893.0
08 Oct1996	20:00	0.250	80.820	71.5	784.0
08 Oct1996	20:30	0.300	73.913	70.3	627.0
08 Oct1996	21:00	0.060	159.837	688	913.0
08 Oct1996	21:30	0.070	266.093	231.4	954.0
08 Oct1996	22:00	0.070	194.309	140.5	2202.0
08 Oct1996	22:30	0.070	155.160	95.0	1258.0
08 Oct1996	23:00	0.080	139.824	81.4	1198.0
08 Oct1996	23:30	0.070	127.584	73.4	2096.0
09 Oct1996	00:00	0.050	124.417	74.8	1364.0
09 Oct1996	00:30	0.030	126.743	73.2	648.0

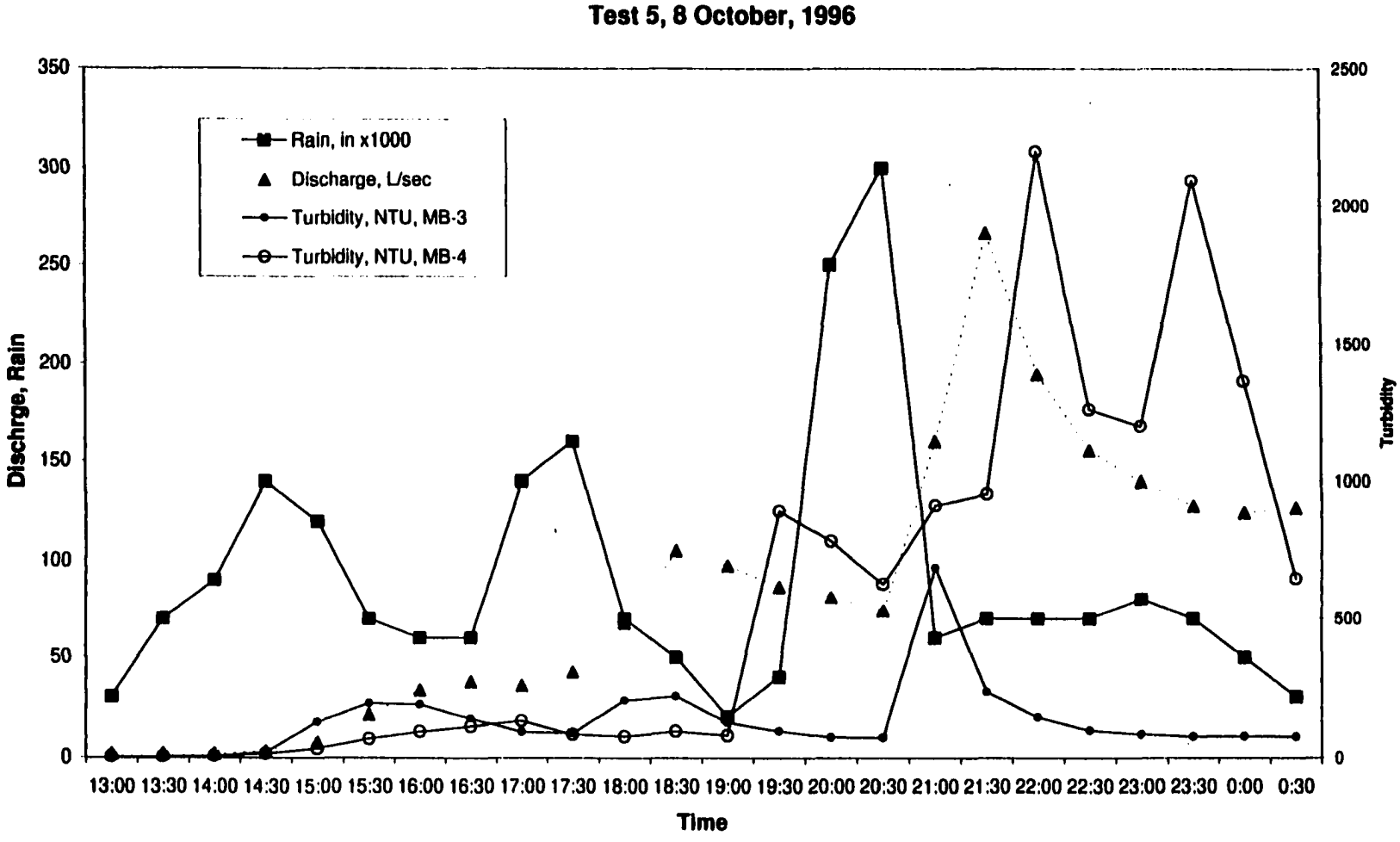

Test 6

Date	Time	Rain (in)	Discharge (l/sec) MB-1	Turbidity (NTU) MB-3	Turbidity (NTU) MB-4
13 Aug 1996	02:19	0.100	1.682	0	0
13 Aug 1996	03:19	0.060	3.448	5	0
13 Aug 1996	04:19	0.040	4.882	8	0
13 Aug 1996	05:19	0.020	5.665	7.5	0
13 Aug 1996	06:19	0.020	4.962	4	0
13 Aug 1996	07:19	0.190	5.163	1	7.5
13 Aug 1996	08:19	0.140	21.589	133	480
13 Aug 1996	09:19	0.040	39.628	165	570
13 Aug 1996	10:19	0.030	34.732	60	100

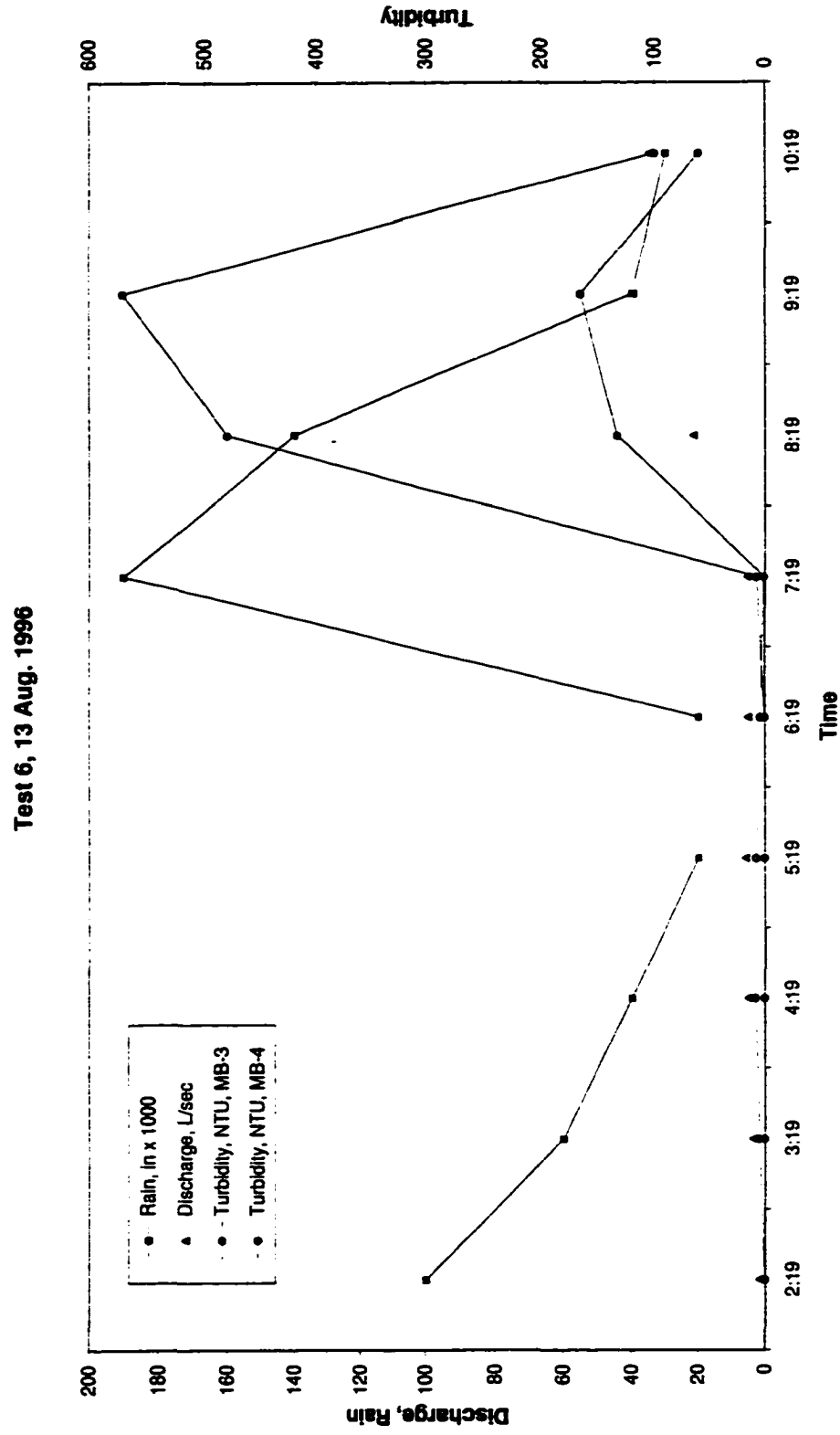

Test 7

Date	Time	Rain(in)	Discharge(l/sec) MB-1	Turbidity (NTU) MB-3	Turbidity (NTU) MB-4
28 Sep1996	20:10	0.150	1.604	0.0	0.0
28 Sep1996	20:50	0.220	3.159	74.0	47.0
28 Sep1996	21:30	0.060	39.936	186.0	108.5
28 Sep1996	22:10	0.150	26.759	152.0	132.0
28 Sep1996	22:50	0.180	28.904	104.0	126.5
28 Sep1996	23:30	0.110	100.304	247.0	133.0
29 Sep1996	00:10	0.100	92.654	112.0	104.5
29 Sep1996	00:50	0.040	104.011	93.0	78.0
29 Sep1996	01:30	0.050	87.610	68.0	69.0
29 Sep1996	02:10	0.040	76.060	65.0	65.0
29 Sep1996	02:50	0.030	67.962	60.0	65.0

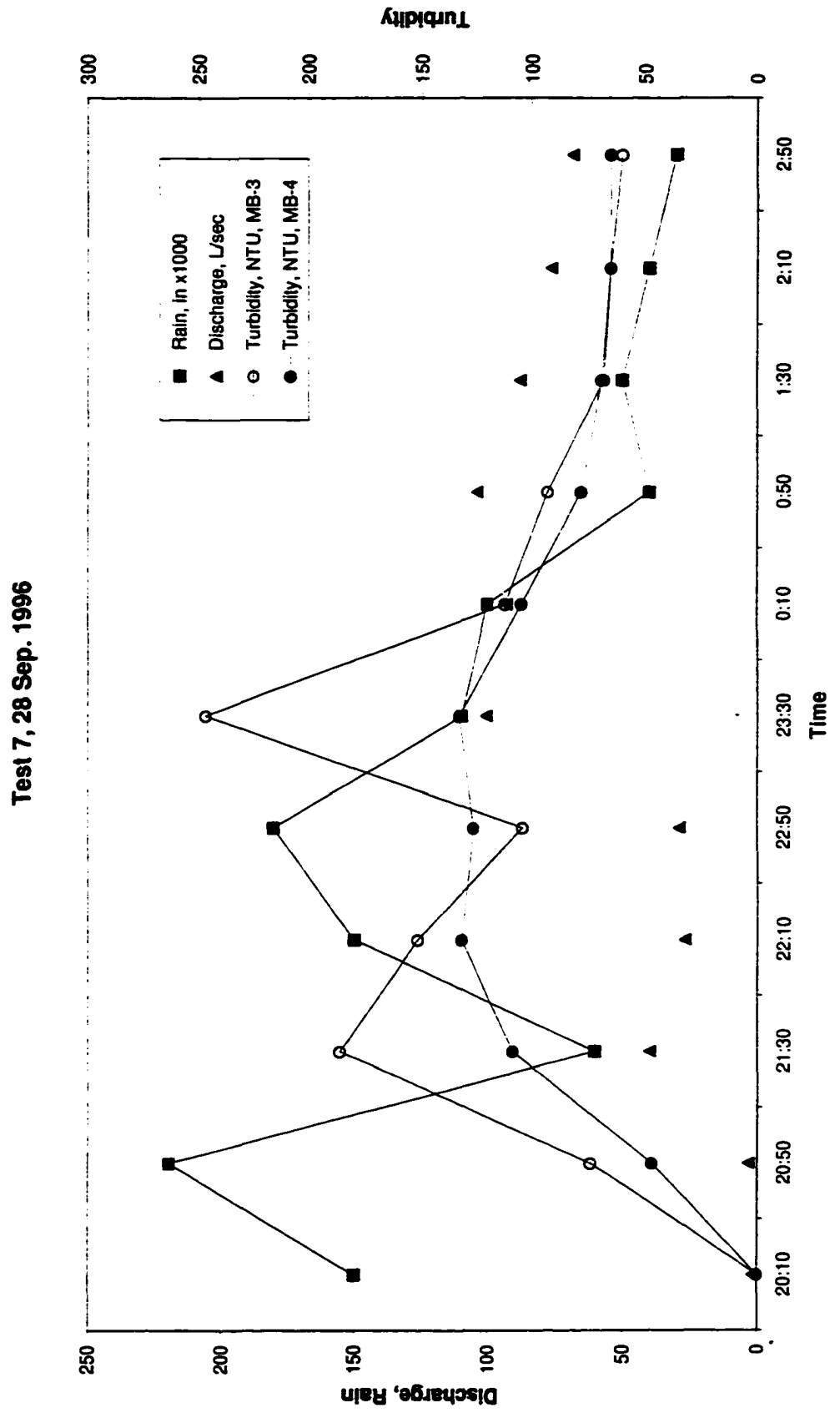

Test 8

Date	Time	Rain (in)	Discharge (l/sec) MB-1	Turbidity (NTU) MB-3	Turbidity (NTU) MB-4
19 Oct 1996	05:20	0.090	2.277	0.2	0.0
19 Oct 1996	06:20	0.140	2.248	1.3	2.0
19 Oct 1996	07:20	0.100	10.454	30.8	12.0
19 Oct 1996	08:20	0.130	12.879	30.5	22.0
19 Oct 1996	09:20	0.080	24.688	37.8	66.0
19 Oct 1996	10:20	0.040	28.877	30.2	90.0
19 Oct 1996	11:20	0.180	25.636	19.1	83.0
19 Oct 1996	12:20	0.310	39.404	32.9	56.0
19 Oct 1996	13:20	0.280	100.197	126.7	83.0
19 Oct 1996	14:20	0.170	160.738	58.7	96.0
19 Oct 1996	15:20	0.070	132.869	40.5	79.0
19 Oct 1996	16:20	0.170	95.282	30.4	57.0
19 Oct 1996	17:20	0.570	93.390	36.4	59.0
19 Oct 1996	18:20	0.580	343.342	113.6	76.0
19 Oct 1996	19:20	0.340	461.138	93.3	156.0
19 Oct 1996	20:20	0.290	409.072	62.9	135.0
19 Oct 1996	21:20	0.220	318.429	47.6	115.0
19 Oct 1996	22:20	0.110	302.368	36.6	110.0
19 Oct 1996	23:20	0.290	205.454	34.4	99.0
20 Oct 1996	00:20	0.120	261.665	34.7	124.0
20 Oct 1996	01:20	0.060	216.099	28.0	193.0

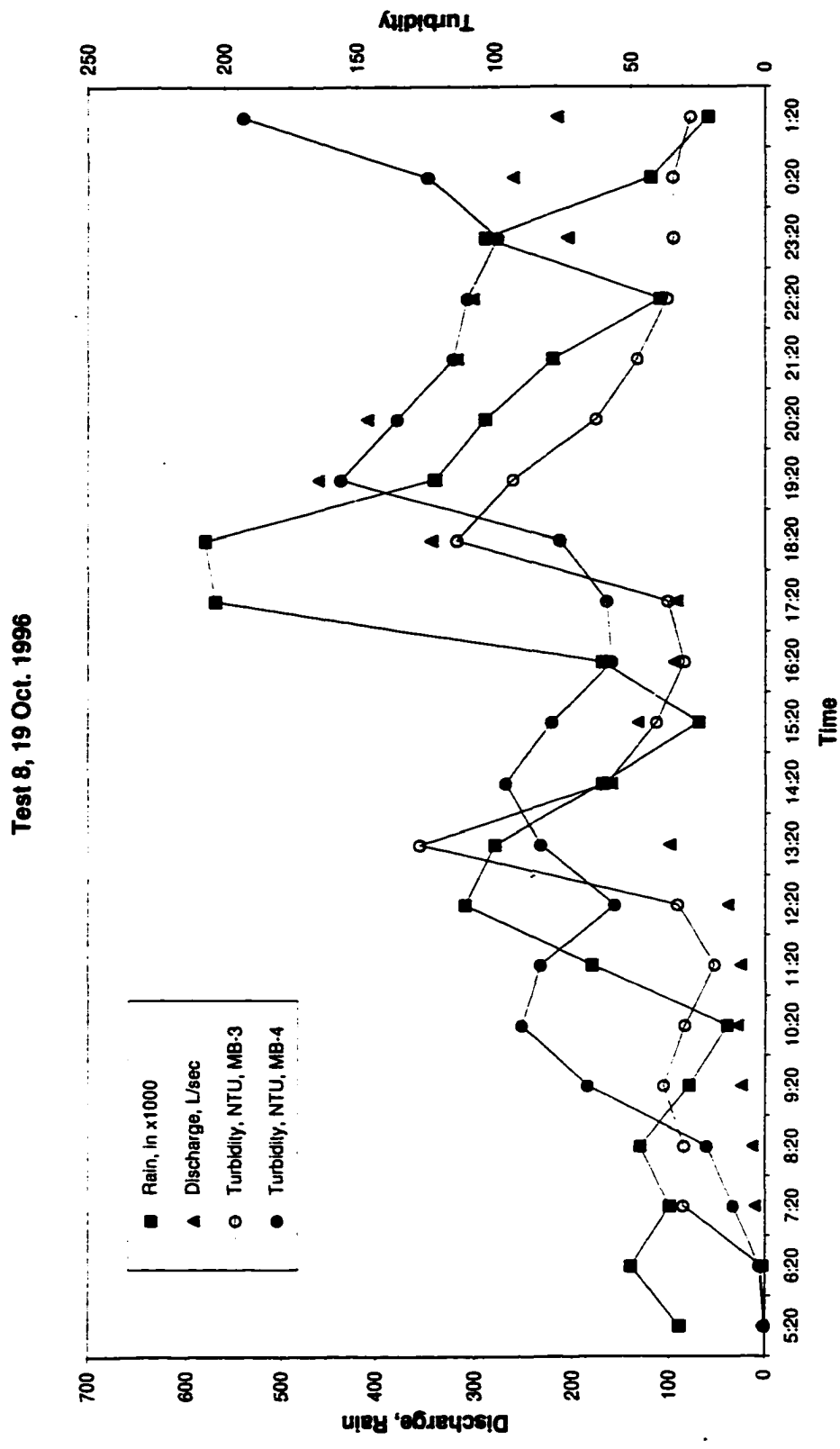

Test 9

Date	Time	Rain (in)	Discharge (l/sec) MB-1	Turbidity (NTU) MB-3
08 NOV 1996	23:06	0.000	9.80	0
08 NOV 1996	23:36	0.000	10.68	0
09 NOV 1996	0:06	0.030	11.65	0
09 NOV 1996	0:36	0.000	11.76	0
09 Nov 1996	1:06	0.040	12.05	0
09 Nov 1996	1:36	0.010	13.23	8
09 Nov 1996	2:06	0.020	20.91	47
09 Nov 1996	2:36	0.050	32.59	51
09 Nov 1996	3:06	0.020	42.47	90
09 Nov 1996	3:36	0.070	84.98	186
09 Nov 1996	4:06	0.020	109.84	280
09 Nov 1996	4:36	0.020	120.67	196
09 Nov 1996	5:06	0.000	112.43	135

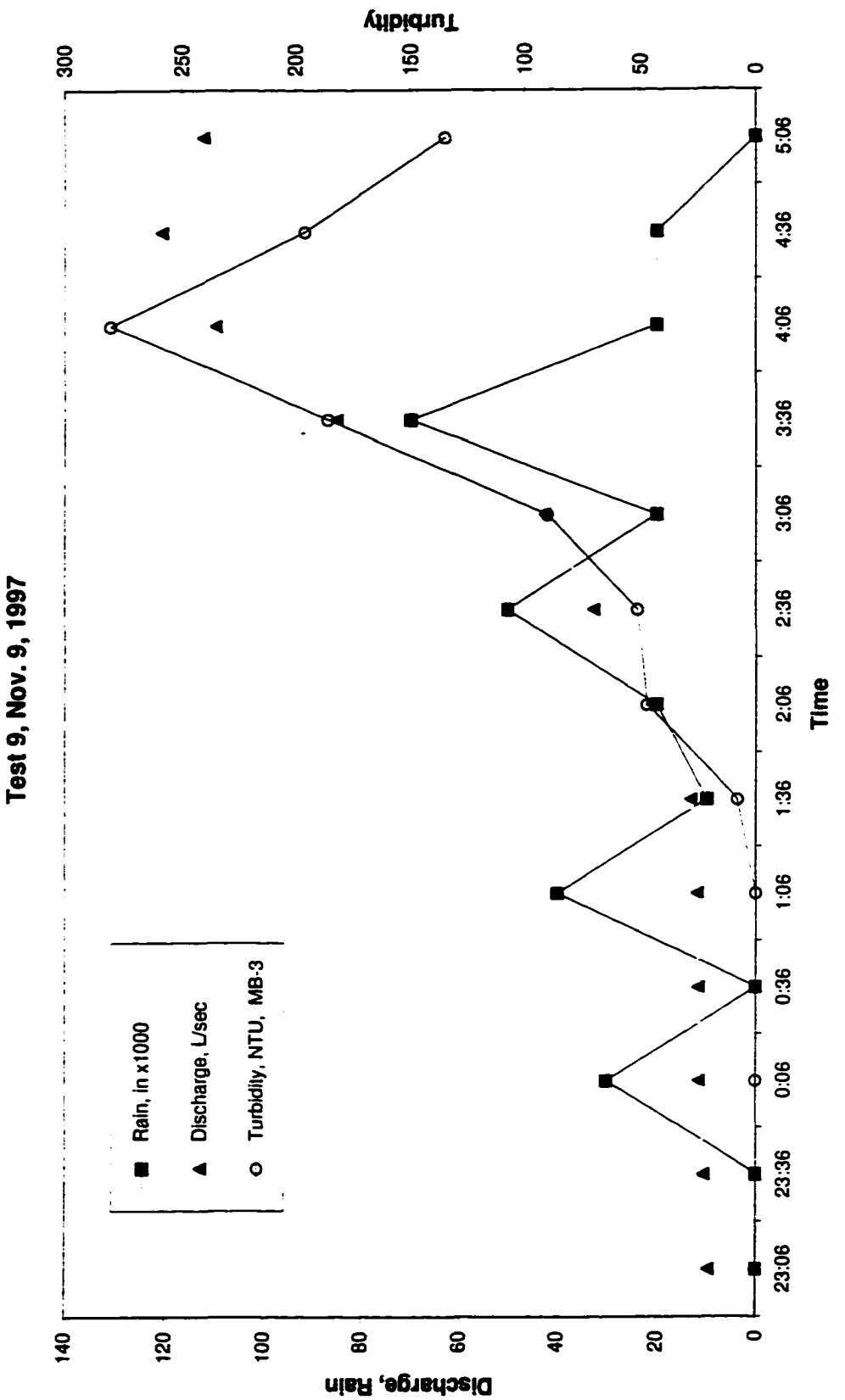

Test 10

Date	Time	Rain (in)	Discharge (l/sec) MB-1	Turbidity (NTU) MB-4	Turbidity (NTU) MB-8
1 May 1997	17:50	0.04	6.29	2	0
1 May 1997	18:00	0.02	6.62	2	0
1 May 1997	18:10	0.00	6.72	2	0
1 May 1997	18:20	0.00	7.01	17	0.8
1 May 1997	18:30	0.01	7.14	28	1.8
1 May 1997	18:40	0.00	7.24	22	2
1 May 1997	18:50	0.01	7.61	18	2.2
1 May 1997	19:00	0.02	7.66	13	3.3
1 May 1997	19:10	0.03	8.33	11	4
1 May 1997	19:20	0.04	9.10	11	3.8
1 May 1997	19:30	0.00	10.65	11	5
1 May 1997	19:40	0.01	12.27	12	5.1

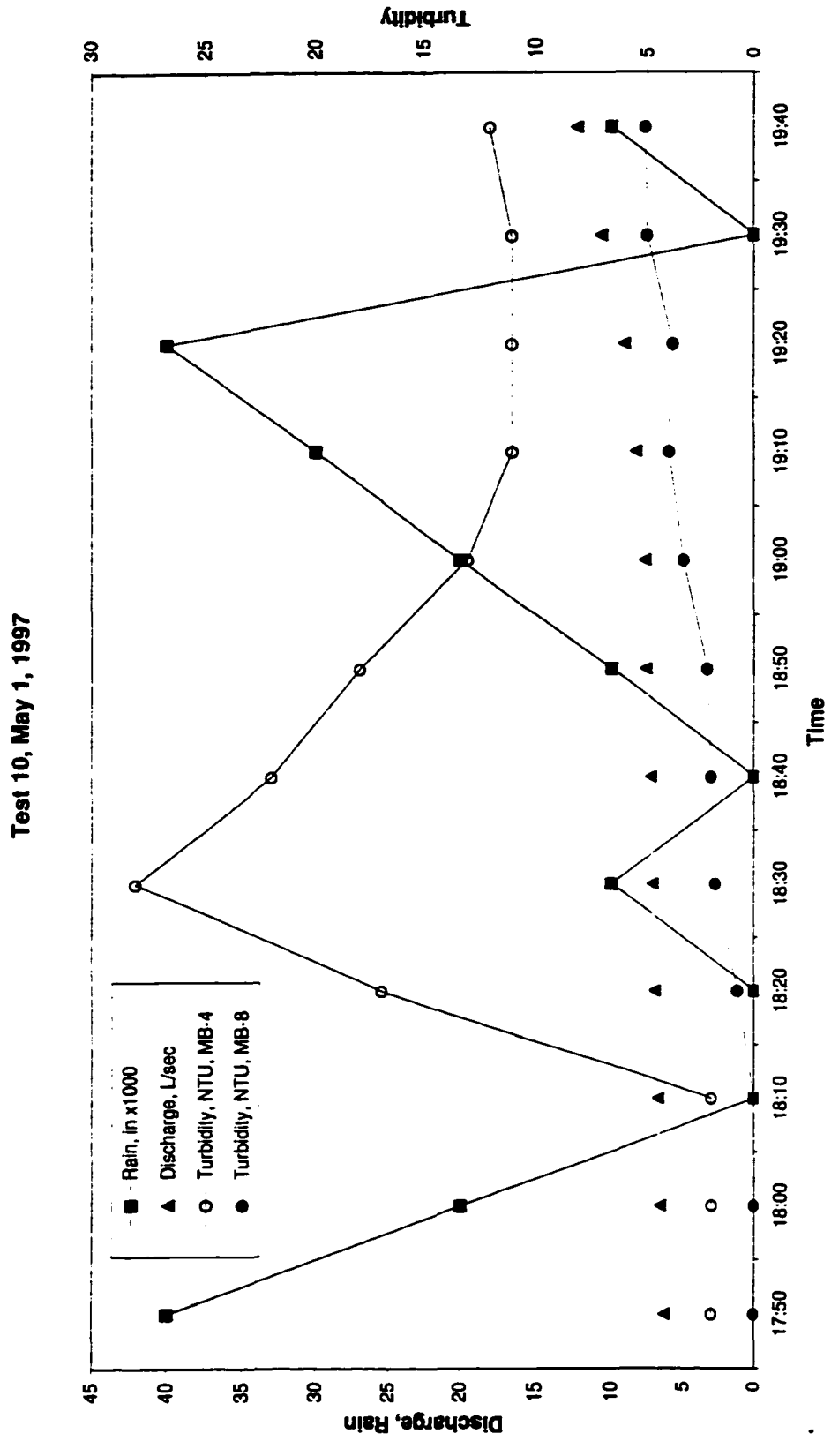

Test 11

Date	Time	Rain (in)	Disch(l/sec) MB-1	Turbidity (NTU) MB-4	Turbidity (NTU) MB-8
6 May 1997	5:30	0.01	8.25	50	50
6 May 1997	5:40	0.02	8.45	53	48
6 May 1997	5:50	0.01	8.72	55	48
6 May 1997	6:00	0.02	9.27	53	49
6 May 1997	6:10	0.03	10.23	54	49
6 May 1997	6:20	0.02	11.35	56	49
6 May 1997	6:30	0.02	13.08	55	49
6 May 1997	6:40	0.02	15.14	52	49
6 May 1997	6:50	0.02	17.32	53	60
6 May 1997	7:00	0.02	19.11	54	84
6 May 1997	7:10	0.01	21.24	56	82
6 May 1997	7:20	0.02	23.02	56	83

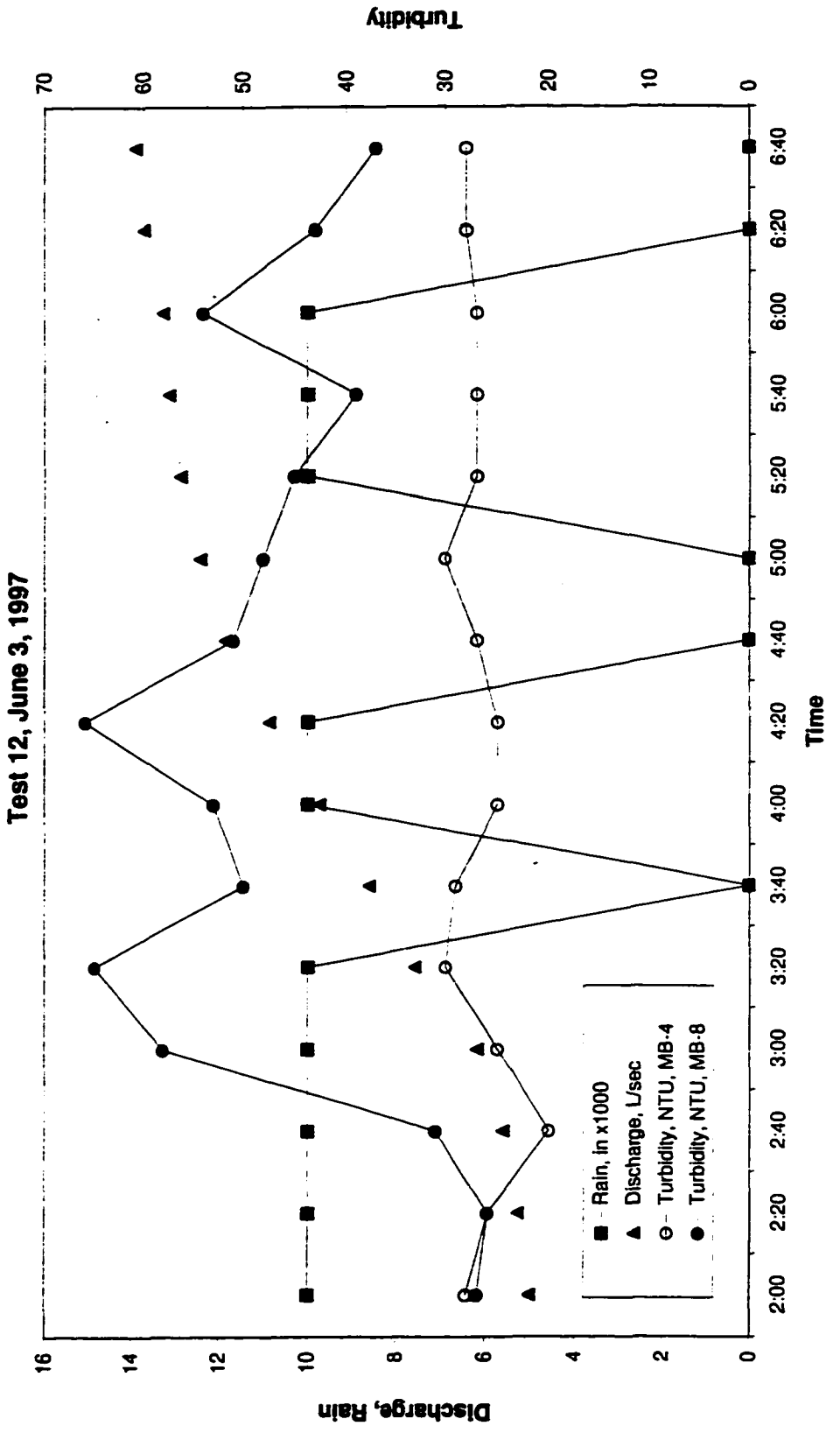

Test 13

Date	Time	Rain (in)	Discharge (l/sec) MB-1	Turbidity (NTU) MB-4	Turbidity (NTU) MB-8
24 Jul 1997	5:50	0.00	4.01	19	28
24 Jul 1997	6:40	0.00	5.15	71	23
24 Jul 1997	7:30	0.00	4.93	51	24
24 Jul 1997	8:20	0.01	4.91	56	16
24 Jul 1997	9:10	0.01	5.30	61	32
24 Jul 1997	10:00	0.00	5.77	75	30
24 Jul 1997	10:50	0.00	5.55	47	26
24 Jul 1997	11:40	0.01	6.04	65	24
24 Jul 1997	12:30	0.01	9.93	81	60
24 Jul 1997	13:20	0.00	12.73	109	36
24 Jul 1997	14:10	0.00	13.25	80	42
24 Jul 1997	15:00	0.00	12.80	48	31
24 Jul 1997	15:50	0.00	12.23	42	26
24 Jul 1997	16:40	0.00	11.12	65	25
24 Jul 1997	17:30	0.00	9.91	29	21
24 Jul 1997	18:20	0.00	8.72	26	16
24 Jul 1997	19:10	0.00	8.12	25	12
24 Jul 1997	20:00	0.00	7.85	28	28
24 Jul 1997	20:50	0.02	7.78	31	18
24 Jul 1997	21:40	0.04	26.74	41	30
24 Jul 1997	22:30	0.04	71.75	61	80
24 Jul 1997	23:20	0.02	79.16	147	121
25 Jul 1997	0:10	0.02	65.62	120	270
25 Jul 1997	1:00	0.11	247.91	70	65
25 Jul 1997	1:50	0.05	165.60	174	697
25 Jul 1997	2:40	0.04	123.68	75	89

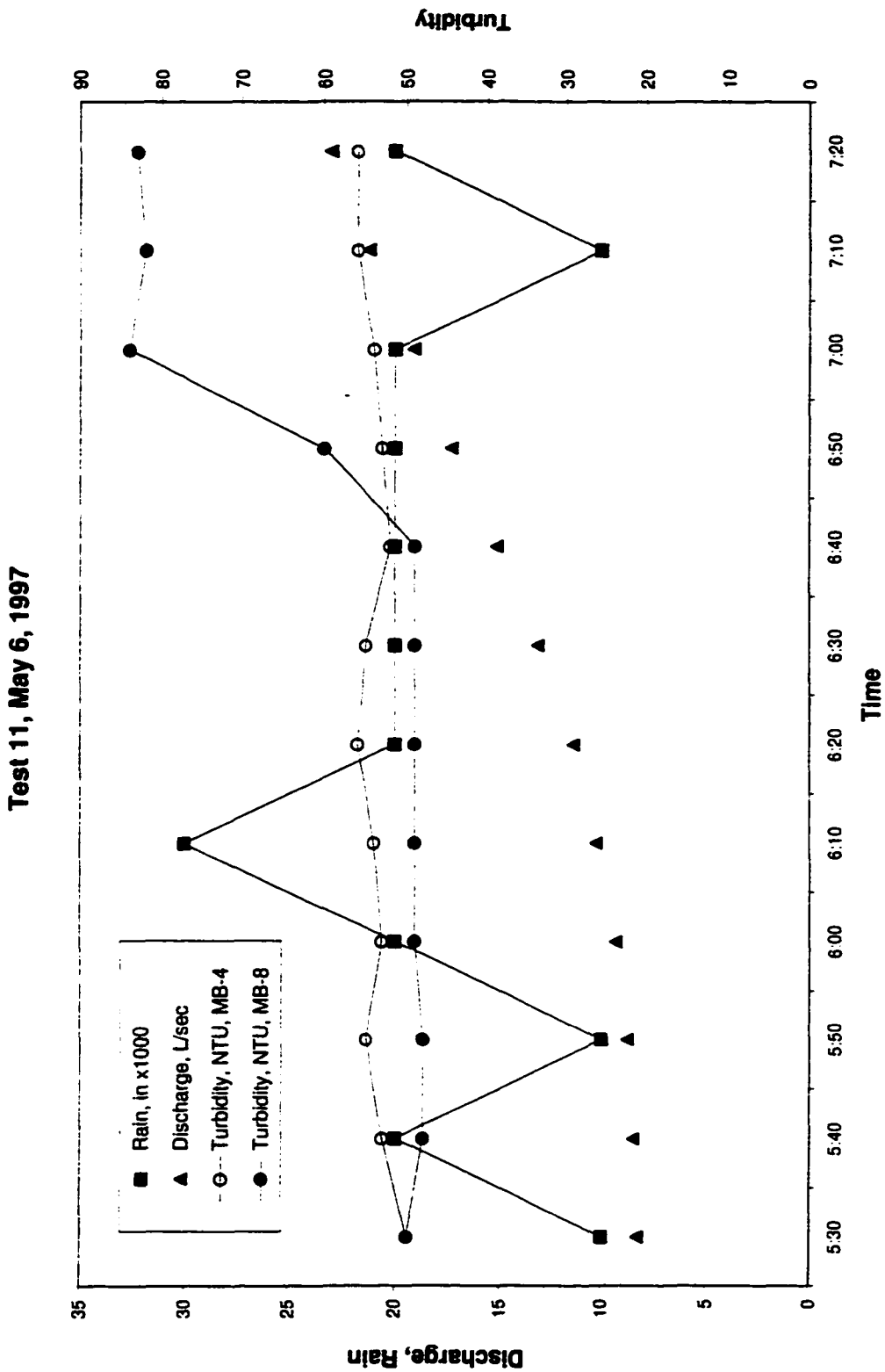

Test 12

Date	Time	Rain (in)	Discharge (l/sec) MB-1	Turbidity (NTU) MB-4	Turbidity (NTU) MB-8
3 June 1997	2:00	0.01	5.01	28	27
3 June 1997	2:20	0.01	5.28	26	26
3 June 1997	2:40	0.01	5.60	20	31
3 June 1997	3:00	0.01	6.17	25	58
3 June 1997	3:20	0.01	7.56	30	65
3 June 1997	3:40	0	8.62	29	50
3 June 1997	4:00	0.01	9.74	25	53
3 June 1997	4:20	0.01	10.85	25	66
3 June 1997	4:40	0	11.84	27	51
3 June 1997	5:00	0	12.41	30	48
3 June 1997	5:20	0.01	12.86	27	45
3 June 1997	5:40	0.01	13.11	27	39
3 June 1997	6:00	0.01	13.26	27	54
3 June 1997	6:20	0	13.70	28	43
3 June 1997	6:40	0	13.89	28	37

Test 13

Date	Time	Rain (in)	Discharge (l/sec) MB-1	Turbidity (NTU) MB-4	Turbidity (NTU) MB-8
25 Jul 1997	3:30	0.01	97.66	75	210
25 Jul 1997	4:20	0.00	76.74	65	290
25 Jul 1997	5:10	0.00	56.97	67	210

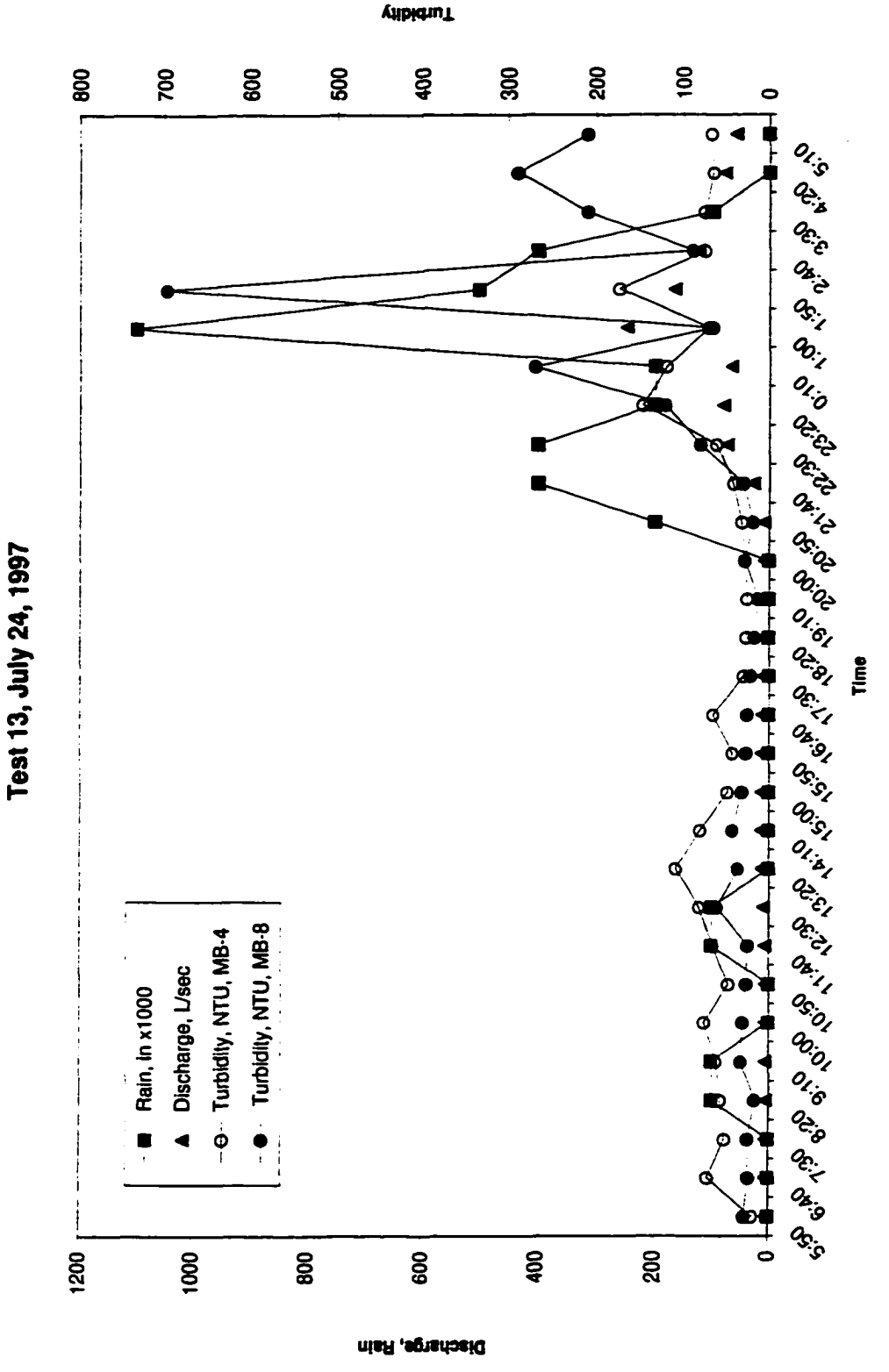

Test 14

Date	Time	Rain (in)	Discharge (l/sec) MB-1	Turbidity (NTU) MB-4	Turbidity (NTU) MB-8
20 Aug 1997	20:20	0.01	5.35	33	40
20 Aug 1997	21:00	0.00	7.18	34	36
20 Aug 1997	21:40	0.01	10.30	44	59
20 Aug 1997	22:20	0.00	11.34	51	46
20 Aug 1997	23:00	0.00	11.07	66	56
20 Aug 1997	23:40	0.01	10.60	80	51
21 Aug 1997	0:20	0.01	10.28	86	53
21 Aug 1997	1:00	0.02	16.49	82	49
21 Aug 1997	1:40	0.00	27.01	96	64
21 Aug 1997	2:20	0.01	28.82	113	59
21 Aug 1997	3:00	0.01	26.94	125	61
21 Aug 1997	3:40	0.01	24.17	95	53
21 Aug 1997	4:20	0.00	22.21	76	53
21 Aug 1997	5:00	0.01	20.11	67	43

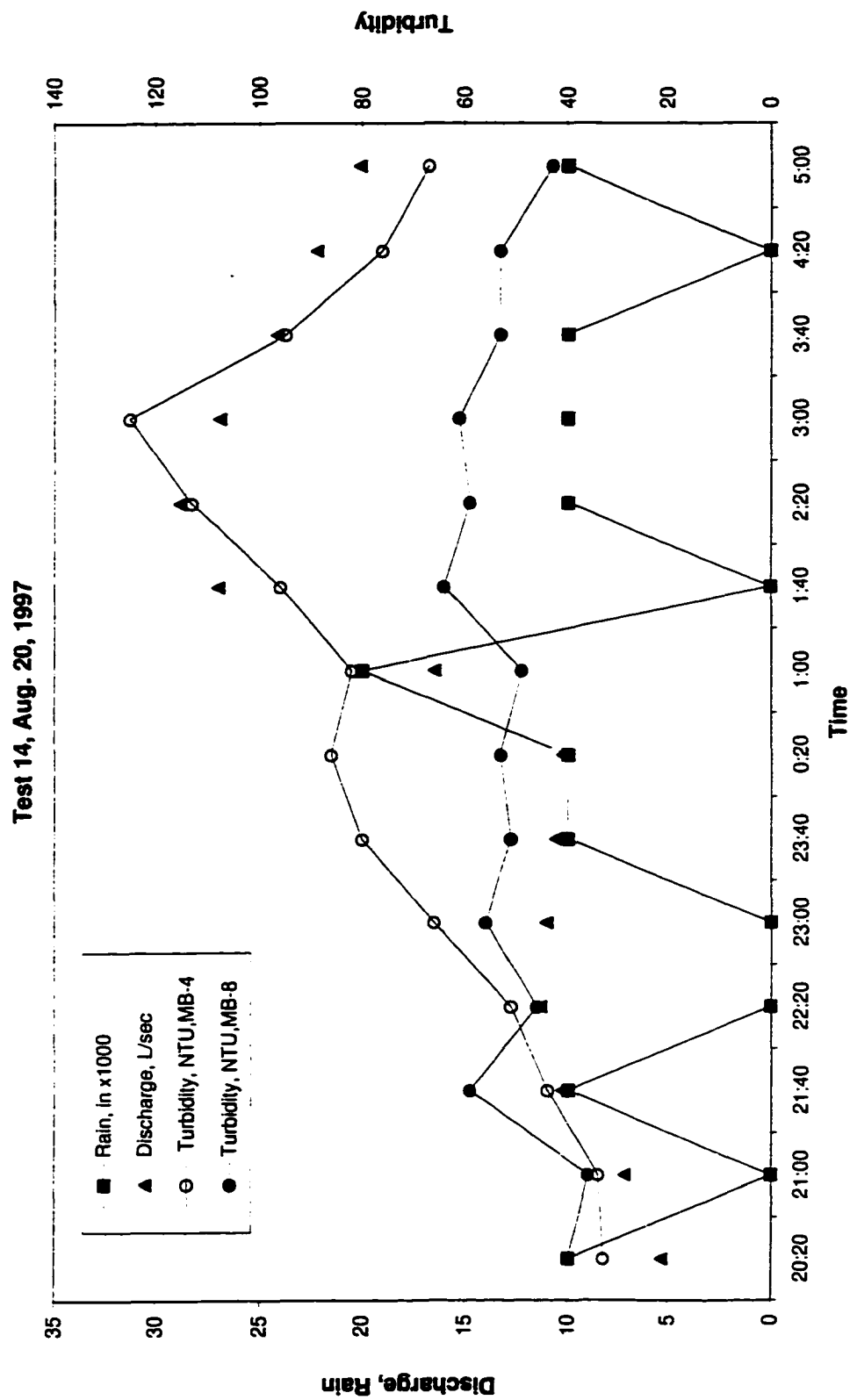

Test 15

Date	Time	Rain (in)	Discharge (l/sec) MB-1	Turbidity (NTU) MB-4	Turbidity(NTU) MB-8
24 Oct 1997	23:40	0.01	0.69	10	2
25 Oct 1997	0:30	0.00	0.69	10	2
25 Oct 1997	1:20	0.02	0.79	10	9
25 Oct 1997	2:10	0.01	1.66	8	130
25 Oct 1997	3:00	0.00	1.73	8	50
25 Oct 1997	3:50	0.02	2.28	8	45
25 Oct 1997	4:40	0.00	2.63	7	50
25 Oct 1997	5:30	0.02	4.28	7	36
25 Oct 1997	6:20	0.03	8.12	7	41
25 Oct 1997	7:10	0.04	20.53	7	40
25 Oct 1997	8:00	0.01	29.54	78	58
25 Oct 1997	8:50	0.01	26.17	76	60
25 Oct 1997	9:40	0.01	26.10	90	37
25 Oct 1997	10:30	0.00	26.00	60	42

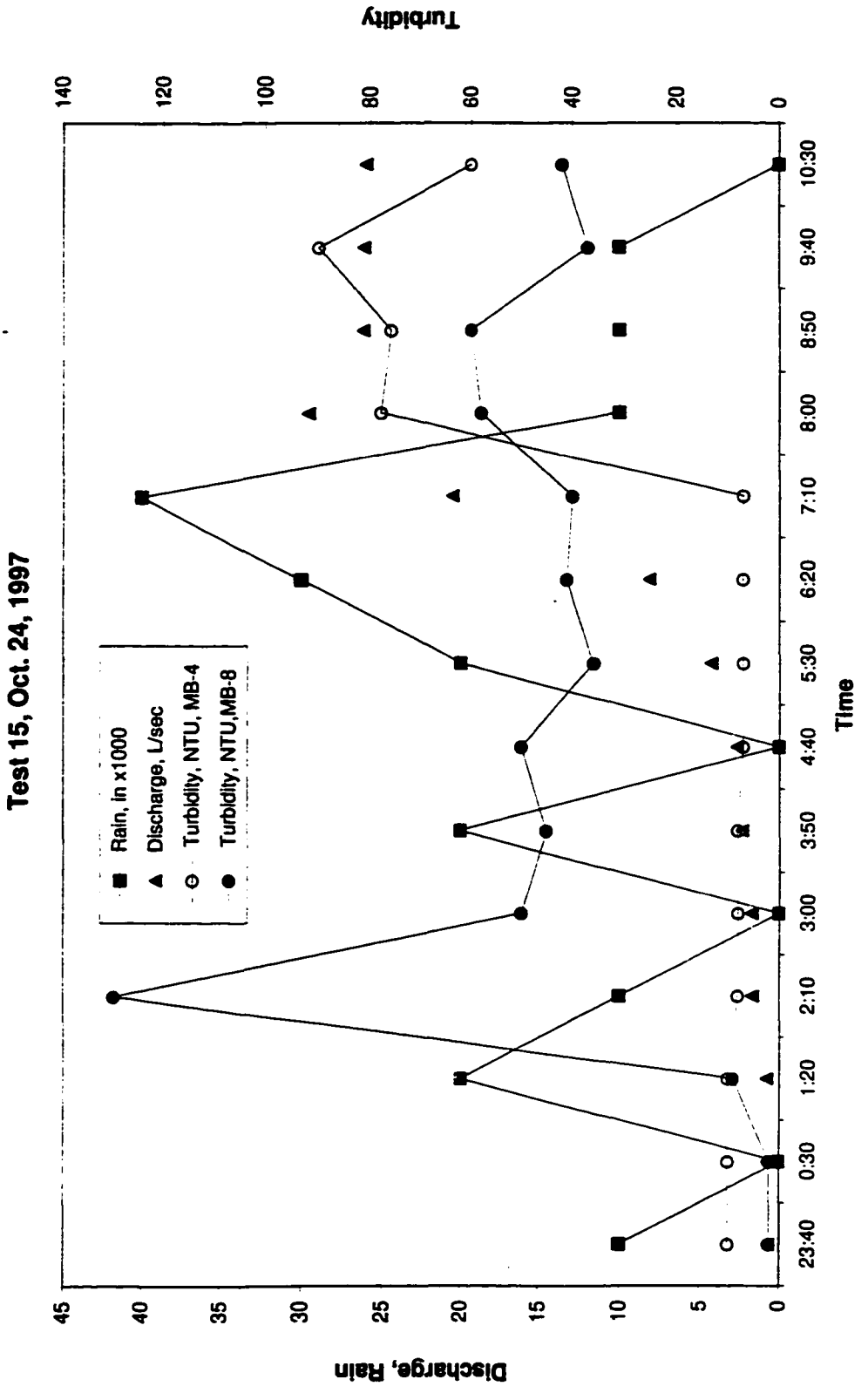

Test 16

Date	Time	Rain (in)	Discharge (l/sec) MB-1	Turbidity (NTU) MB-4	Turbidity (NTU) MB-8
26 Oct 1997	17:10	0.01	1.43	25	47
26 Oct 1997	17:50	0.01	1.46	25	47
26 Oct 1997	18:30	0.01	1.66	25	50
26 Oct 1997	19:10	0.01	2.45	13	28
26 Oct 1997	19:50	0.01	3.05	13	25
26 Oct 1997	20:30	0.01	5.55	14	13
26 Oct 1997	21:10	0.01	8.96	612	23
26 Oct 1997	21:50	0.01	11.44	50	24
26 Oct 1997	22:30	0.00	13.15	48	22
26 Oct 1997	23:10	0.00	14.01	51	33
26 Oct 1997	23:50	0.02	15.20	43	37
27 Oct 1997	0:30	0.01	18.94	50	31
27 Oct 1997	1:10	0.02	22.93	43	150
27 Oct 1997	1:50	0.01	27.11	44	63
27 Oct 1997	2:30	0.00	27.04	45	280
27 Oct 1997	3:10	0.00	24.83	60	75
27 Oct 1997	3:50	0.00	22.06	47	57
27 Oct 1997	4:30	0.02	19.86	43	42
27 Oct 1997	5:10	0.00	20.53	38	39
27 Oct 1997	5:50	0.00	22.21	38	68
27 Oct 1997	6:30	0.00	20.95	37	42
27 Oct 1997	7:10	0.00	18.42	39	41
27 Oct 1997	7:50	0.01	16.74	35	37
27 Oct 1997	8:30	0.00	15.73	33	46

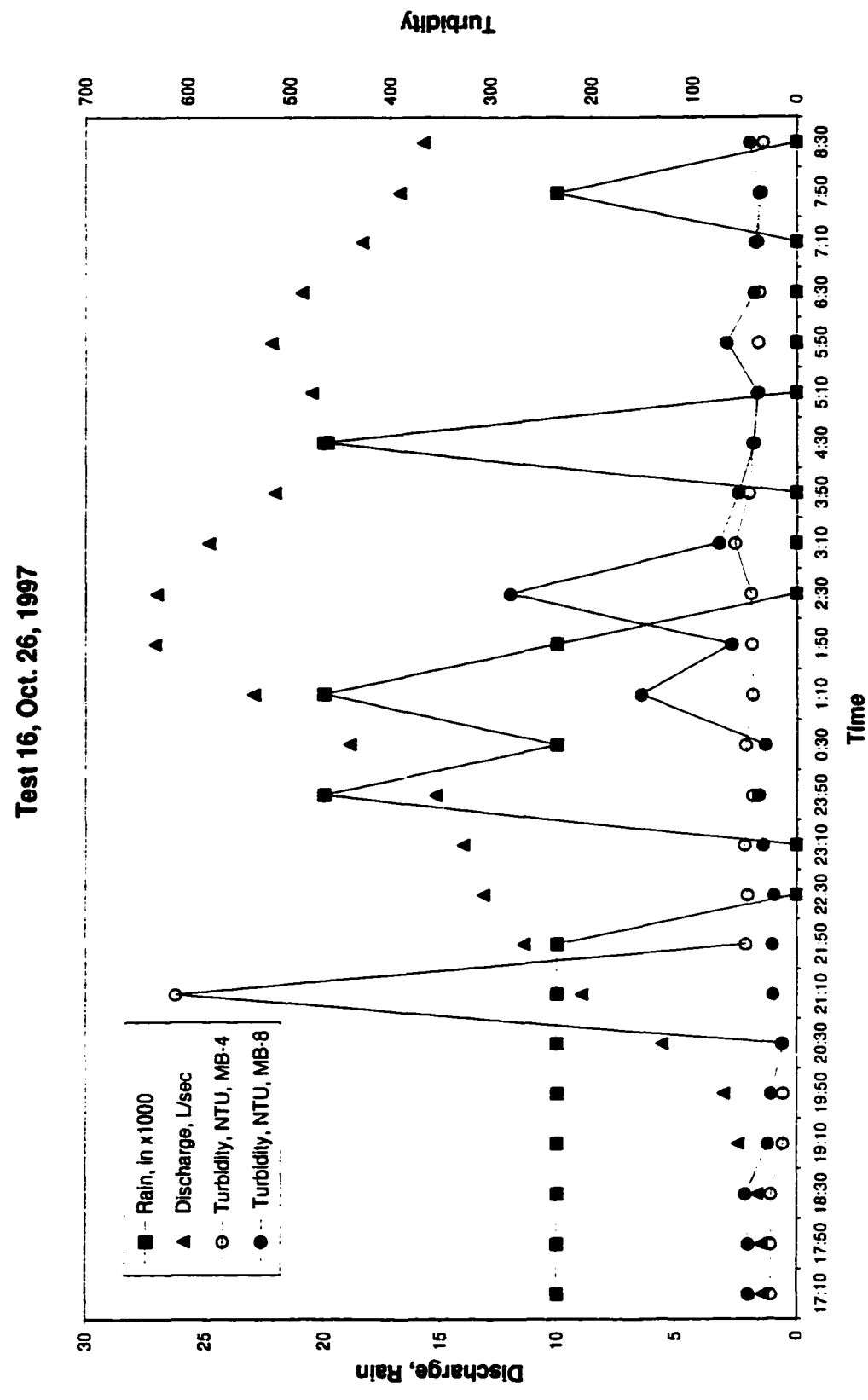

Appendix C. Input Data for Modeling.

Filename of the input file with rainfall data	Data File Content NOTE: "&sv" is an AML syntax for setting variable value; .P# - rainfall variables; .cycle - number of intervals; .time_interval - time between measured intervals;
test1.aml	/* July 3, 1996 rainstorm, 1.2 hour length /* Time interval = 10 min; 10 min x 60 sec = 600 sec; /* &sv .P1 = 0.07 &sv .P2 = 0.14 &sv .P3 = 0.08 &sv .P4 = 0.06 &sv .P5 = 0.1 &sv .P6 = 0.23 &sv .P7 = 0.13 &sv .P8 = 0.01 &sv .cycle = 8 &sv .time_interval = 10
test2.aml	/* June 30, 1996 rainstorm, 5.3 hour length /* Time interval = 40 min; 40 min x 60 sec = 2400 sec; /* &sv .P1 = 0.05 &sv .P2 = 0.06 &sv .P3 = 0.11 &sv .P4 = 0.11 &sv .P5 = 0.06 &sv .P6 = 0.05 &sv .P7 = 0.03 &sv .P8 = 0.02 &sv .P9 = 0.02 &sv .cycle = 9 &sv .time_interval = 40

Filename of the input file with rainfall data	Data File Content NOTE: "&sv" is an AML syntax for setting variable value; .P# - rainfall variables; .cycle - number of intervals; .time_interval - time between measured intervals;
test3.aml	/* July 31, 1996 rainstorm, 2.5 hour length /* Time interval = 10 min; 10 min x 60 sec = 600 sec; /* &sv .P1 = 0.03 &sv .P2 = 0.03 &sv .P3 = 0.02 &sv .P4 = 0.04 &sv .P5 = 0.02 &sv .P6 = 0.03 &sv .P7 = 0.03 &sv .P8 = 0.02 &sv .P9 = 0.03 &sv .P10 = 0.06 &sv .P11 = 0.05 &sv .P12 = 0.04 &sv .P13 = 0.04 &sv .P14 = 0.05 &sv .P15 = 0.02 &sv .P16 = 0.01 &sv .cycle = 16 &sv .time_interval = 10

Filename of the input file with rainfall data	Data File Content NOTE: "&sv" is an AML syntax for setting variable value; .P# - rainfall variables; .cycle - number of intervals; .time_interval - time between measured intervals;
test4.aml	/* September 16-17, 1996 rainstorm, 8.5 hour length /* Time interval = 30 min; 30 min x 60 sec = 1800 sec; /* &sv .P1 = 0.01 &sv .P2 = 0.01 &sv .P3 = 0.01 &sv .P4 = 0.01 &sv .P5 = 0.07 &sv .P6 = 0.06 &sv .P7 = 0.06 &sv .P8 = 0.07 &sv .P9 = 0.08 &sv .P10 = 0.11 &sv .P11 = 0.05 &sv .P12 = 0.09 &sv .P13 = 0.12 &sv .P14 = 0.17 &sv .P15 = 0.16 &sv .P16 = 0.12 &sv .P17 = 0.04 &sv .P18 = 0.04 &sv .cycle = 18 &sv .time_interval = 30

Filename of the input file with rainfall data	Data File Content NOTE: "&sv" is an AML syntax for setting variable value; .P# - rainfall variables; .cycle - number of intervals; .time_interval - time between measured intervals;
test5.aml	/* October 8, 1996 rainstorm, 11.5 hour length /* Time interval = 30 min; 30 min x 60 sec = 1800 sec; /* &sv .P1 = 0.03 &sv .P2 = 0.07 &sv .P3 = 0.09 &sv .P4 = 0.14 &sv .P5 = 0.12 &sv .P6 = 0.07 &sv .P7 = 0.06 &sv .P8 = 0.06 &sv .P9 = 0.14 &sv .P10 = 0.16 &sv .P11 = 0.07 &sv .P12 = 0.05 &sv .P13 = 0.02 &sv .P14 = 0.04 &sv .P15 = 0.25 &sv .P16 = 0.30 &sv .P17 = 0.06 &sv .P18 = 0.07 &sv .P19 = 0.07 &sv .P20 = 0.07 &sv .P21 = 0.08 &sv .P22 = 0.07 &sv .P23 = 0.05 &sv .P24 = 0.03 &sv .cycle = 24 &sv .time_interval = 30

Filename of the input file with rainfall data	Data File Content NOTE: "&sv" is an AML syntax for setting variable value; .P# - rainfall variables; .cycle - number of intervals; .time_interval - time between measured intervals;
test6.aml	/* August 13, 1996 rainstorm, 8 hour length /* Time interval = 60 min; 60 min x 60 sec = 3600 sec; /* &sv .P1 = 0.1 &sv .P2 = 0.06 &sv .P3 = 0.04 &sv .P4 = 0.02 &sv .P5 = 0.02 &sv .P6 = 0.19 &sv .P7 = 0.14 &sv .P8 = 0.04 &sv .P9 = 0.03 &sv .cycle = 9 &sv .time_interval = 60
test7.aml	/* September 28, 1996 rainstorm, 6.7 hour length /* Time interval = 40 min; 40 min x 60 sec = 2400 sec; /* &sv .P1 = 0.15 &sv .P2 = 0.22 &sv .P3 = 0.06 &sv .P4 = 0.15 &sv .P5 = 0.18 &sv .P6 = 0.11 &sv .P7 = 0.10 &sv .P8 = 0.04 &sv .P9 = 0.05 &sv .P10 = 0.04 &sv .P11 = 0.03 &sv .cycle = 11 &sv .time_interval = 40

Filename of the input file with rainfall data	Data File Content NOTE: "&sv" is an AML syntax for setting variable value; .P# - rainfall variables; .cycle - number of intervals; .time_interval - time between measured intervals;
test8.aml	/* October 19, 1996 rainstorm, 20.0 hour length /* Time interval = 60 min; 60 min x 60 sec = 3600 sec; /* &sv .P1 = 0.09 &sv .P2 = 0.14 &sv .P3 = 0.10 &sv .P4 = 0.13 &sv .P5 = 0.08 &sv .P6 = 0.04 &sv .P7 = 0.18 &sv .P8 = 0.31 &sv .P9 = 0.28 &sv .P10 = 0.17 &sv .P11 = 0.07 &sv .P12 = 0.17 &sv .P13 = 0.57 &sv .P14 = 0.58 &sv .P15 = 0.34 &sv .P16 = 0.29 &sv .P17 = 0.22 &sv .P18 = 0.11 &sv .P19 = 0.29 &sv .P20 = 0.12 &sv .P21 = 0.06 &sv .cycle = 21 &sv .time_interval = 60

Filename of the input file with rainfall data	Data File Content NOTE: "&sv" is an AML syntax for setting variable value; .P# - rainfall variables; .cycle - number of intervals; .time_interval - time between measured intervals;
test9.aml	/* November 9, 1996 rainstorm, 6.0 hour length /* Time interval = 30 min; 30 min x 60 sec = 1800 sec; /* Rain started 08Nov, 22:46 &sv .P1 = 0.02 &sv .P2 = 0.01 &sv .P3 = 0.03 &sv .P4 = 0.03 &sv .P5 = 0.07 &sv .P6 = 0.06 &sv .P7 = 0.06 &sv .P8 = 0.15 &sv .P9 = 0.11 &sv .P10 = 0.13 &sv .P11 = 0.05 &sv .P12 = 0.03 &sv .P13 = 0.02 &sv .cycle = 13 &sv .time_interval = 30

Filename of the input file with rainfall data	Data File Content NOTE: "&sv" is an AML syntax for setting variable value; .P# - rainfall variables; .cycle - number of intervals; .time_interval - time between measured intervals;
test10.aml	/* May 1, 1997 rain storm, 1.8 hours; /* Time interval = 10 min; 10 min x 60 sec = 600 sec; /* Rain started 5/1/97 at 17:50 &sv .P1 = 0.04 &sv .P2 = 0.02 &sv .P3 = 0.0 &sv .P4 = 0.0 &sv .P5 = 0.01 &sv .P6 = 0.00 &sv .P7 = 0.01 &sv .P8 = 0.02 &sv .P9 = 0.03 &sv .P10 = 0.04 &sv .P11 = 0.0 &sv .P12 = 0.01 &sv .cycle = 12 &sv .time_interval = 10

Filename of the input file with rainfall data	Data File Content NOTE: "&sv" is an AML syntax for setting variable value; .P# - rainfall variables; .cycle - number of intervals; .time_interval - time between measured intervals;
test11.aml	/* May 6, 1997 rain storm, 1.8 hours; /* Time interval = 10 min; 10 min x 60 sec = 600 sec; /* Rain started 5/6/97, 5:30 &sv .P1 = 0.01 &sv .P2 = 0.02 &sv .P3 = 0.01 &sv .P4 = 0.02 &sv .P5 = 0.03 &sv .P6 = 0.02 &sv .P7 = 0.02 &sv .P8 = 0.02 &sv .P9 = 0.02 &sv .P10 = 0.02 &sv .P11 = 0.01 &sv .P12 = 0.02 &sv .cycle = 12 &sv .time_interval = 10

Filename of the input file with rainfall data	Data File Content NOTE: "&sv" is an AML syntax for setting variable value; .P# - rainfall variables; .cycle - number of intervals; .time_interval - time between measured intervals;
test12.aml	/* June 3, 1997 rain storm, 4.7 hours length /* Time interval = 20 min; 20 min x 60 sec = 1200 sec; /* Rain started 6/3/97, 1:50 &sv .P1 = 0.02 &sv .P2 = 0.01 &sv .P3 = 0.01 &sv .P4 = 0.02 &sv .P5 = 0.01 &sv .P6 = 0.01 &sv .P7 = 0.02 &sv .P8 = 0.01 &sv .P9 = 0.01 &sv .P10 = 0.01 &sv .P11 = 0.01 &sv .P12 = 0.01 &sv .P13 = 0.01 &sv .P14 = 0.01 &sv .P15 = 0.01 &sv .cycle = 15 &sv .time_interval = 20

Filename of the input file with rainfall data	Data File Content NOTE: "&sv" is an AML syntax for setting variable value; .P# - rainfall variables; .cycle - number of intervals; .time_interval - time between measured intervals;
test13.aml	/* July 24, 1997; 23.3 hour length /* Time interval = 50 min = 3000 sec /* &sv .P1 = 0.04 &sv .P2 = 0.01 &sv .P3 = 0.01 &sv .P4 = 0.04 &sv .P5 = 0.03 &sv .P6 = 0.01 &sv .P7 = 0 &sv .P8 = 0.06 &sv .P9 = 0.05 &sv .P10 = 0.05 &sv .P11 = 0.02 &sv .P12 = 0.03 &sv .P13 = 0.02 &sv .P14 = 0.01 &sv .P15 = 0.01 &sv .P16 = 0 &sv .P17 = 0.06 &sv .P18 = 0.02 &sv .P19 = 0.05 &sv .P20 = 0.2 &sv .P21 = 0.23 &sv .P22 = 0.16 &sv .P23 = 0.12 &sv .P24 = 0.56 &sv .P25 = 0.29 &sv .P26 = 0.1 &sv .P27 = 0.12 &sv .P28 = 0.04 &sv .P29 = 0.03 &sv .cycle = 29 &sv .time_interval = 50

Filename of the input file with rainfall data	Data File Content NOTE: "&sv" is an AML syntax for setting variable value; .P# - rainfall variables; .cycle - number of intervals; .time_interval - time between measured intervals;
test14.aml	/* August 20, 1997; 8.7 hour length /* Time interval = 40 min = 2400 sec. /* &sv .P1 = 0.06 &sv .P2 = 0.03 &sv .P3 = 0.02 &sv .P4 = 0.02 &sv .P5 = 0 &sv .P6 = 0.01 &sv .P7 = 0.12 &sv .P8 = 0.08 &sv .P9 = 0.02 &sv .P10 = 0.02 &sv .P11 = 0.02 &sv .P12 = 0.02 &sv .P13 = 0.01 &sv .P14 = 0.02 &sv .cycle = 14 &sv .time_interval = 40

Filename of the input file with rainfall data	Data File Content NOTE: "&sv" is an AML syntax for setting variable value; .P# - rainfall variables; .cycle - number of intervals; .time_interval - time between measured intervals;
test15.aml	/* October 24, 1997; 10.8 hour length /* Time int. = 50 min = 3000 sec; /* &sv .P1 = 0.02 &sv .P2 = 0.04 &sv .P3 = 0.08 &sv .P4 = 0.04 &sv .P5 = 0.04 &sv .P6 = 0.03 &sv .P7 = 0.06 &sv .P8 = 0.09 &sv .P9 = 0.13 &sv .P10 = 0.09 &sv .P11 = 0.03 &sv .P12 = 0.05 &sv .P13 = 0.04 &sv .P14 = 0.01 &sv .cycle = 14 &sv .time_interval = 50

Filename of the input file with rainfall data	Data File Content NOTE: "&sv" is an AML syntax for setting variable value; .P# - rainfall variables; .cycle - number of intervals; .time_interval - time between measured intervals;
test16.aml	/* October 26, 1997, 15.3 hour length /* Time interval = 40 min; 40 x 60 = 2400 sec; /* &sv .P1 = 0.02 &sv .P2 = 0.05 &sv .P3 = 0.04 &sv .P4 = 0.04 &sv .P5 = 0.05 &sv .P6 = 0.05 &sv .P7 = 0.03 &sv .P8 = 0.04 &sv .P9 = 0.01 &sv .P10 = 0.05 &sv .P11 = 0.04 &sv .P12 = 0.06 &sv .P13 = 0.04 &sv .P14 = 0.02 &sv .P15 = 0 &sv .P16 = 0.01 &sv .P17 = 0.02 &sv .P18 = 0.05 &sv .P19 = 0.01 &sv .P20 = 0 &sv .P21 = 0.01 &sv .P22 = 0.02 &sv .P23 = 0.02 &sv .P24 = 0.02 &sv .cycle = 24 &sv .time_interval = 40

Appendix D. Flow Modeling Results.

Each modeled test has two corresponding figures: one with comparison between simulated and measured flow, another with 1:1 (ideal match) and regression line.

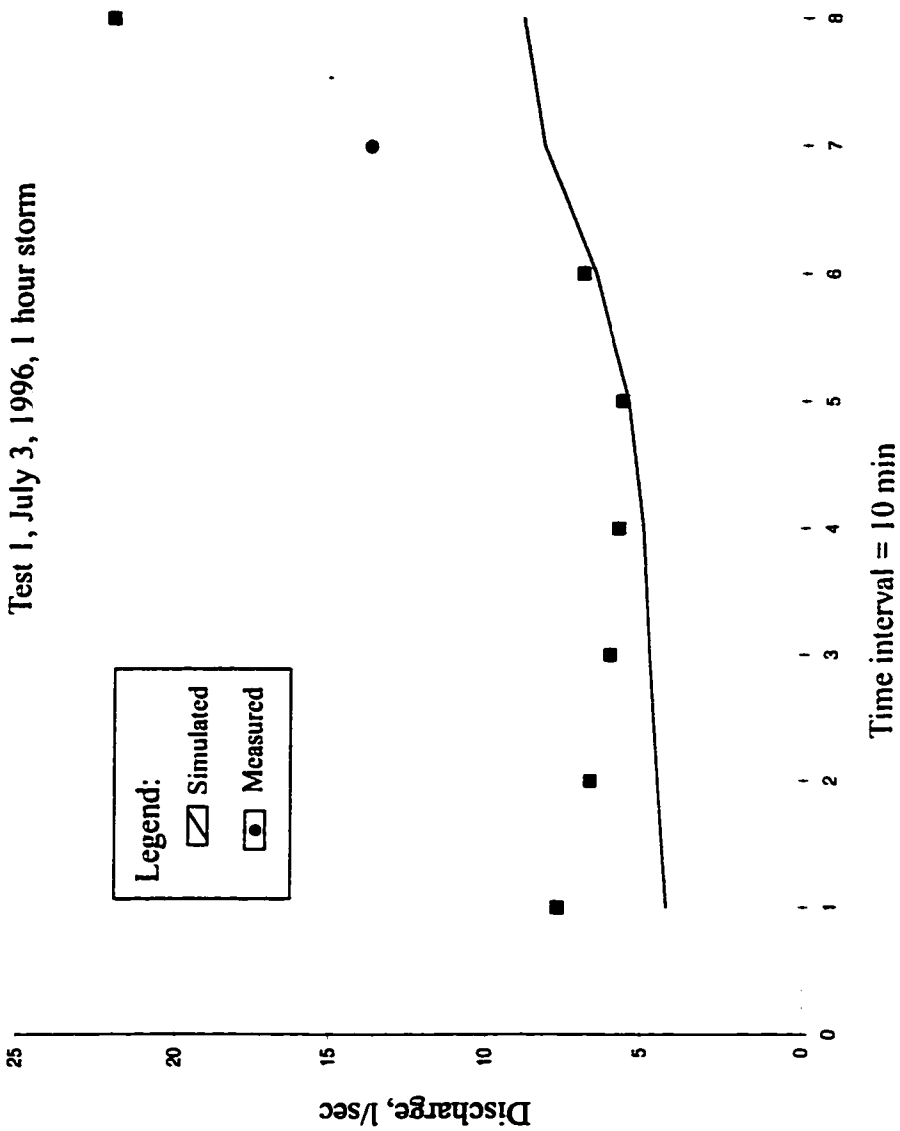

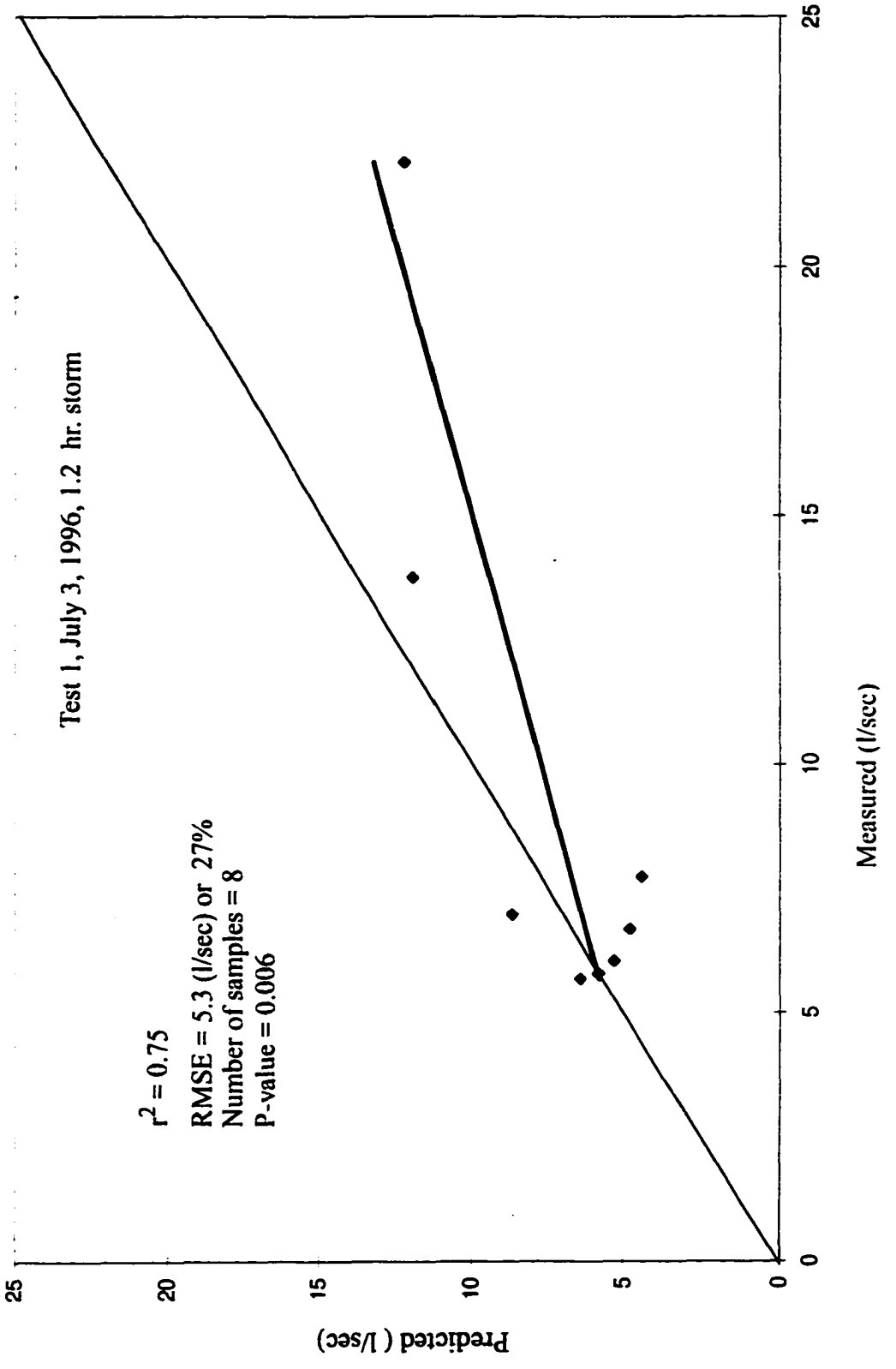

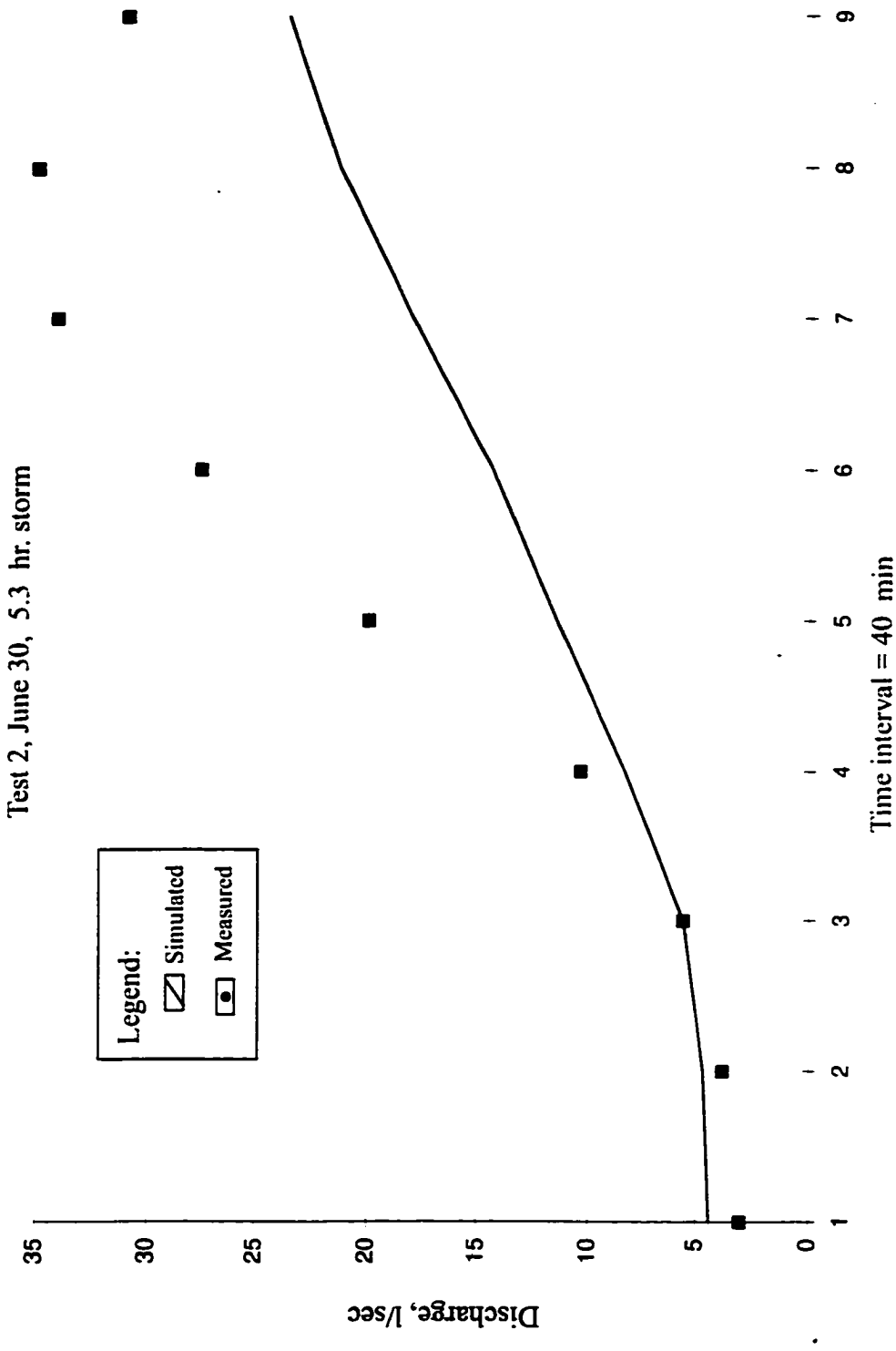

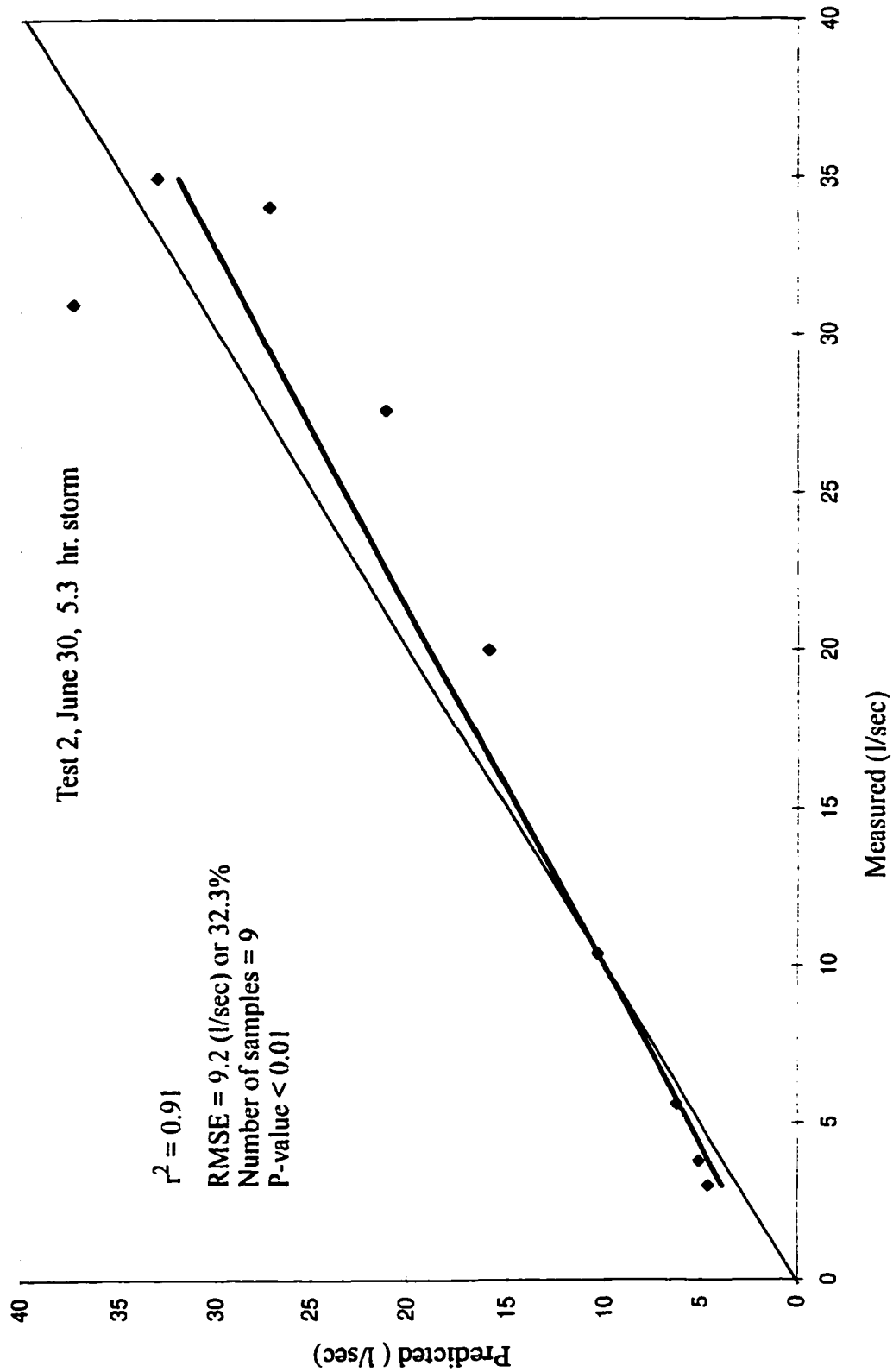

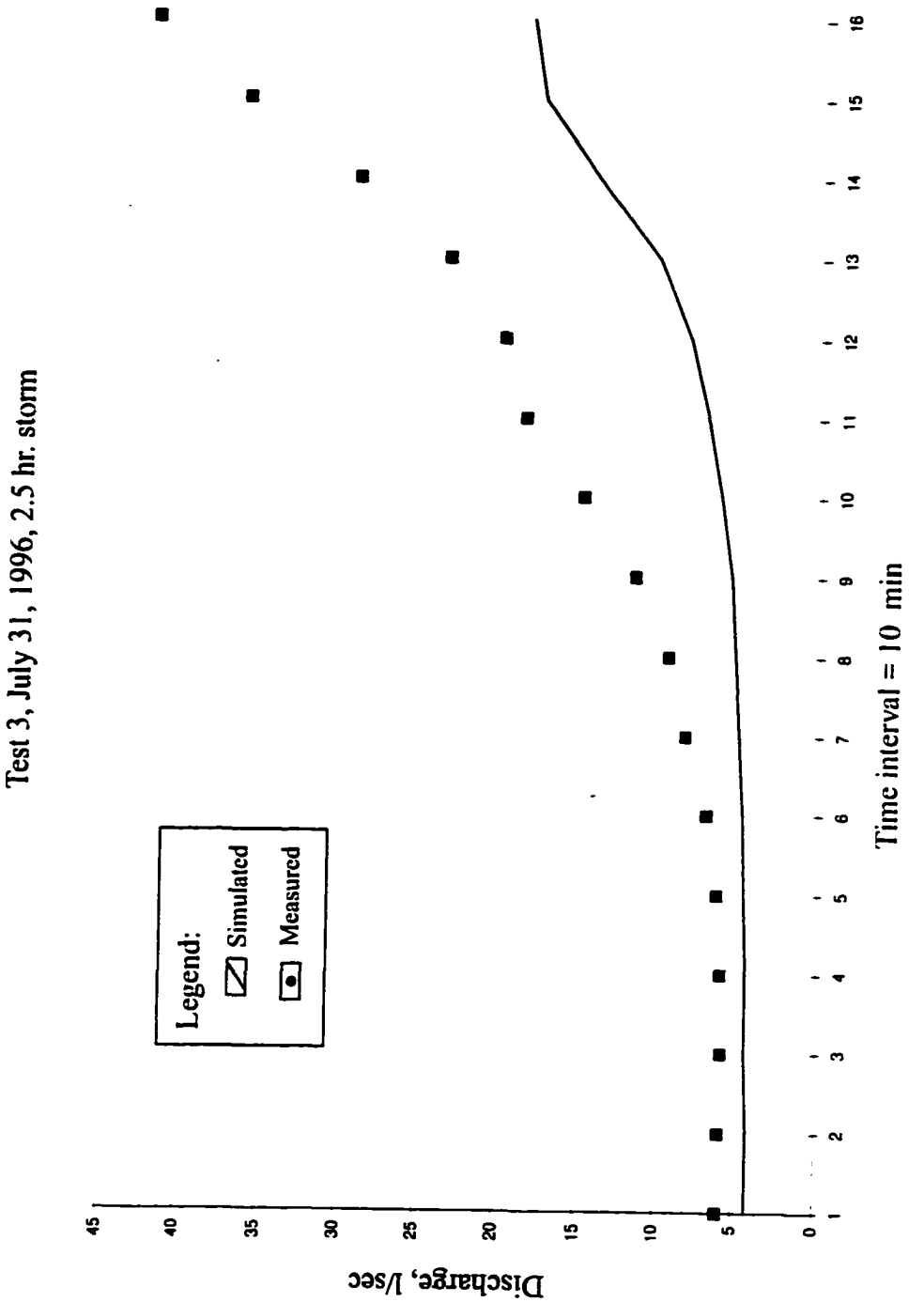

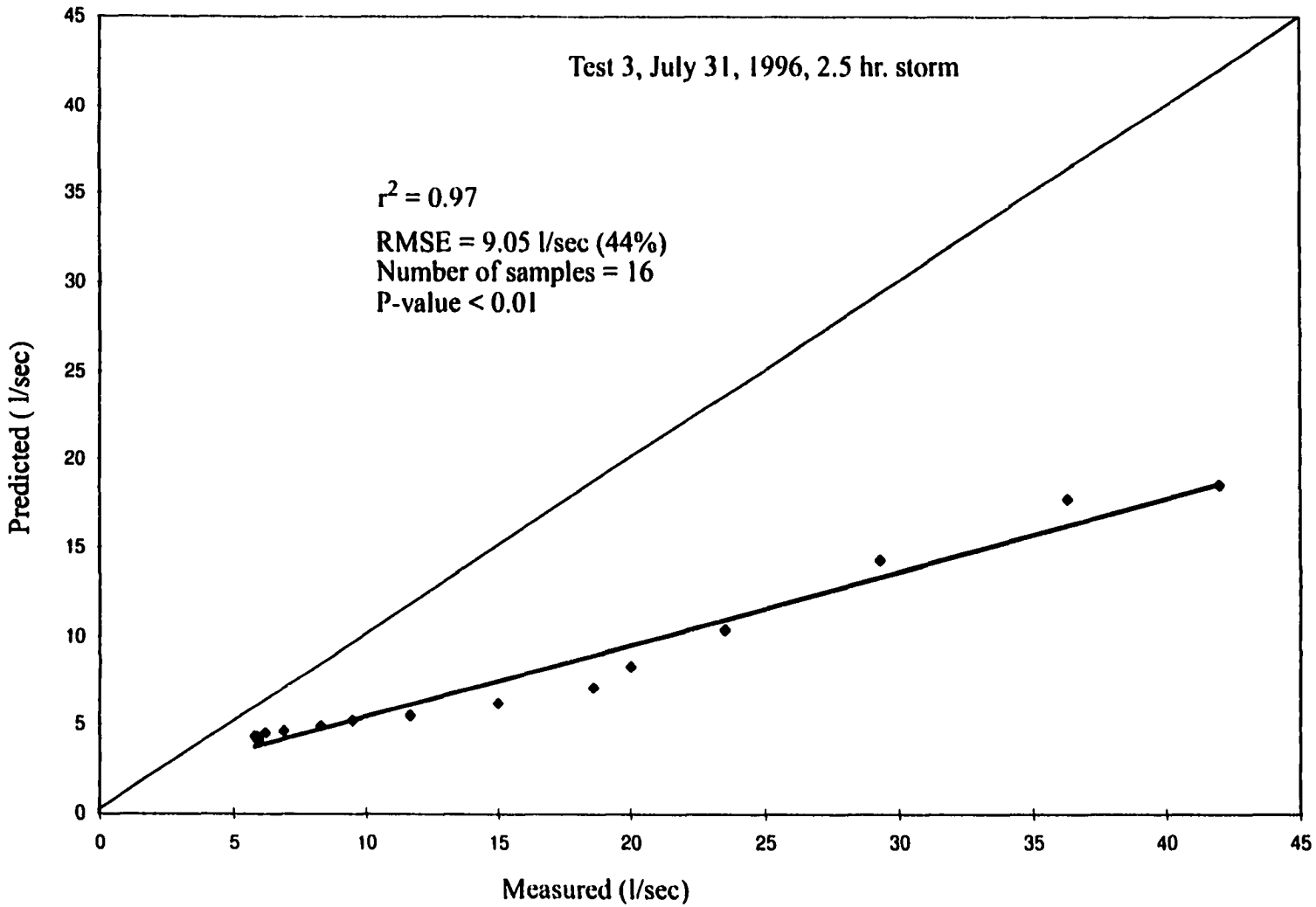

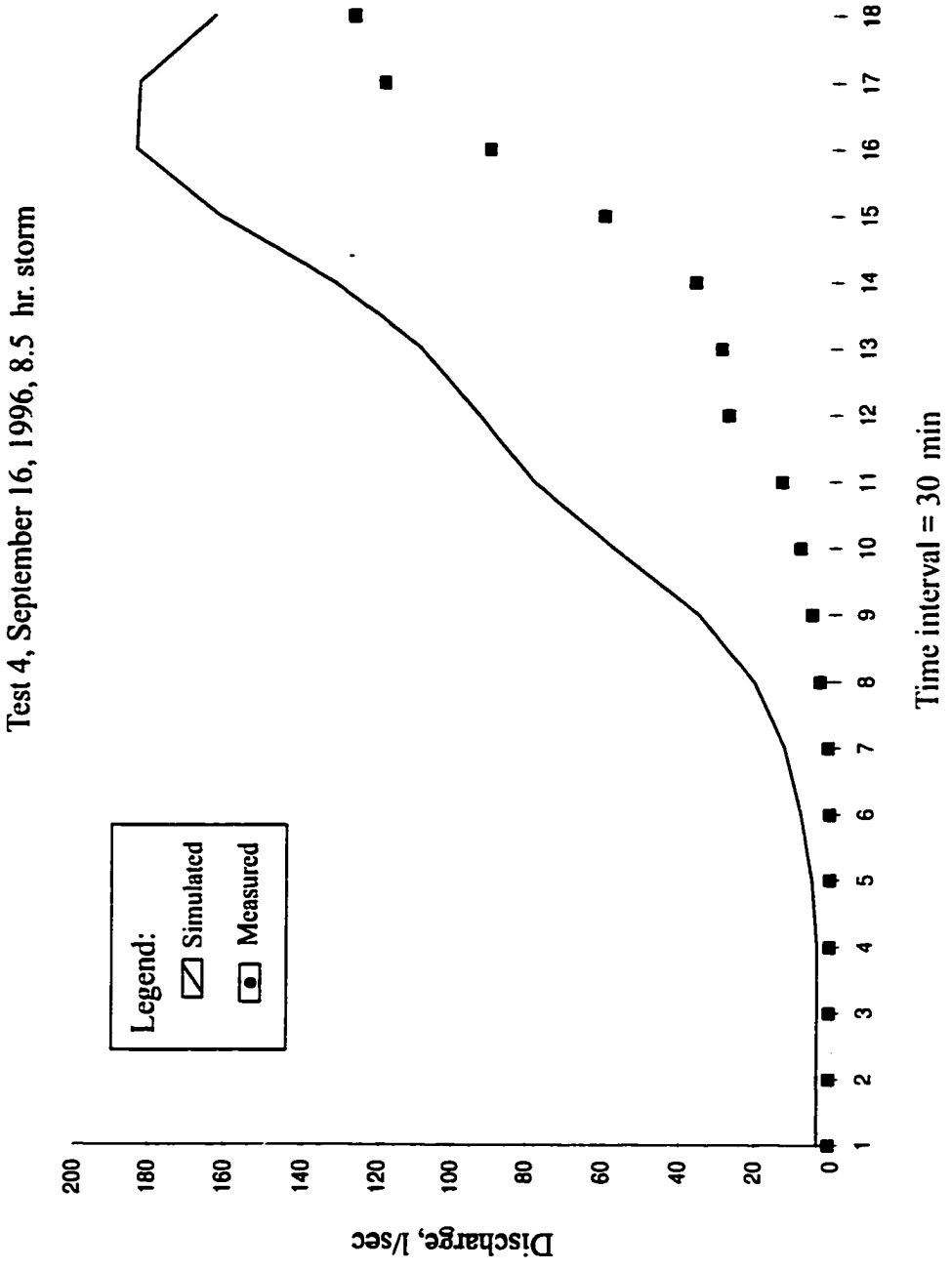

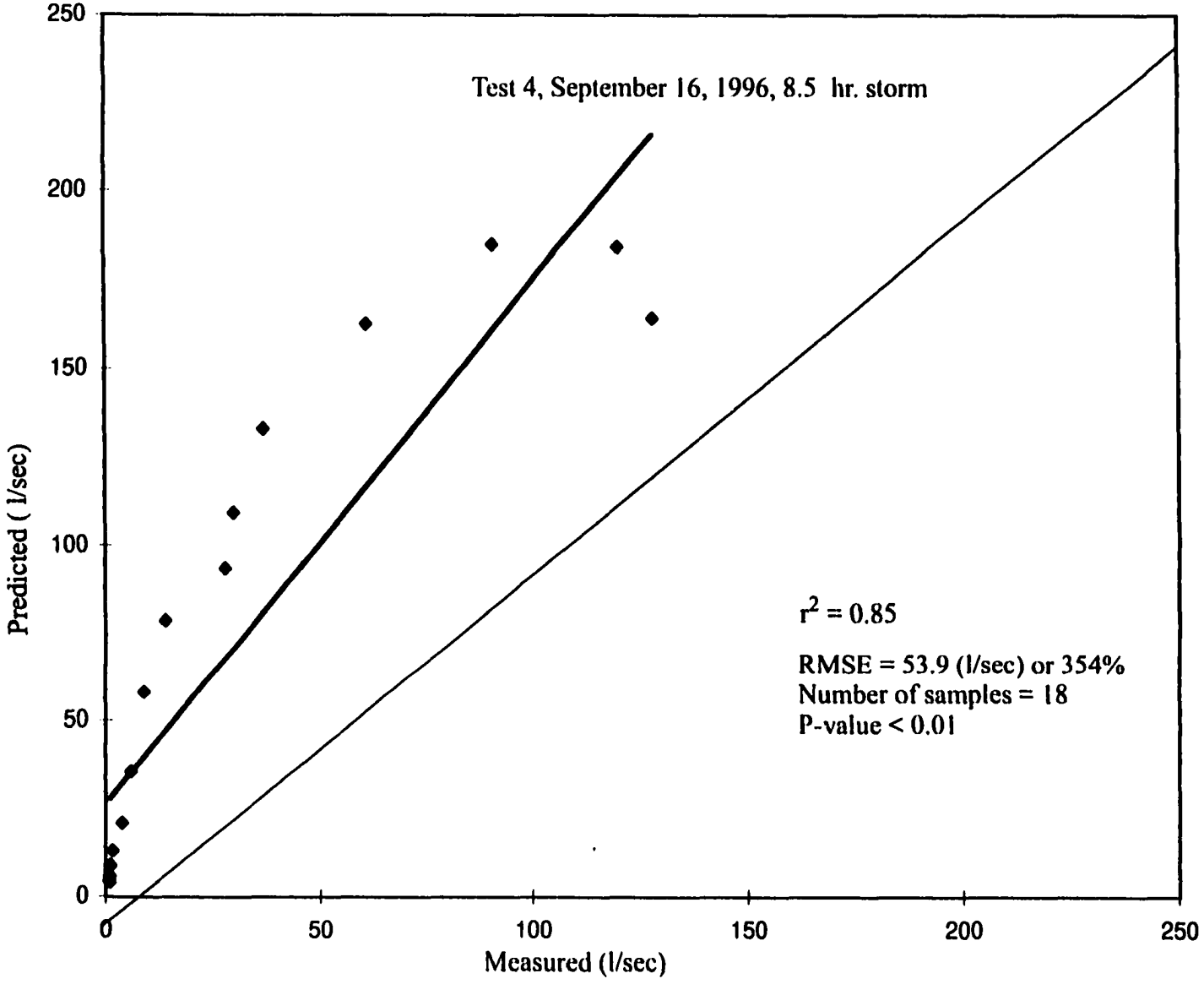

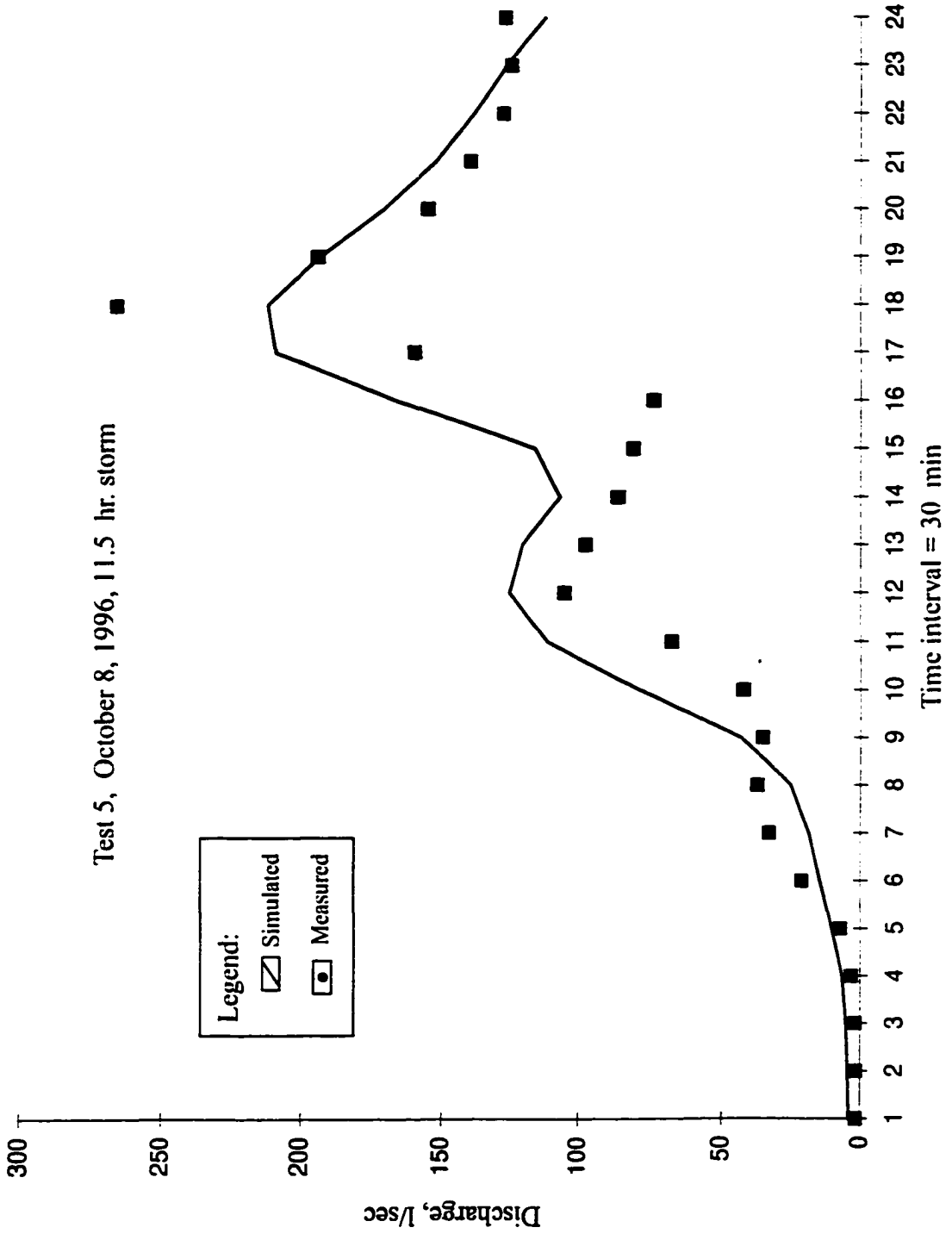

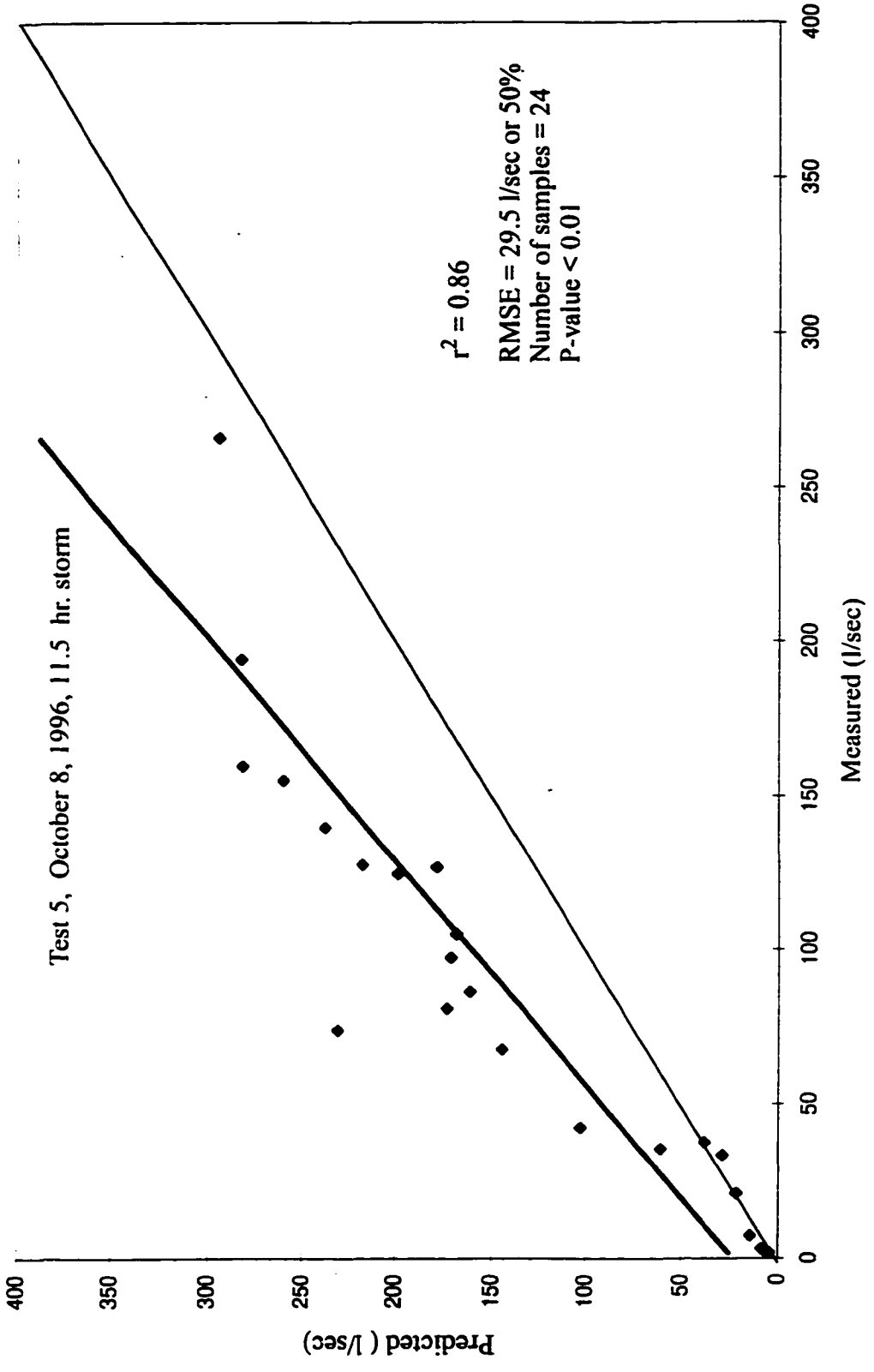

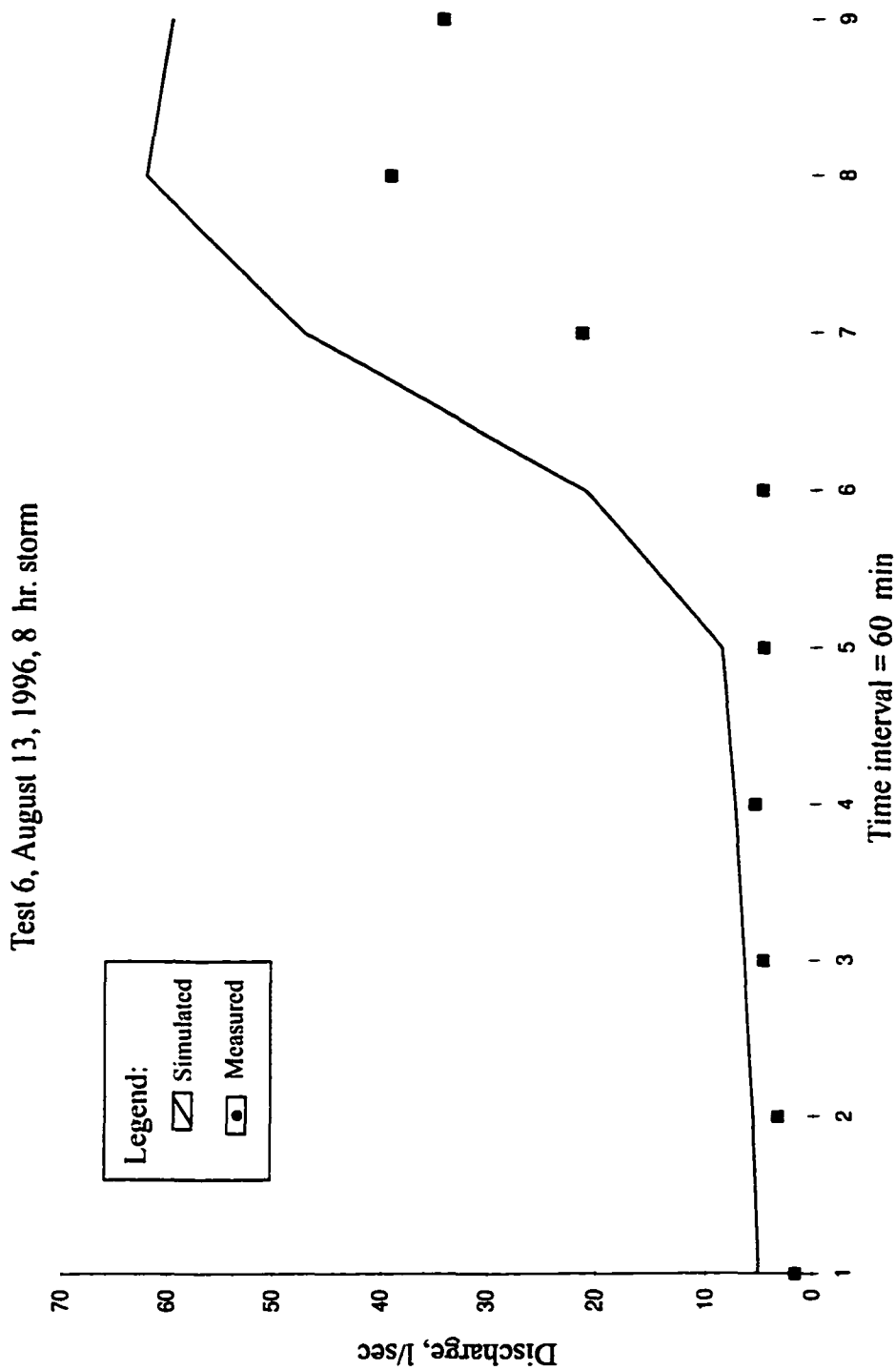

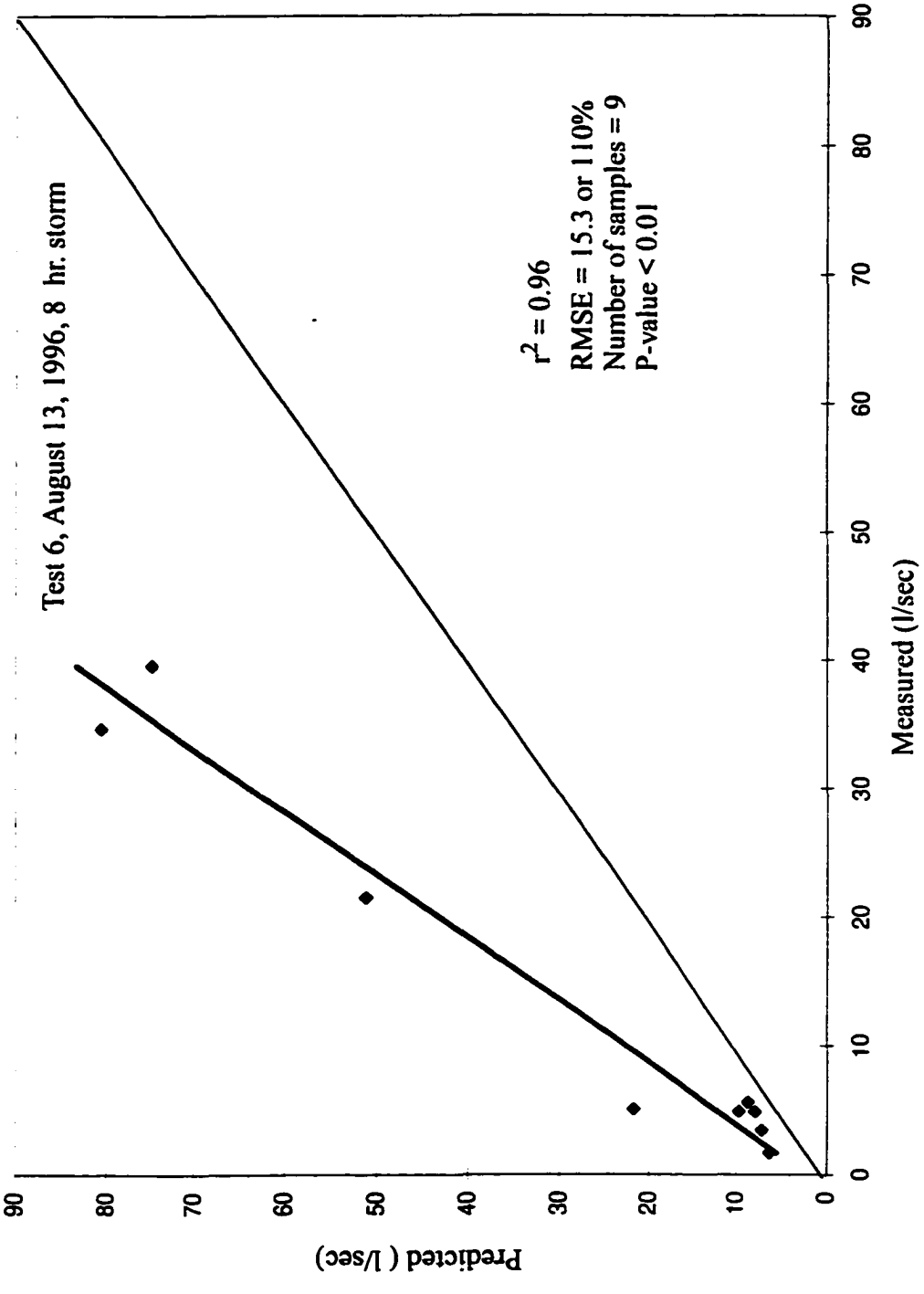

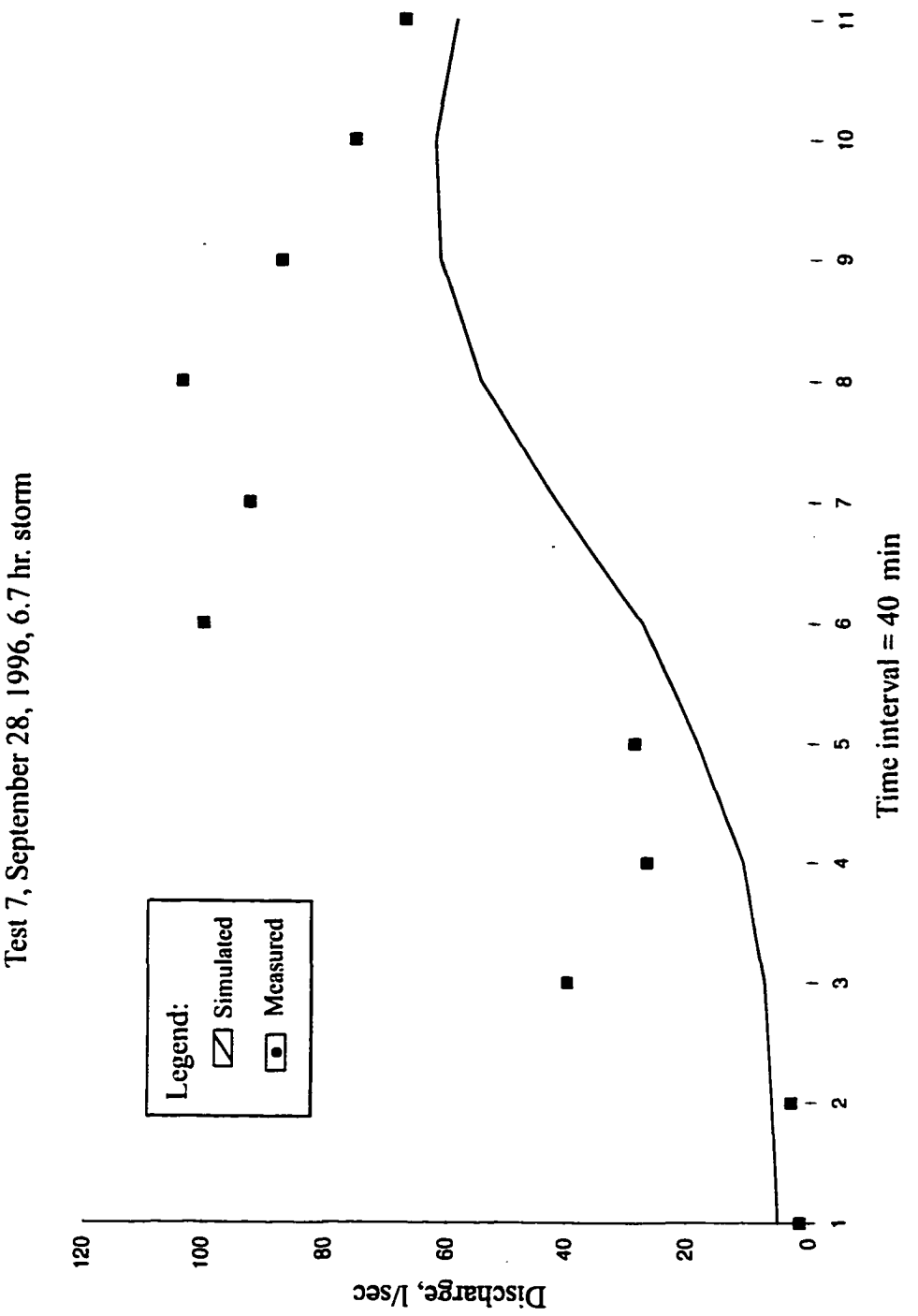

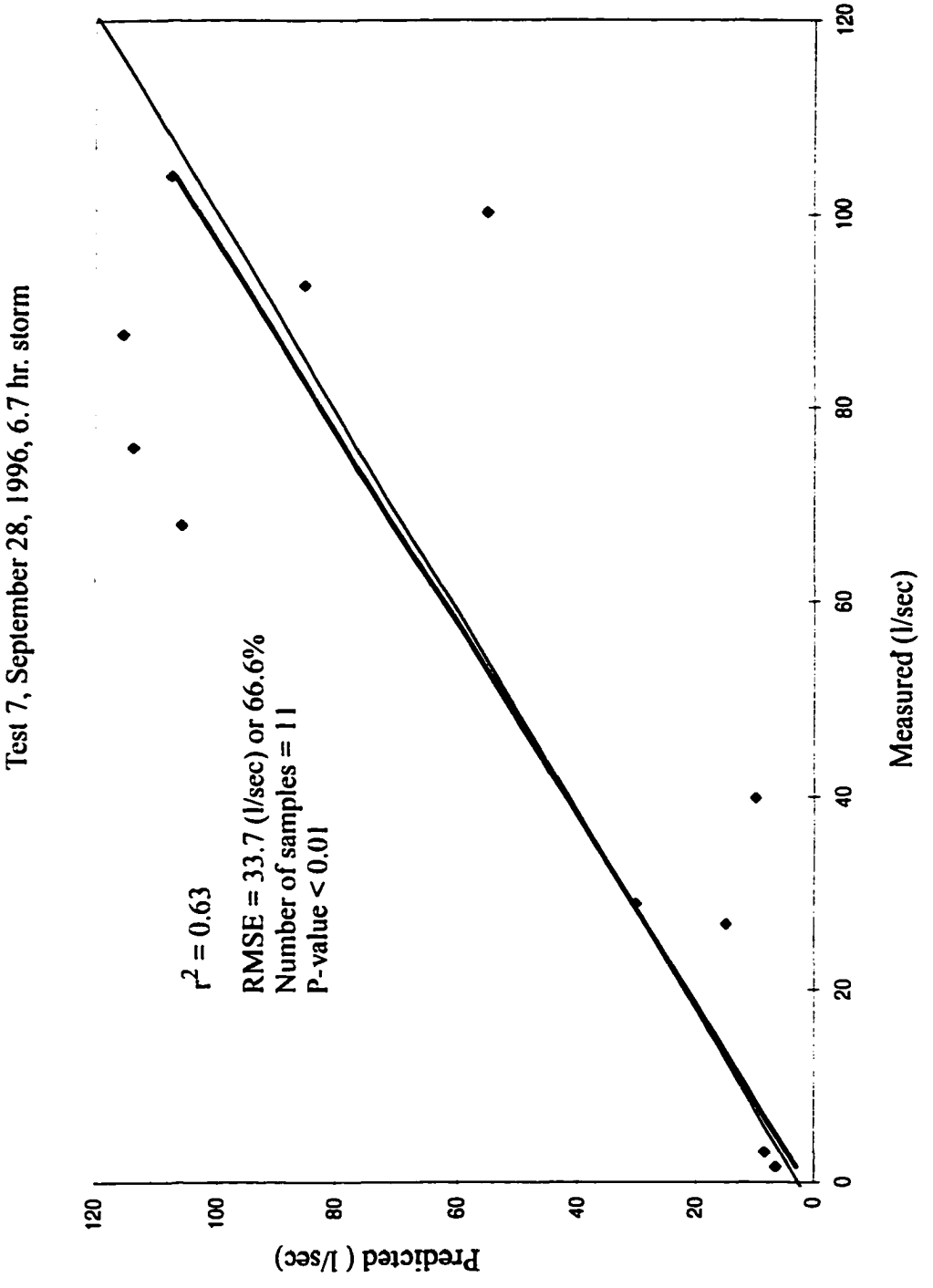

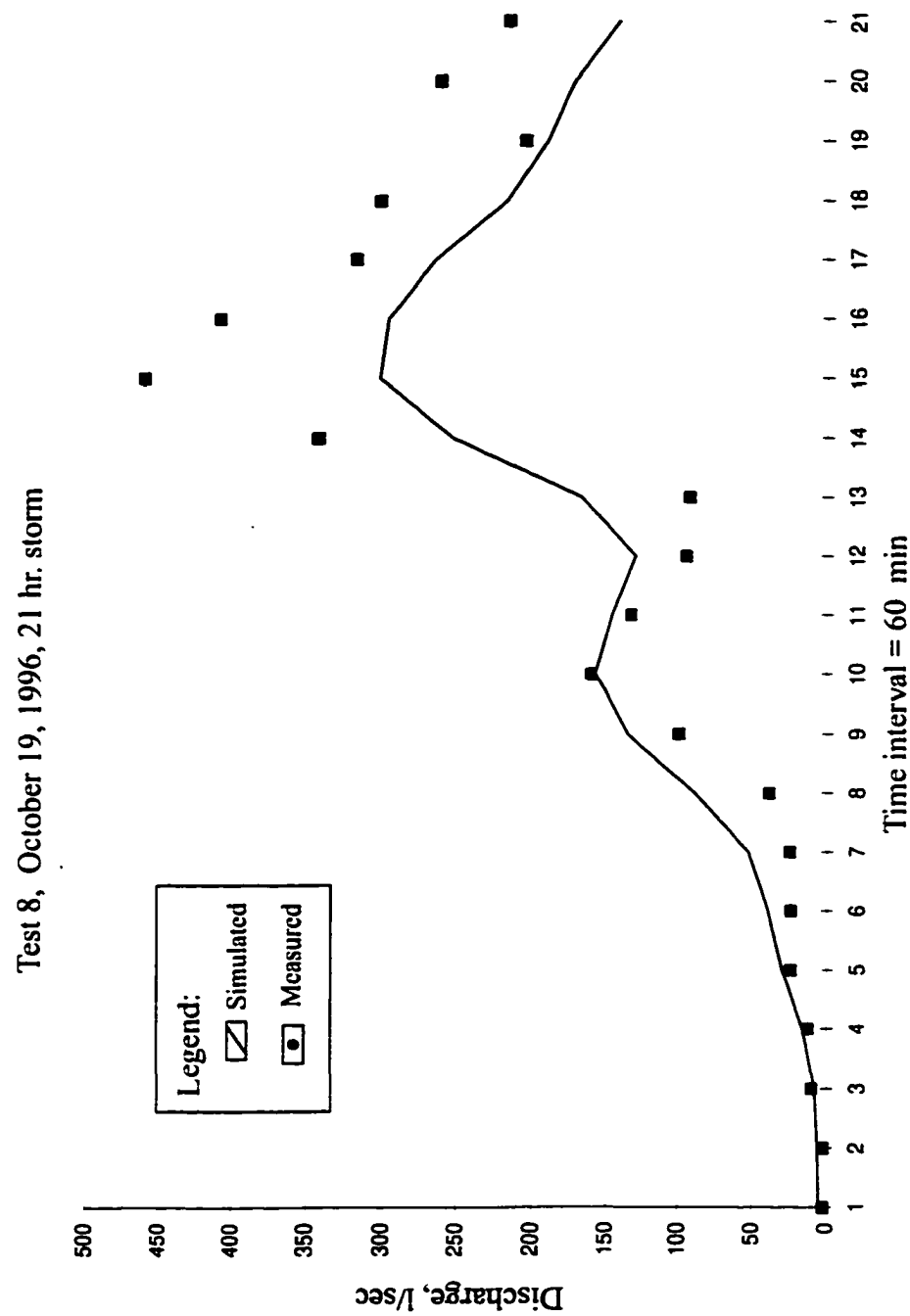

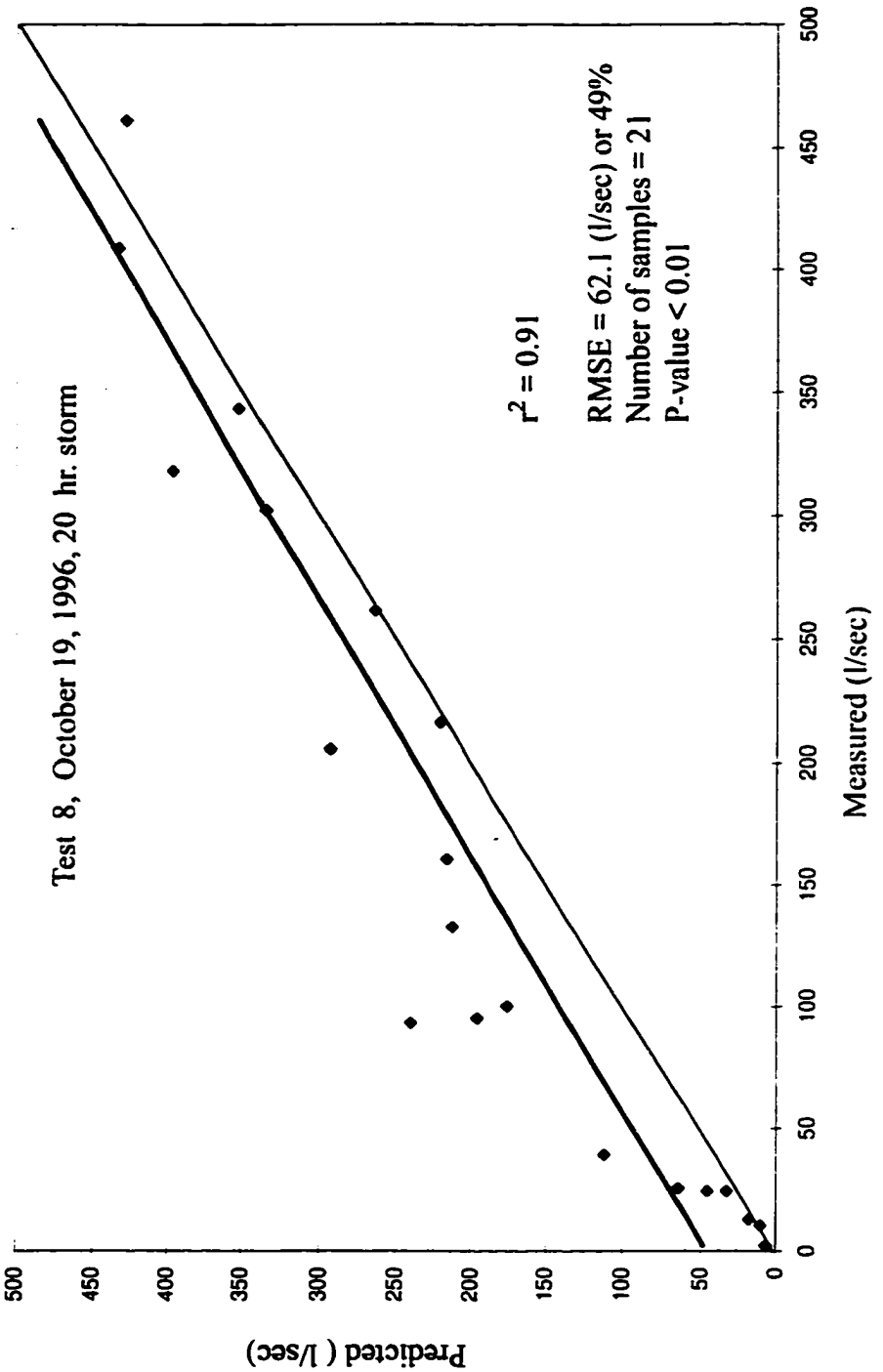

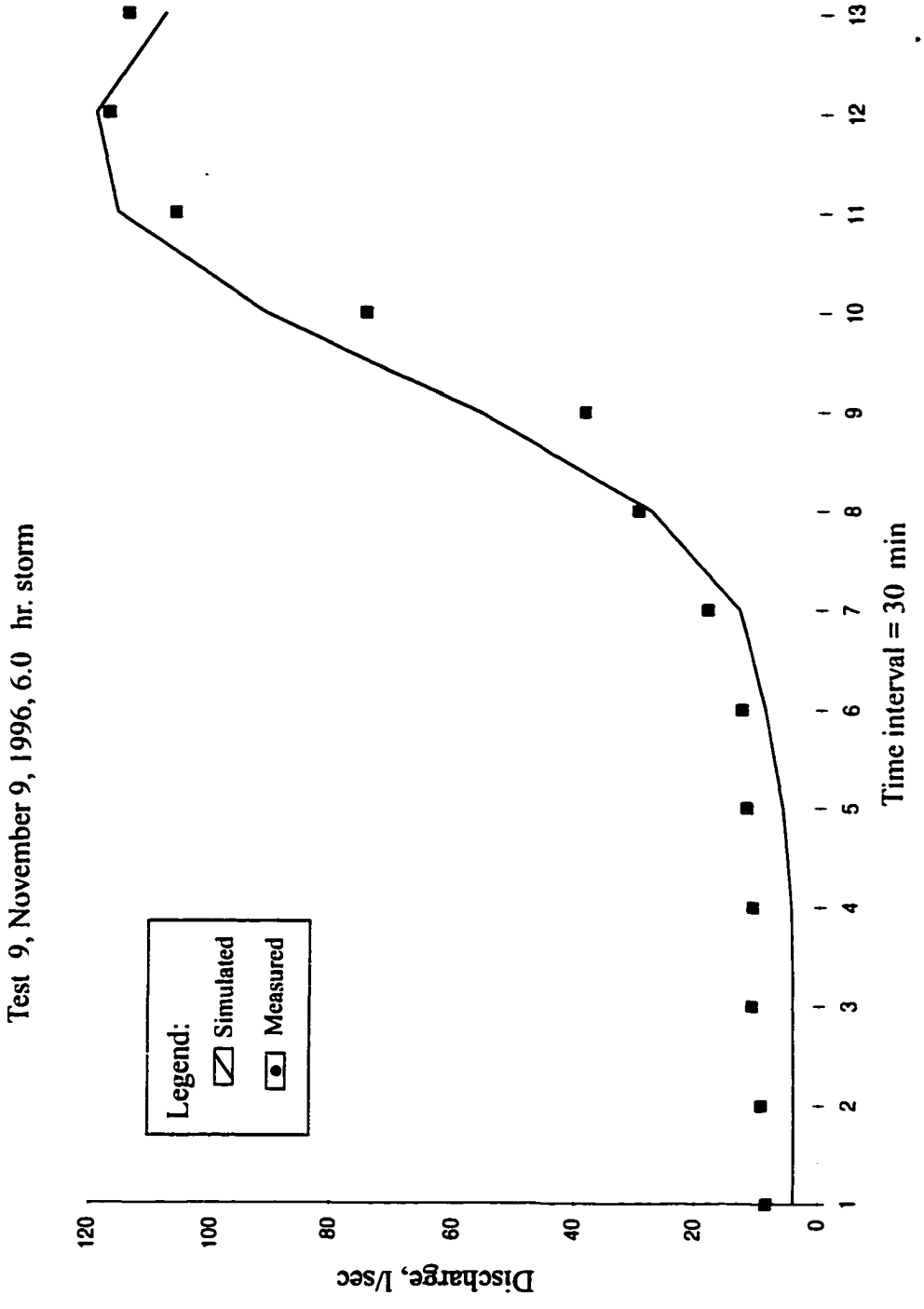

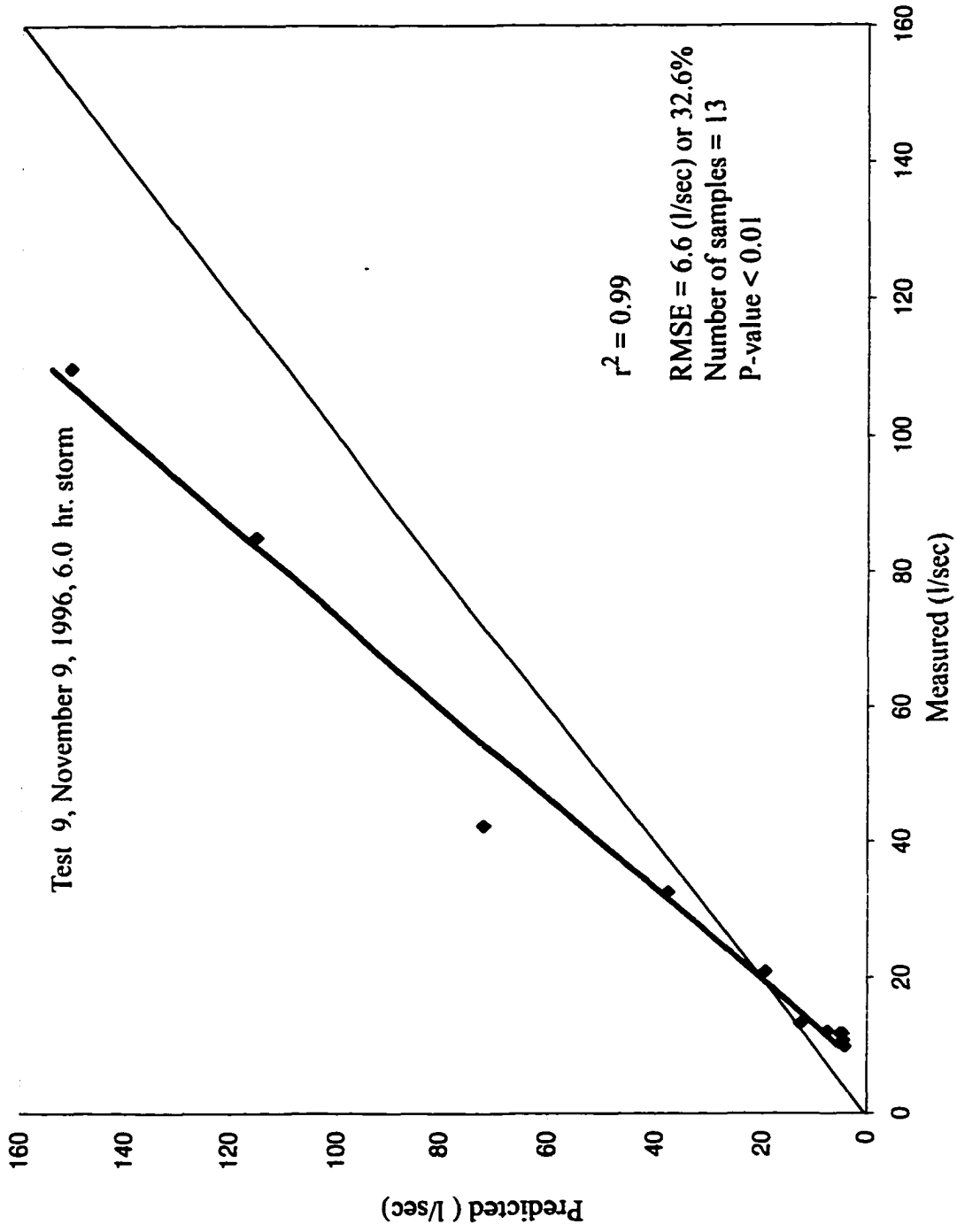

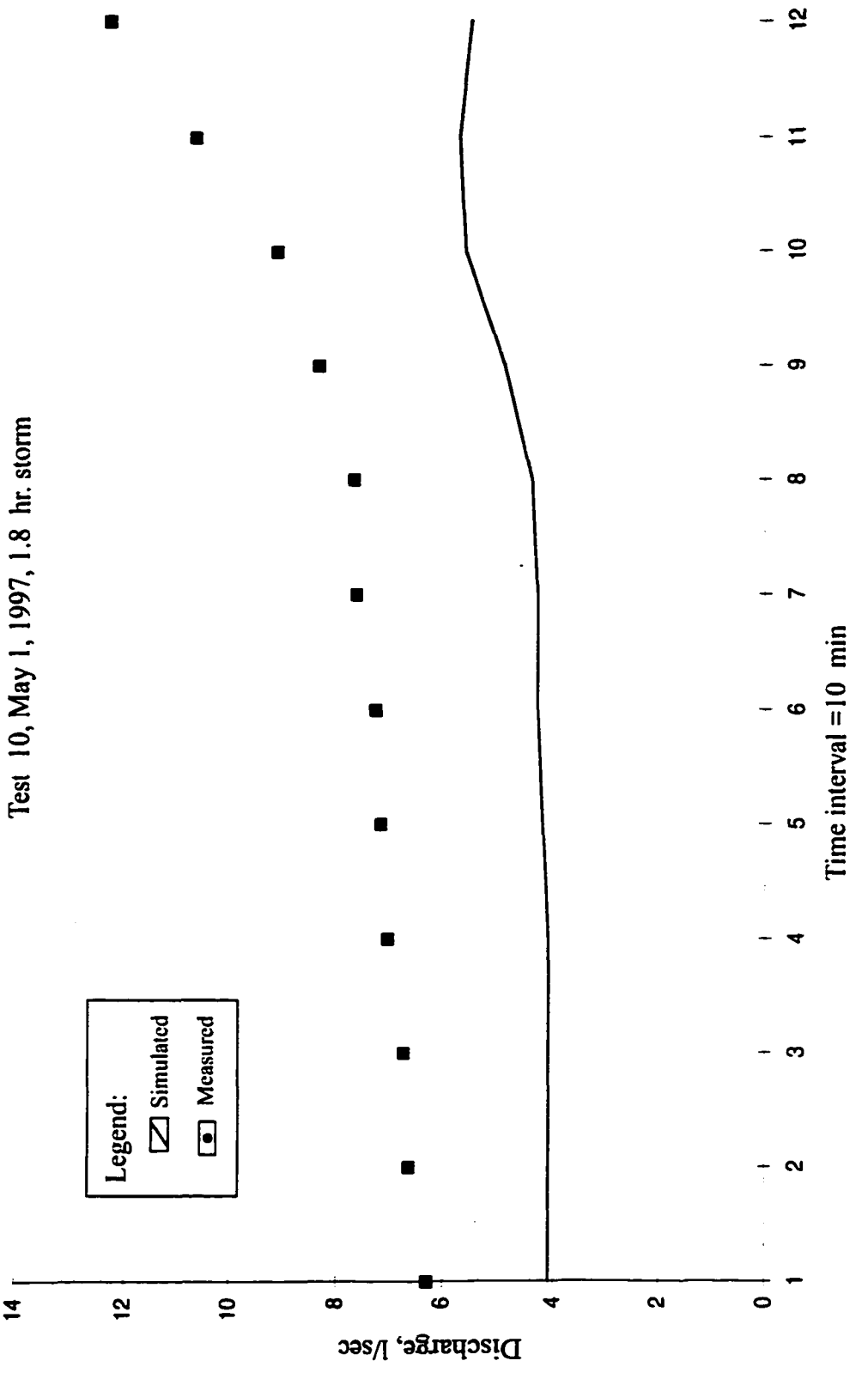

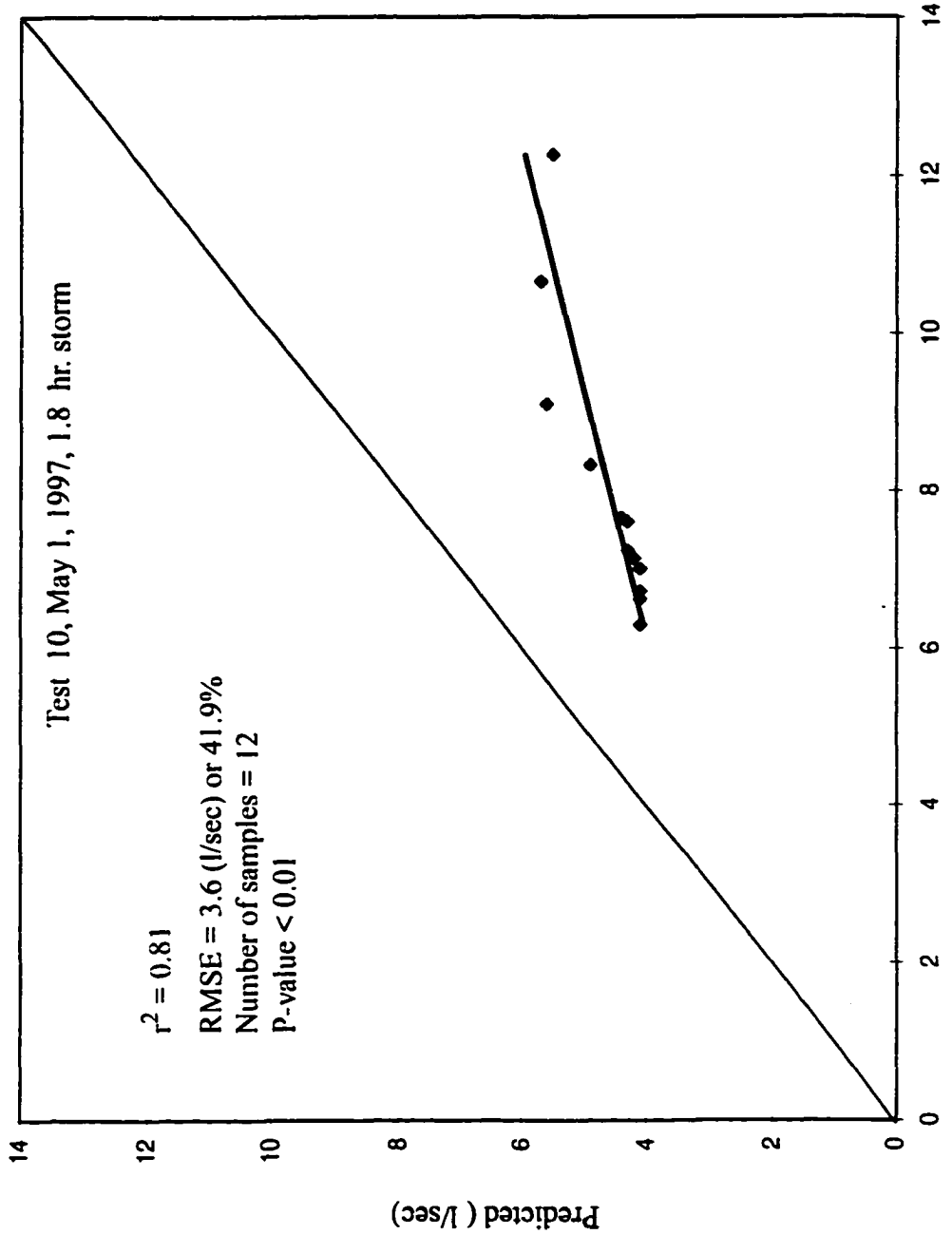

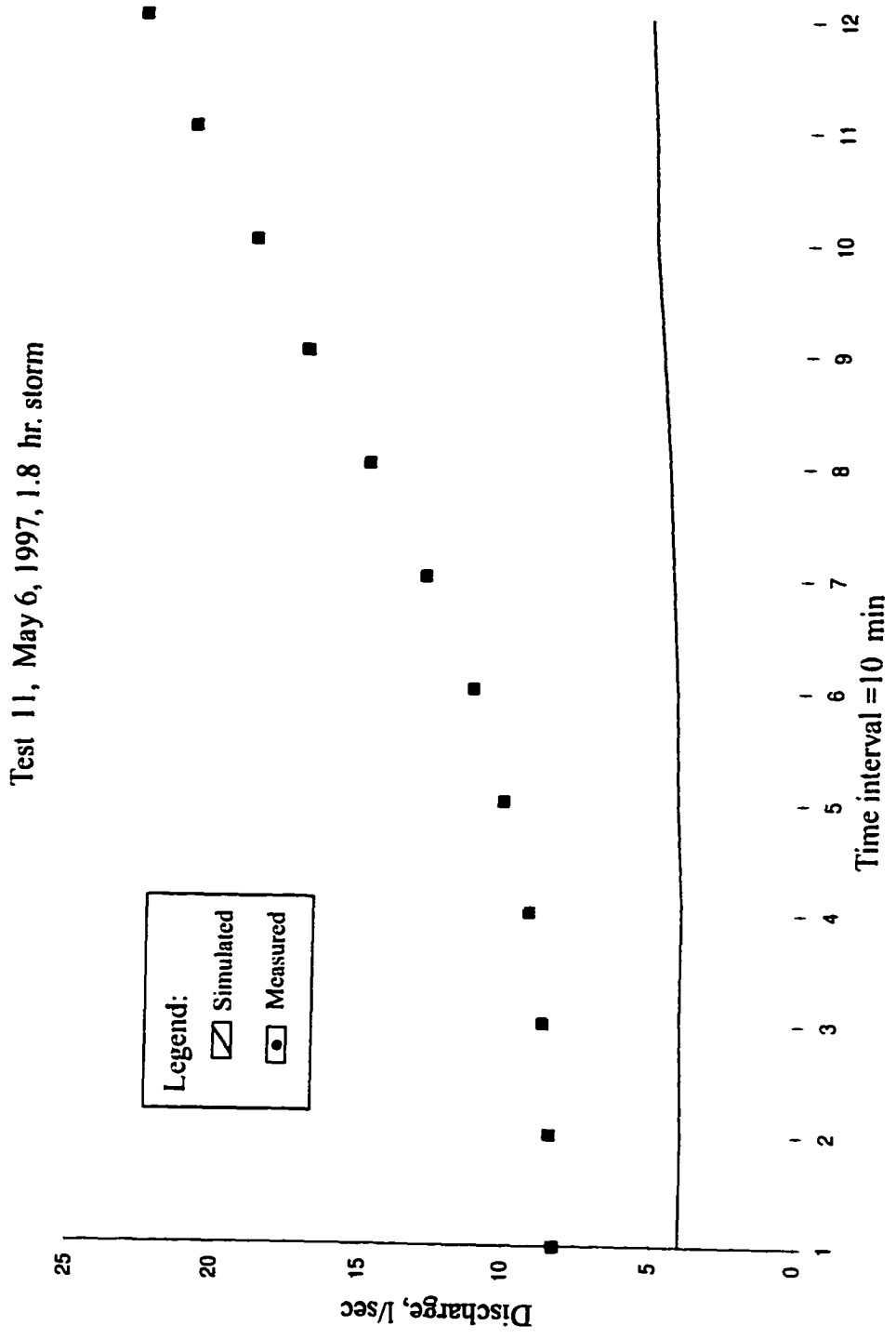

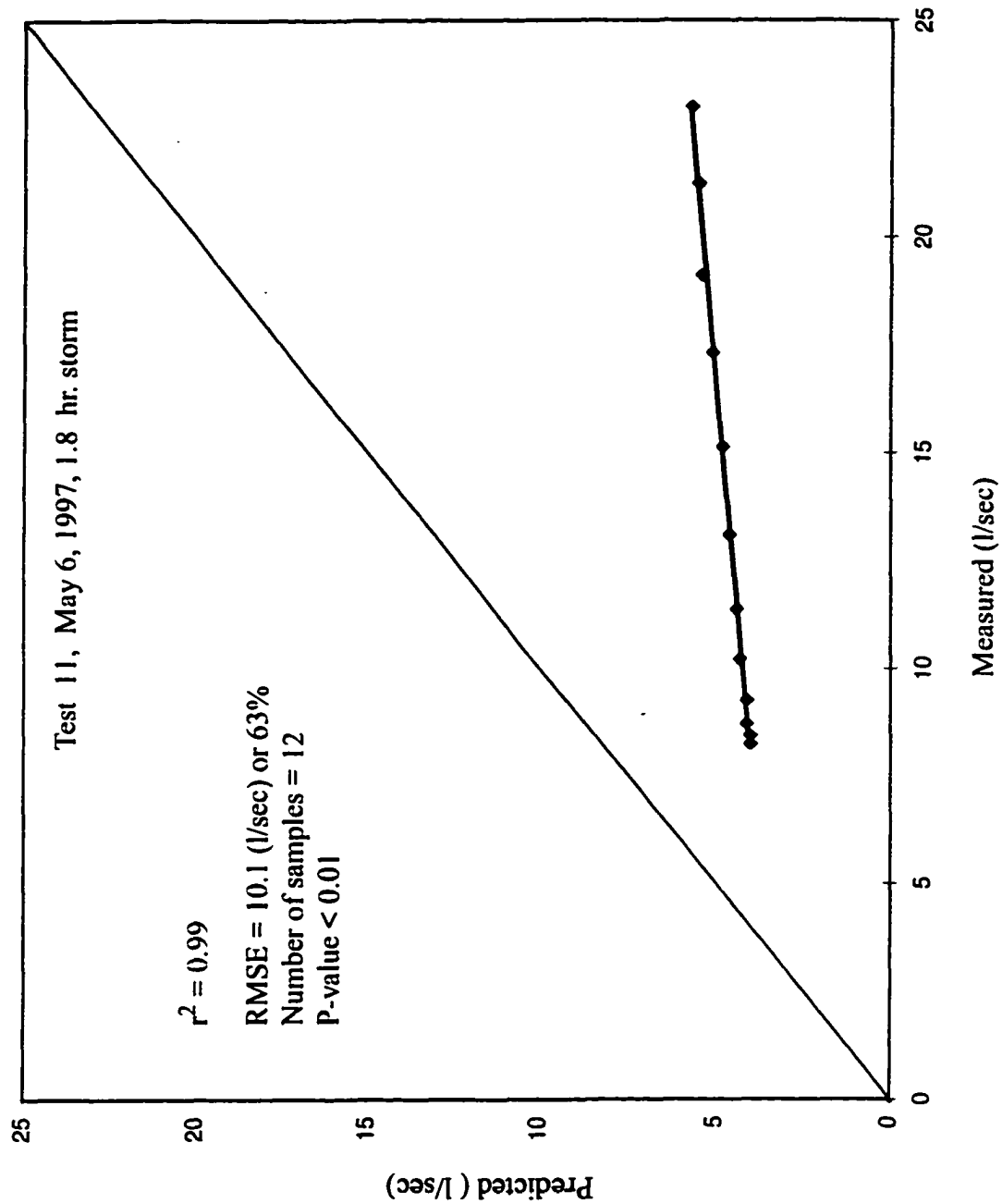

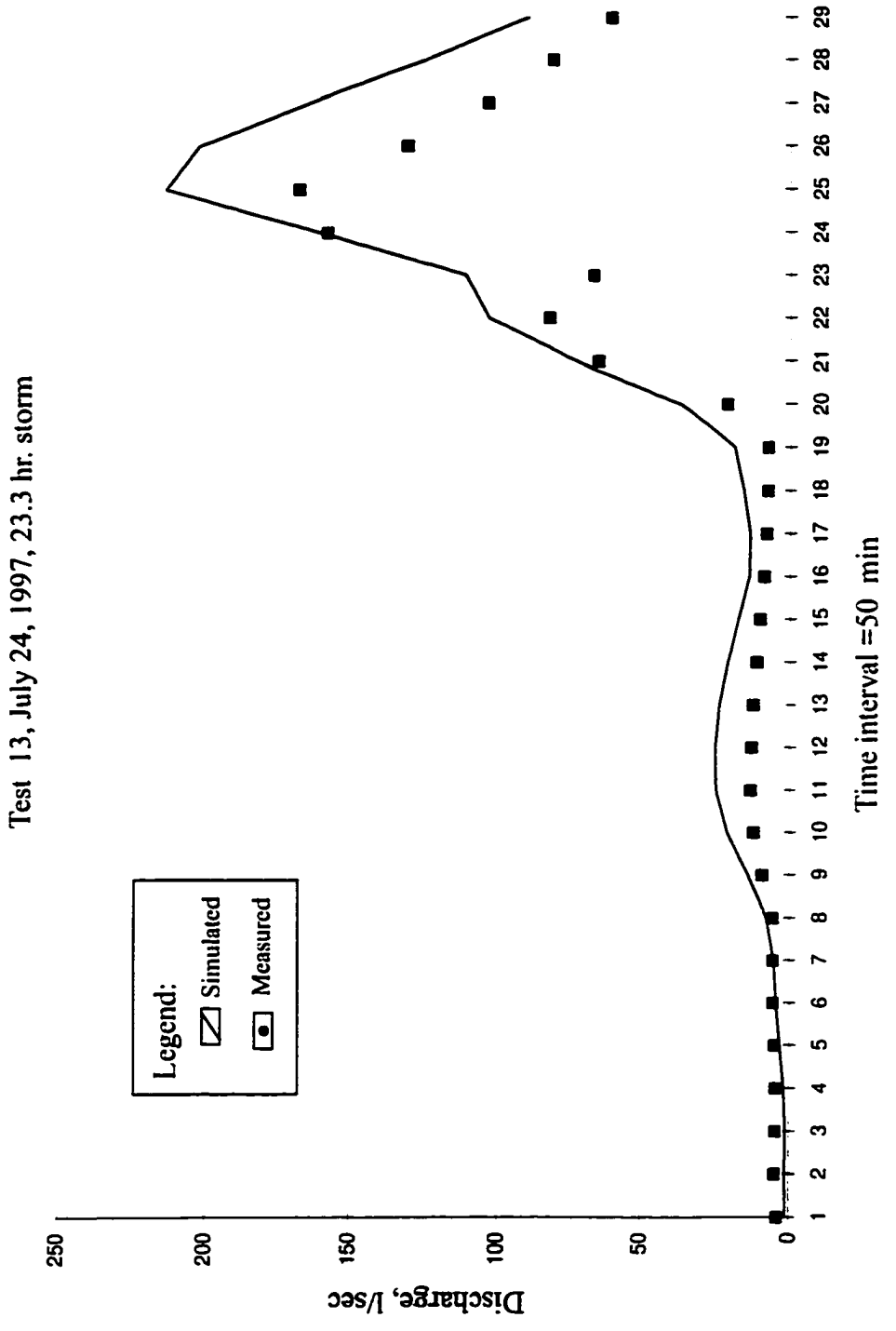

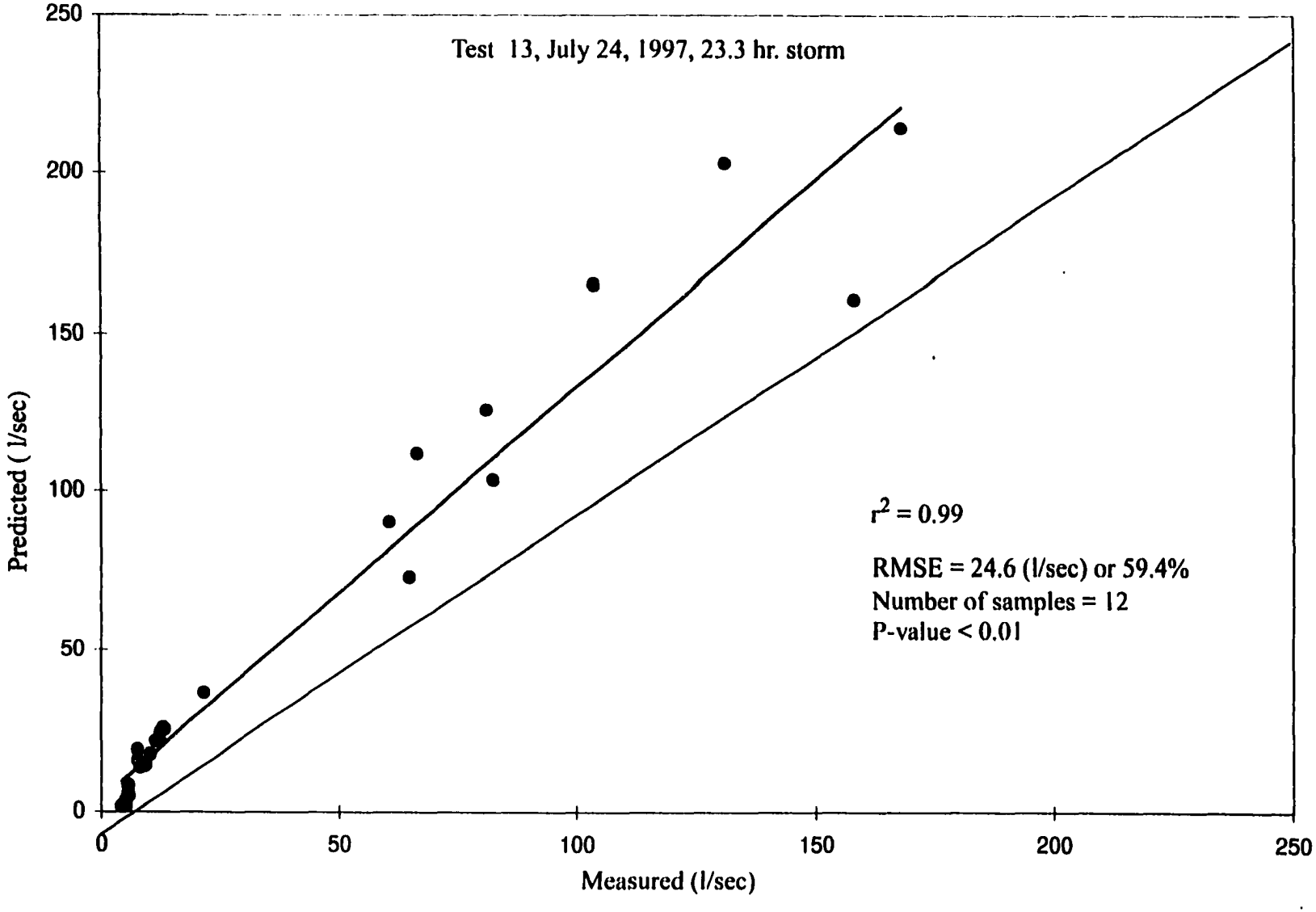

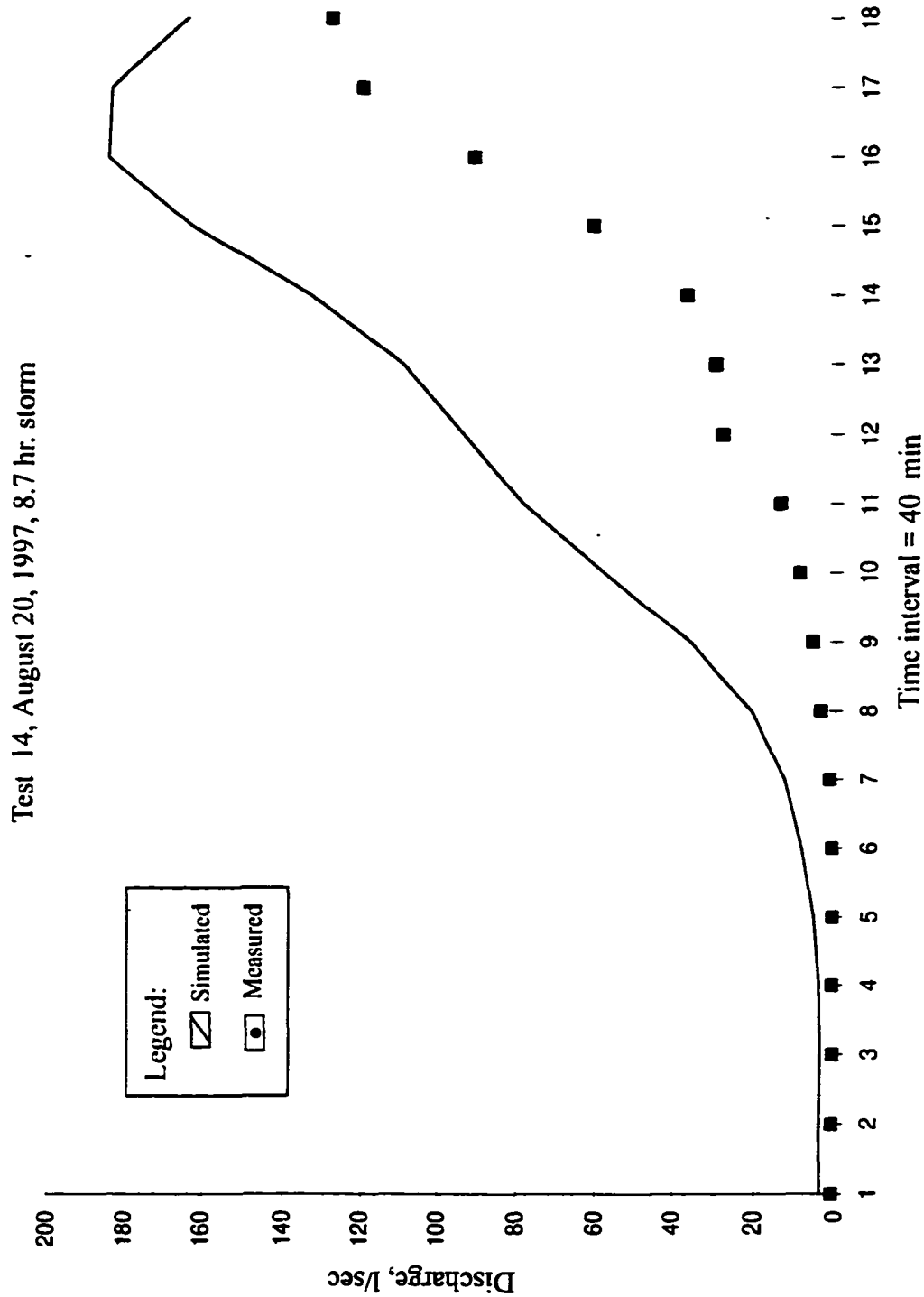

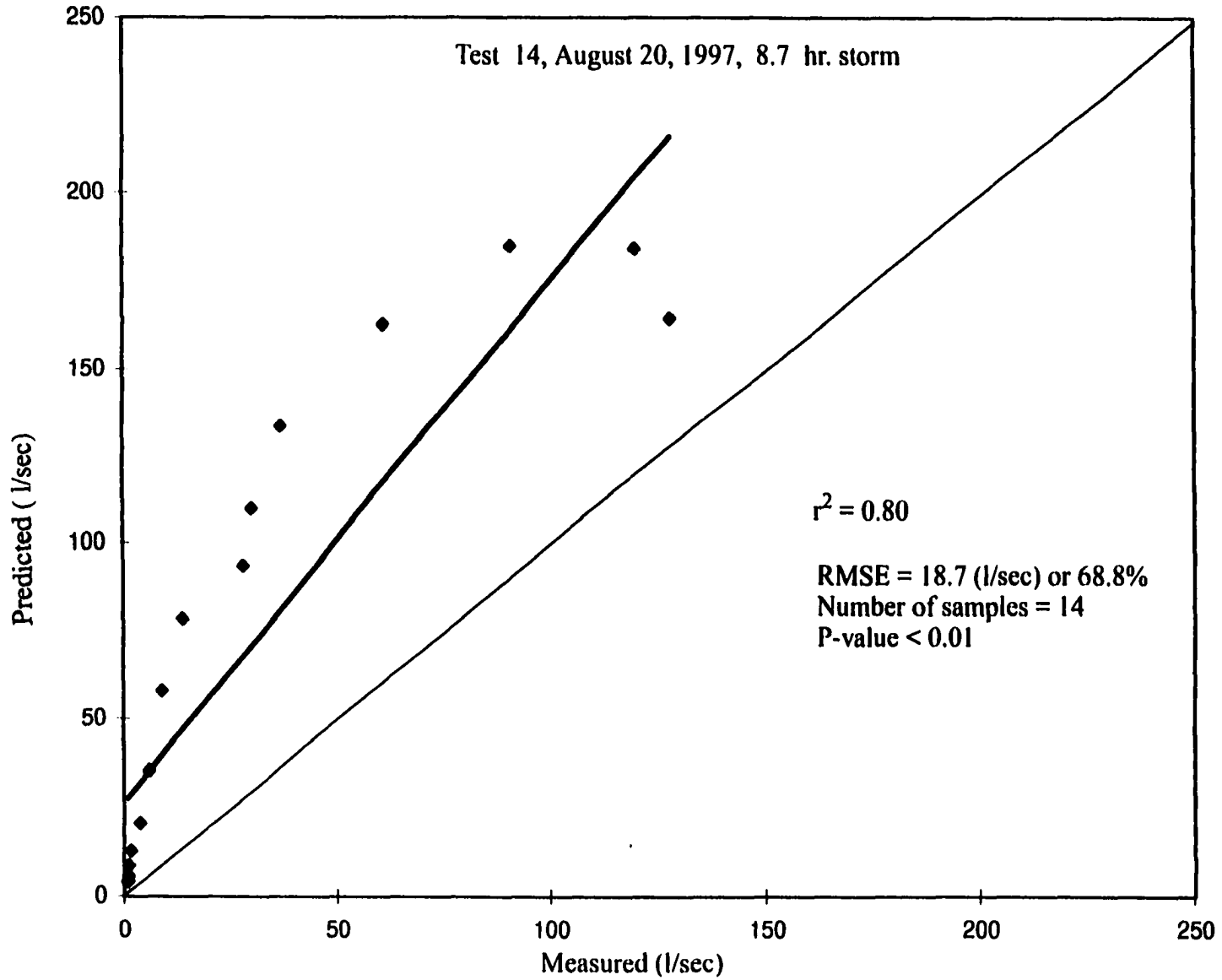

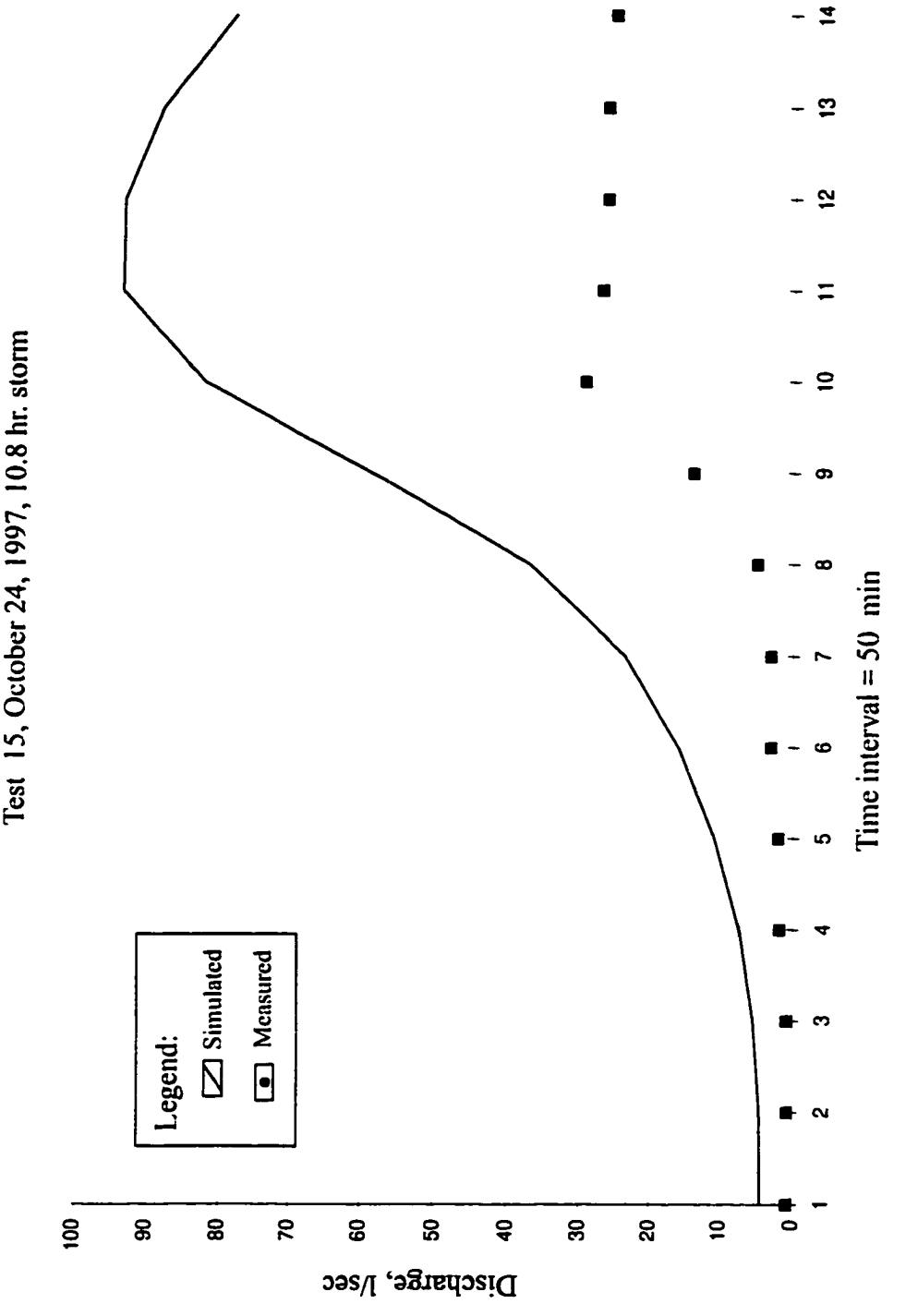

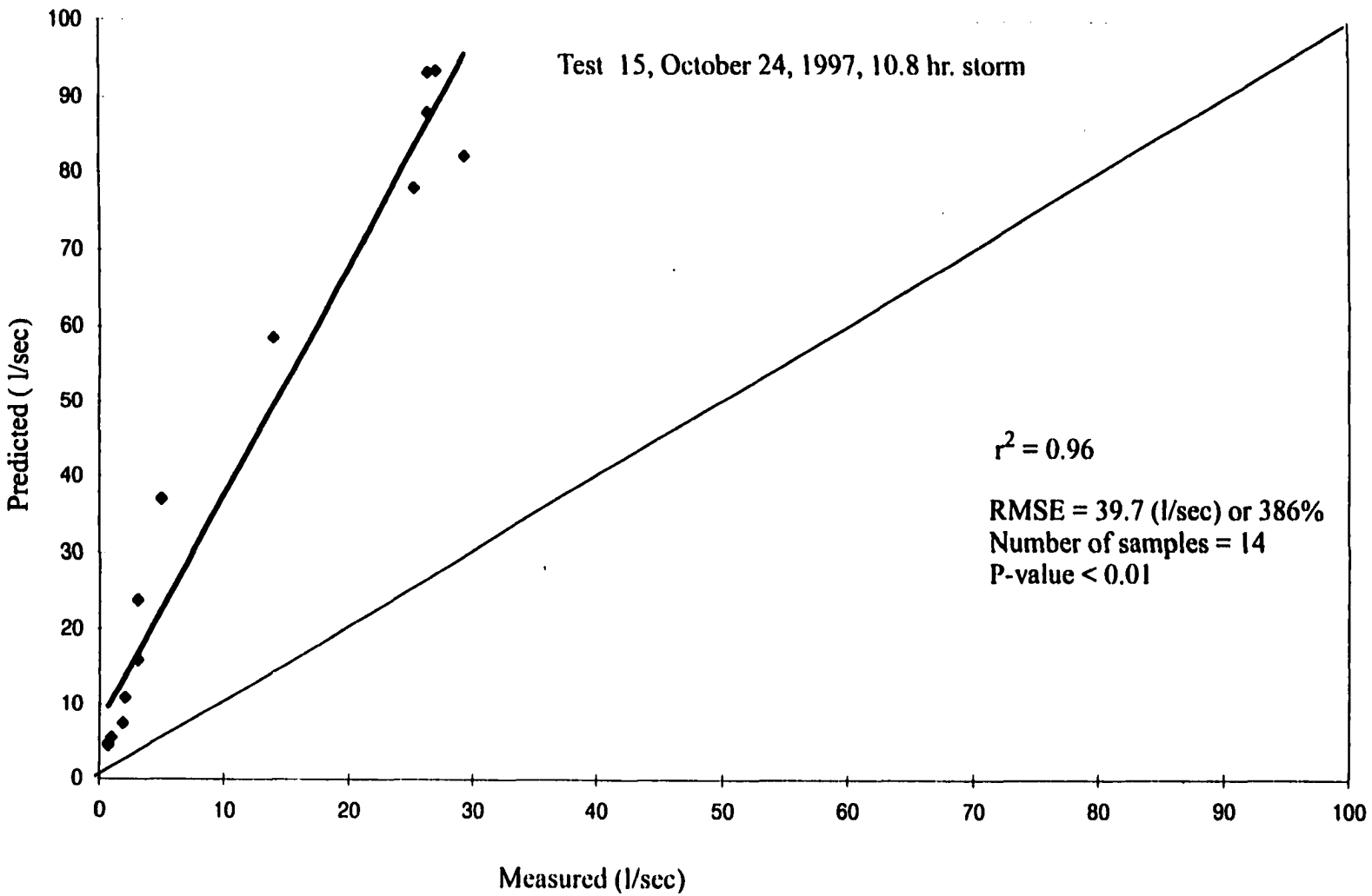

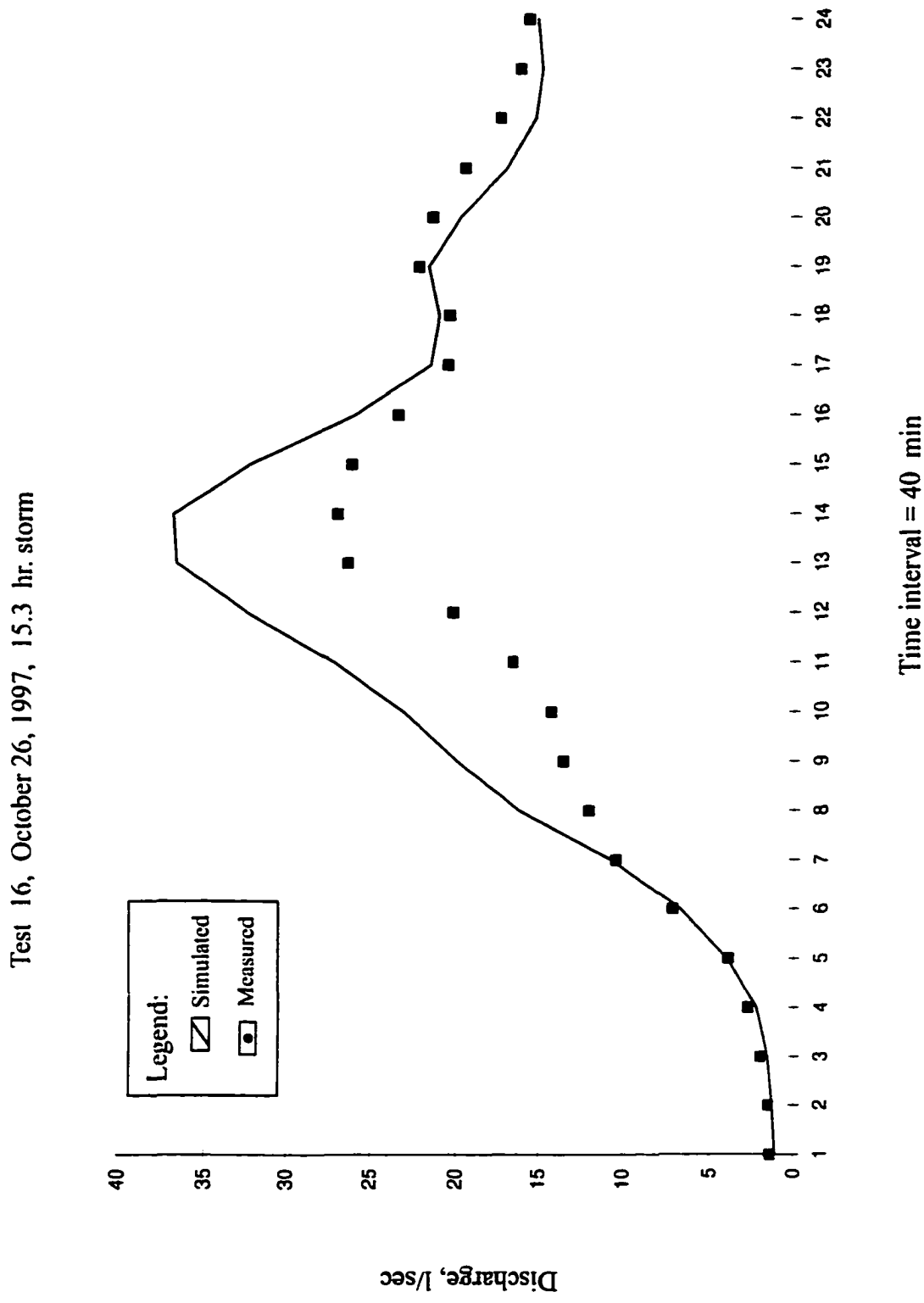

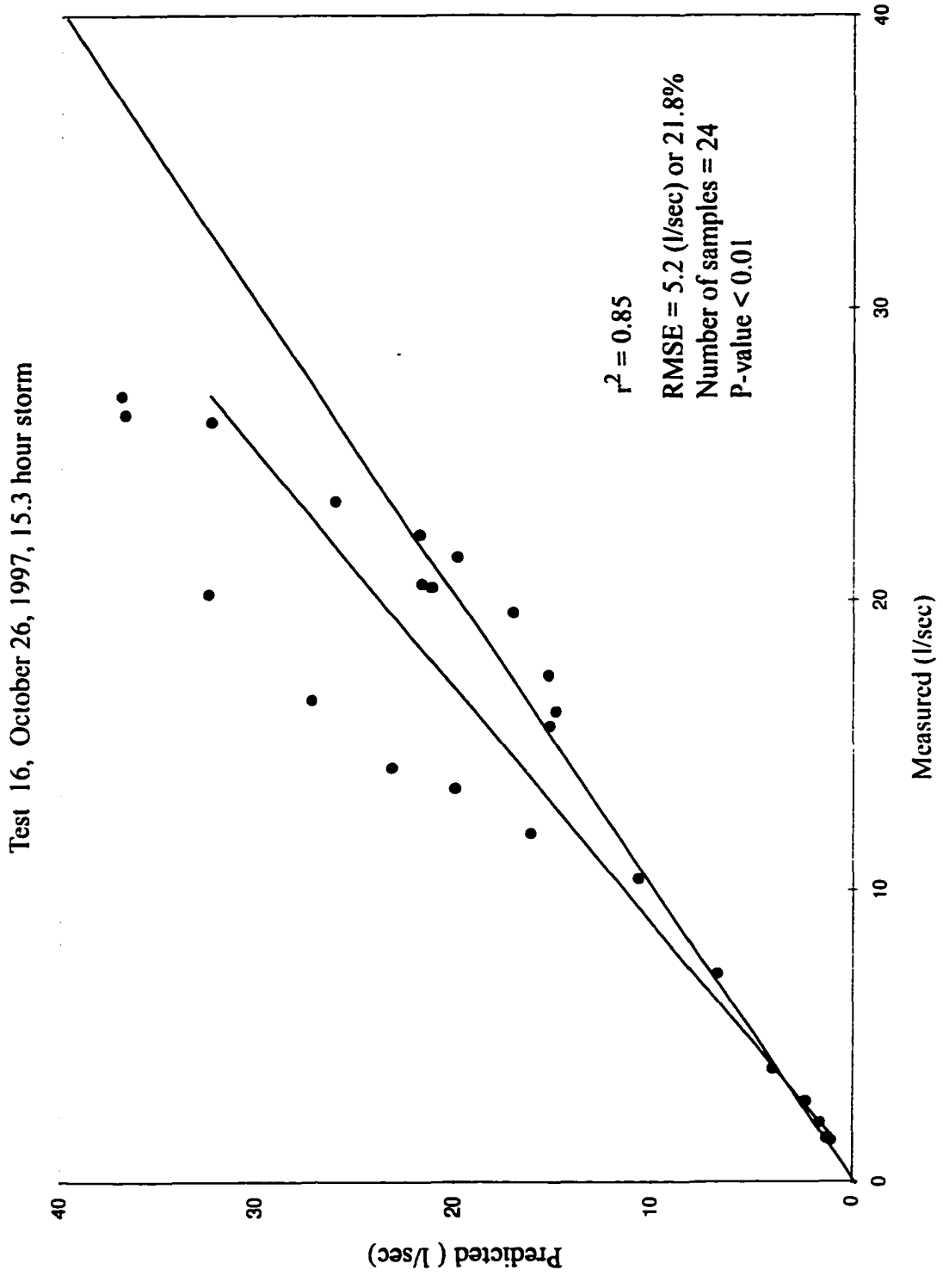

Appendix E. Turbidity Modeling Results.

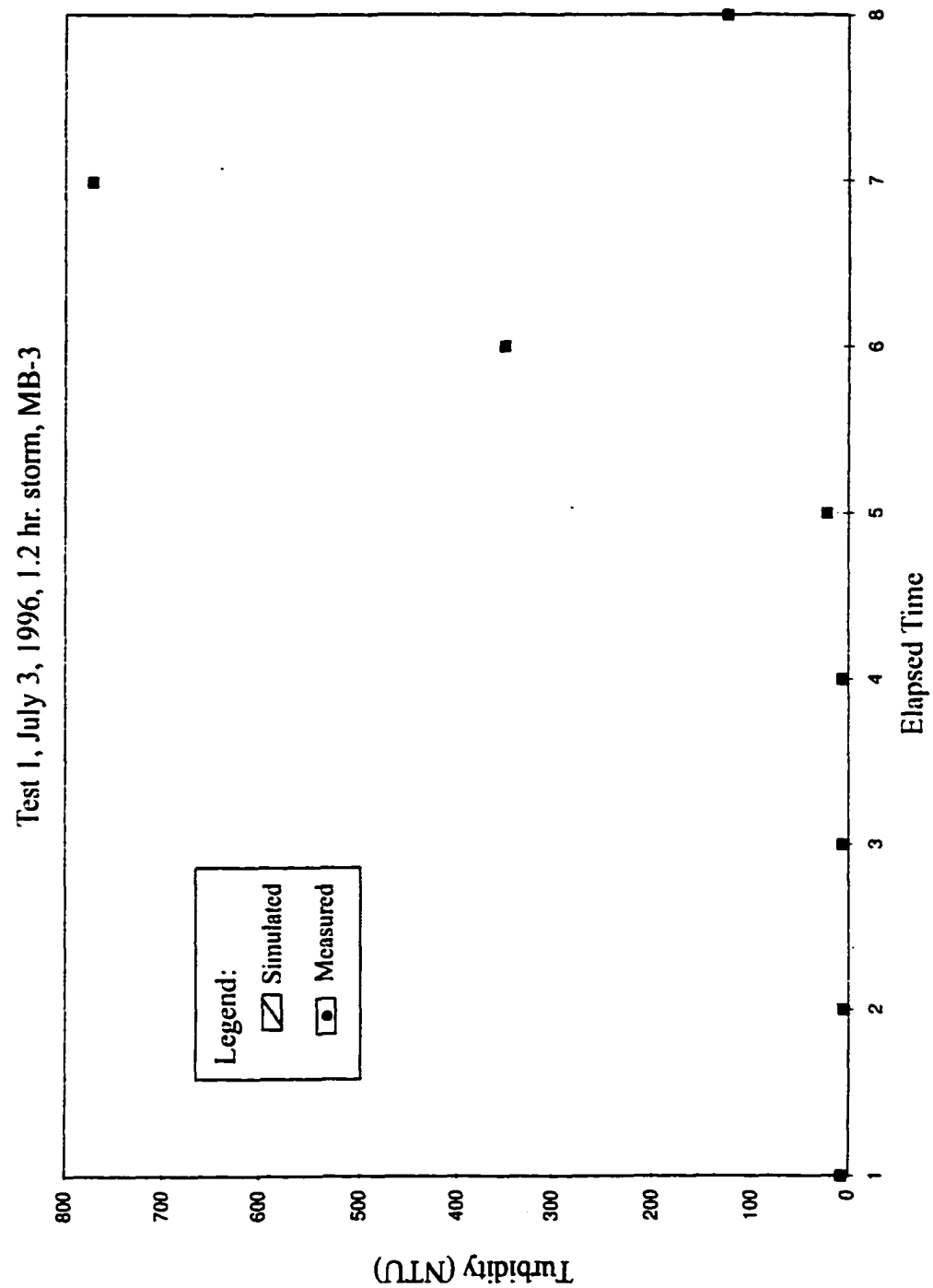

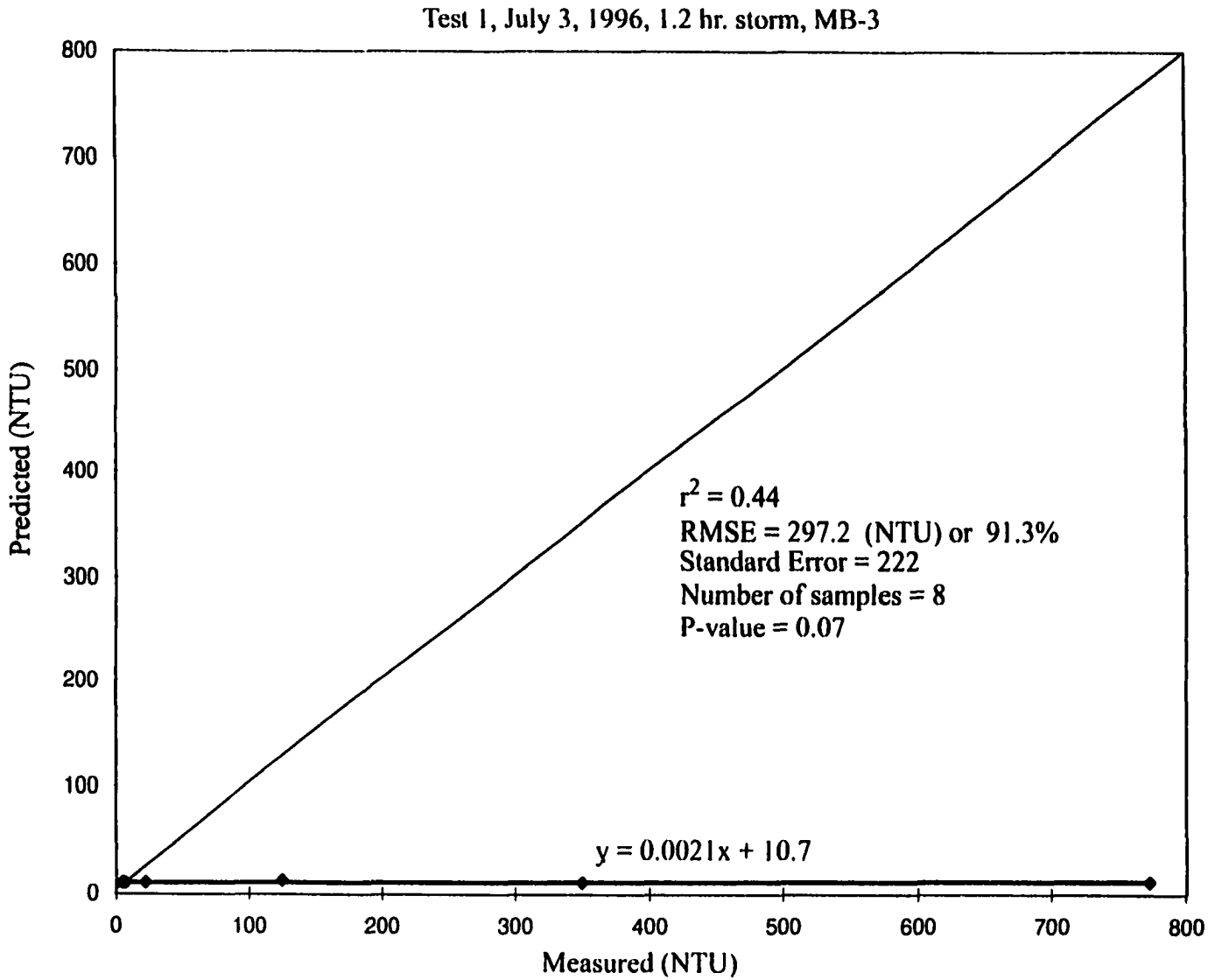

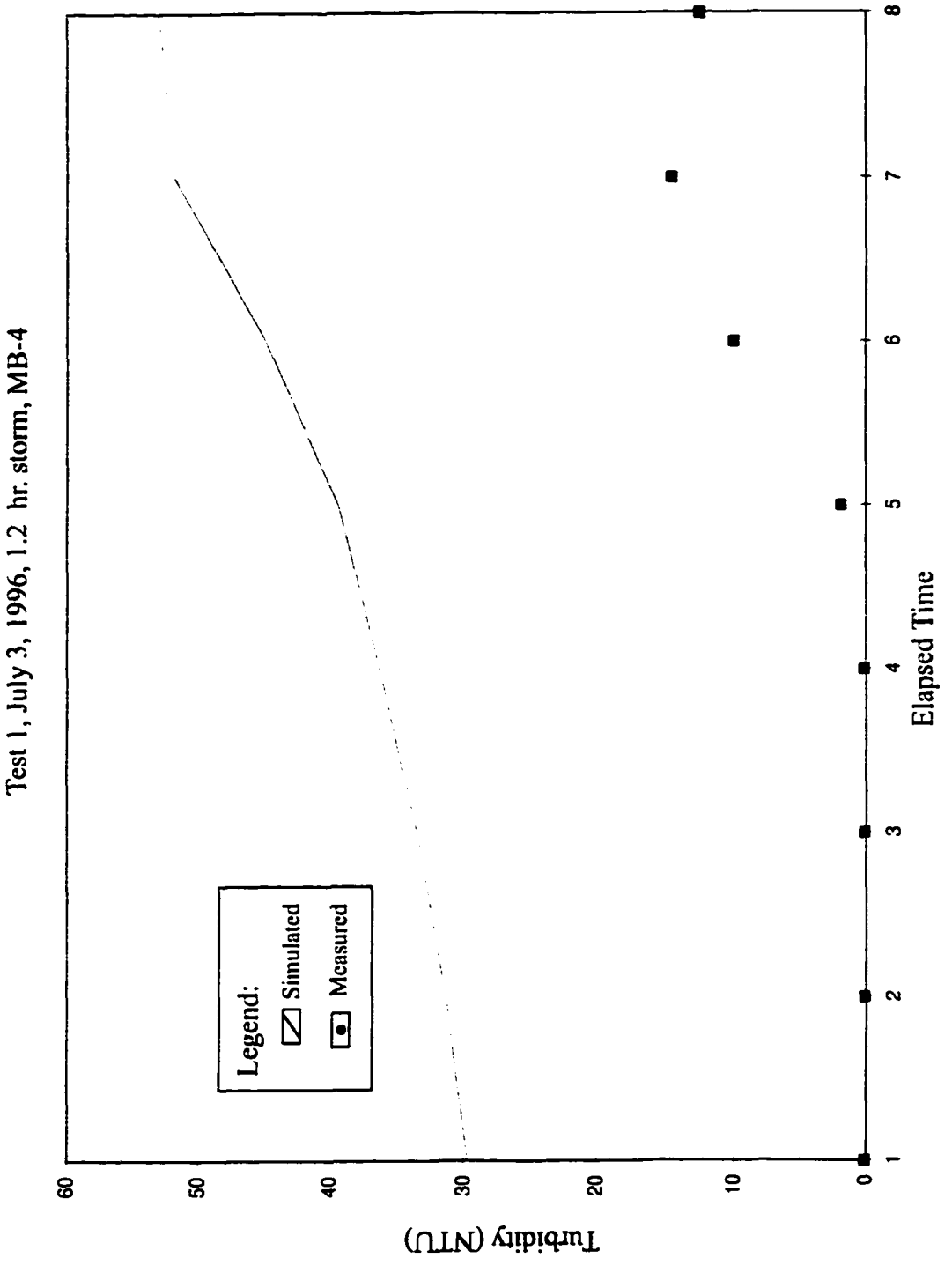

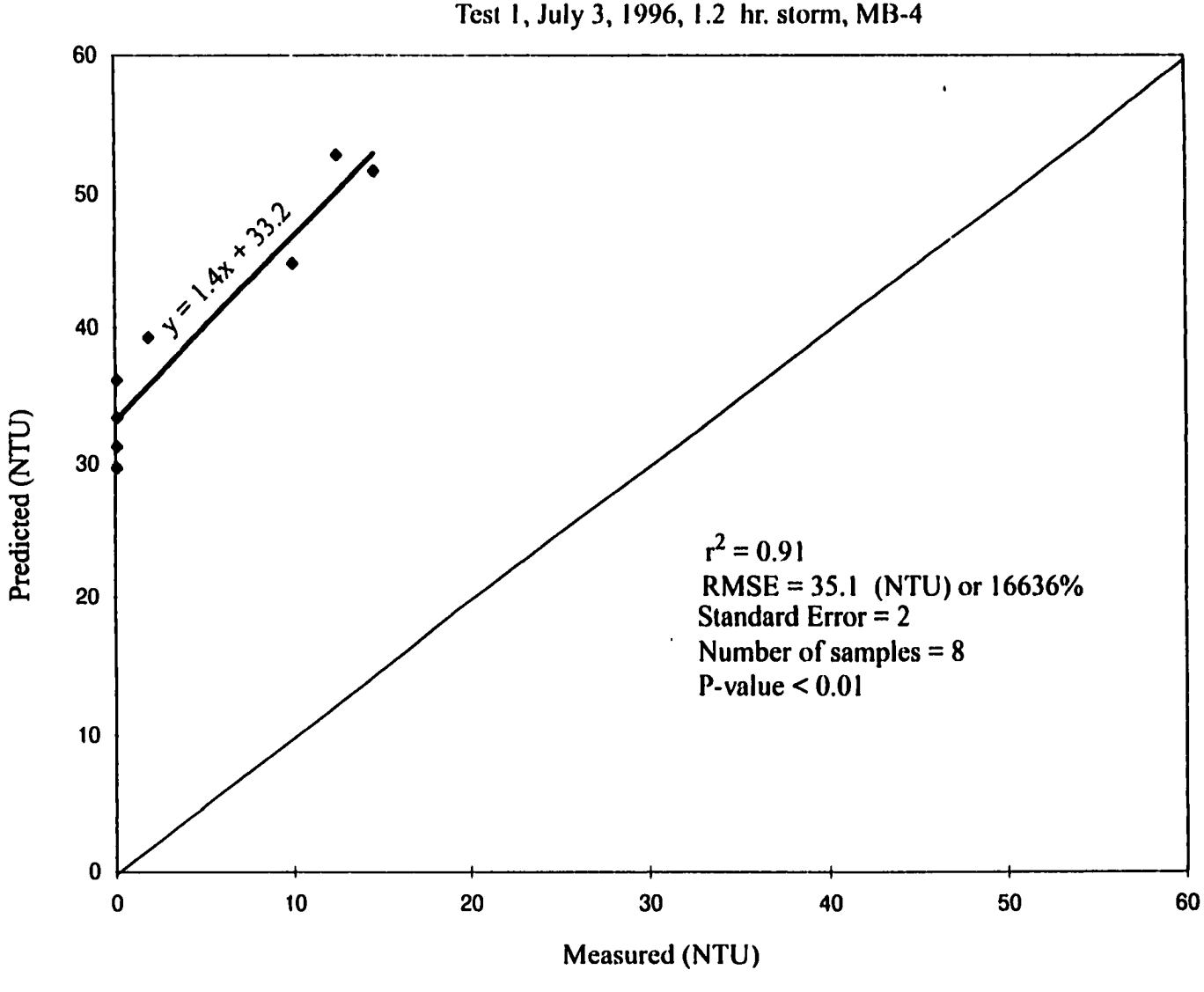

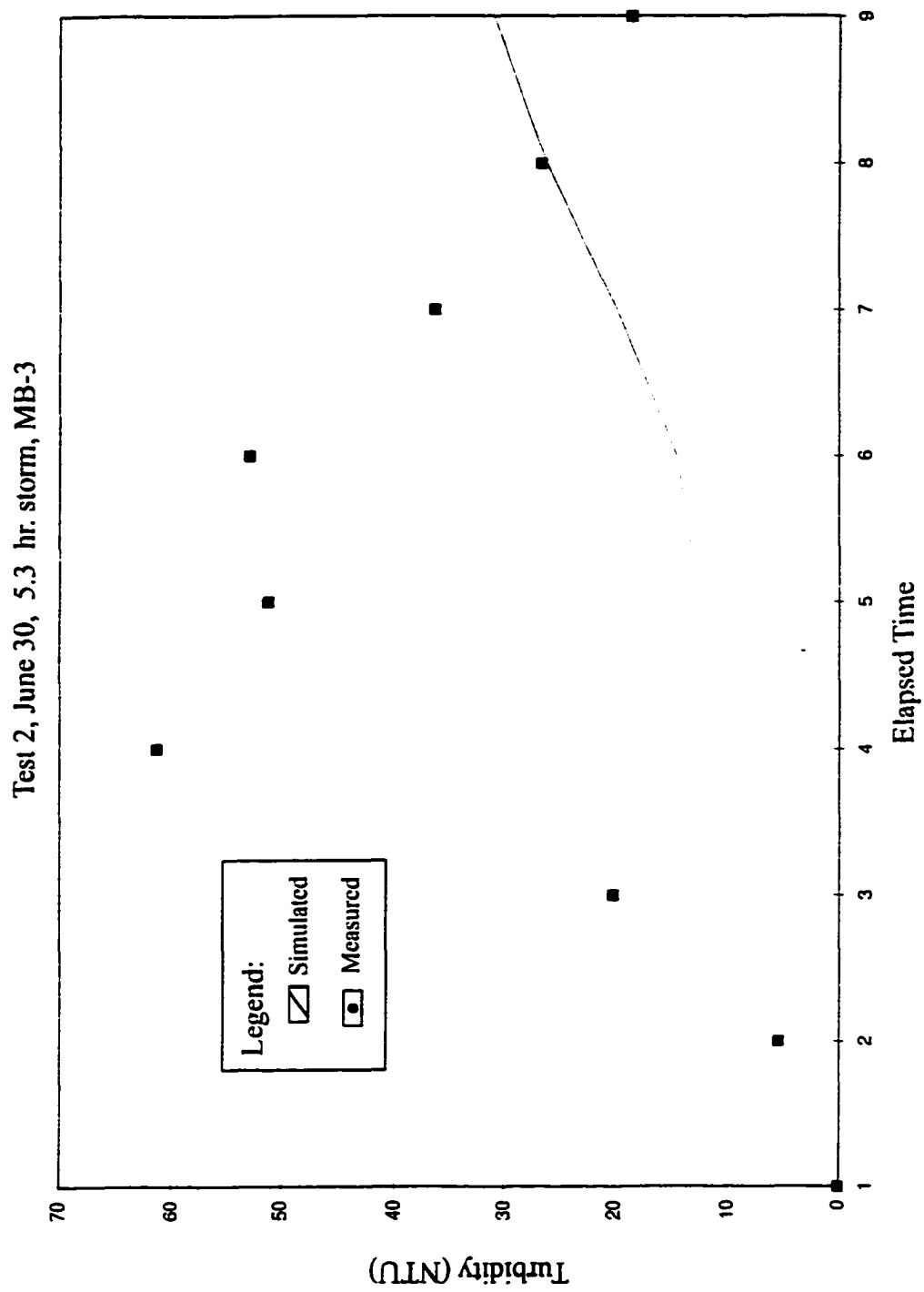

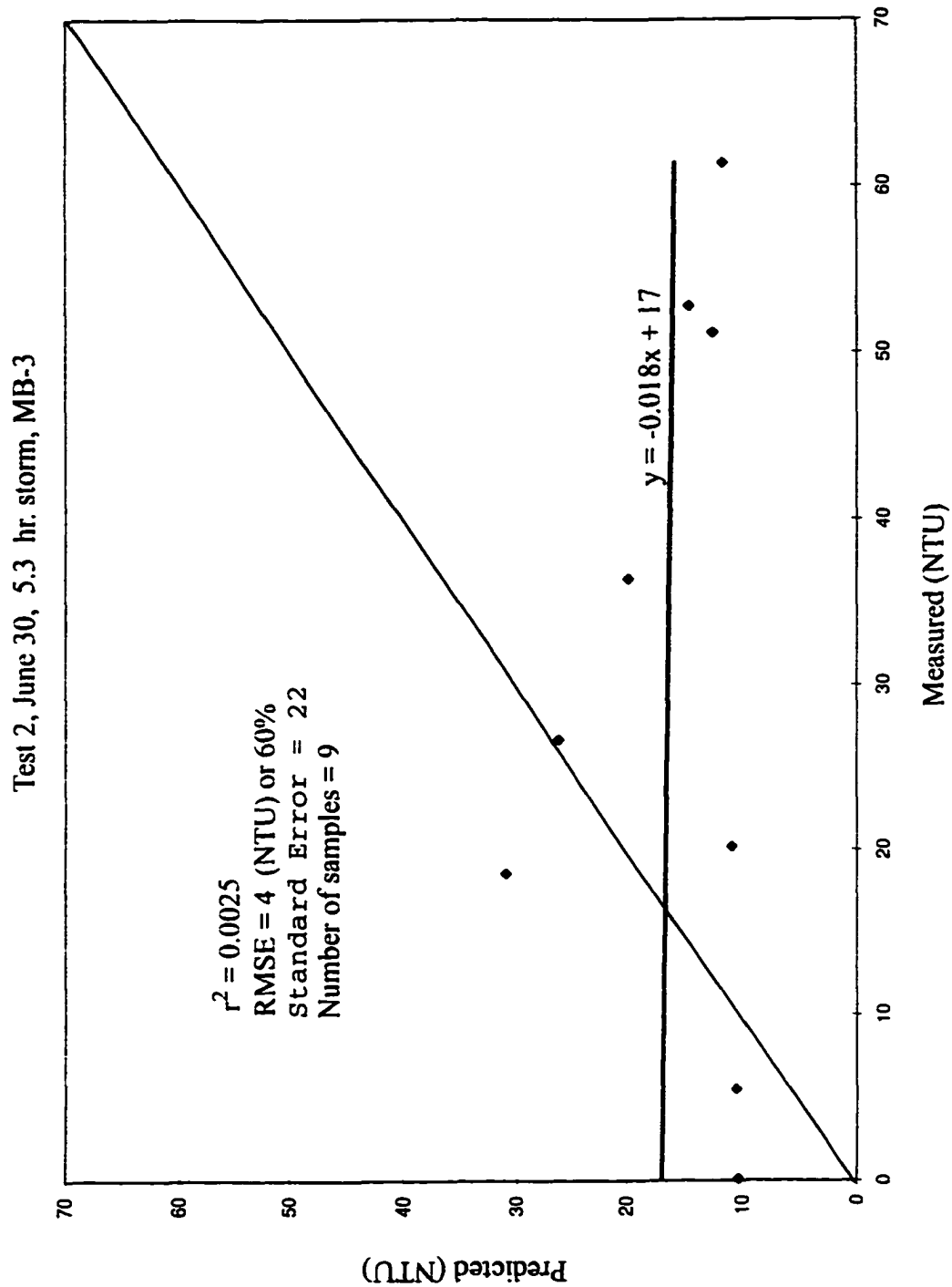

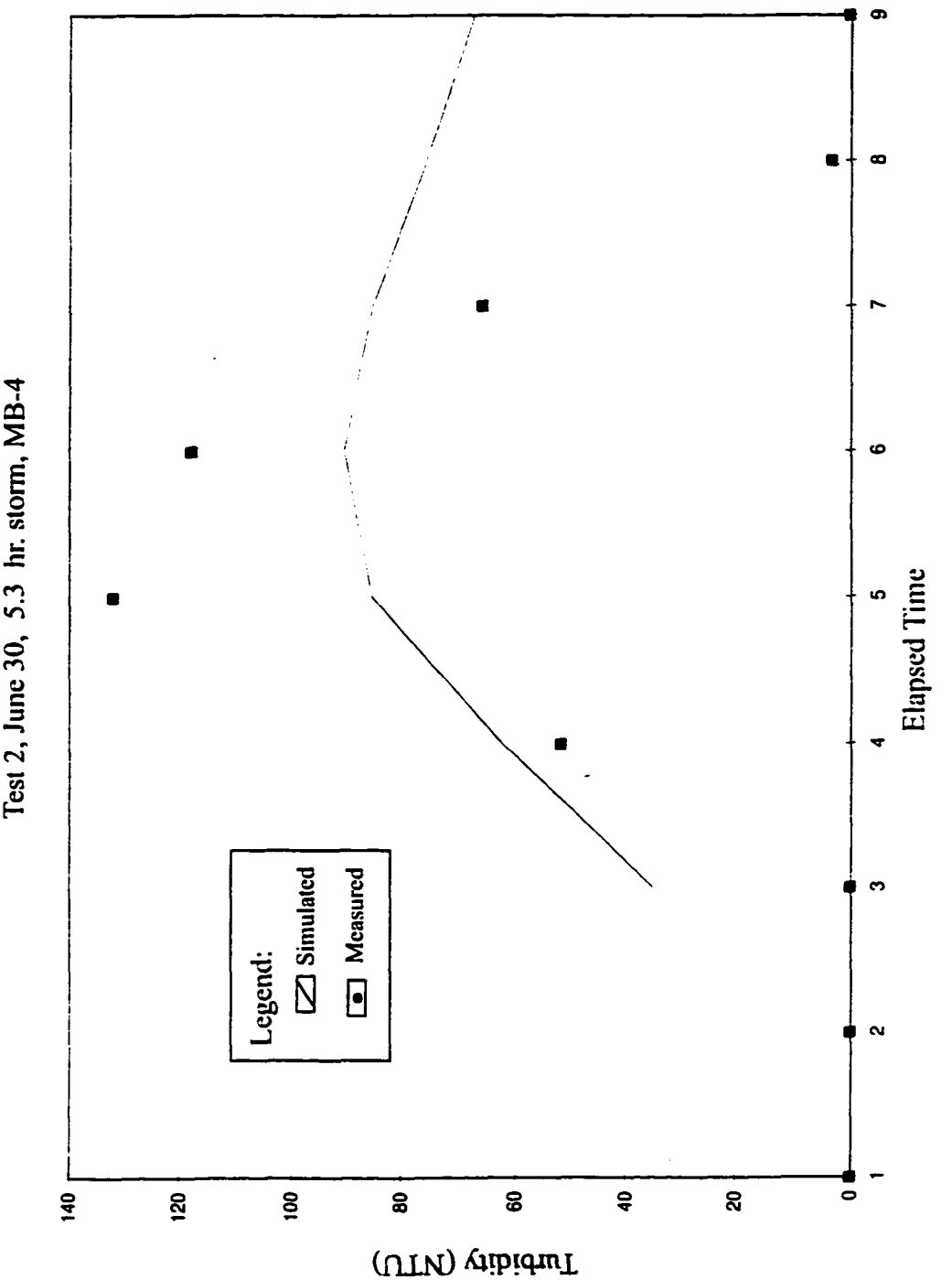

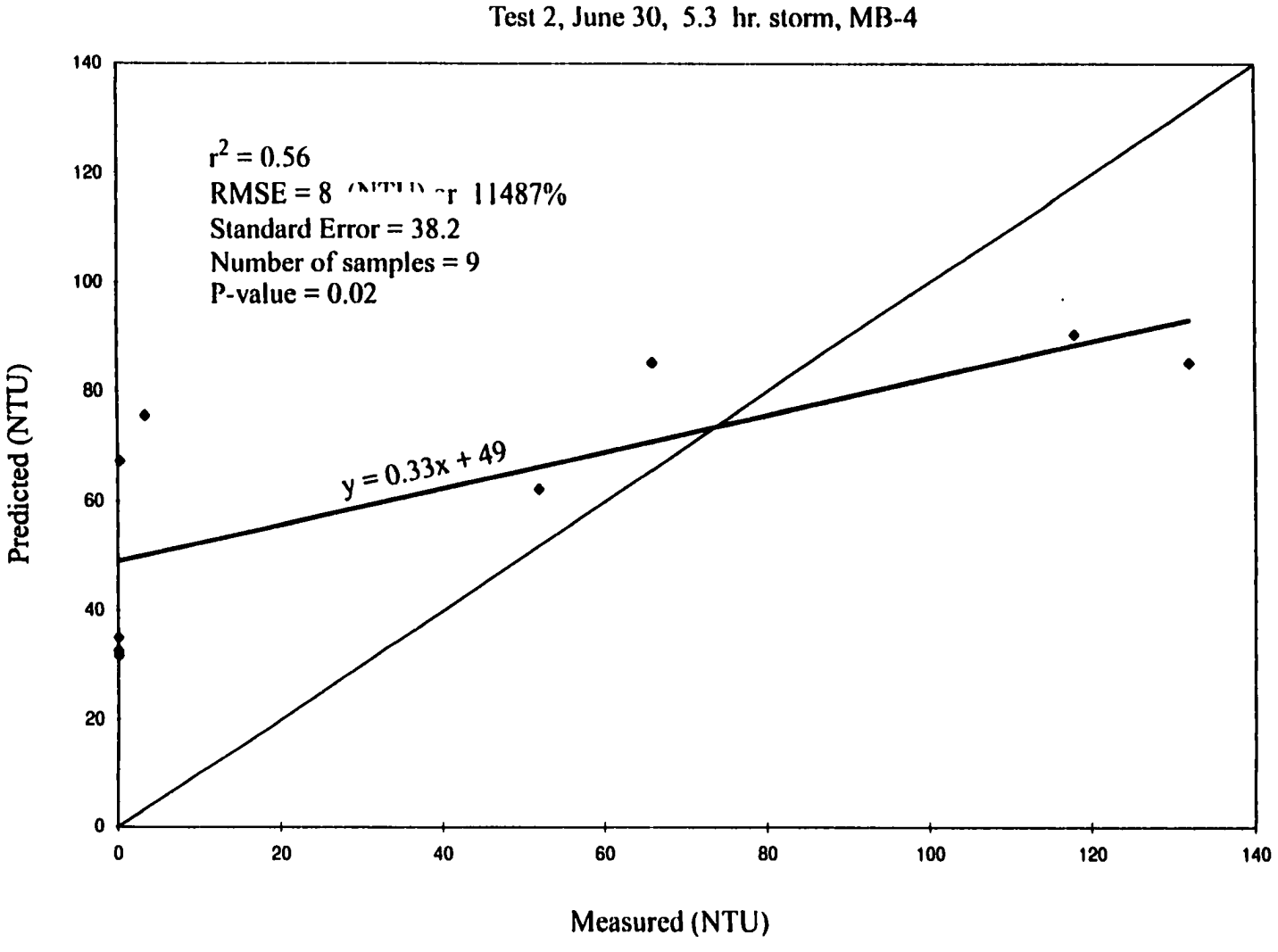

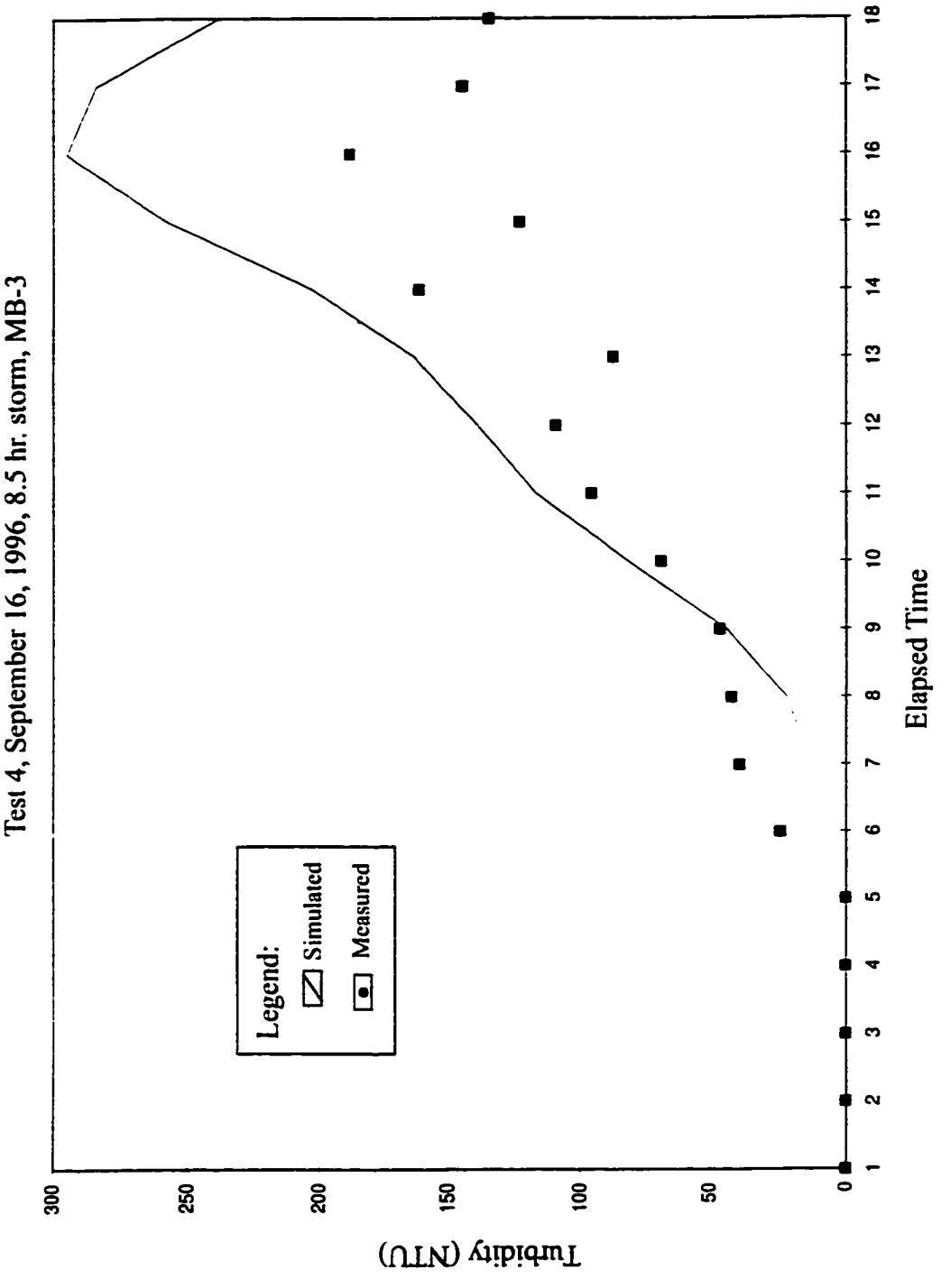

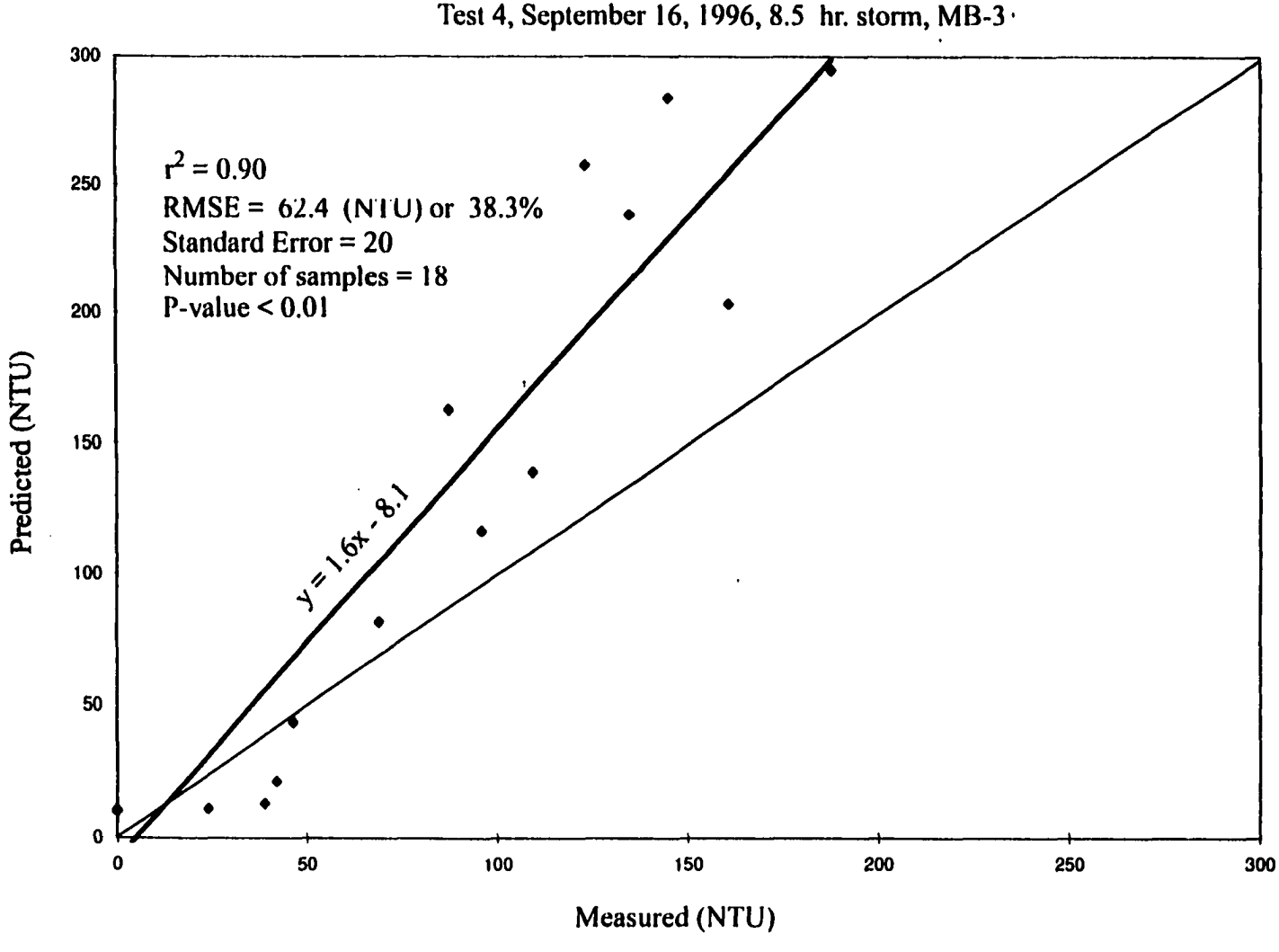

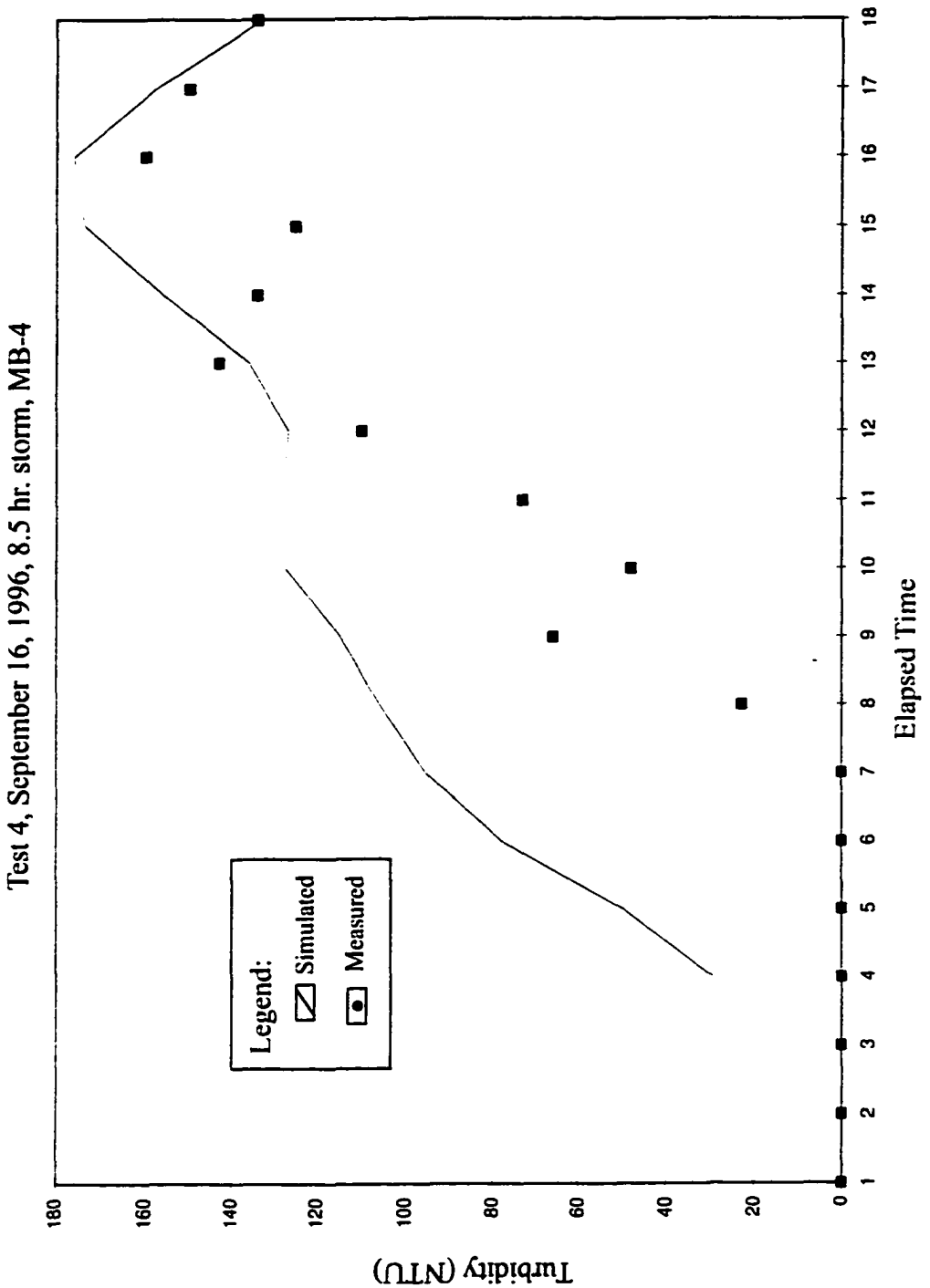

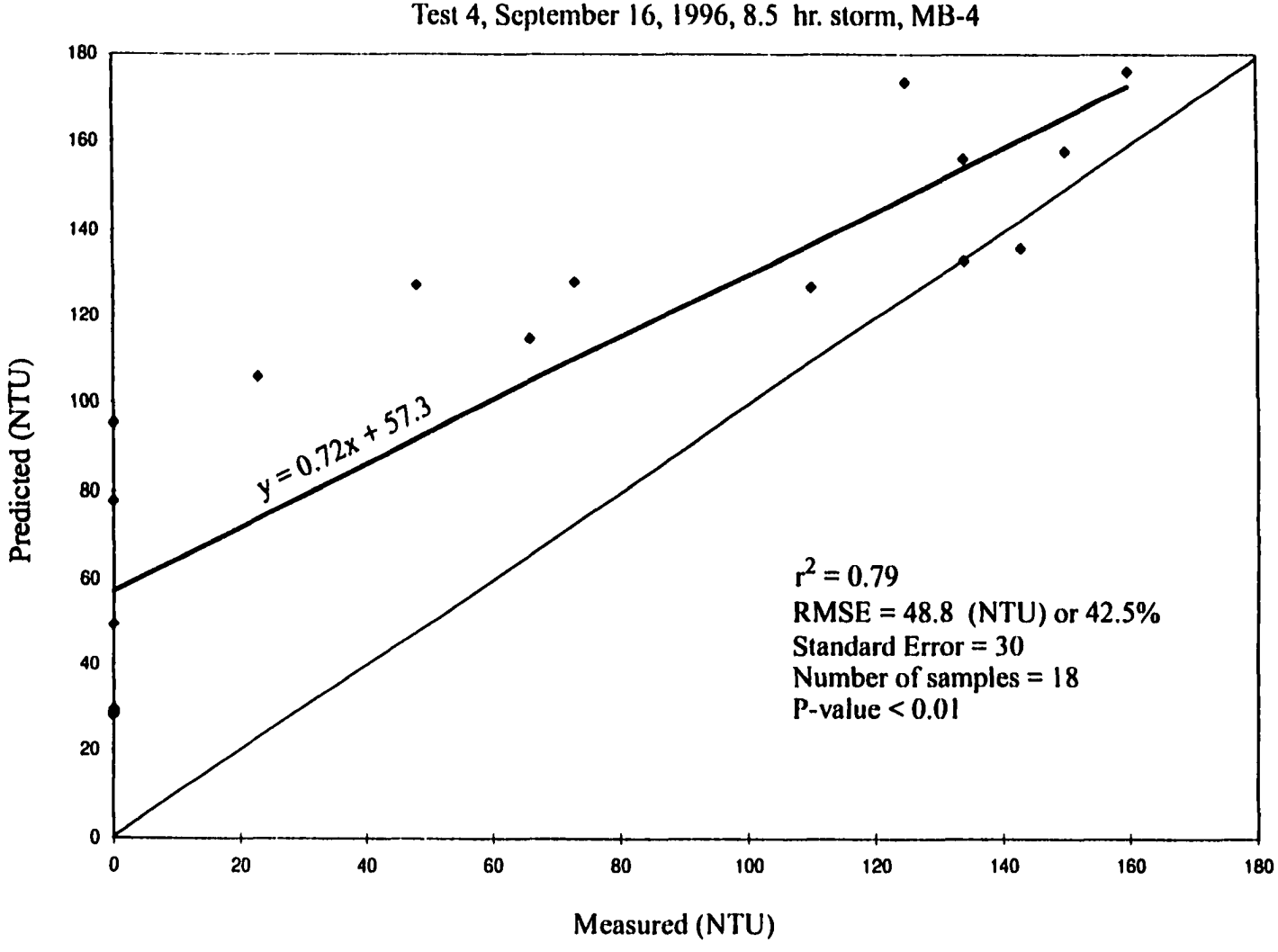

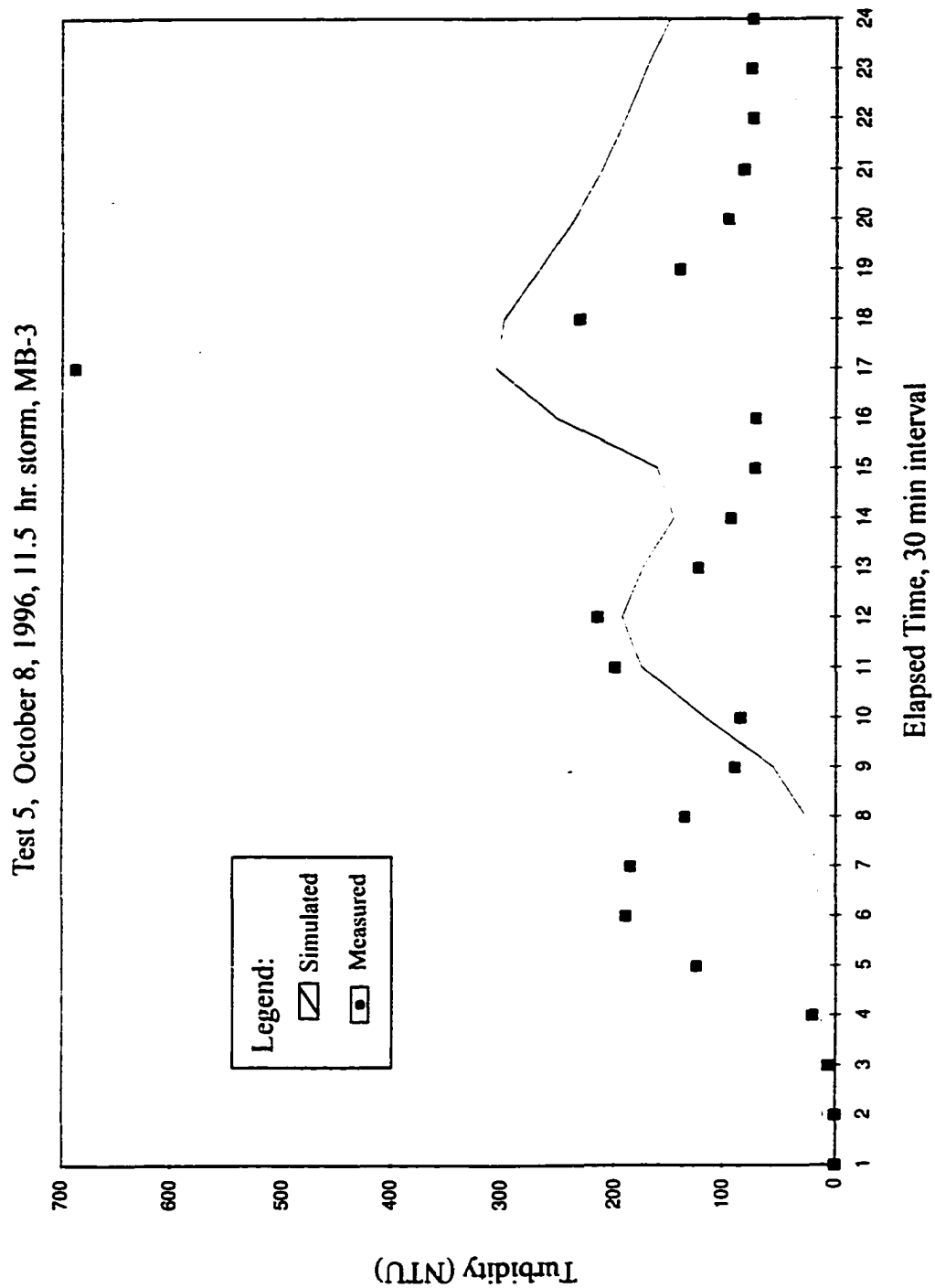

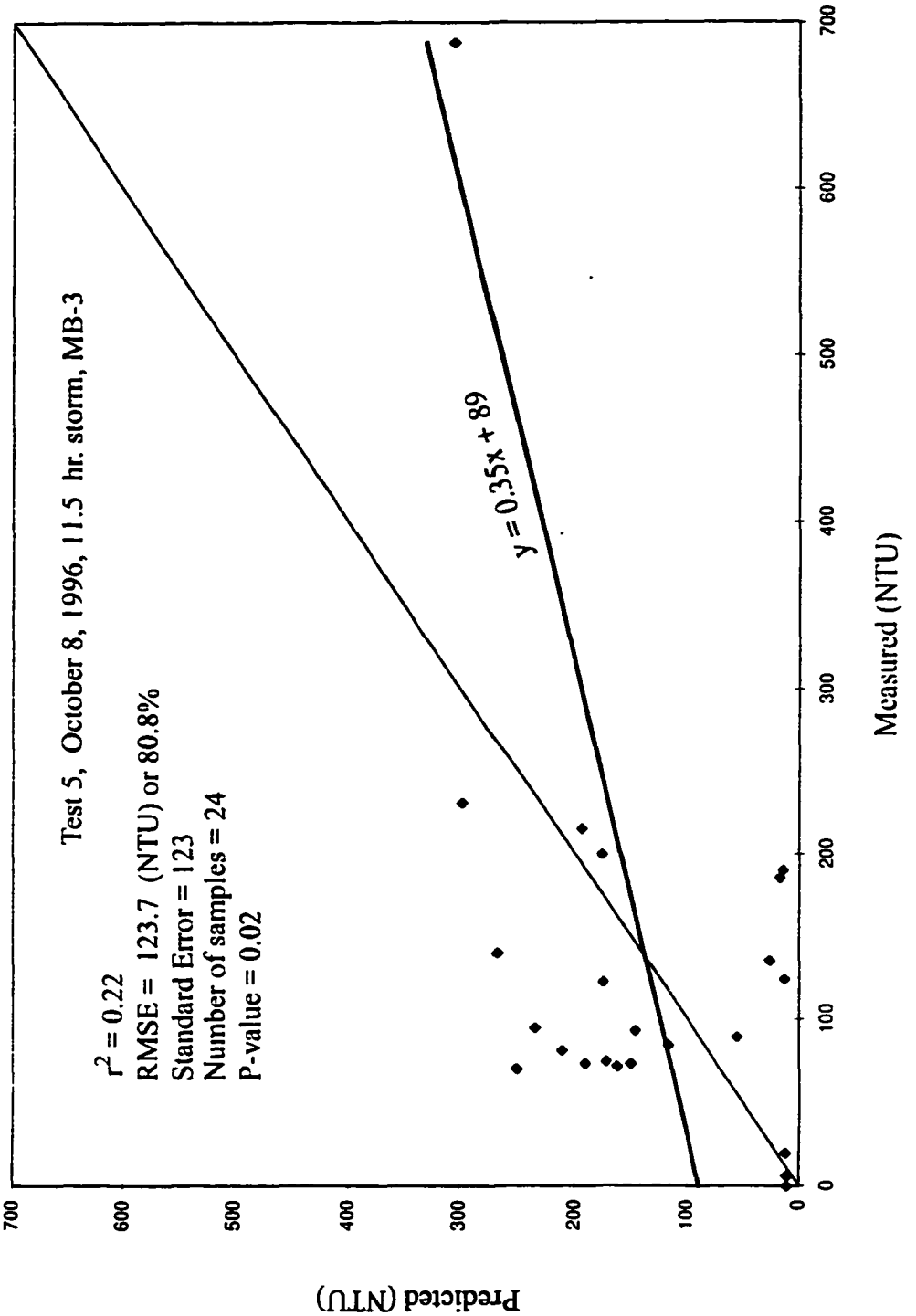

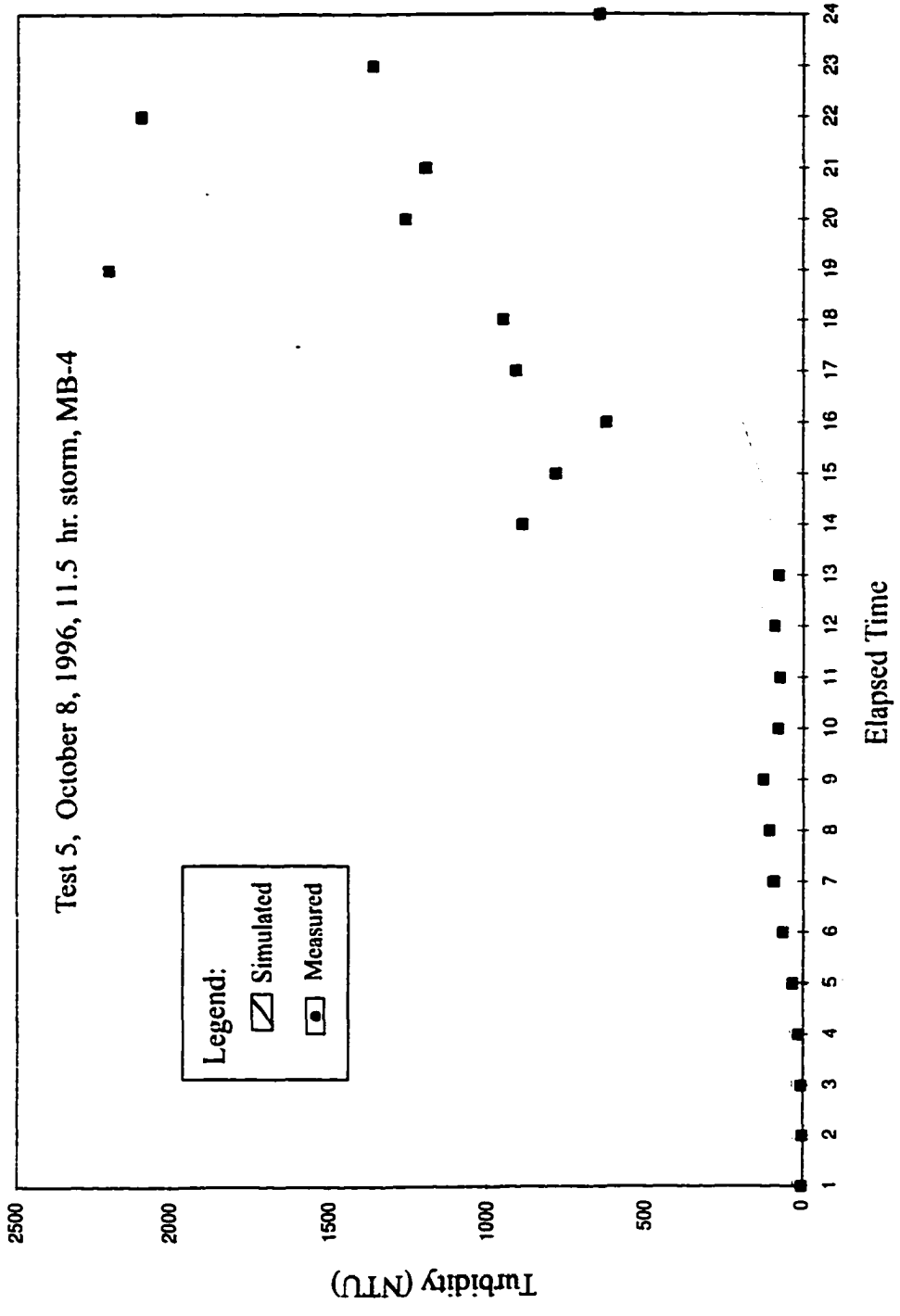

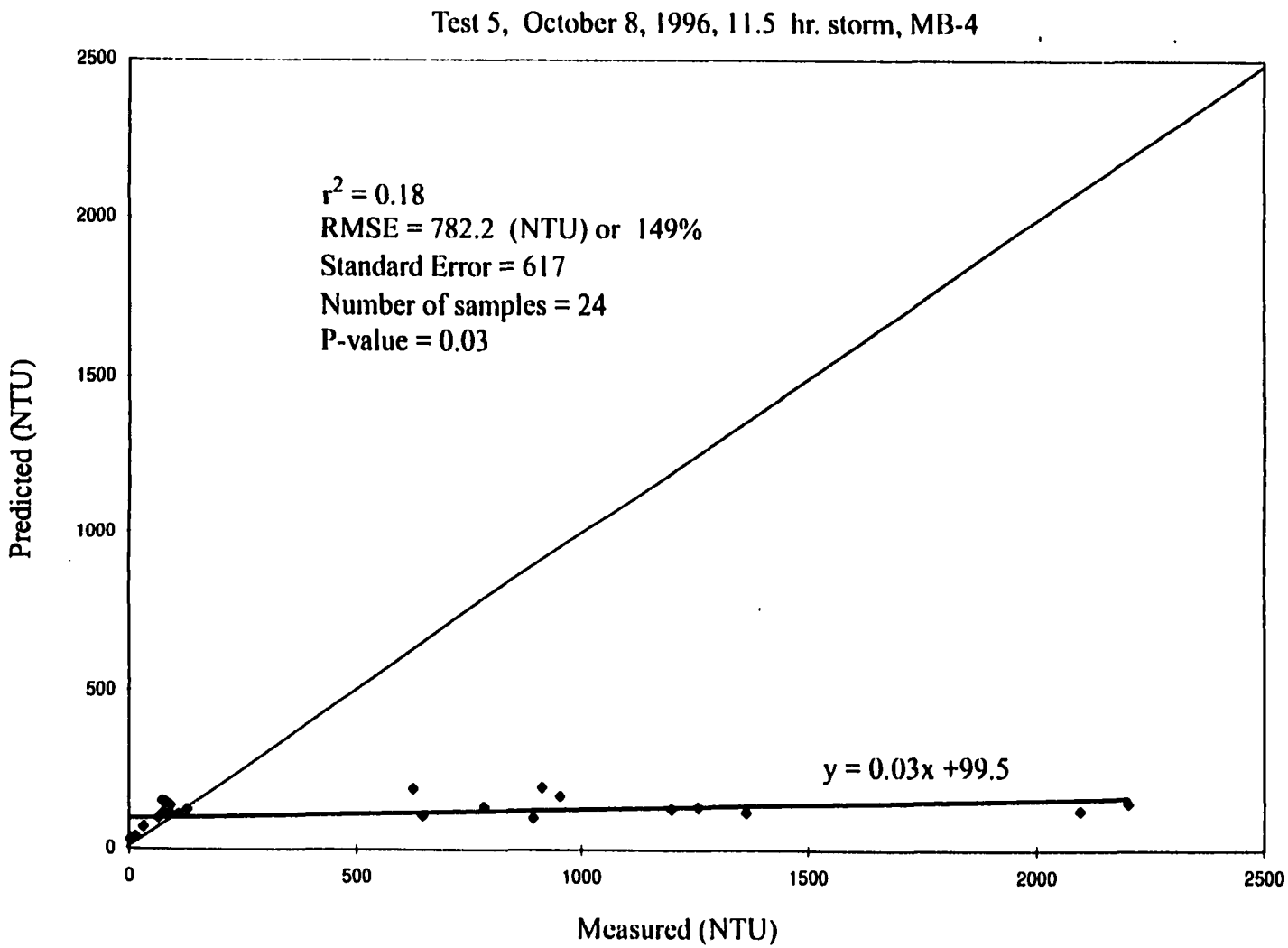

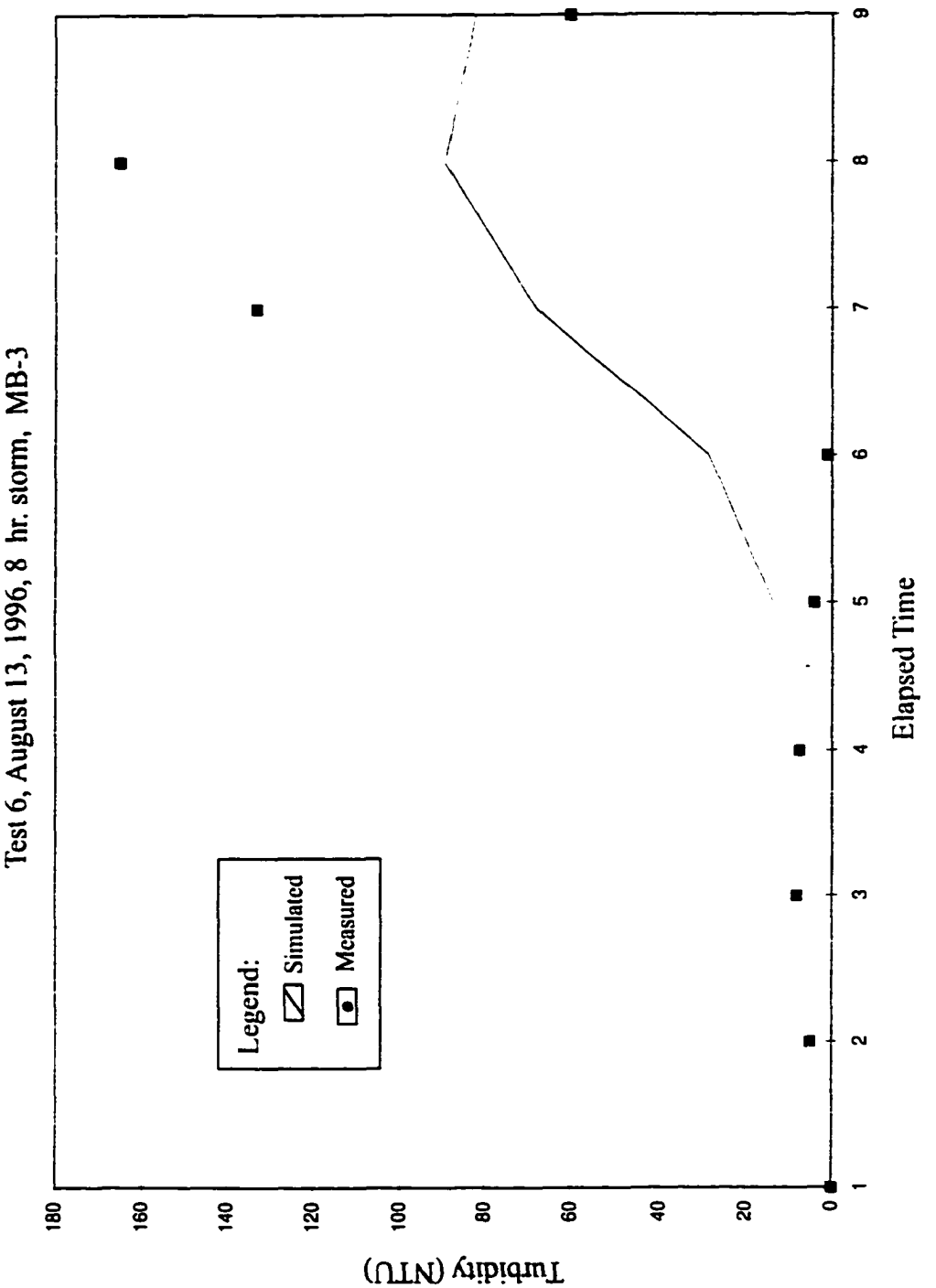

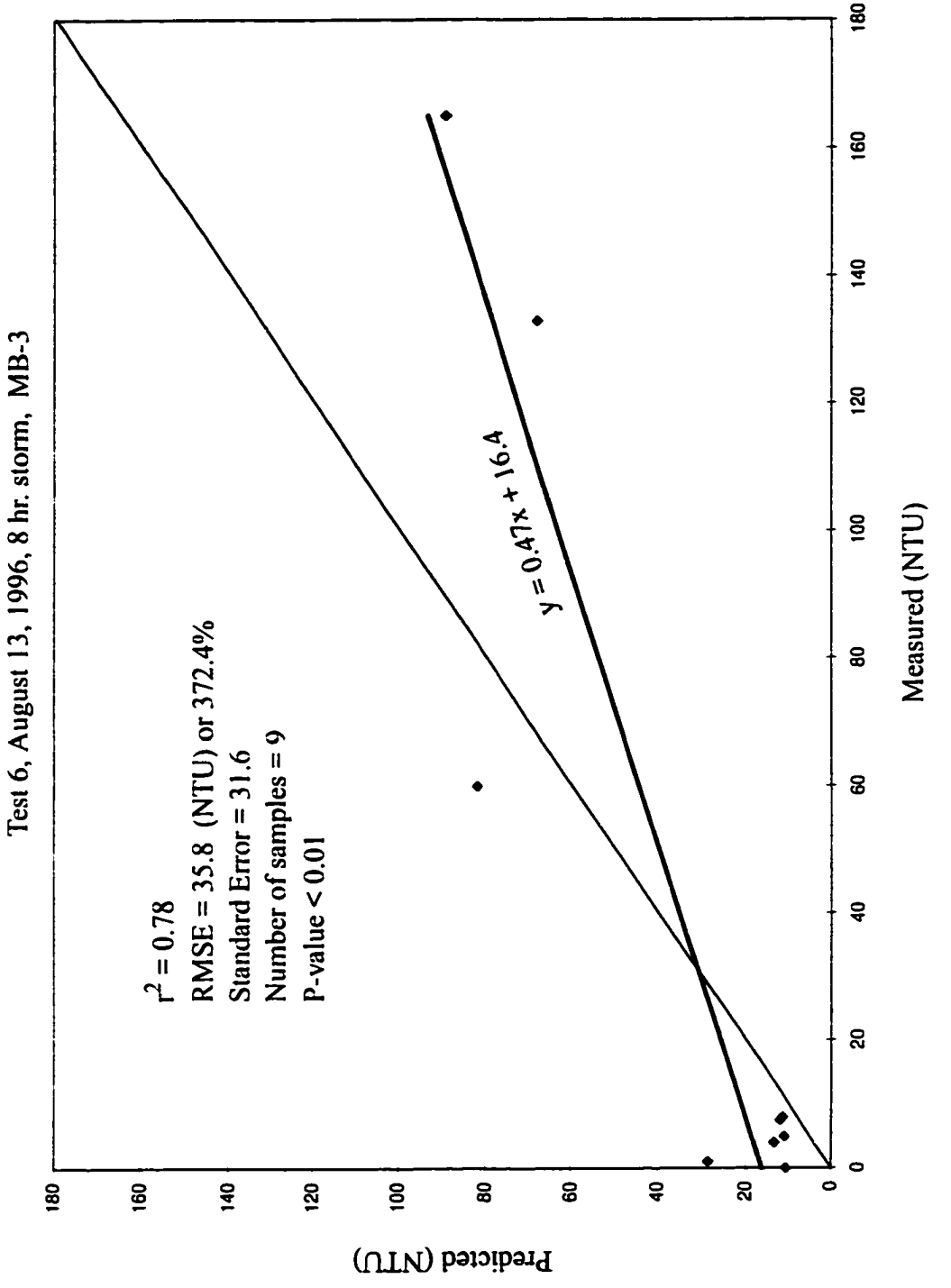

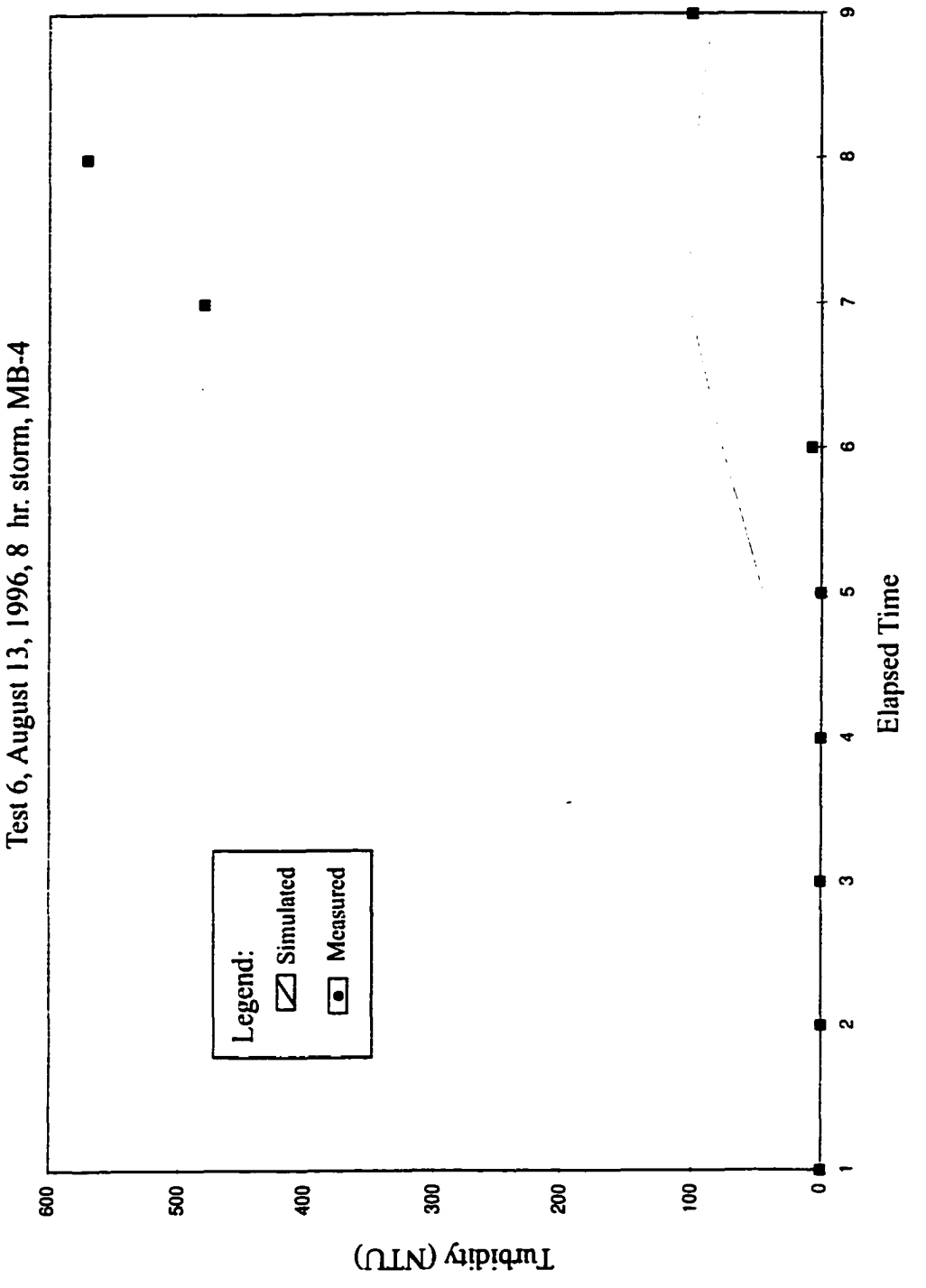

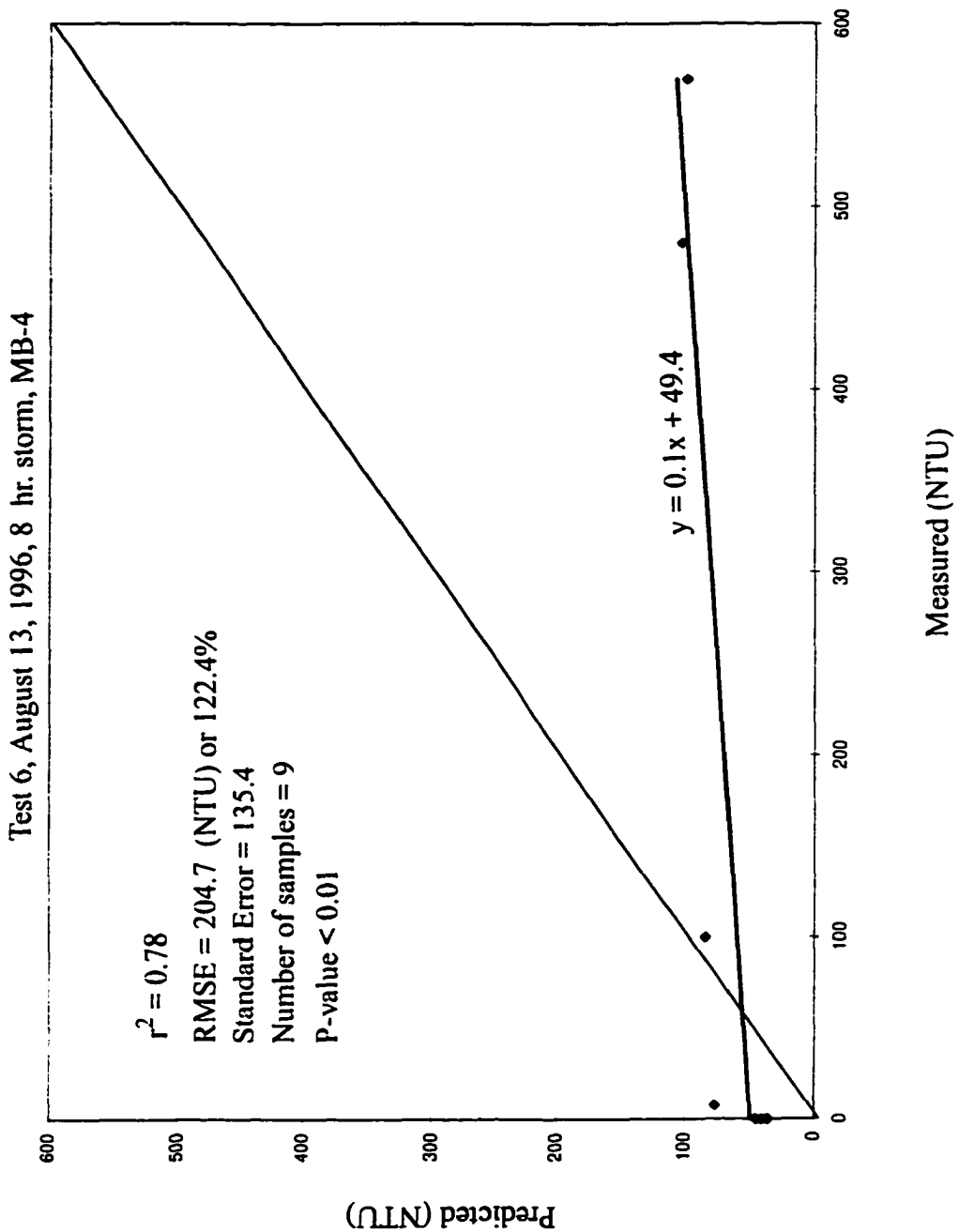

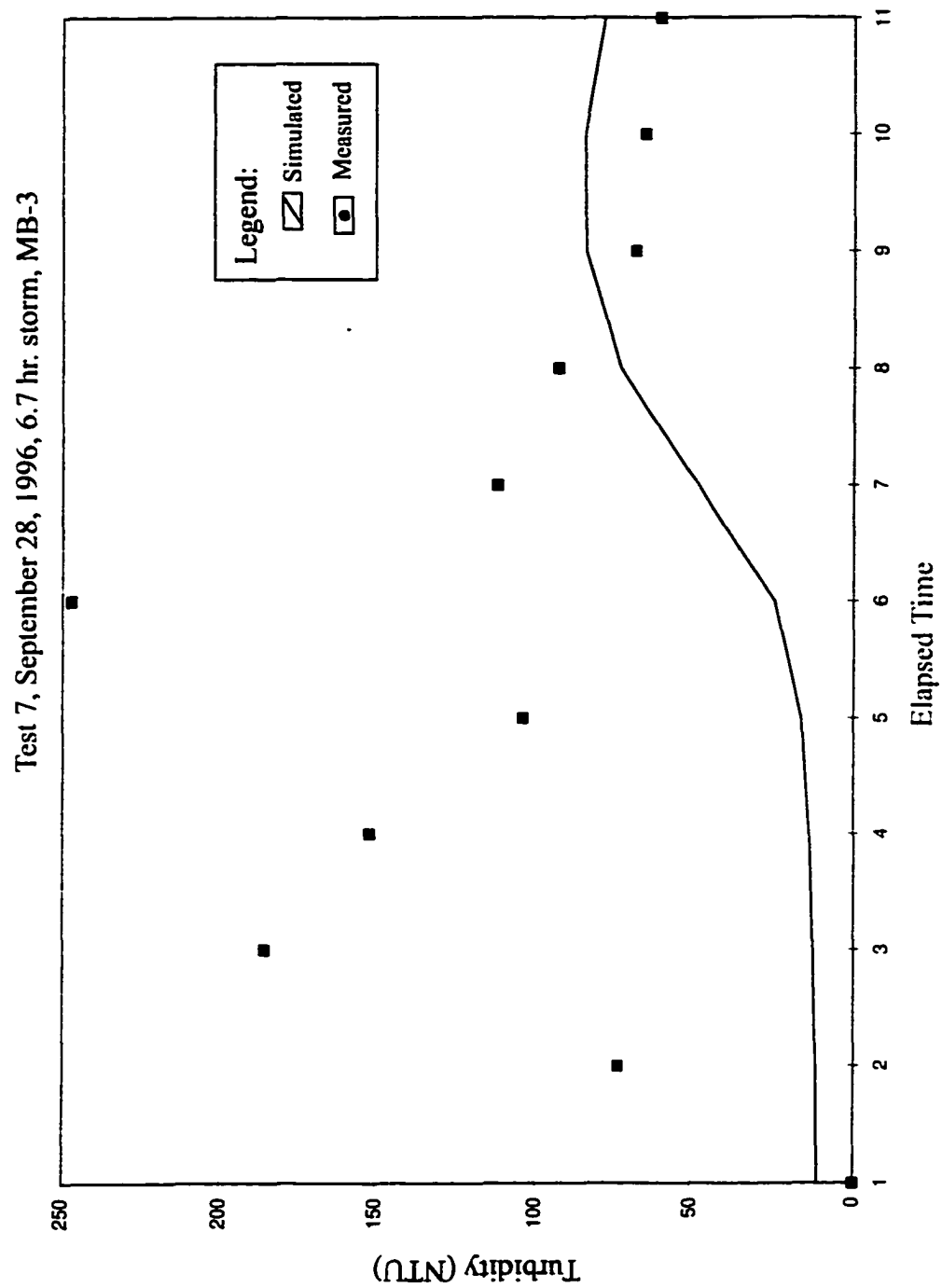

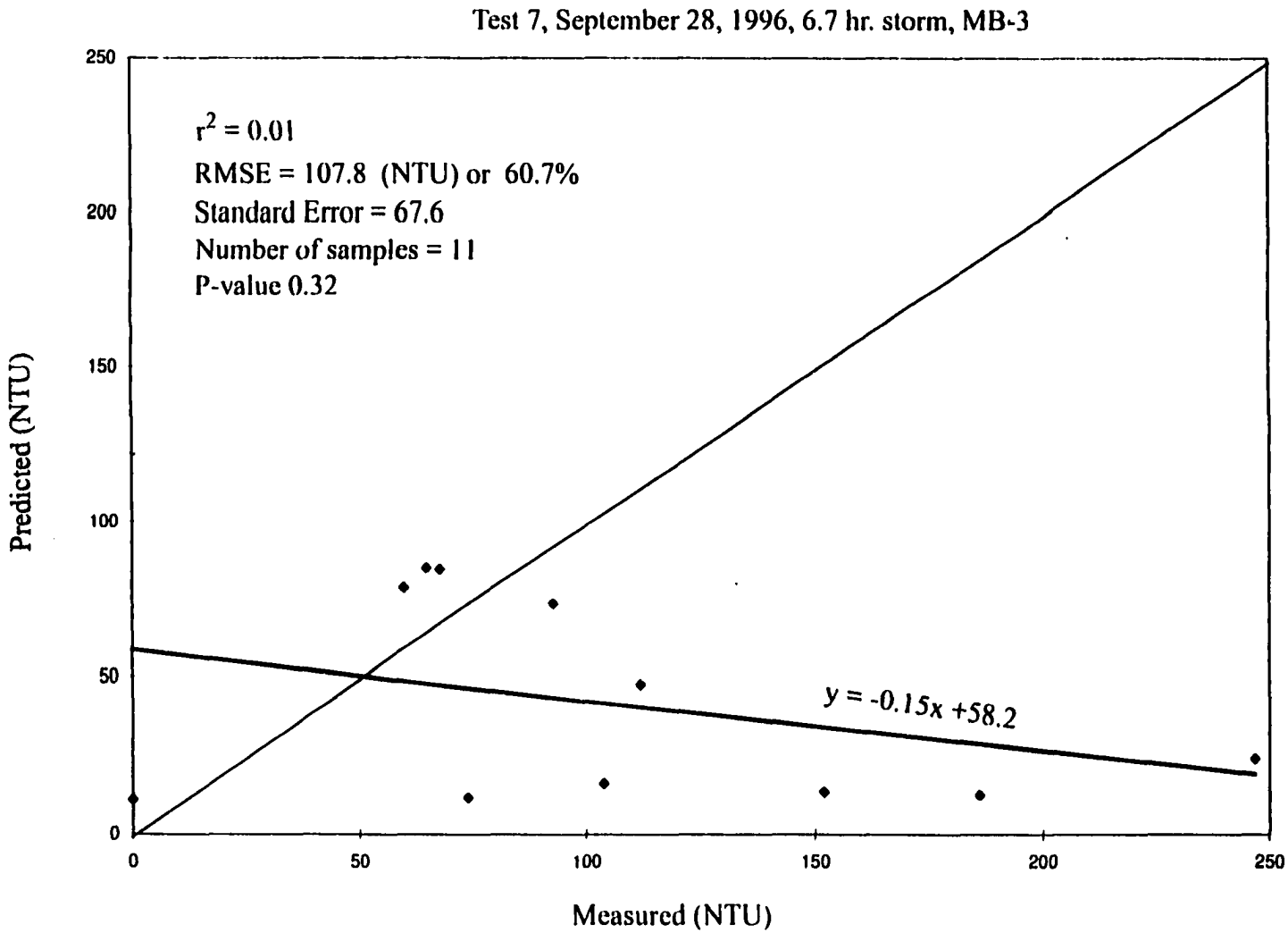

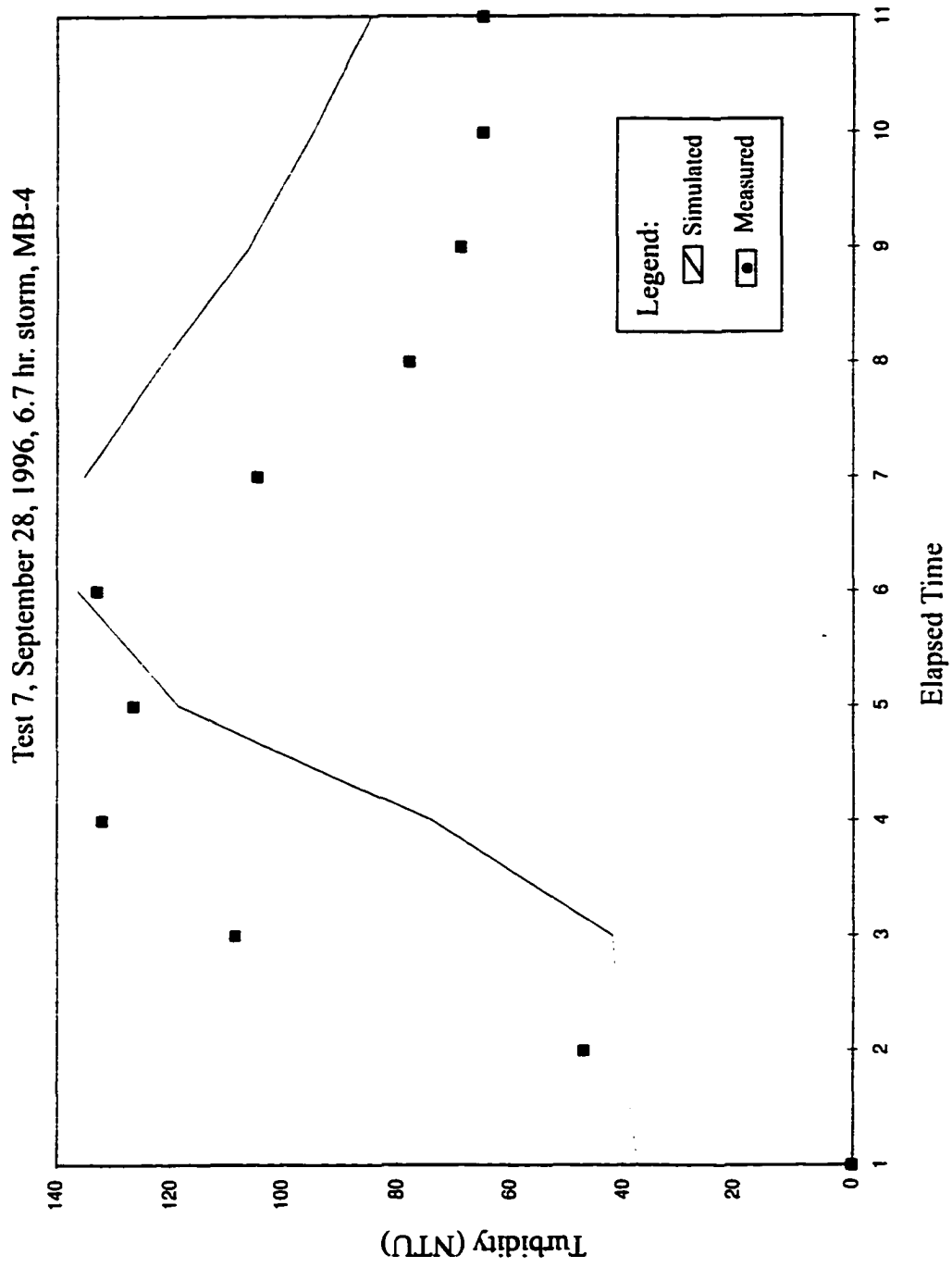

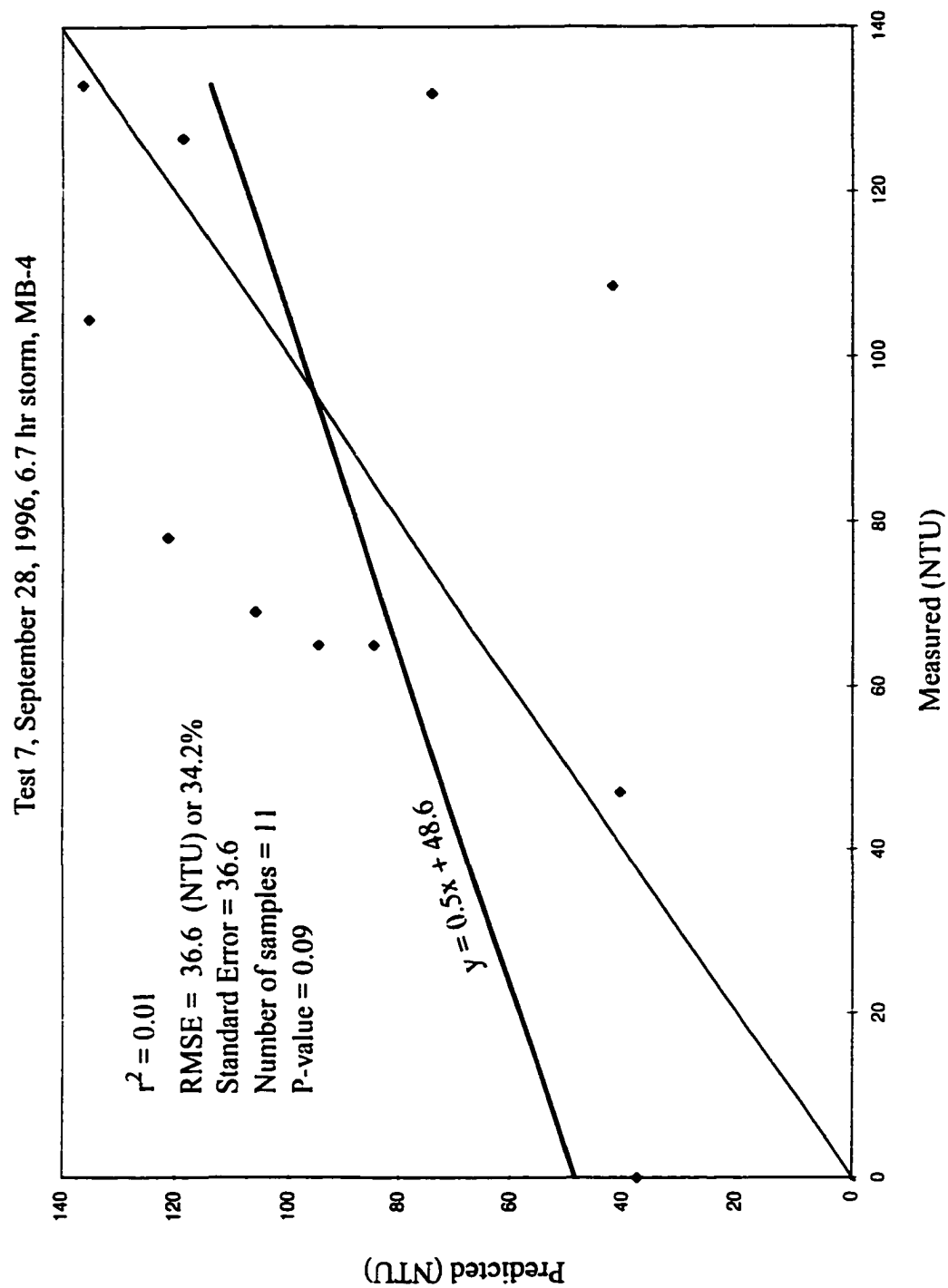

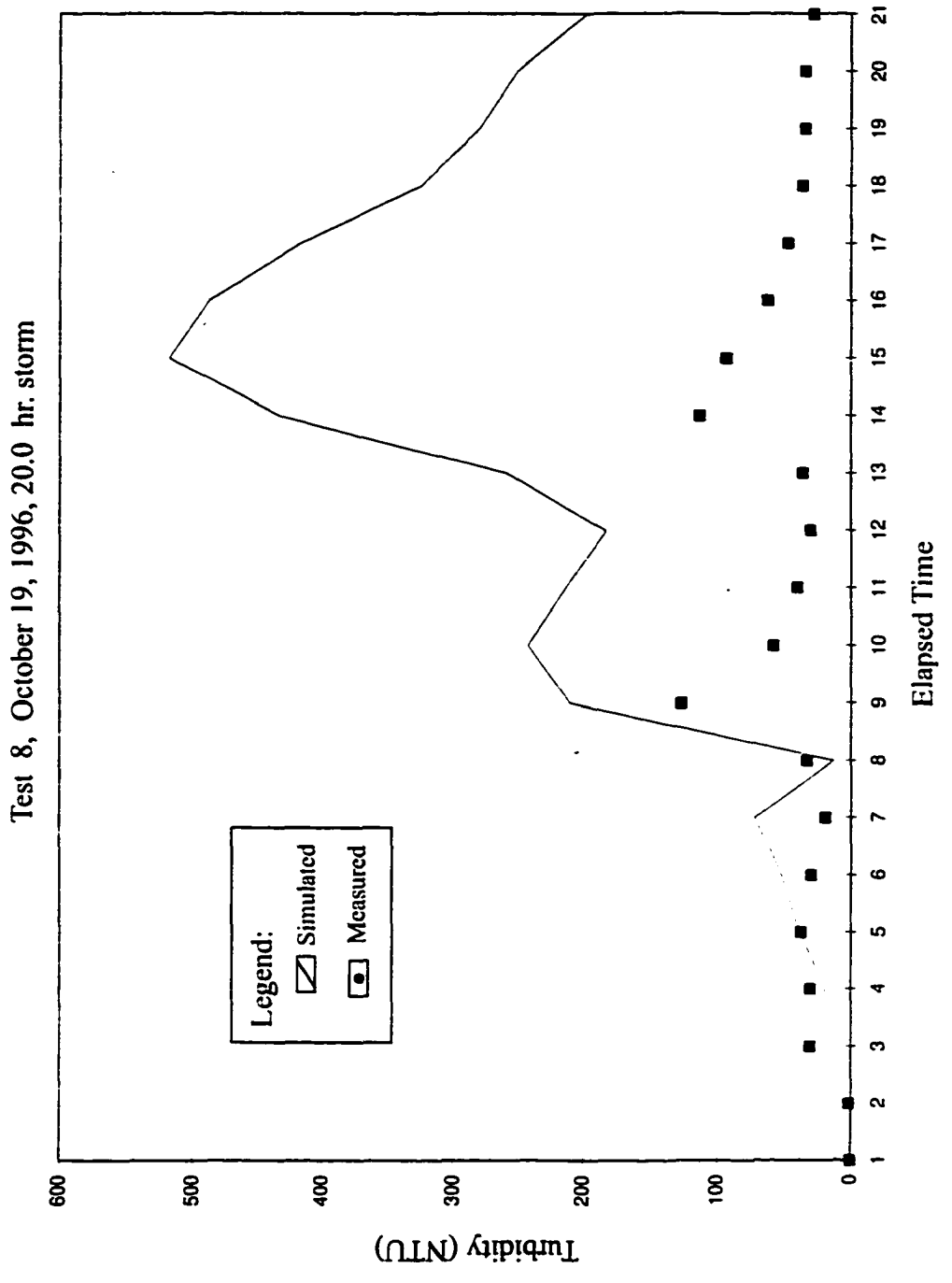

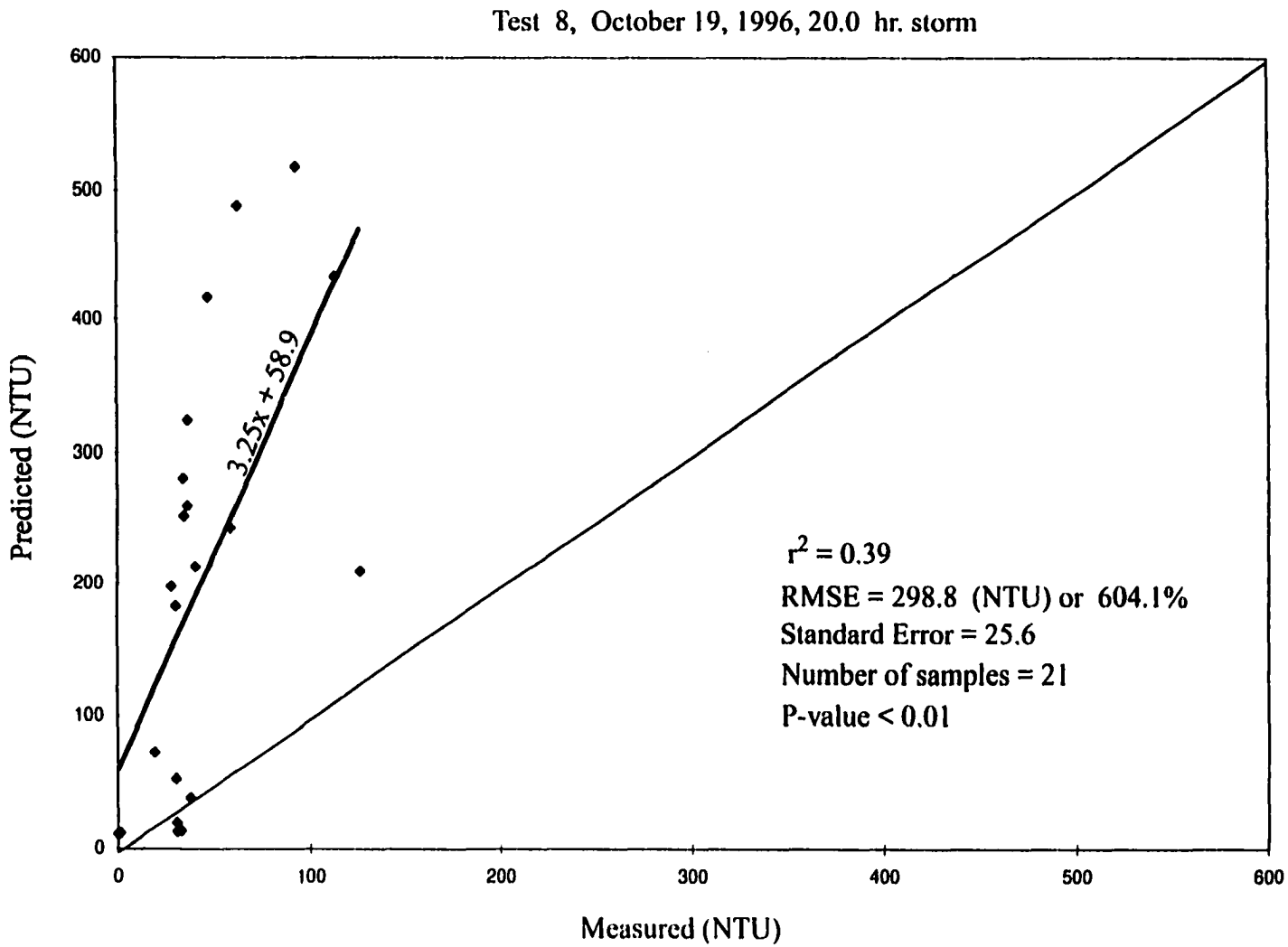

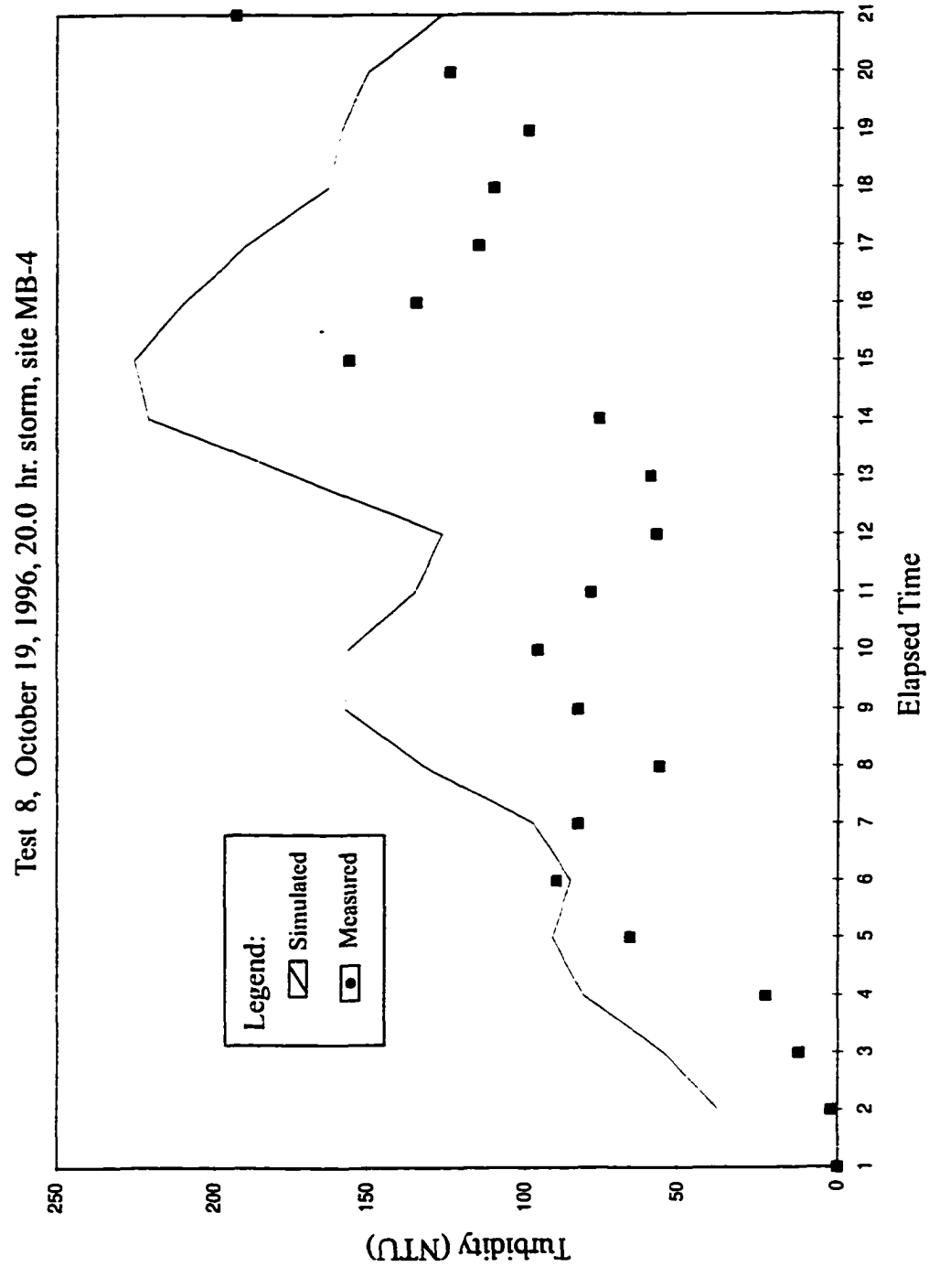

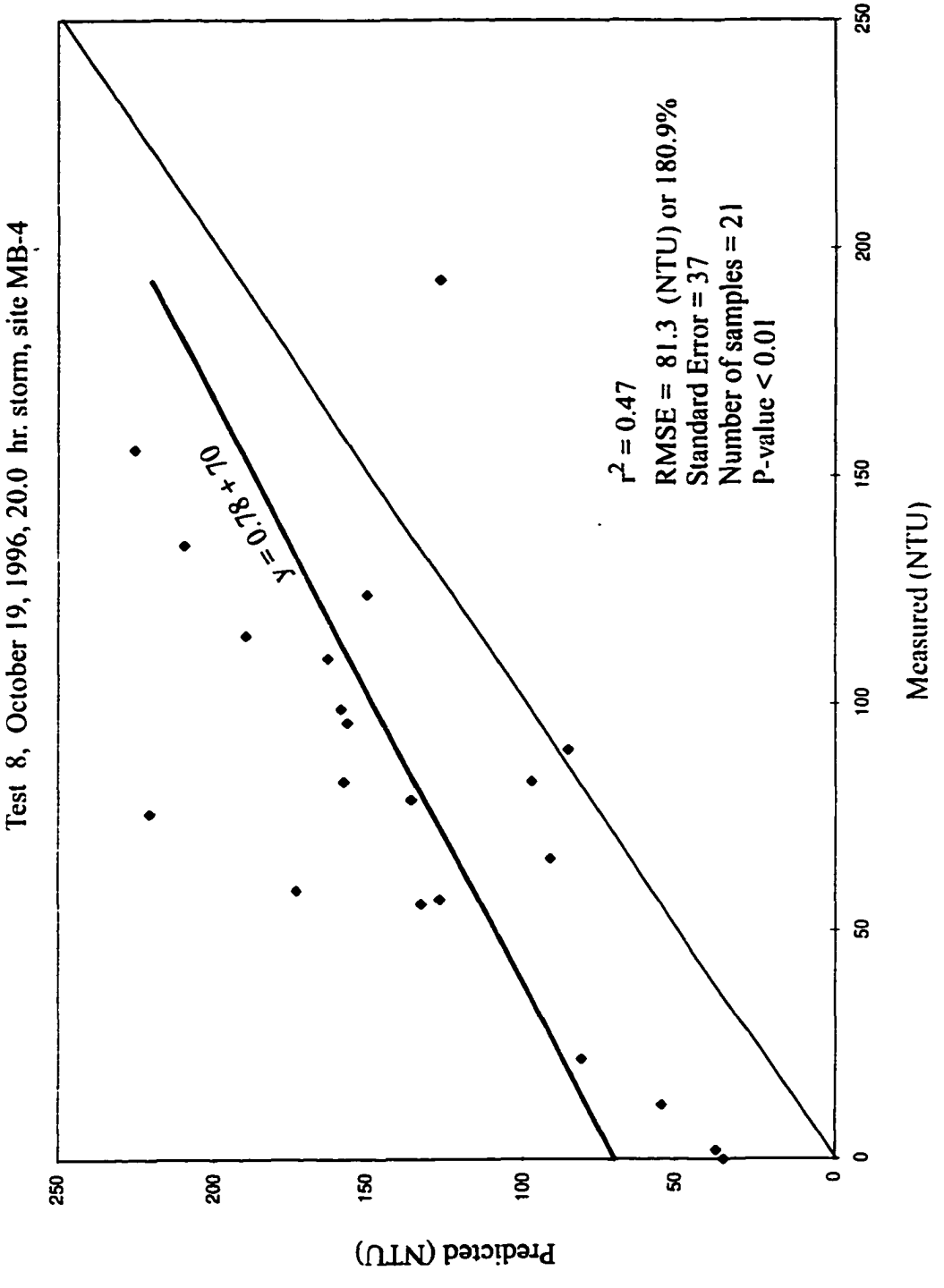

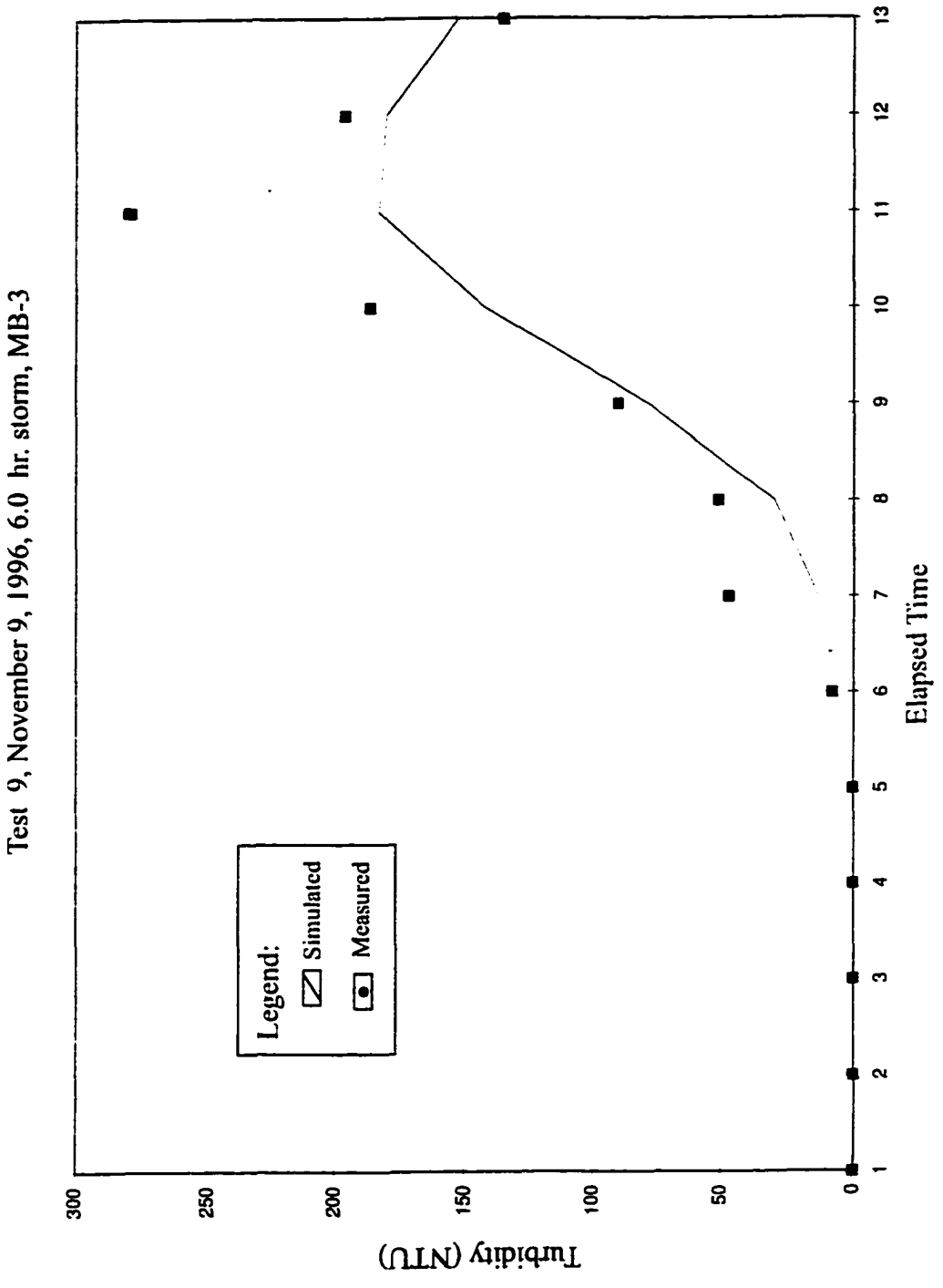

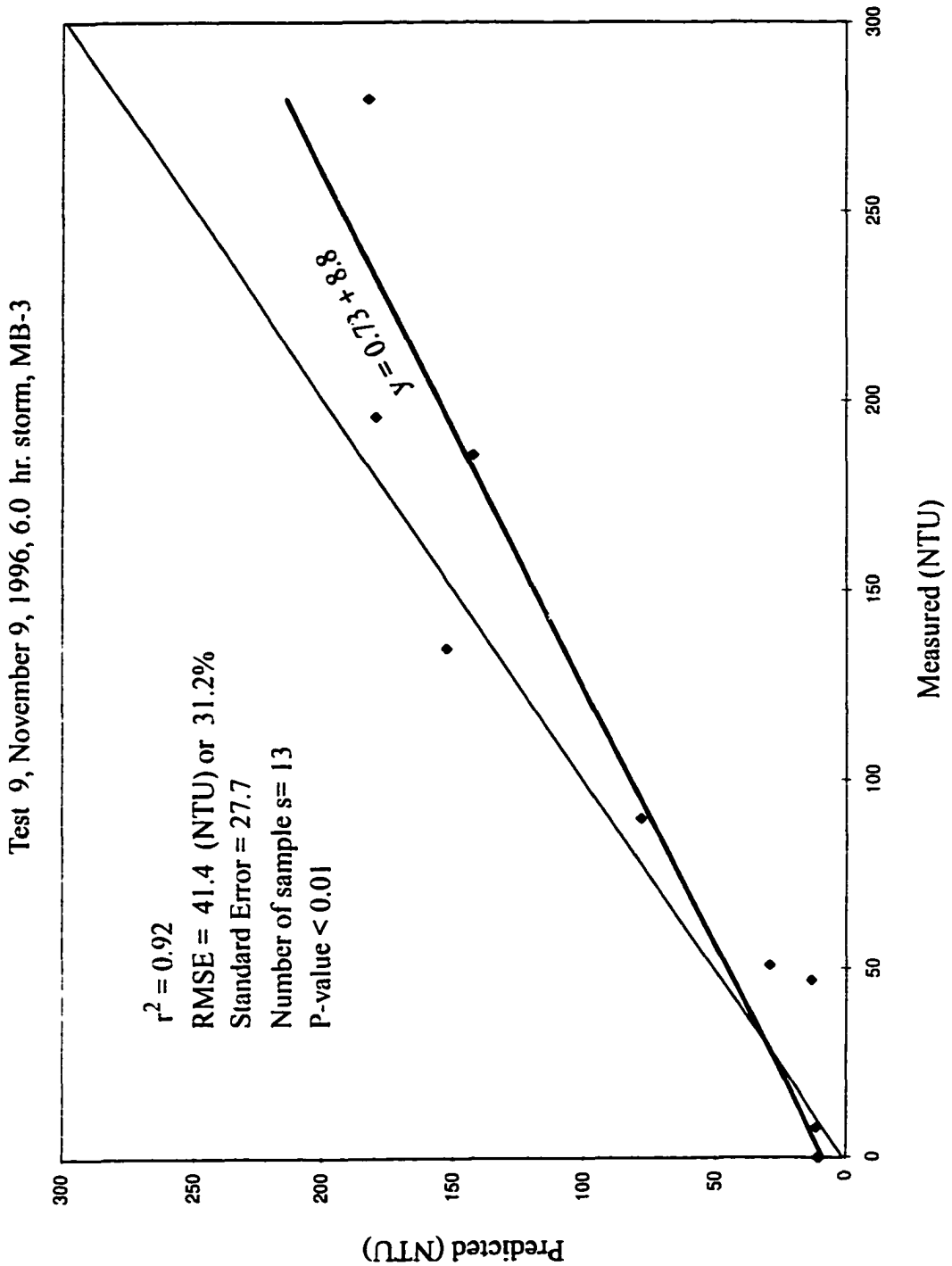

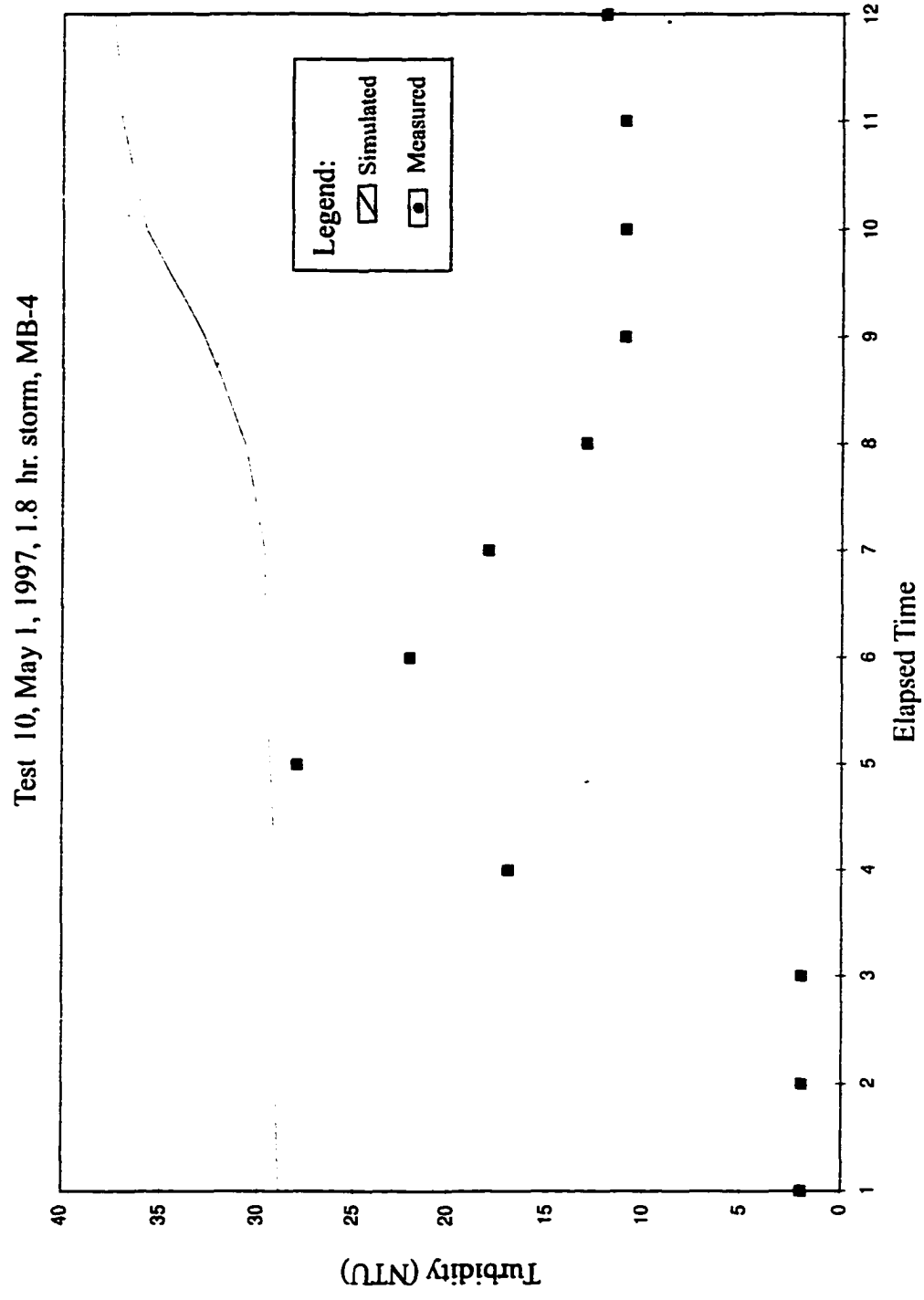

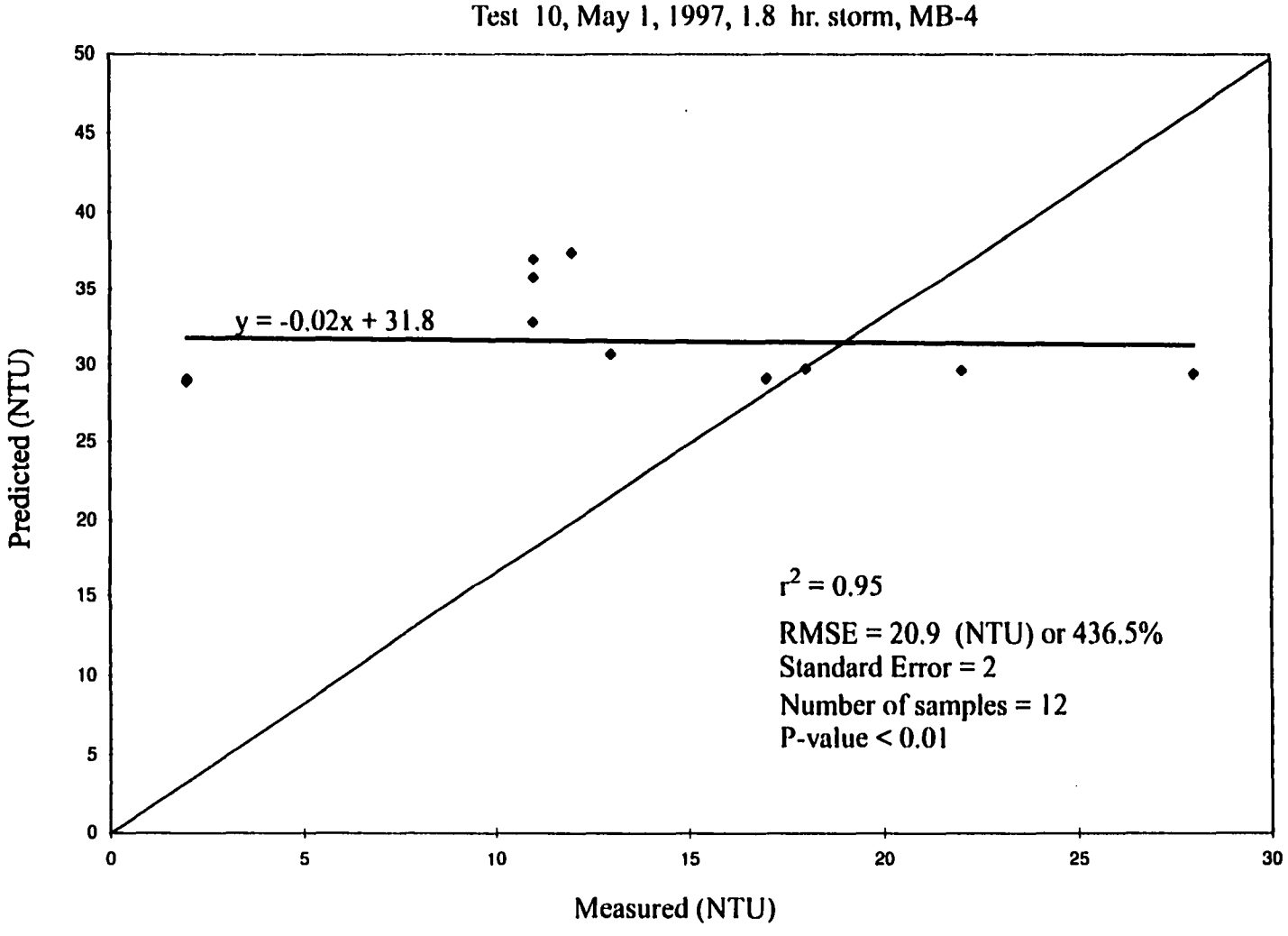

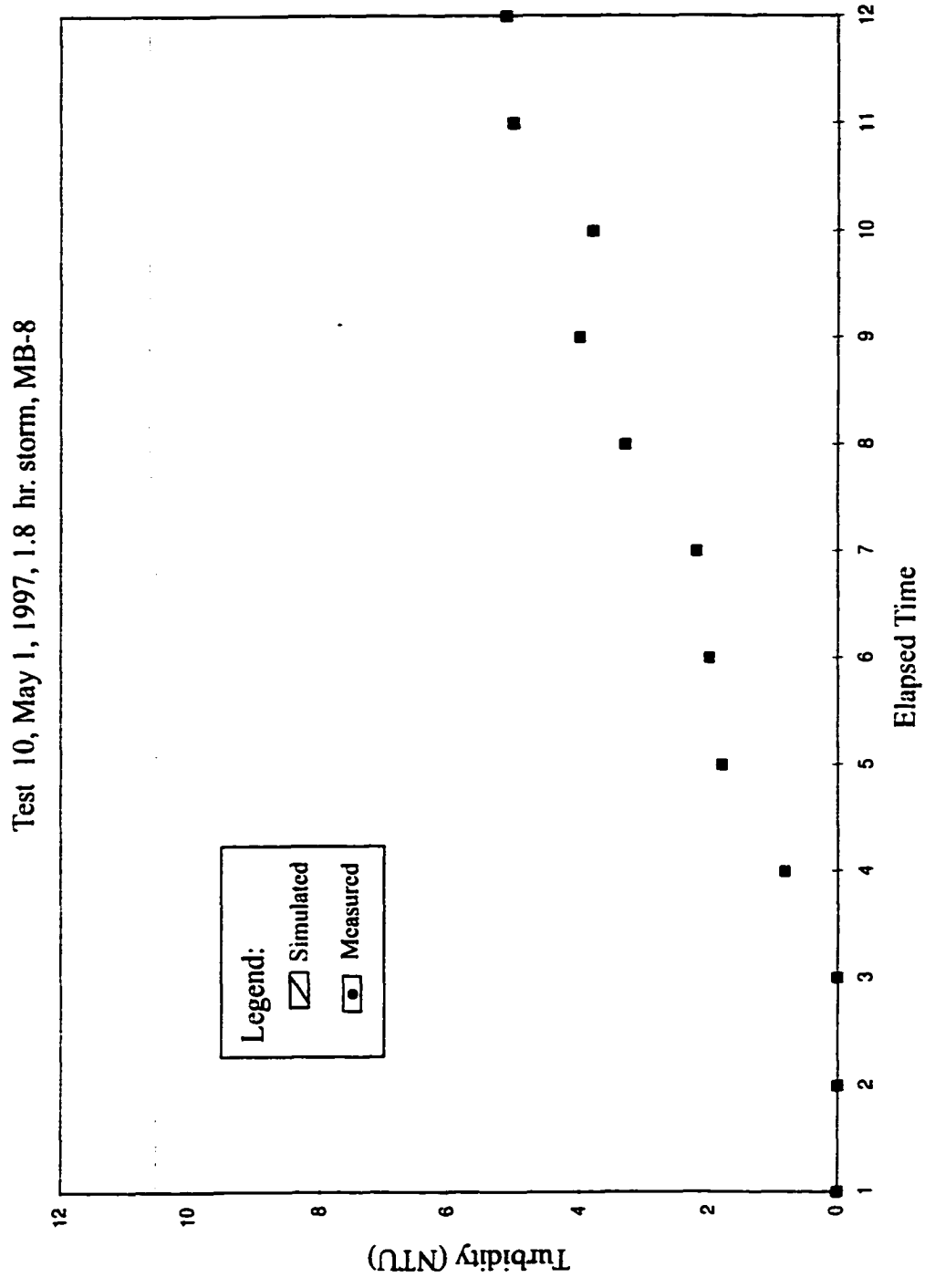

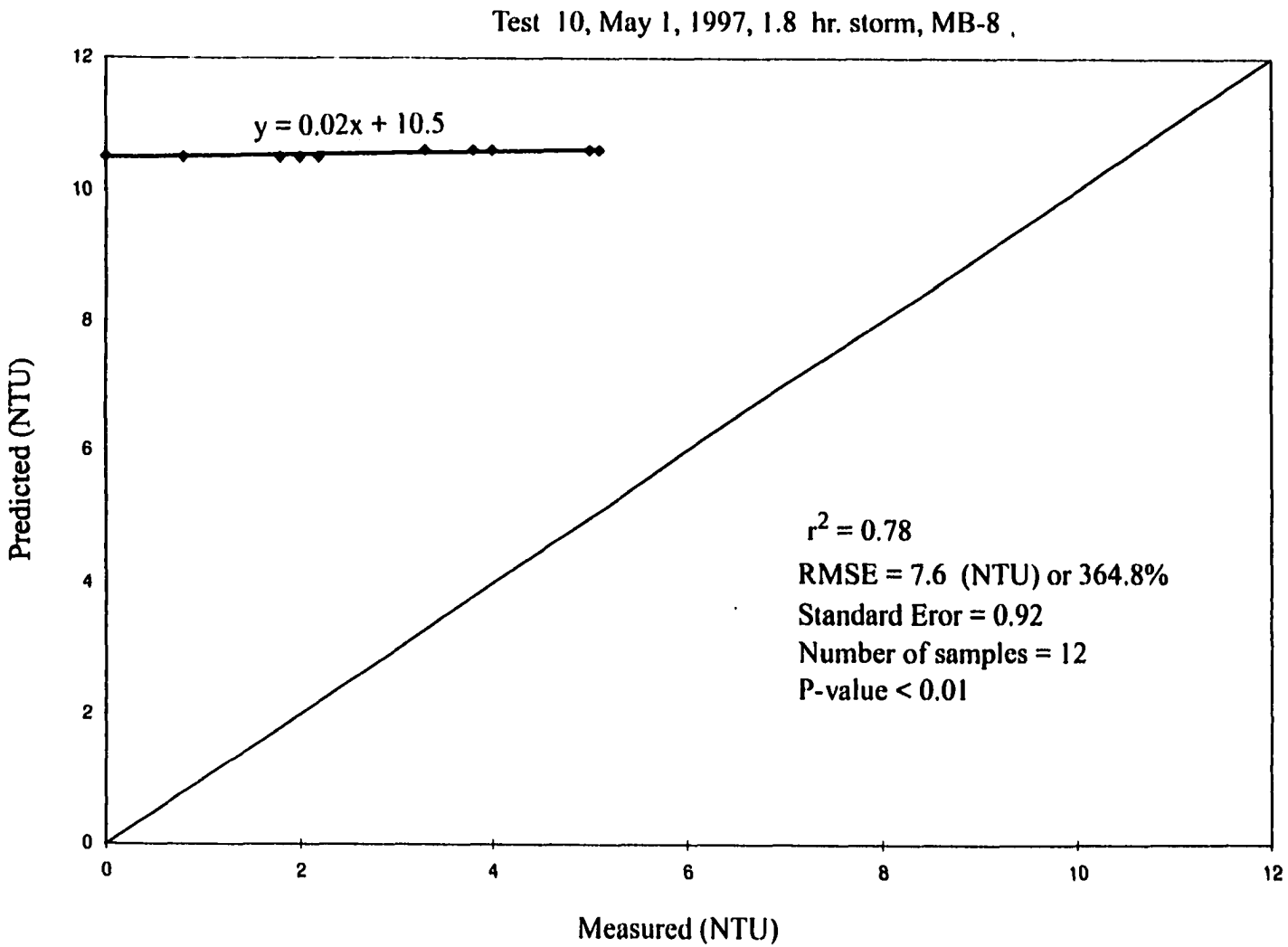

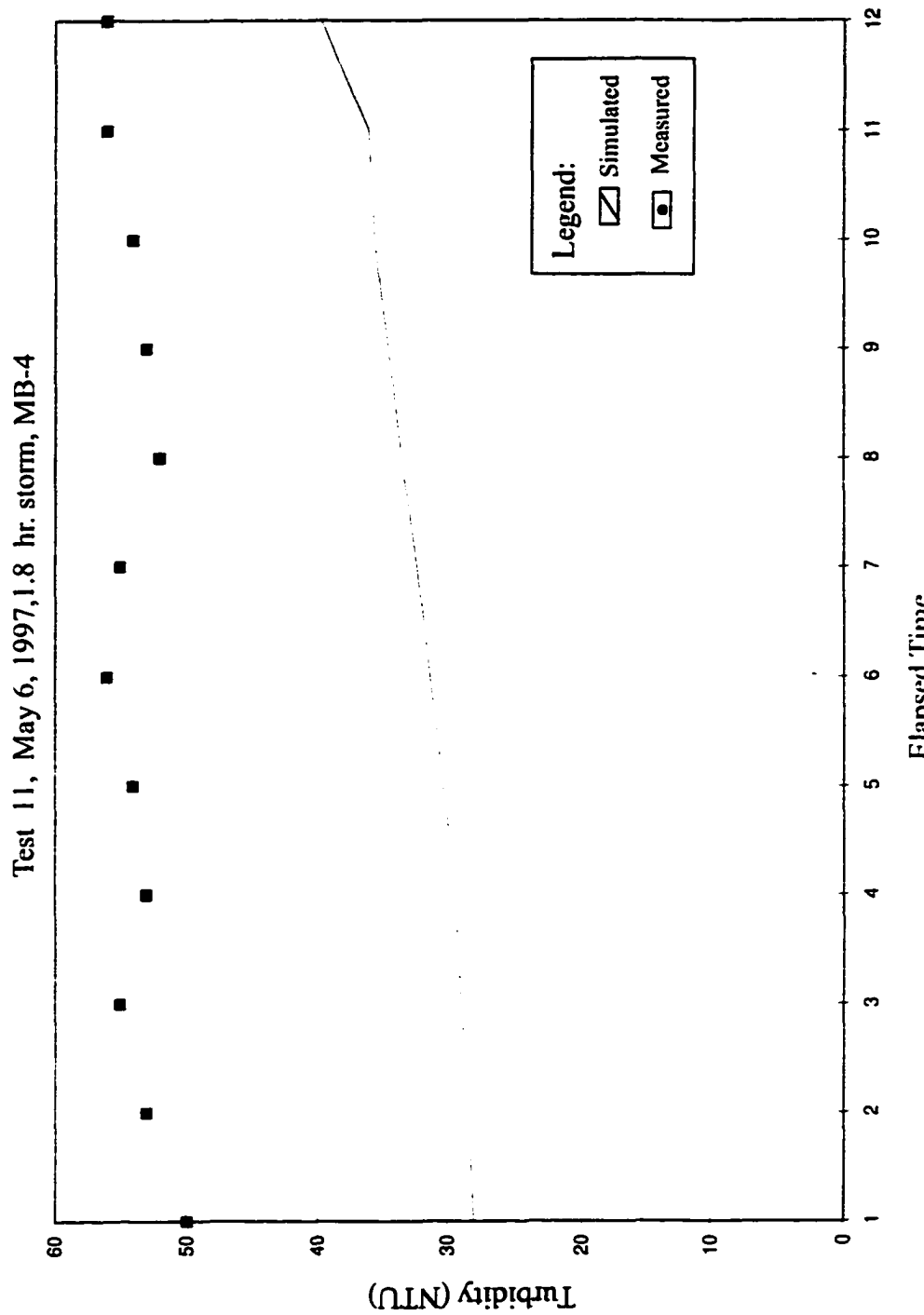

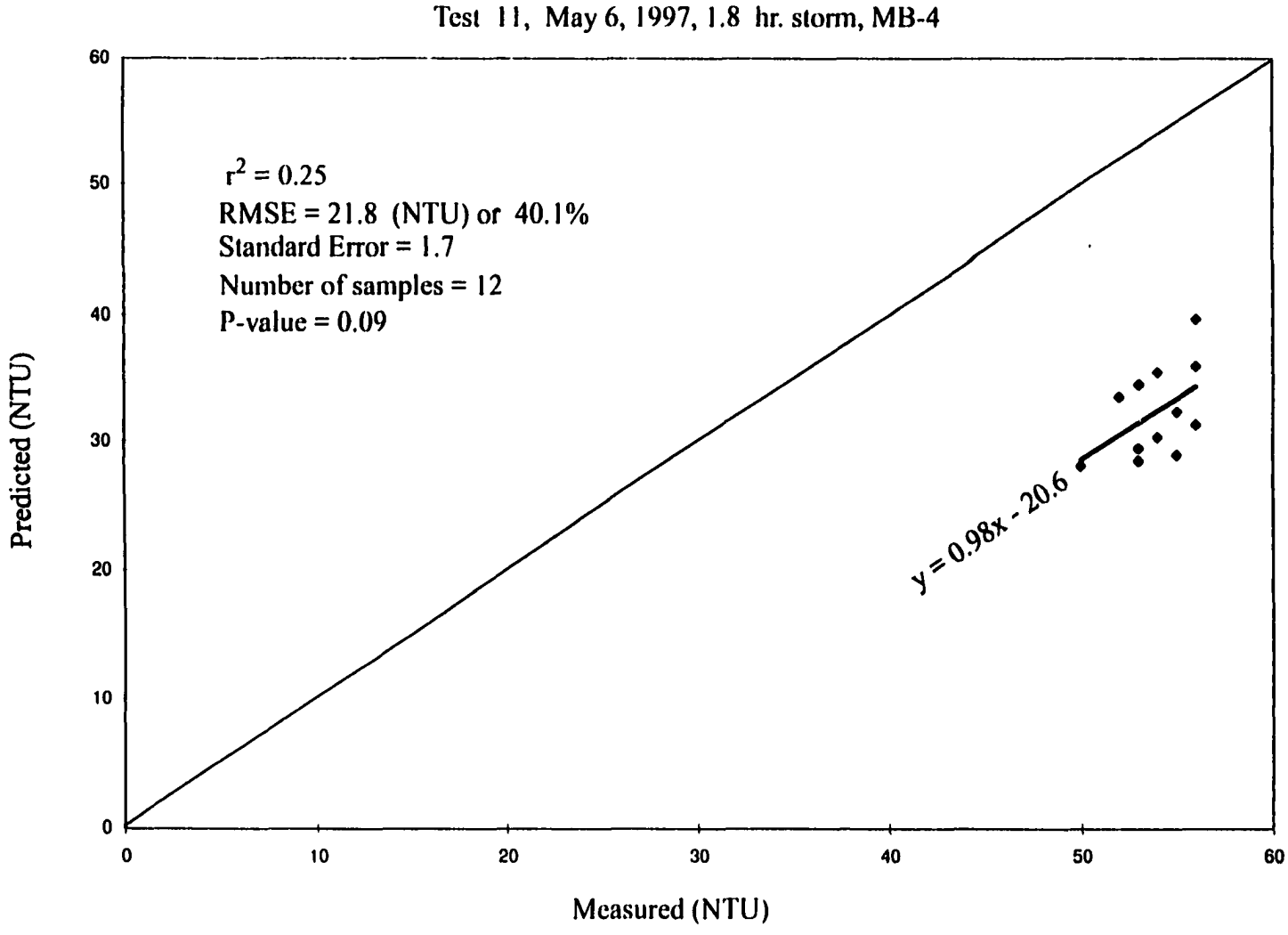

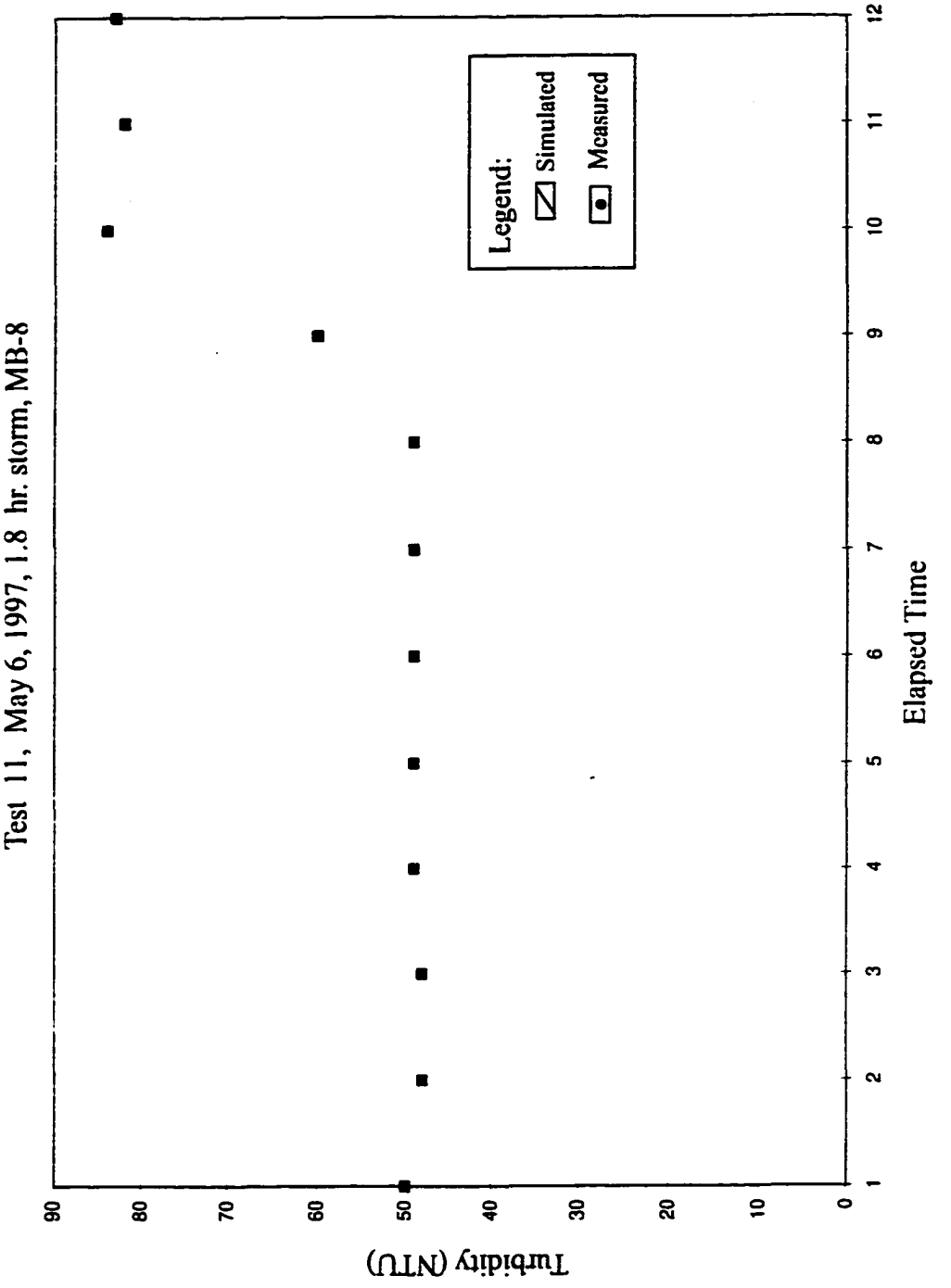

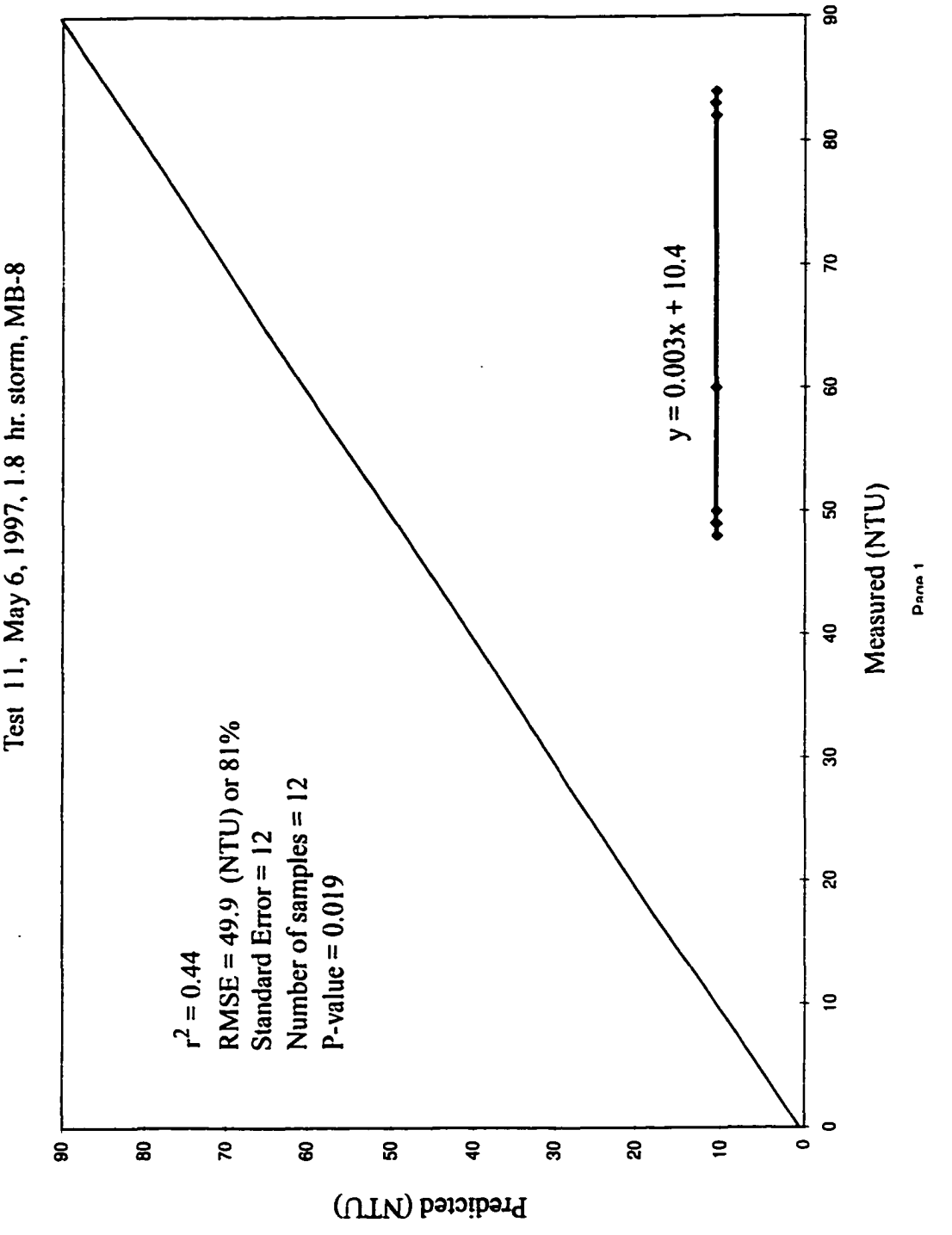

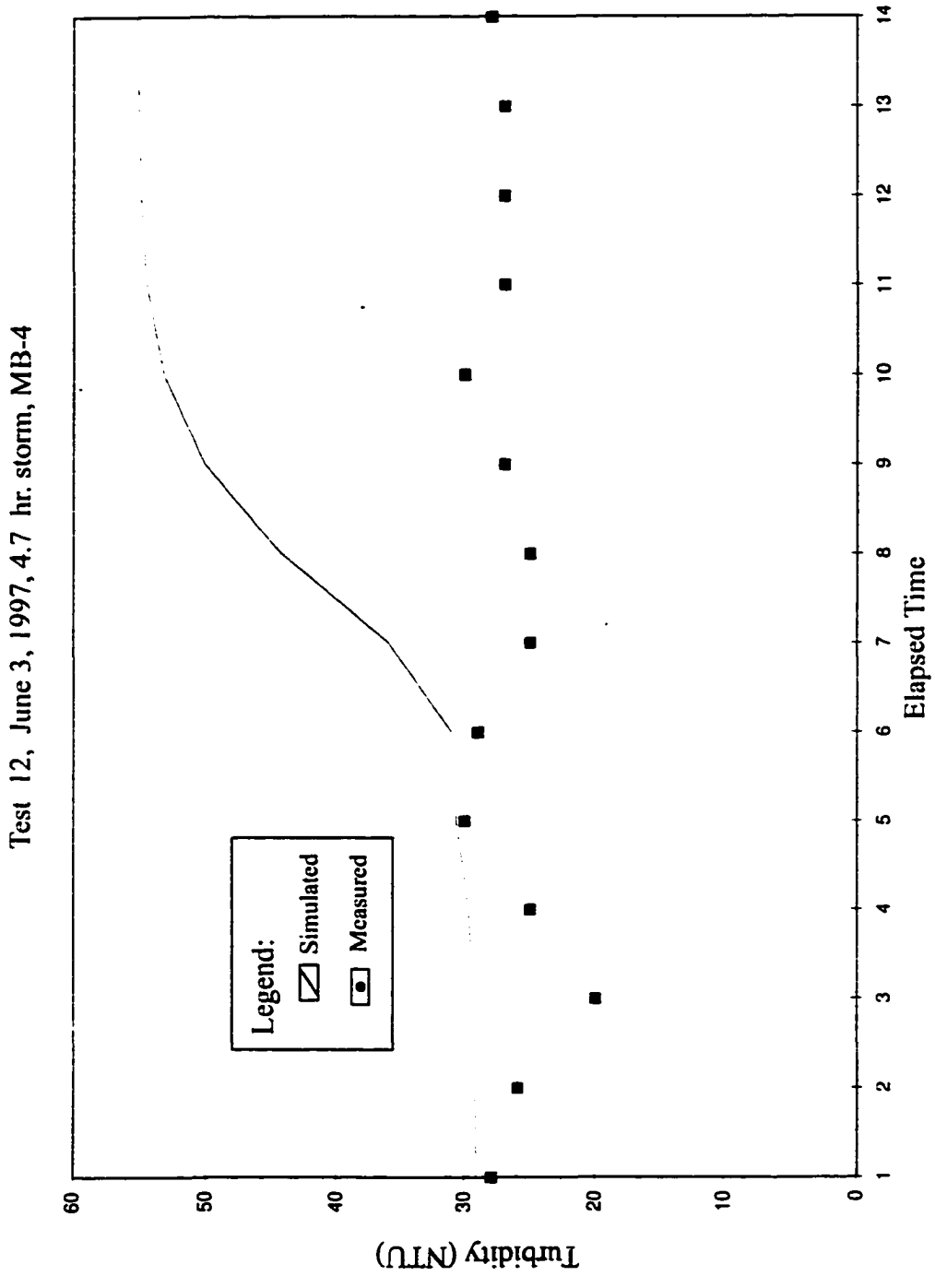

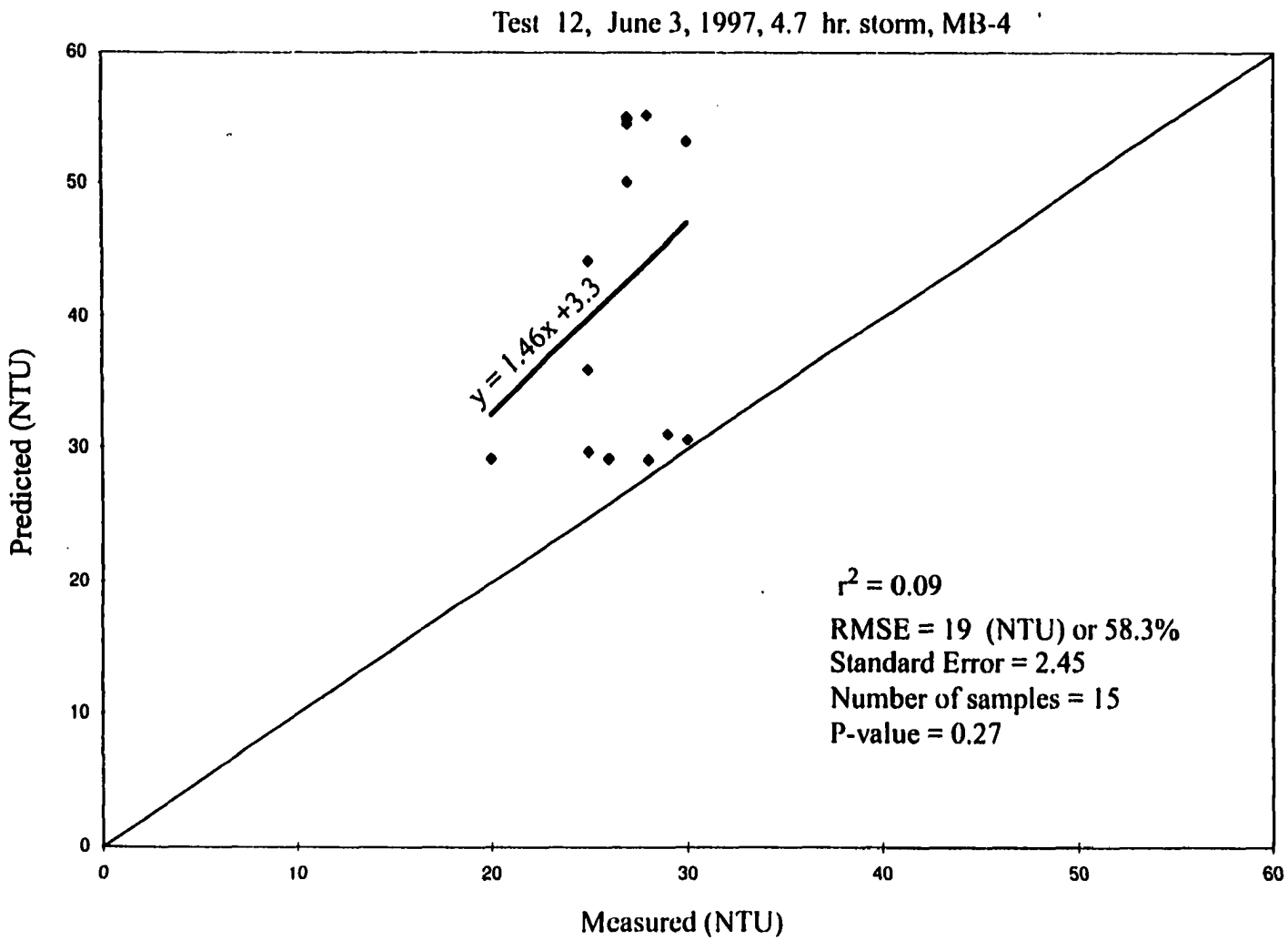

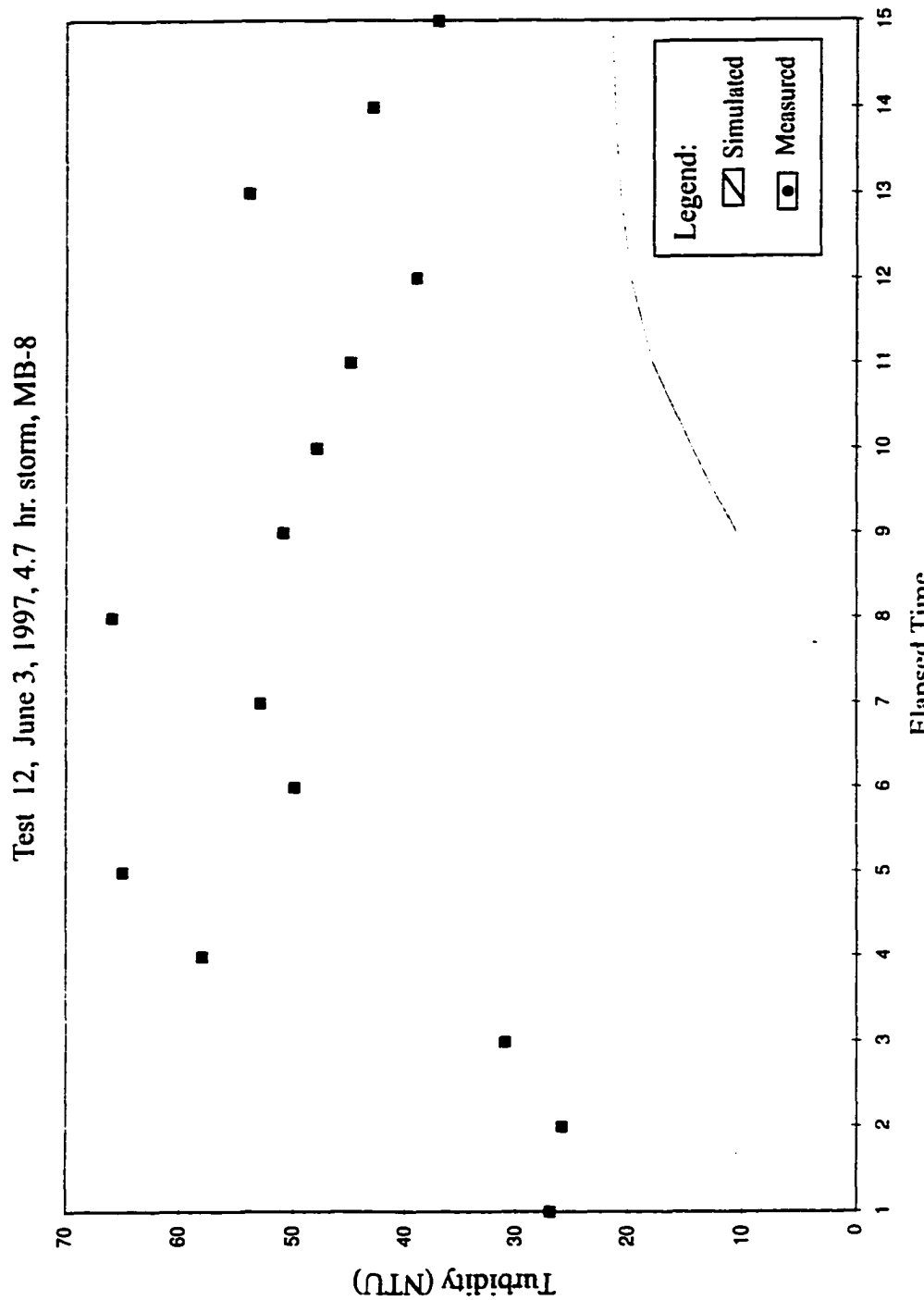

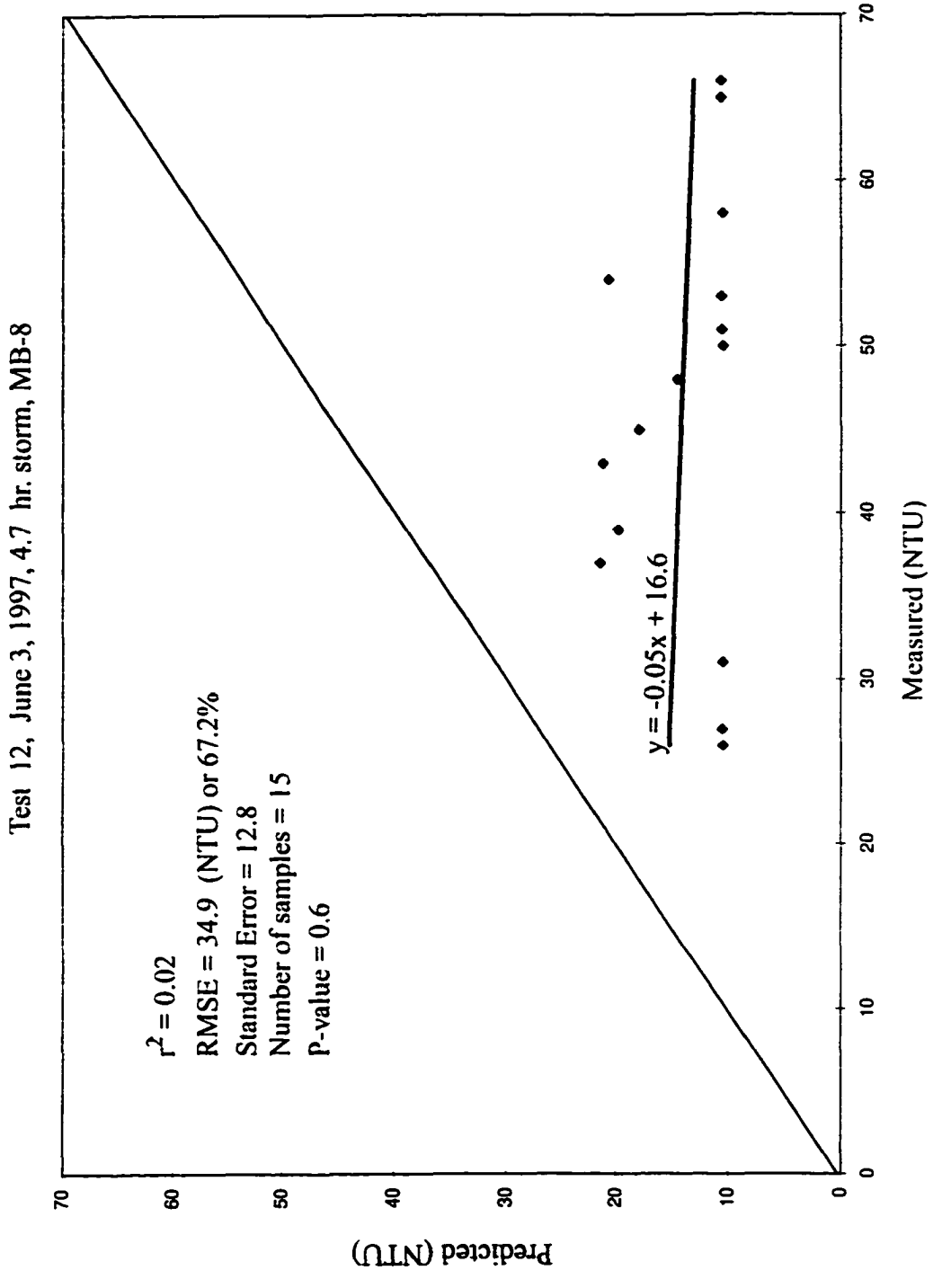

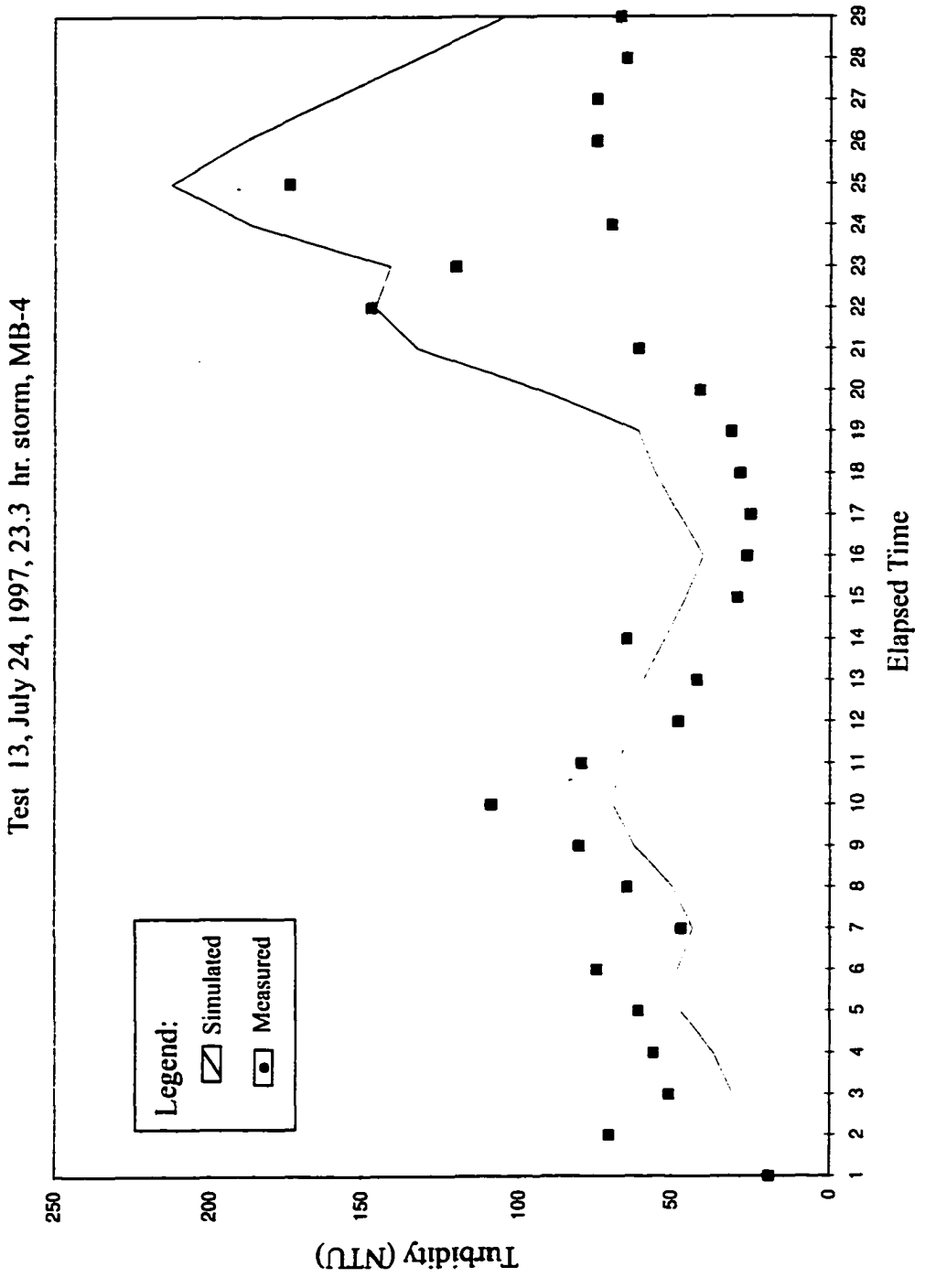

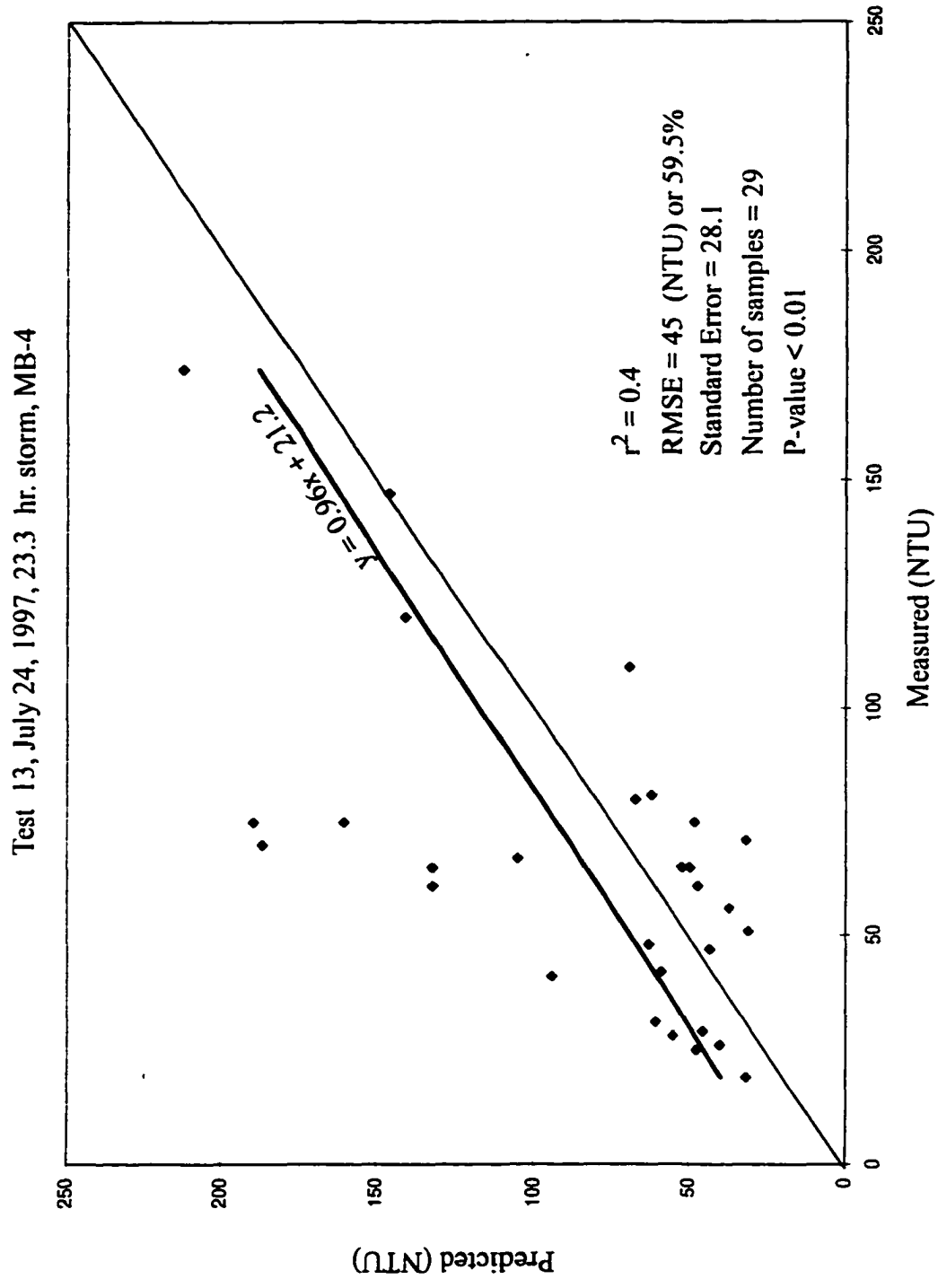

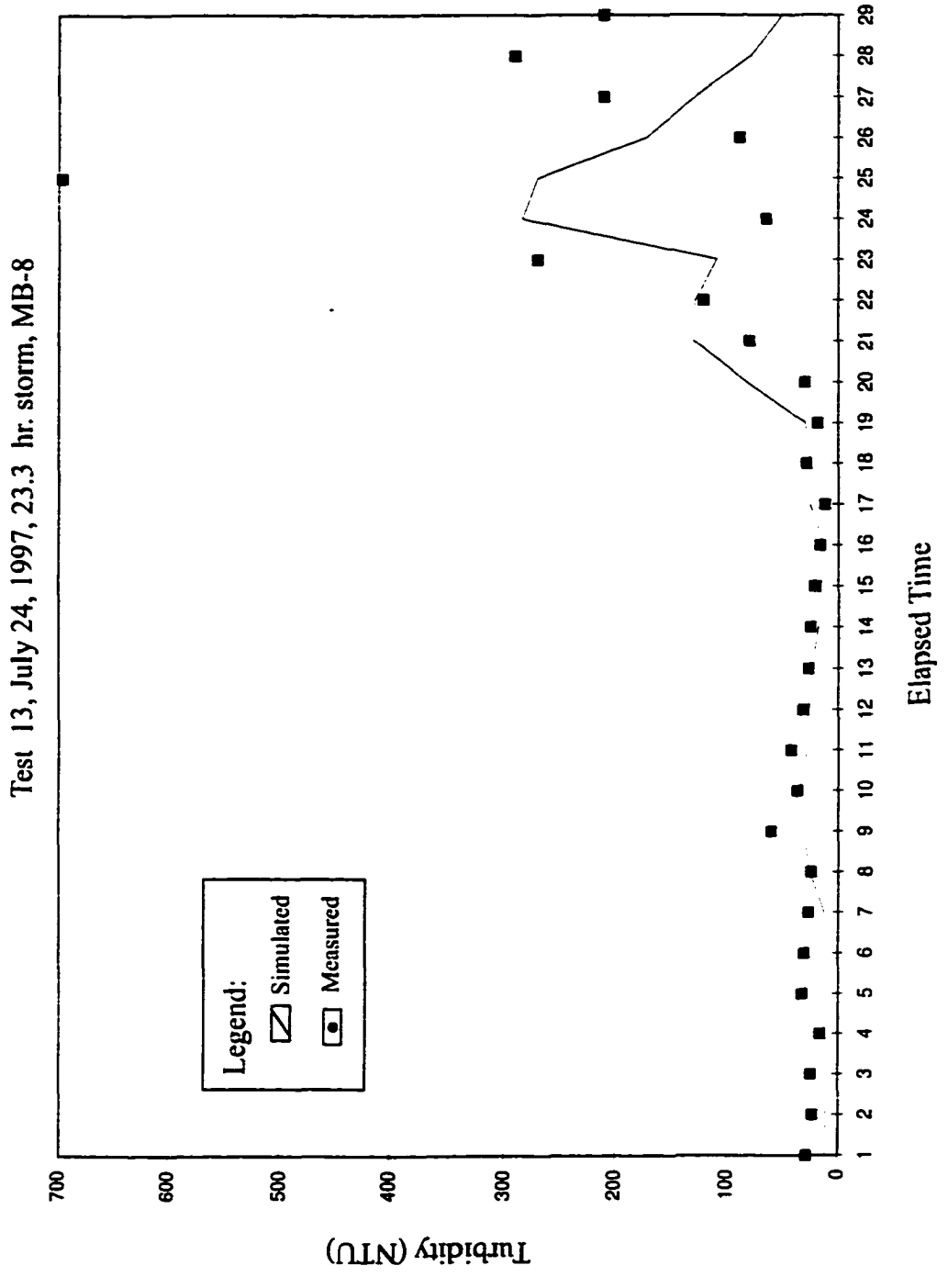

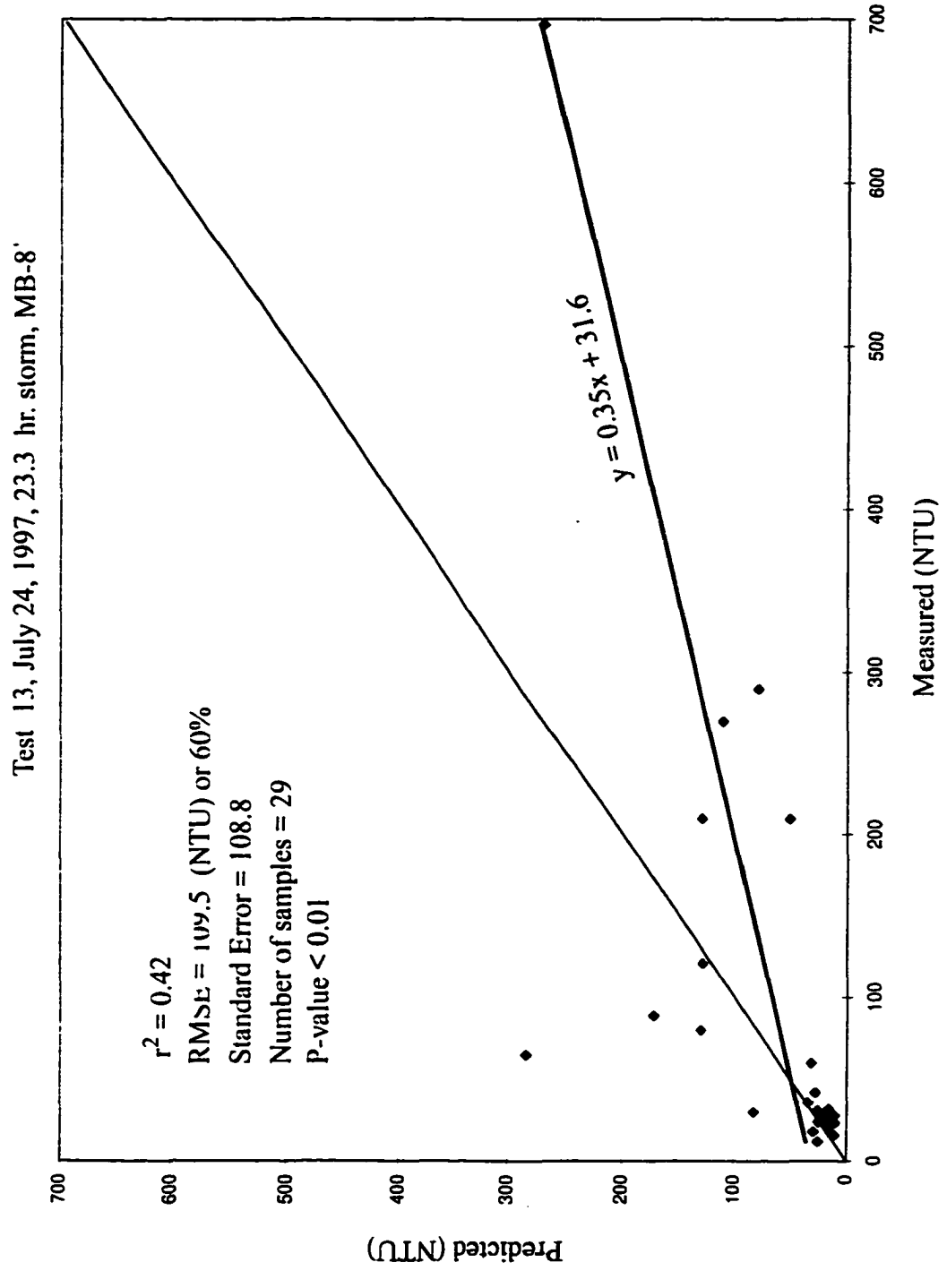

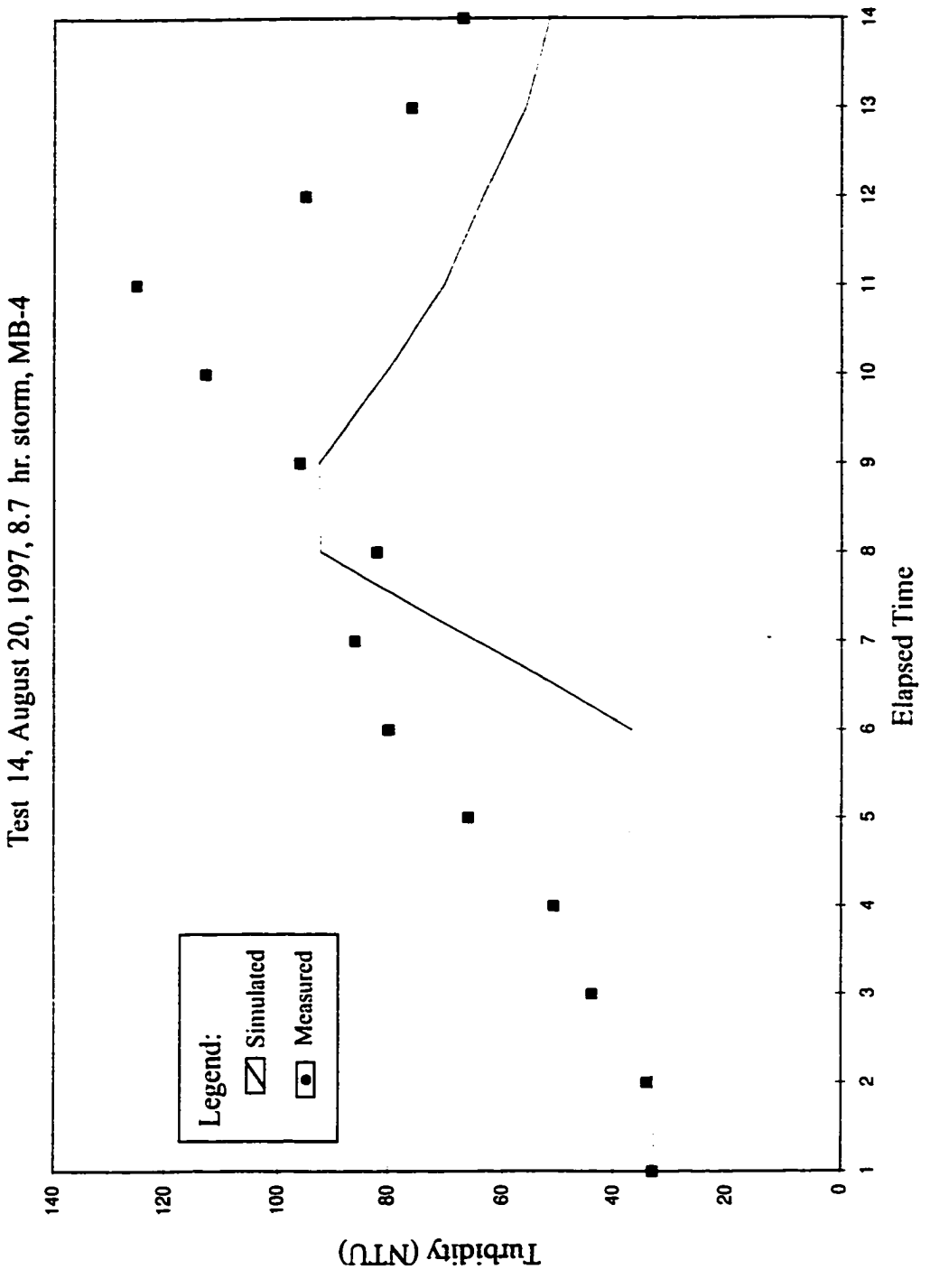

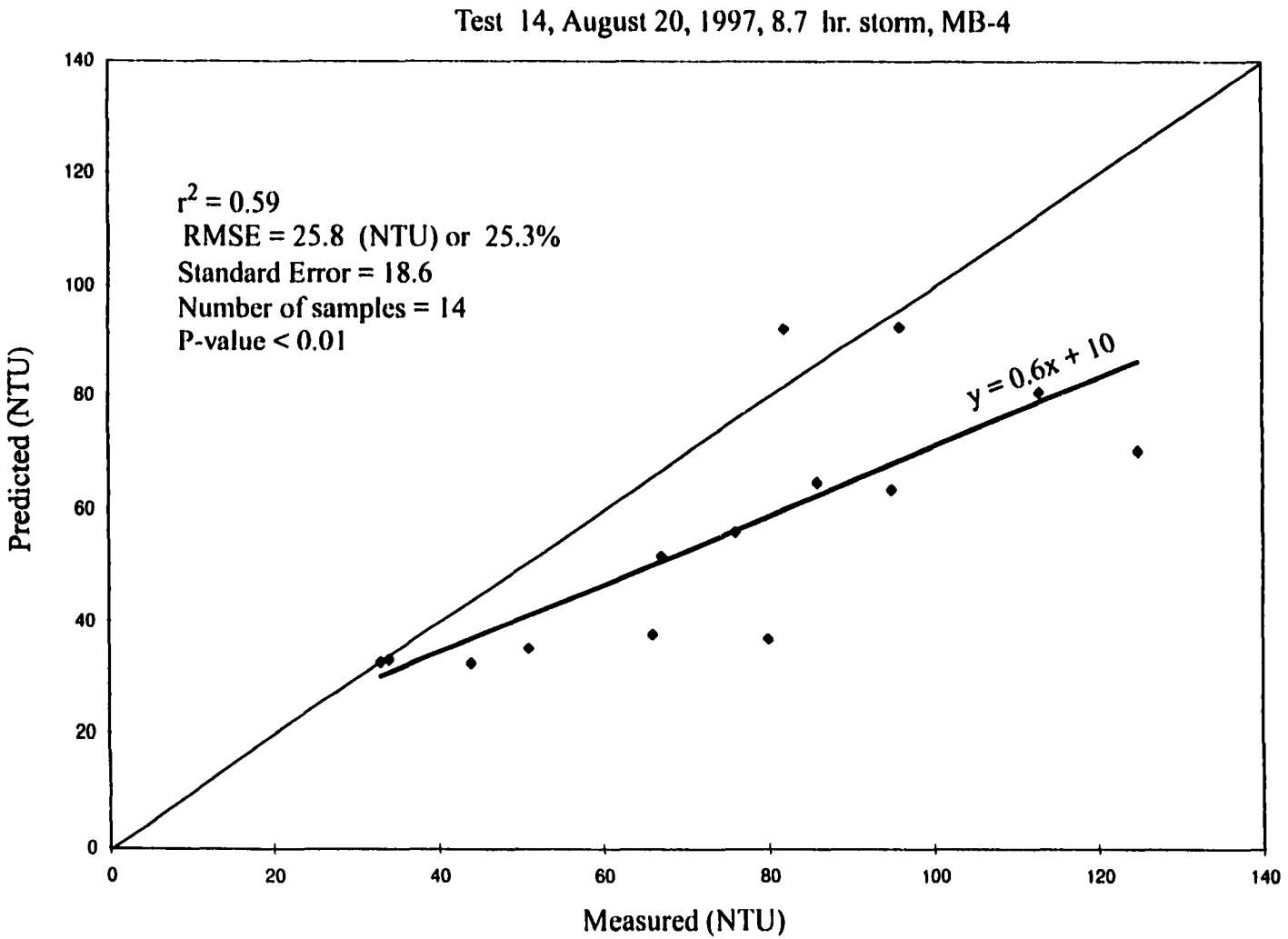

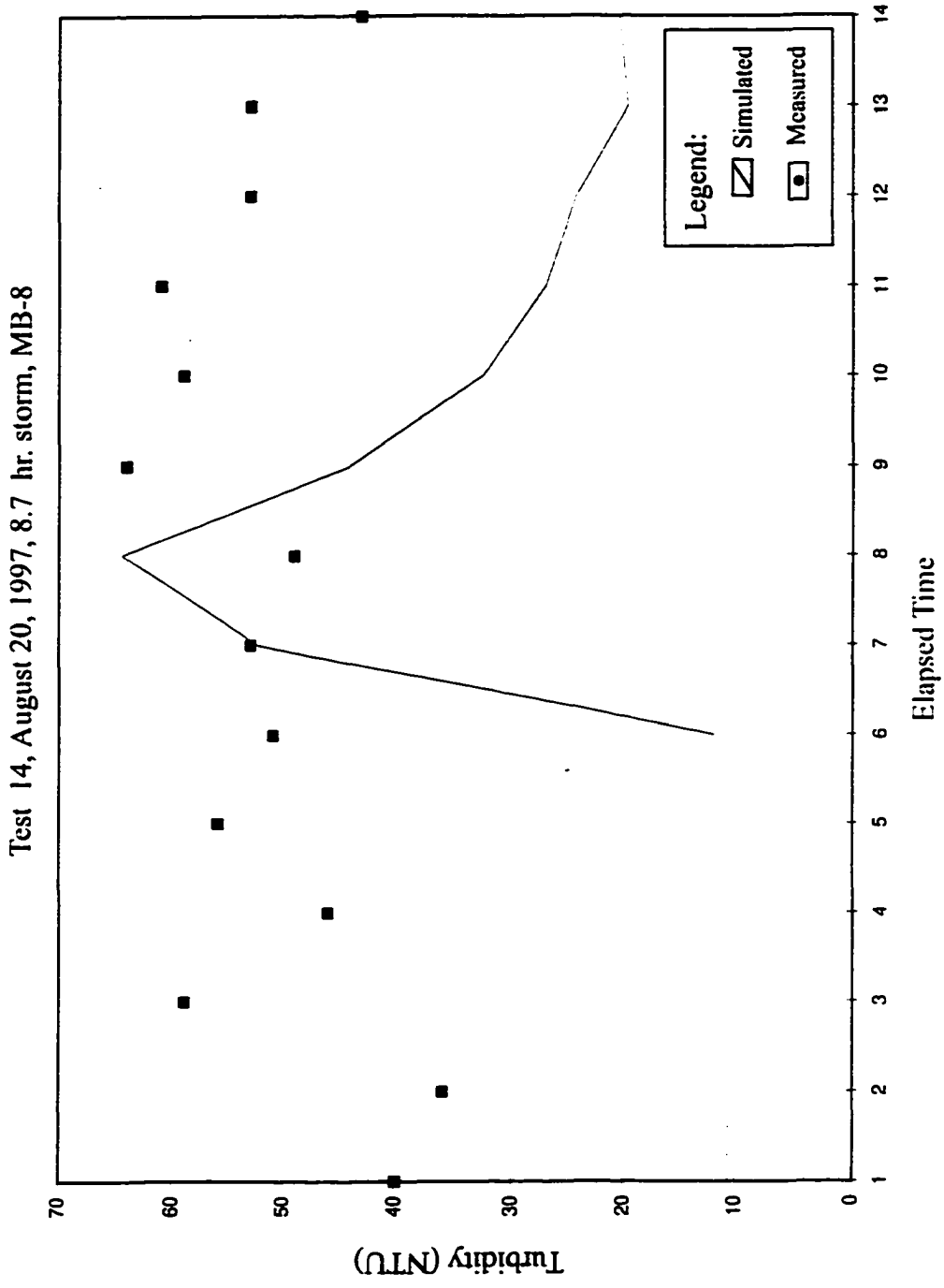

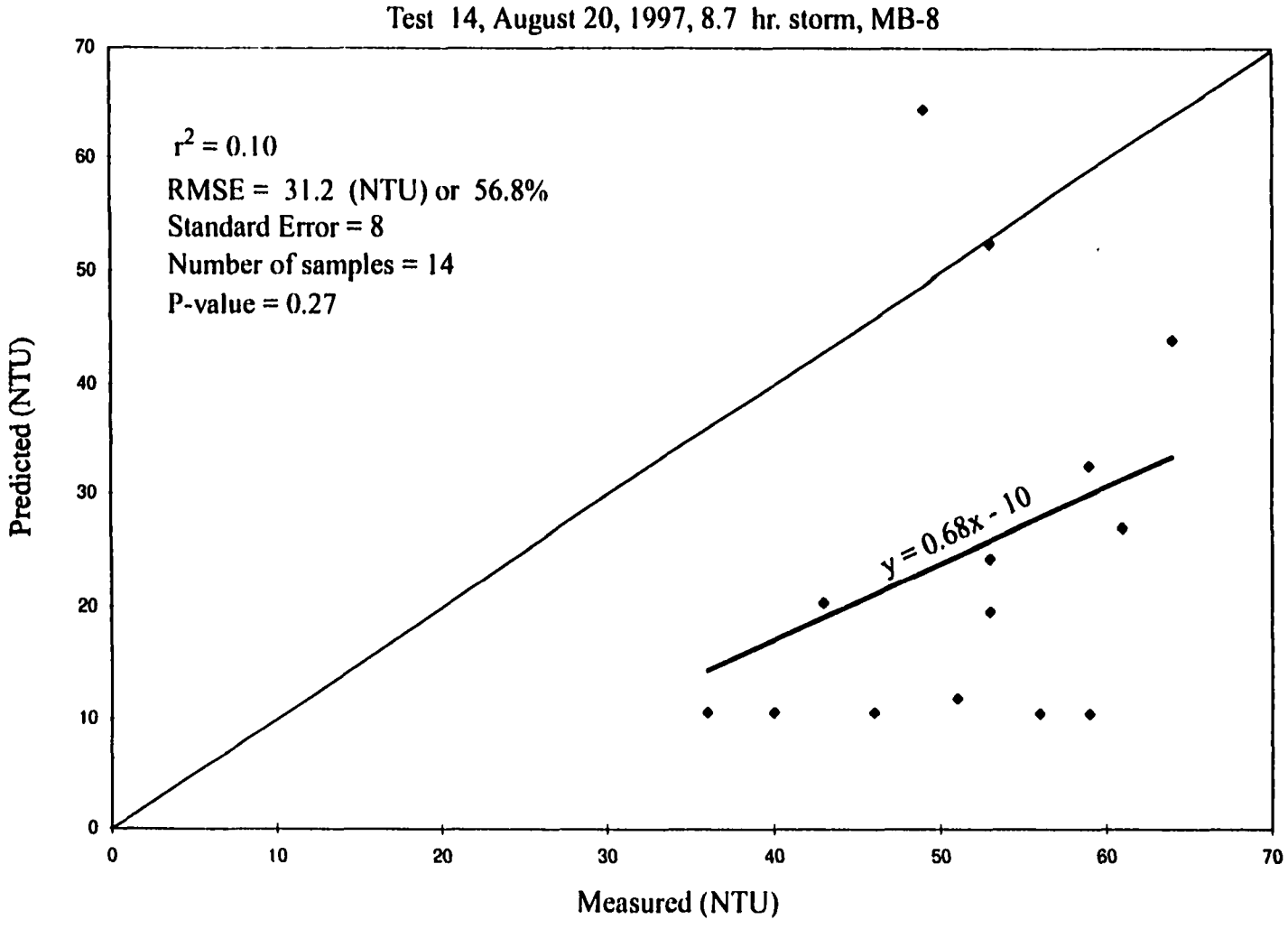

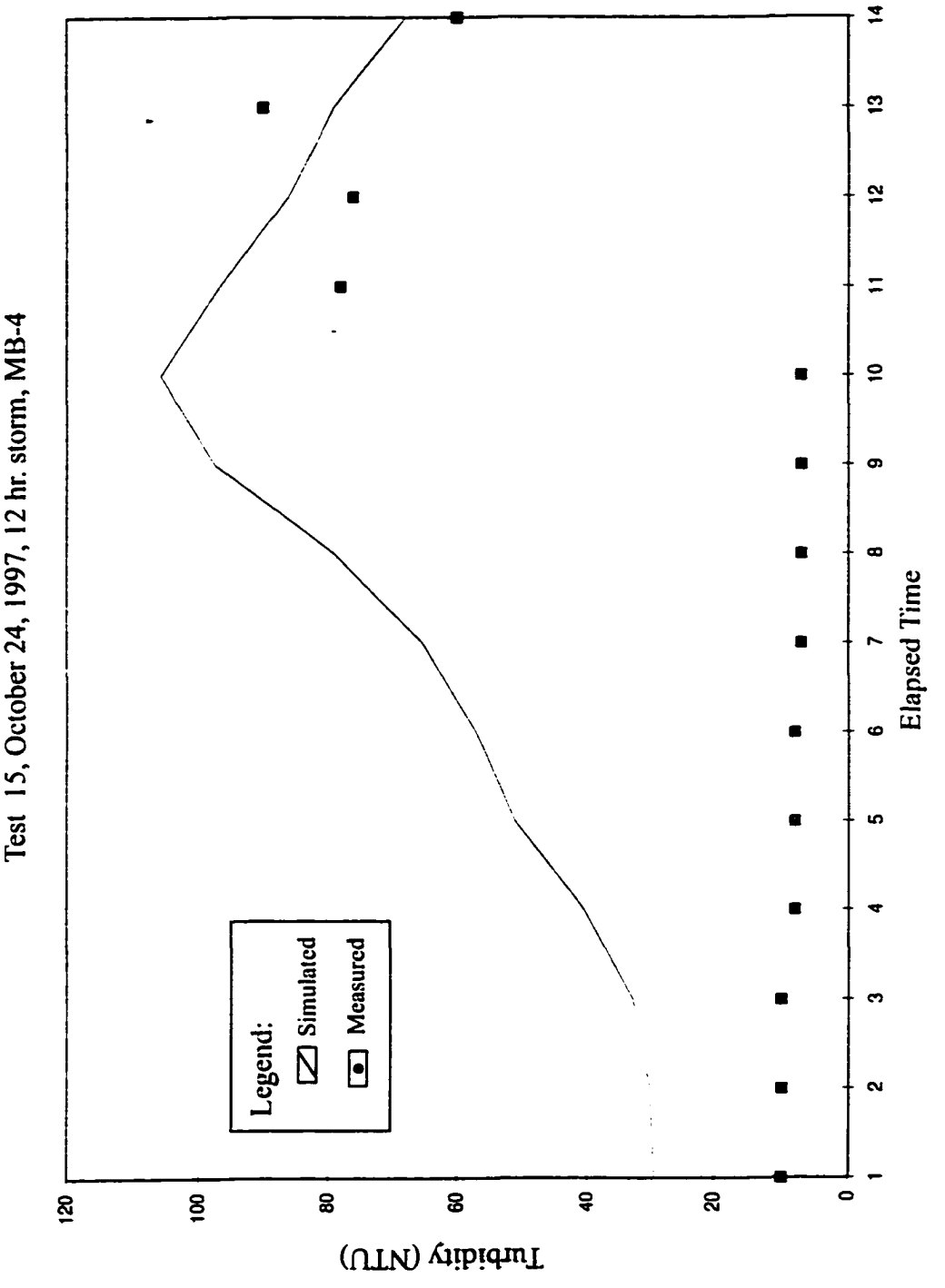

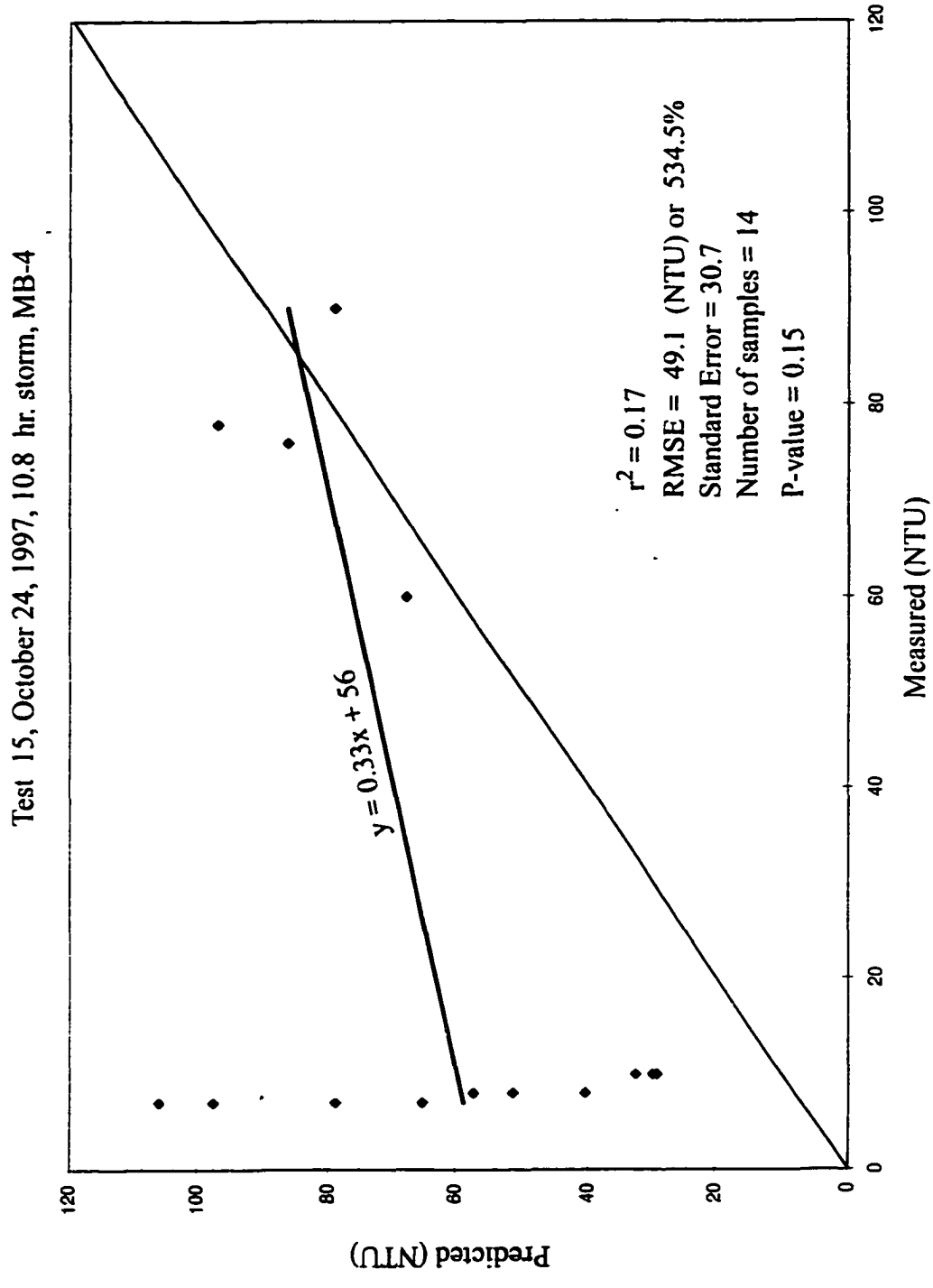

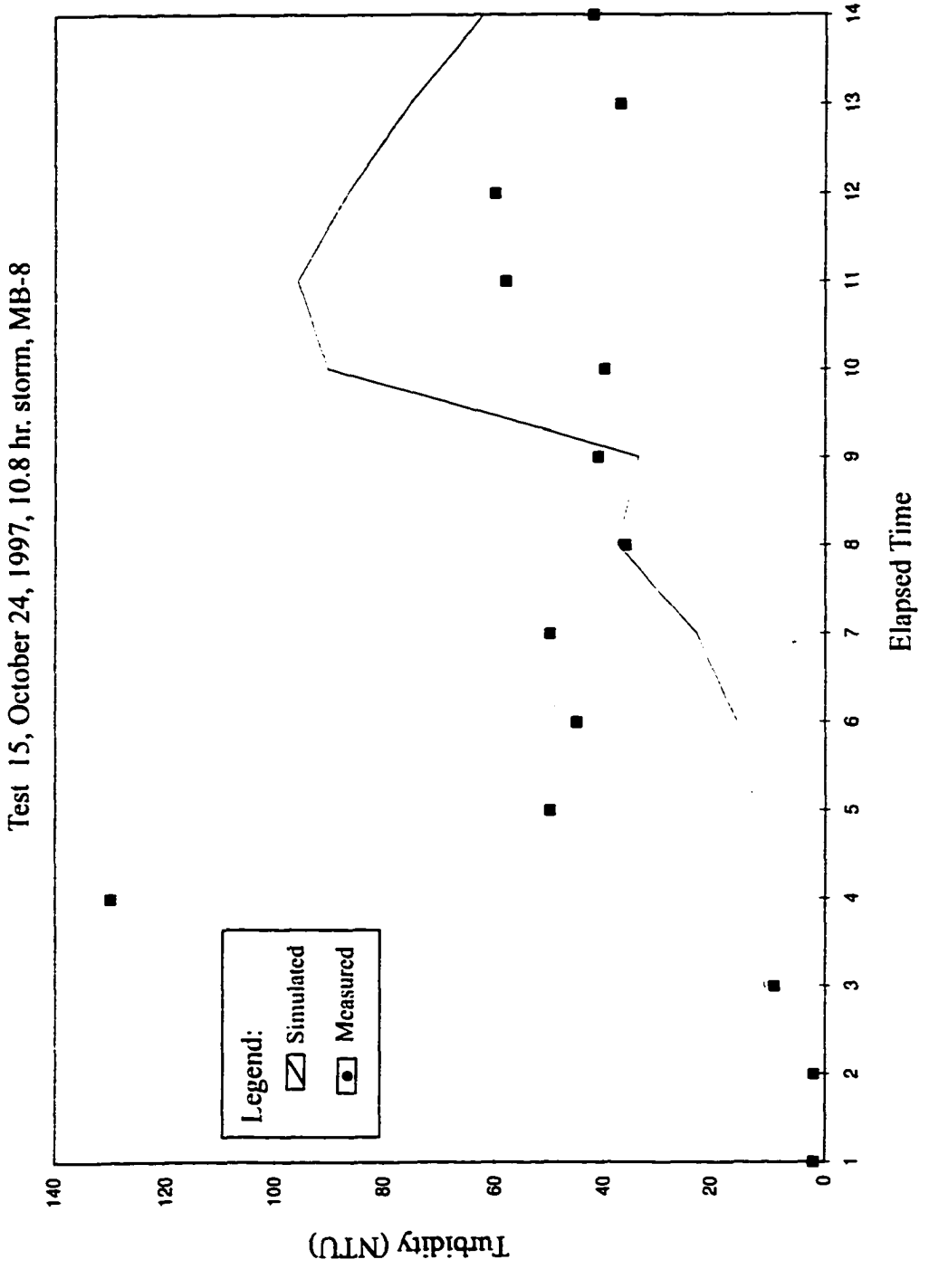

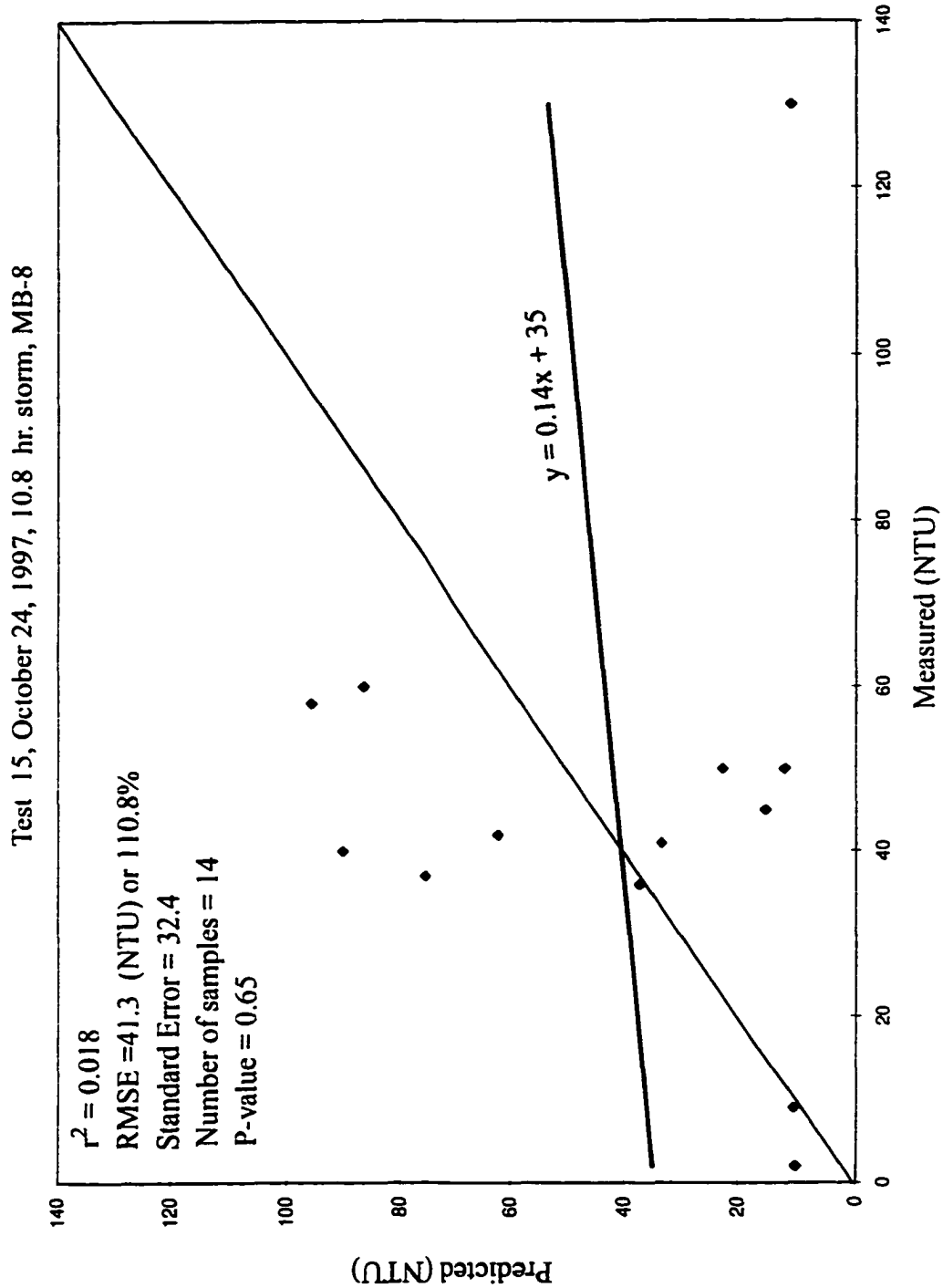

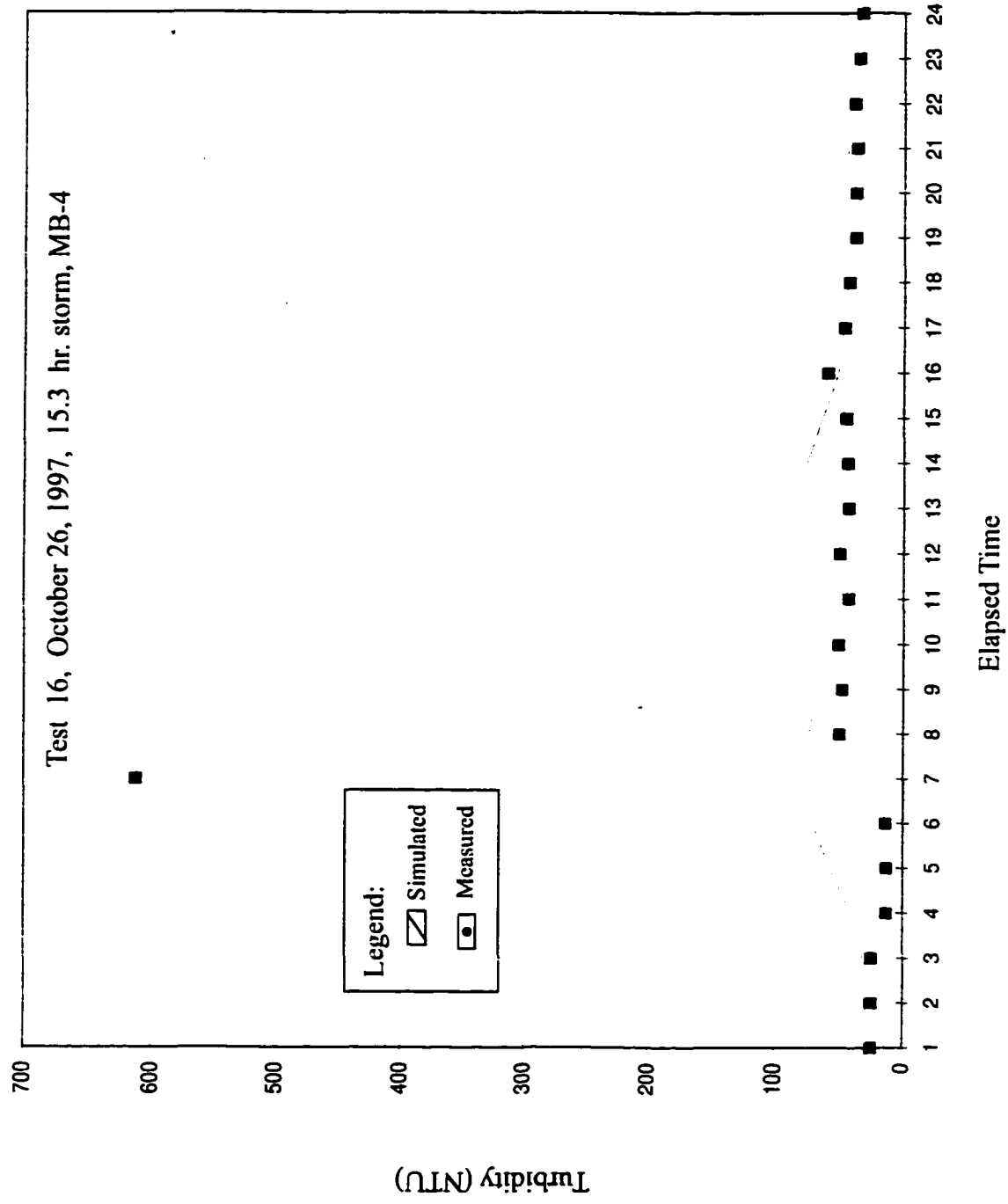

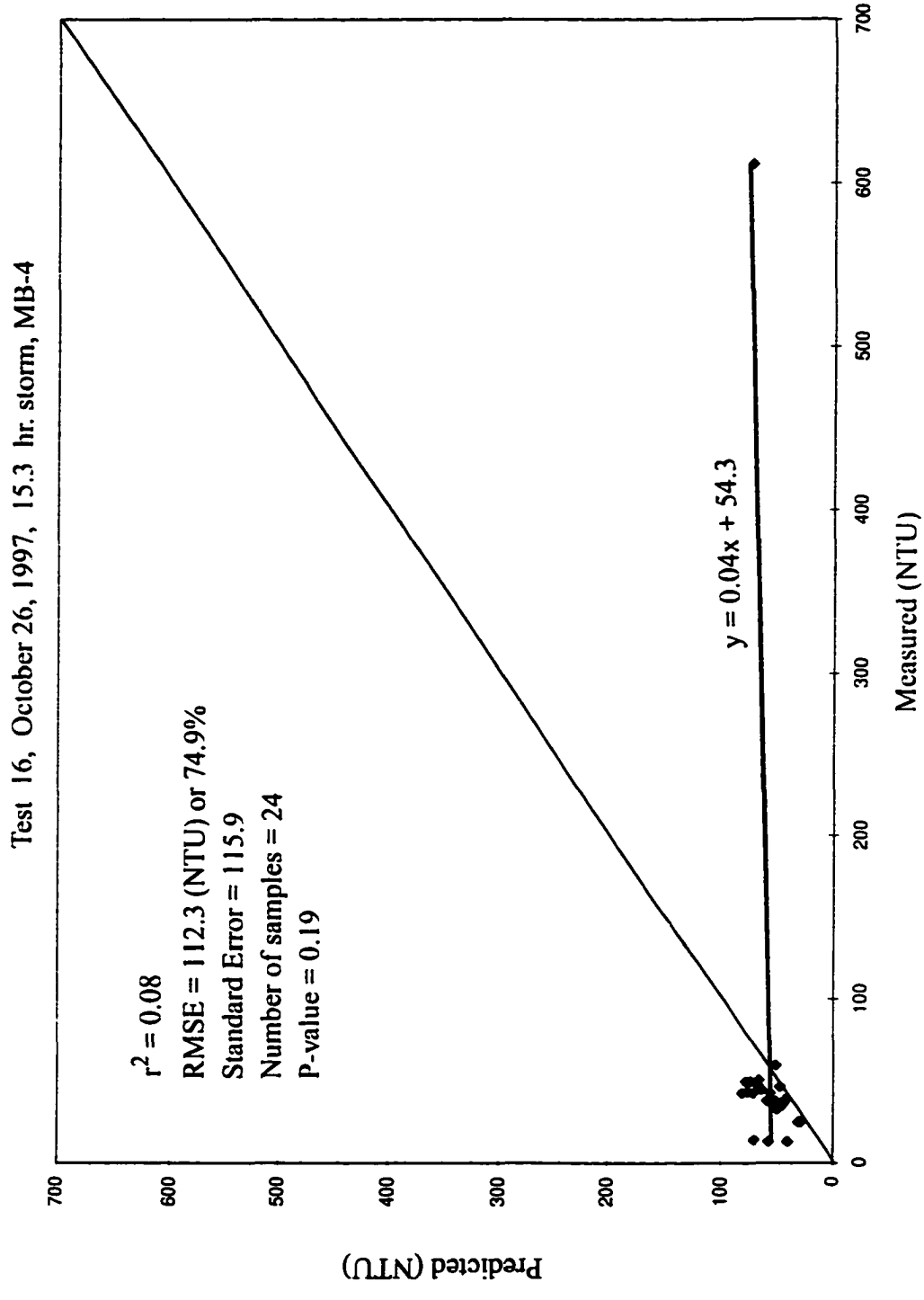

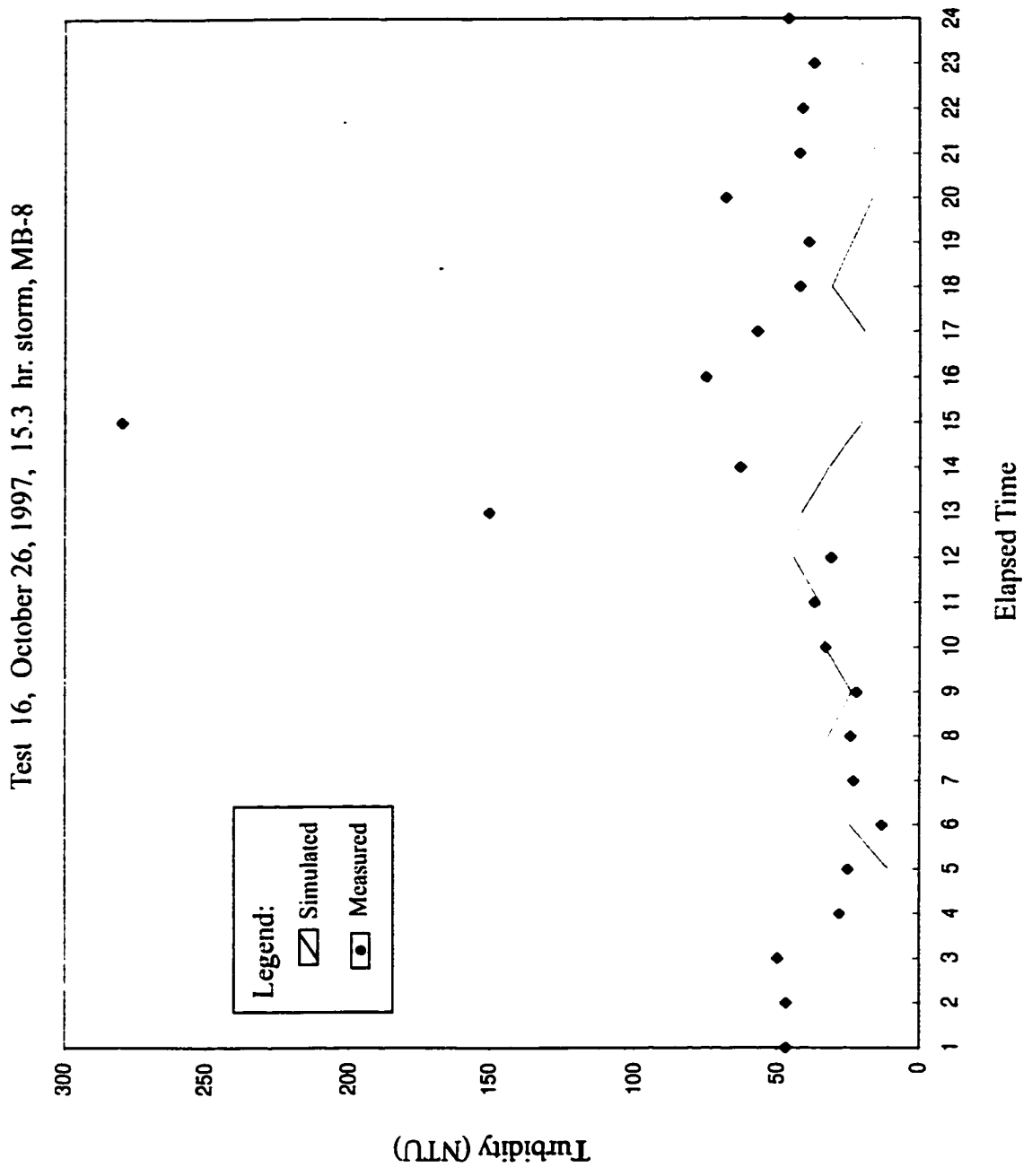

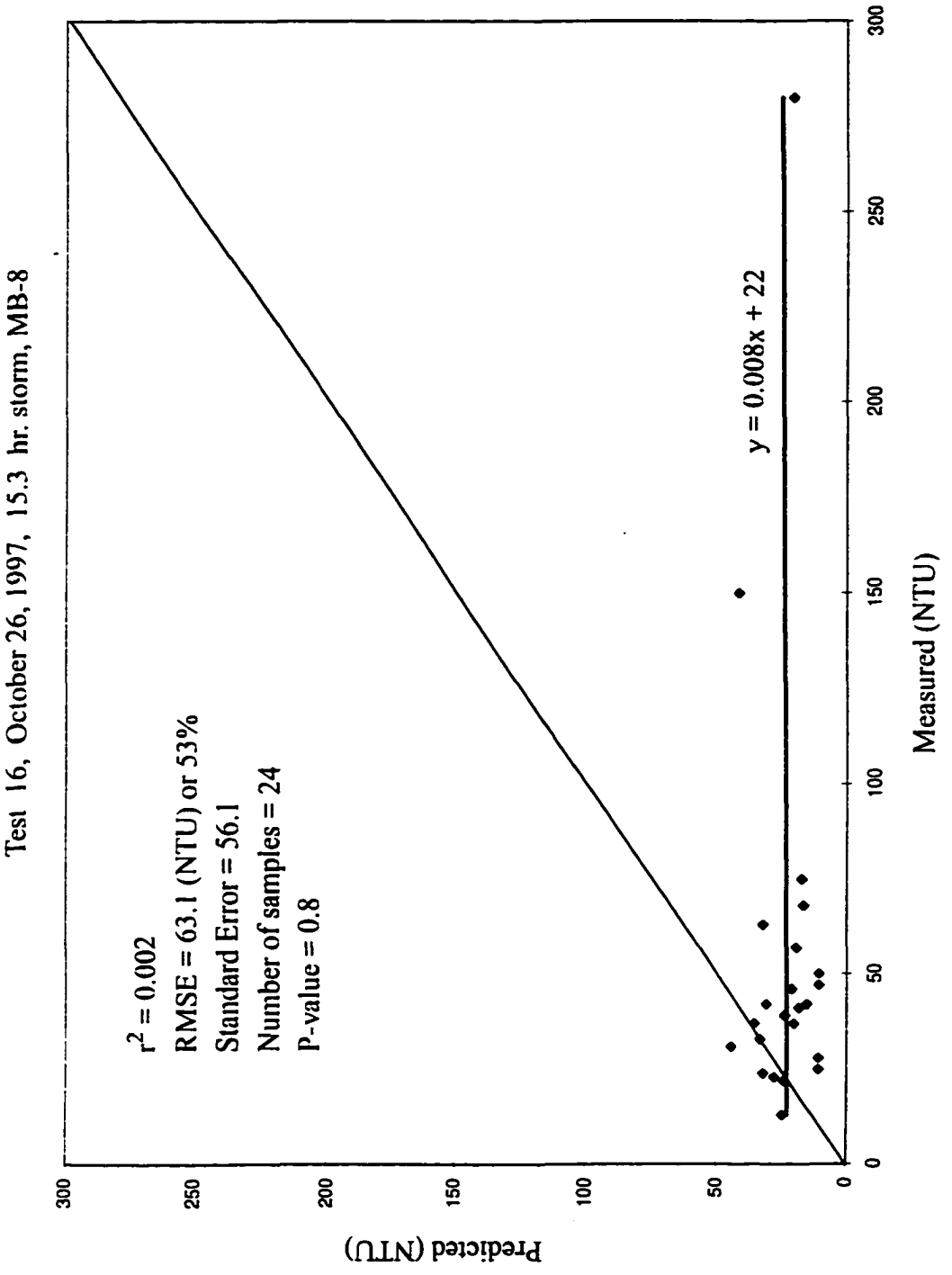

Bibliography.

Althausen, J.D. and B. Kjerfve. 1992. Distribution of Suspended Sediment in a Partially Mixed Estuary, Charleston Harbor, South Carolina, USA. Estuarine, Coastal and Shelf Science, 35, (5): 517-531.

Bagnold, R.A. 1977. Bedload Transport by Natural Rivers. Water Resources Research.13:303-311.

Burrough, P.A. 1986. Principles of Geographical Information Systems for Land Resources Assessment. Clarendon Press, Oxford. 193 pp.

Cahill, T.H., J.McGuire and C.Smith. 1993. Hydrologic and Water Quality Modeling with Geographic Information Systems. In: Proceedings of Symposium on Geographic Information Systems and Water Resources. J.M.Harlin (Ed.), 640 pp.

Carter, C.E. J.D.Greer, H.Brand, and J.Floyd1974. Raindrop Characteristics in South Central United States. Transactions of American Society of Agricultural Engineers, 17:1033-1037.

Chapra, S.C. 1996. Surface Water-Quality Modeling. Preliminary Edition. McGraw-Hill Companies, Inc. 844 pp.

Chien, N. and S.W. Wan. 1983. Mechanics of Sediment Transport. Science Press, Beijing.

Chow, V.T, D.R.Maidment and L.W. Mays. 1988. Applied Hydrology. McGraw-Hill, New York, 572 pp.

Clarke, K. 1995. Analytical and Computer Cartography. Prentice Hall, NJ, 334 pp.

Colby, B.R. 1964. Practical Computations of Bed Material Discharge. Journal of Hydrological Engineering. 90:217-246.

Collins, Michael A., and Roger O. Dickey. 1989. Stochastic Modeling of the Runoff-Process for Nonpoint Source Pollutant Load Estimation. Technical Report No. 148, Texas Water Resources Institute, College Station, TX. 326 pp.

Courant, R., and K.O. Friedrichs. 1948. Supersonic Flow and Shock Waves. Interscience Publishers, New York. 464 pp.

Darlington, T. 1905. Report on Filtration of the Water Supply of the City of New York. Martin B. Brown Press. New York.

Davies-Colley, R.J. C.W.Hickey, J.M.Quinn, and P.A.Ryan. 1992. Effects of Clay Discharge on Streams: 1. Optical Properties and Epilithon. Hydrobiologia, 248 (3):215-234.

Decamps, H., J.Capblancq, H.Casanova, and J.N. Tourenq. 1979. Hydrobiology of Some Regulated Rivers in the Southwest of France. Ecology of Regulated Streams. Plenum, New York. 398 pp.

DePinto, J.V. , J.F.Atkinson, H.W.Calkins, P.J.Densham, W.Guan, H.Lin, F.Xia,P.W.Rodgers, T.Slawecki and W.L.Richardson. 1993. Development of GEO-WAMS: A Modeling Support System for Integrating GIS With Watershed Analysis Models. First International Conference/Workshop Integrating GIS and Environmental Modeling. Breckenridge, Colorado, 1993.

Dickinson, W.T., and R. Pall. 1982. Identification and Control of Soil Erosion and Fluvial Sedimentation in Agricultural Areas of the Canadian Great Lakes Basin. Contract No.2360. 0152-S-1-0433. Final Report to Supply and Services, Canada, Ottawa, Ontario.

Dueker, K. and D. Kjerne. 1989. Multipurpose Cadastre: Terms and Definitions. Bethesda, MD. American Congress on Surveying and Mapping, pp. 7.

Dunne, T., and L.B. Leopold. 1978. Water in Environmental Planning. W.H.Freeman and Co. New York. 818 pp.

Effler, S.W. and D. Johnson. 1987. Calcium Carbonate Precipitation and Turbidity Measurements in Otsico Lake, New York. Water Resources Bulletin, 23 (1):73-79.

Einstein, H.A. 1942. Formulas for the Transportation of Bed Load. Transactions of ASCE, 107:561-573.

Einstein, H.A. 1950. The Bed Load Function for Sediment Transportation in Open Channel Flows. USDA Technical Bull. 1026.

Emmet, W.W. 1975. The channels and waters of the Upper Salmon River Area, Idaho. USGS Professional Paper 870-A. 115 pp.

Engel, B. A., R. Srinivasan and C. Rewerts, 1993. Spatial Decision Support System for Modeling and Managing Agricultural Non-Point-Source-Pollution. pp. 231-237. In: GIS and Environmental Modeling. New York, Oxford University Press.

Federal Aviation Administration. 1970. Airport Drainage. AC 150/5320-5B.

Foster G. R. 1982. Modeling the Erosion Process. In: Hann C.T. Hydrologic Modeling of Small Watersheds. American Society of Agricultural Engineers Monography. 5:297-379.

Foster G.R., L.D.Meyer, C.A. Onstad. 1977. A Runoff Erosivity Factor and Variable Slope Length Exponents for Soil Loss Estimates. Transactions of the ASAE. 683-687 pp.

Foster, G.R., and L.D. Meyer. 1972. A closed-form soil erosion equation for upland areas. In: H.W. Shen (ed.) Sedimentation, 1-19 pp.

Gao X., S. Sorooshian and D. Goodrich, 1993. Linkage of a GIS to a Distributed Rainfall-Runoff model. pp.182-187. In: GIS and Environmental Modeling. New York, Oxford University Press.

Gippel, CJ. 1995. Potential of Turbidity Monitoring For Measuring The Transport of Suspended Solids in Streams. Hydrological Processes, 9:83-97

Gippel, C.J. 1989. Use of Turbidimeters in Suspended Sediment Research. Hydrobiologia, 176(17):465-480

Goodchild, M.F (Ed.).1993. GIS and Environmental Modeling. New York, Oxford University Press. pp.488

Gorokhovich,Y. and L. Janus. 1996. The NYC Water Quality Division Geographical Information System (GIS) and Its Applications for the Watershed Management. Proceedings, Watershed'96 Technical Conference, June 8-12, 1996, Baltimore, Maryland. pp.530-532.

Gorokhovich Y., and P. O'Hara. 1995. Geographic Information Systems as a Tool for Modeling Turbidity Generated During Storm Events. American Geophysical Union, Spring Meeting, April 1995, Baltimore.

Graf, W.H. 1984. Hydraulics of Sediment Transport. Water Resources Publications, Denver, Colorado. 513 pp.

Grayson, R.B. T.Blake and J.Doolan. 1994. Latrobe Sediment and Nutrient Study. Report, Centre for Environmental Applied Hydrology, University of Melbourne, Parkville. pp 190 - 207.

Hairsine, P.B., Rose C.W. 1991. Rainfall Detachment and Deposition: Sediment Transport in the Absence of Flow-driven Processes. Journal of Soil Science Society of America, (55):320-324

Hairsine P.B., Rose C.W. 1992a. Modeling Water Erosion Due to Overland Flow Using Physical Principles 1. Sheet flow. Water Resources Research, 28:237-250.

Hairsine P.B., Rose C.W. 1992b. Modeling Water Erosion Due to Overland Flow Using Physical Principles 1. Rill flow. Water Resources Research, 28:245-250.

Haith, D.A., and R.C.Loehr. 1979. Effectivness of Soil and Water Conservation Practices for Pollution Control. New York State College of Agriculture and Life Sciences, Ithaca. Report EPA-600/3-79-106, prepared for Environmental Research Lab, Athens, GA, October 1979.

Harris, E. 1868. Sanitary Qualities of the Water Supply of New York and Brooklyn. Wescott. New York, N.Y.

Hathaway, G.A. 1945. Design of Drainage Facilities. Transactions, ASCE, (110):697-730.

Hillel, D. 1986. Modeling in Soil Physics: A Critical Review. Future Developments in Soil Science Research (A Collection of Soil Science Society of America Golden Anniversary Contributions). Presented at the Annual meeting, Soil Science Society of America, New Orleans, Louisiana, pp. 35-42

Hudson , N.W. 1971. Raindrop Size. In: Soil Conservation. Cornell University Press, Ithaca, New York, pp.50-56.

HydroQual, Inc., 1997. SWMM Modeling for the Kensico Tributaries Management Plan, October 9, 1997, Project#:HAZE0450, 200 pp.

Iwan G.R. 1987. Drinking Water Quality Concerns of New York City, Past and Present. Annals of the New York Academy of Sciences, (502):183-204.

Julien, P.Y. 1995. Erosion and Sedimentation. Cambridge University Press. 280 pp.

Kelly L.A. 1992. Estimating Sediment Yield Variation in a Small Forested Upland Catchment. Hydrobiologia, 235(6):199-203.

Kirkby M.J. 1978. Hillslope Hydrology. Chichester, John Wiley and Sons.

Kirpich, Z.P. 1940. Time of Concentration of Small Agricultural Watersheds. Civil Engineering, 10:362

Krysanova V., Dirk-Ingmar Mueller-Wohlfeil, A. Becker, 1996. Mesoscale Integrated Modeling of Hydrology and Water Quality with GIS Interface. In: Proceedings of the Third International Conference/Workshop on Integrating Geographic Information Systems and Environmental Modeling, January 21-25, 1996, Santa-Fe.

Lal R.(Ed.). 1994. Soil Erosion Research Methods. Soil and water Conservation Society.

LeChevallier M.W., Norton W.D., Lee R.G. 1991. Occurence of Giardia and Cryptosporidium spp. in Surface Water Supplies. Applied and Environmental Microbiology, 57 (9):2610-2616.

LeChevallier, M.W., and W.D.Norton. 1992. Examining Relationships Between Particle Counts and Giardia, Cryptosporidium, and Turbidity. Journal of the American Water Works Association, 84(12):54-60.

Leopold L.B, and T.Maddock. 1953. The Hydraulic Geometry of Stream Channels and Some Physiographic Implications. Geological Survey Professional Paper 252. Washington D.C. pp.57

Letterman, R.D. 1991. An Evaluation of Alternative Surface Water Treatment Technologies, Report to the New York State Department of Health, Bureau of Public Water Supply Protection, Albany, N.Y.

Letterman, R.D. 1994. What Turbidity Measurements Can Tell Us. Opflow, 20(8):1-7

Lewis J. 1996. Turbidity Controlled Suspended Sediment Sampling for Runoff-event Load Estimation. Waster Resources Research, 32(7):2299-2310.

Liang L., J.F. McCarthy. 1993. Iron Dynamics: Transformation of Fe(II)/Fe(III) during Injection of Natural Organic Matter in a Sandy Aquifer. Geochimica et Cosmochimica Acta GCACAK,57(9):1987-1999.

Lovell, C.J., C.W. Rose. 1988. Measurement of Soil Aggregate Settling Velocities. A Modified Bottom Withdrawal Tube Method. Australian Journal of Soil Research, 26:55-71.

Mack, F. Stephen, 1988. Using Turbidity To Predict Total Suspended Solids in Mined Streams in Interior Alaska. Report of Investigation 88-2. State of Alaska, Department of Natural Resources, Division of Geological and Geophysical Surveys.

Maidment, D.R. 1992. Handbook of Hydrology. McGraw-Hill, Inc.

McCutcheon, S.C. 1989. Water Quality Modeling. (R.H. French, editor).Vol.I. Transport and Surface Exchange in Rivers. CRC Press, Inc. Boca Raton, Florida.

McIsaac G.F., J.K.Mitchell, J.W.Hummel, and W.J.Elliot. 1992. An Evaluation of Unit Stream Power Theory for Estimating Soil Detachment and Sediment Discharge From Tilled Soils. Transactions of the ASAE.35:535 - 544.

Moore, I.D. and J.C. Gallant. 1991. Overview of Hydrologic and Water Quality Modeling. In I.D. Moore (ed), Modeling the Fate of Chemicals in the Environment, Canberra: Center for Resource and Environmental Studies, the Australian National University, pp. 1-8.

NCGIA. 1996. Proceedings of the Third International Conference/Workshop on Integrating Geographic Information Systems and Environmental Modeling, Santa Fe, New Mexico.

NRCS (former SCS), 1992a. National Soils Handbook: Draft 1992.United States Department of Agriculture. Soil Conservation Service, 430-VI-NSH, Draft, September 1992.

NRCS (former SCS), 1992b. National Soil Survey Interpretations Handbook: Draft 1992.United States Department of Agriculture, Soil Conservation Service, 430-VI-NSH, Draft, September 1992.

New York City Department of Environmental Protection, DWQC. 1993. Annual Report.

New York City Department of Environmental Protection, DWQC. 1994. Kensico Watershed Study Augmented Annual Research Report , January 1993- March 1994. 192 pp.

Novotny V. and G. Chesters.1989. Delivery of Sediment and Pollutants From Nonpoint Sources: A Water Quality Perspective. Journal of Soil and Water Conservation, Nov.-Dec., 1989. pp. 568-576.

Oksiiuk O.P., L.A.Zhuravleva, L.V.Liashechenko, I.K.Bashmakova, and I.I.Karpezo. 1992. Gidrobiologicheskii Zhurnal GBZUAM, 28(6):3-11.

Onstad, C.A., and G.R. Foster.1975. Erosion Modeling on a Watershed. Transactions of the American Society of Agricultural Engineers, 18(2):288-292.

Panuska J.C., Moore I.D., Kramer L.A. 1991. Terrain Analysis: Integration into the Agricultural Nonpoint Source (AGNPS) Pollution Model. Journal of Soil and Water Conservation., January-February 1991, pp. 59-63.

Pickering, R.J. 1976. Measurement of 'Turbidity' and Related Characteristics of Natural Waters. Open-file report 76-153, USGS. 13 pp.

Ponce, V.M. 1989. Engineering Hydrology. Prentice Hall, Englewood Cliffs, New Jersey.

Proffitt A.P.B., C.W.Rose, and P.B.Hairsine. 1991. Rainfall Detachement and Deposition: Experiments with Low Slopes and Significant Water Depths. Soil Science Society of America Journal, 55:325-332.

Proffitt A.P.B. , P.B.Hairsine, and C.W.Rosel. 1993. Modelling Soil Erosion by Overland Flow: Application over a Range of Hydraulic Conditions. Transactions of the American Society of Agricultural Engineers, vol. 36.

Quinn J.M., R.J.Davies-Cooley, C.W.Hickey, M.L.Vickers, and P.A.Ryan. 1992. Effects of Clay Dischargees on Streams: 2. Benthic Invertebrates. Hydrobiologia HYDRB8, 248(3):235-247.

Roehl, J.E. 1962. Sediment Source Areas and Delivery Ratios Influencing Morphological Factors. Int. Assoc. Hydro. Sci., 59:202-213.

Rose C.W. , J.Y.Parlange, G.C.Sander, S.Y.Campbell and D.A.Barry. 1983. Kinematic Approximation to Runoff on a Plane: An Approximate Analytical Solution. Journal of Hydrology, 62:363-369.

Rose C.W., Hairsine P.B. 1988. Process of Water Erosion. In: Steffen W.L., Denmead O.T. Flow and Transport in Natural Environment: Advances and Applications. Springer Verlag, Berlin. pp. 312-326.

Rose C.W. , P.B.Hairsine, A.P.B.Profifitt, and R.K.Misra. 1990. Interpreting the role of soil strength in erosion processes. Catena Supplement 17: 153-165.

Rutgers University. 1995. HEC-1 Hands-On Workshop on the Flood Hydrograph Package, March 13-17, 1995. The State University of New Jersey, Rutgers, Office of Continuing Professional Education, Cook College, New Brunswick, p.28

Schumm, S.A. 1954. The Relation of Drainage Basin Relief to Sediment Loss. Pub. Int. Assoc. of Hydrology, IUCG, Tenth Gen. Assembly, Rome,1:216-219.

Severson, R.K. Harvey, J., Polissar, L. 1981. The Relationship Between Asbestos and Turbidity in Raw Water. Journal of the American Water Works Association, 73(4):223-224.

Simons, D.B., R.M.Li, and W.Fullerton 1981. Theoretically Derived Sediment Transport Equations for Pima County, Arizona. Prepared for Pima County DOT and Flood Control District, Tucson, Arizona, Ft.Collins, Colorado.

Shields, A. 1936. Anwendung der Aehnlichkeitsmechanik und der Turbulenz Forschung auf die Gescheibebewegung. Berlin: Mitteilungen der Preussische Versuchanstalt fur Wasserbau und Schliffbau.

Soil Conservation Service (SCS), 1972. National Engineering Handbook, Section 4, Hydrology, SCS.

Spangberg A., Niemczynowicz. 1992. High Resolution Measurements of Pollution Wash-Off from an Asphalt Surface. Nordic Hydrology, 23(4):245-256.

Strahler A. N. 1952. Dynamic Basis of Geomorphology. Bulletin of the Geological Society of America, 63(9):923-938

Strahler A.N. 1957. Quantitative Analysis of Watershed Geomorphology. Trans. Am. Geophysical Union, 38(6):913-920.

Standard Methods for Examination of Water and Wastewater. 1994.

Stewart, K.M. and P.J.H. Martin. 1982. Turbidity and its Cause in a Narrow Glacial Lake with Winter Ice Cover. Limnology and Oceanography, 27(3):510-517.

Strunk N. 1992. Case Studies of Variations in Suspended Matter Transport in Small Catchments. Hydrobiologia, 235 (6):247-255.

Tanimoto T. and A. Hoshika. 1991. Seasonal Variation of Bottom Turbidity Layer in Etauchi Bay. Journal of the Oceanographical Society of Japan, 47 (6):286-296.

Truhlar, J.F. 1976. Determining Suspended Sediment Loads from Turbidity Records. Proceedings of the Third Federal Inter-Agency Sedimentation Conference 1976, held at Denver, Colorado, March 22-25, 1976: Water Resources Council, Sedimentation Committee, pp. 7-65 - 7-74.

Tufte, E.R. 1983. The Visual Display of Quantitative Information. Graphics Press, Cheshire, Connecticut.

US Army Corps of Engineers. 1994. HEC-1. User's Manual. Water Resources Support Center. Hydrologic Engineering Center, Davis, CA.87 pp.

USEPA. 1989. Surface Water Treatment Regulations, 40 CFR Parts 141 and 142. Federal Register, 54(24).

Waggoner, G.S. 1993. Geographic Information Systems: Proceedings of the Seventh Annual GRASS Users Conference. Technical Report NPS/NRGISD/NRTR-93/13. US Dept. of Interior.

Walling, D.E. 1977. Assessing the Accuracy of Suspended Sediment Rating Curves For a Small Basin. Water Resources Research, 13:531-538

Walling, D.E., and B.W. Webb. 1988. The Reliability of Rating Curve Estimates of Suspended Sediment Yield; Some Further Comments. In: Bordas, M.P. and Walling, D.E. (Eds), Sediment Budgets, Proceedings Porto Alegre Symposium., IAHS Publ. Mo. 174:337-350

Walling, D.E. 1996. Suspended Sediment Transport by Rivers: A Geomorphological and Hydrological Perspective, in: Advances in Limnology 47. Suspended Particulate Matter in Rivers and Estuaries, Proceedings of an International Symposium, Reinbek, Germany. E.Schweizerbart'sche Verlagsbuchhandlung, Stuttgart 1996. pp 1-27.

Ward A.D., and W.J. Elliot. 1995. Environmental Hydrology. CRC Press, Lewis Publishers, 462 pp.

Wilber C.G. 1982. Turbidity in the Aquatic Environment. American Lecture Series; publication no. 1057. A publication in the Bannerstone Division of American Lectures in Environmental Studies. Charles C. Thomas, p.133

Williams, J.R. 1975. Sediment Yield Prediction With Universal Equation Using Runoff Energy Factor. Present and Prospective Technology for Predicting Sediment Yield and Sources. ARS-S-40. U.S. Department of Agriculture. Agriculture Research Service. Washington, D.C. pp. 244-252.

Wischmeier W.H., and D.D. Smith. 1965. Predicting Rainfall Erosion Losses From Cropland East of the Rocky Mountains. Handbook 282. Agricultural Research Service, U.S. Department of Agriculture. Washington, D.C.

Wischmeier, W.H. and D.D. Smith. 1978. Predicting Rainfall Erosion Losses - A Guide To Conservation Planning. Supersedes Agriculture Handbook No. 282. Science and Education Administration United States Department of Agriculture in ooperation with Purdue Agricultural Experiment Station.

Yang, C.T. 1972. Unit Stream Power and Sediment Transport. Journal of the Hydraulics Division, ASCE, vol. 98, No. HY10, Proc. Paper 9295, 10:1805-1826.

Yang, C.T. 1973. Incipient Motion and Sediment Transport. Journal of the Hydraulics Division, ASCE, 10:1679 - 1704.

Young, R.A., Onstad, C.A., Bosch, D.D., Anderson W.P. 1987. AGNPS, Agricultural Non-Point-Source Pollution Model: A Watershed Analysis Tool. Conservation Research Report 35, Washington, DC: U.S. Department of Agriculture.

IMAGE EVALUATION TEST TARGET (QA-3)

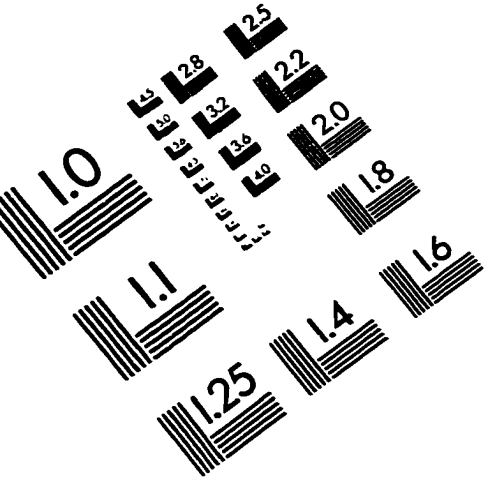

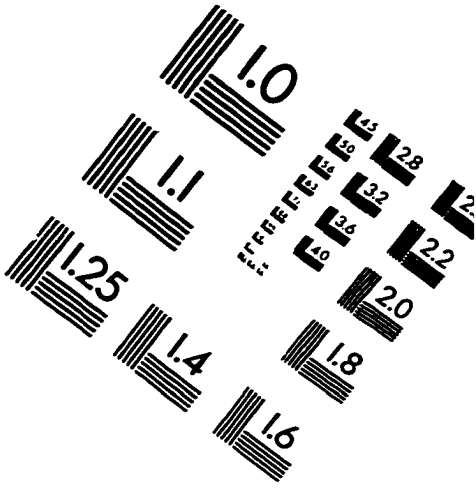

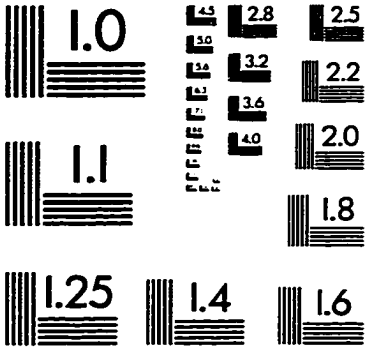

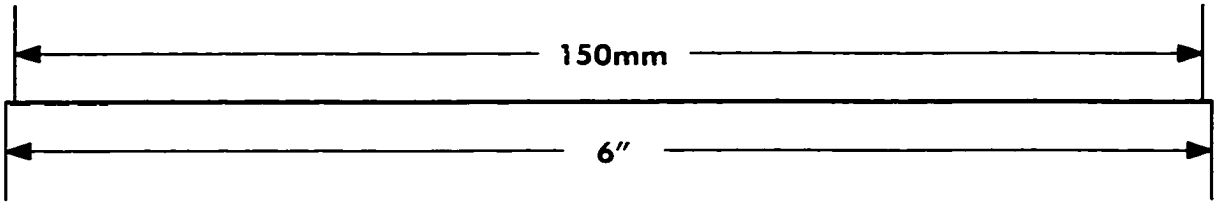

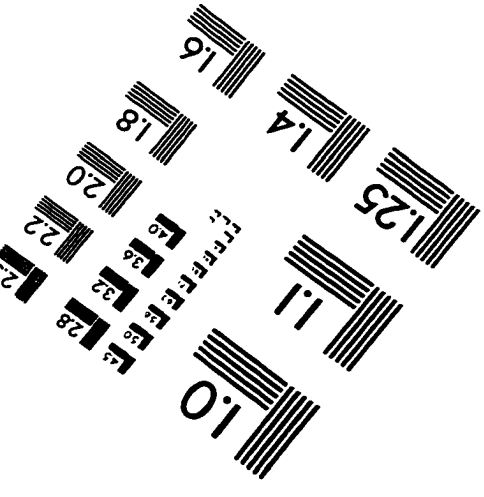

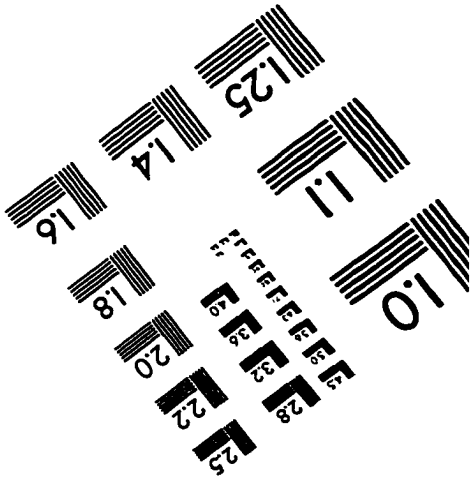

APPLIED IMAGE, Inc
1653 East Main Street
Rochester, NY 14609 USA
Phone: 716/482-0300
Fax: 716/288-5989